1-1-2016

Exploring new chemical entities from traditional medicine: Docking, synthesis and specific bioactivities

Chinni Yalamanchili
University of Mississippi

EXPLORING NEW CHEMICAL ENTITIES FROM TRADITIONAL MEDICINE: DOCKING, SYNTHESIS AND SPECIFIC BIOACTIVITIES

A Dissertation

presented in partial fulfillment of requirements

for the degree of Doctor of Philosophy

in Pharmaceutical Science, Emphasis in Pharmacognosy

The University of Mississippi

by

CHINNI YALAMANCHILI

August 2016

ABSTRACT

Traditional medical systems contributed significantly to medicine with a number of their phytochemicals found to possess good biological properties. Recently, Dr. Youyou Tu was awarded the Nobel Prize (2015) for her discovery/isolation of Artemisinin from the TCM plant *Artemisia annua*. Our first aim is to identify active phytochemicals against botulinum neurotoxin A (BoNT/A), and diabetes from *Ayurveda* and TCM, respectively, by using *in silico*, *in vitro* and *in vivo* approaches. In our second aim, we wanted to enantioselectively synthesize scalable quantities of phytoestrogenic isoflavans such as equol and sativan. The following three chapters summarize results of the three research goals.

Chapter II describes our approach to identify the small molecules effective against BoNT/A, one of the most lethal toxins known to humans, with none of the current known its inhibitors reaching even the clinical trial stages. *Ayurvedic* literature was analyzed and a number of plants were identified based on their usage, frequency and utility in various formulations, for treating diseases with symptoms similar to botulism. The phytochemicals of these plants were studied by docking into the catalytic domain of BoNT/A. From the docking results, thirty-one compounds and their analogues were identified and tested *in vitro* using liquid chromatography-based protease assay. From these results, seven compounds were further tested using *ex vivo* mouse phrenic nerve hemidiaphragm assay (MPNHDA). Results showed a number of compounds including acoric acid **1**, and galangin **3** possessed inhibitory activities of around 40-

50% against BoNT/A in the *in vitro* assay, and in the MPNHDA, initial studies showed that at 20 μM, acoric acid **1** possessed marginal protection. Further testing of the active compounds like acoric acid **1** and their analogues and using more sensitive, reproducible bioassays could yield more active compounds.

Chapter III deals with the identification of small-molecule antidiabetic compounds from the TCM plant, Goji (*Lycium barbarum* and *Lycium chinense*), widely used for treating various diseases including diabetes and hypertension Current clinical antidiabetic drugs, like rosiglitazone display severe side effects like edema, weight gain and heart failure. By docking the twenty-seven selected reported compounds of Goji into the partial and full agonist binding sites of PPARγ (target of rosiglitazone), tyramine derivatives were found to possess good docking scores and binding poses. Henceforth, twenty-four cinnamomyl phenylethyl amide derivatives (termed as tyramine-derivatives) were synthesized and were tested *in vitro* using PPARγ-PPARα luciferase assay. Three compounds showed similar or higher fold induction than the positive control, rosiglitazone. One tyramine-derivative **08**, and tyramine derivatives-enriched fraction (21%) of the root bark of *L. chinense* were further studied *in vivo* using diabetic db/db mice. However, both of them did not possess antidiabetic properties in the tested mice model. *In vivo* results indicate that the antidiabetic property of *Lycium* species is not due to tyramine derivatives.

Chapter IV describes the first large-scale, enantioselective synthesis of both antipodes of

phytoestrogenic isoflavans, equol and sativan, synthesized in >98% ee, with good overall yields starting from the commercially available starting material. Syntheses of these isoflavans were performed using Evans' aldol condensation as a chiral inducing step at C-3 position of isoflavan scaffold. The same flexible methodology can be applied for syntheses of other C-3 chiral isoflavans.

LIST OF ABBREVIATIONS AND SYMBOLS

°C	Degrees Celsius
µg	Microgram
µL	Microliter
µM	Micromole
BoNT/A	Botulinum neurotoxin serotype A
$CaCl_2$	Calcium chloride
CDC	Centers for Disease Control and prevention
Cys	Cysteine
DCM	Dichloromethane
DHT	5α-dihydrotestosterone
DMSO	Dimethyl sulfoxide
ER	Estrogen receptor
FDA	U S Food and Drug Administration
g.	Gram
h	Hours
HC	Heavy Chain
HEPES	4-(2-Hydroxyethyl)-1-piperazineethanesulfonic acid
HPLC	High performance liquid chromatography
IC_{50}	Inhibitory Concentration, 50%

KCl	Potassium Chloride
LBD	Ligand binding domain
LC	Light Chain
LC_{50}	Lethal Dose, 50%
m/z	Mass-to-Charge Ratio
MeOH	Methanol
$MgCl_2$	Magnesium chloride
min.	Minute
mL	Milliliter
MPNHDA	Mouse Phrenic Nerve Hemidiaphragm Assay
NaCl	Sodium Chloride
NaH_2PO_4	Sodium dihydrogen phosphate
$NaHCO_3$	Sodium bicarbonate
NMR	Nuclear Magnetic Resonance
PDA	Photodiode Array Detector
PDB	Protein Data Bank
PPAR	Peroxisome Proliferator-Activated Receptors
RMSD	Root-Mean Square Deviation
RXR	Retinoid X receptor
SNAP-25	Synaptosome Associated Protein 25kD

T2D	Type 2 Diabetes
TCM	Traditional Chinese Medicine
TFA	Trifluoroacetic acid
THF	Tetrahydrofuran
TLC	Thin Layer chromatography
UMMC	University of Mississippi Medical Center, Jackson, MS
UPLC	Ultra-performance liquid chromatography
USAMRIID	The United States Army Medical Research Institute for Infectious Diseases
VSW	Virtual Screening Workflow

ACKNOWLEDGEMENTS

I would like to take this opportunity to recognize the contributions of all the people involved in finishing my doctoral degree, Ph.D. in Pharmaceutical Sciences. First, I would like to thank Dr. Ikhlas A. Khan for admitting me into the department, for his guidance, and financial support throughout my studies. His support, criticism, wisdom and leadership were critical for my development as a scientist, and his achievements and persona serve as a true inspiration to me. Next, I would like to thank Dr. Amar G. Chittiboyina, for serving as my research advisor along with Dr. Khan, without whom I would have not finished this work. His training, guidance, wisdom and support cannot be forgotten and are very significant for finishing my Ph.D. He encouraged me be a better scientist, enhanced my competence, and was my go-to person in need at every stage. I would like to thank my other dissertation committee members-Drs. Larry Walker, Jordan K. Zjawiony, Samir Ross, for serving in the committee, going through my dissertation, evaluating my ORP and providing valuable suggestions in spite of their busy schedules. I would like to thank Dr. Jon F. Parcher for correcting my dissertation and publications.

Next, I would like to thank our collaborators at USAMRIID, particularly Dr. Bob Webb for his collaboration and technical help with BoNT/A project, and our collaborators at UMMC to assess the cardio-metabolic profiles of samples *in vivo*. Also, I would like to thank the researchers at the University of Mississippi, Drs. Shabana Khan, Vamsi Manda, Bharathi Avula,

Sathyanarayana raju Sagi, Yelkaira Vasquez, for helping in bioassays and analytical instrumentation, Drs. Sateesh Chandra Kumar Rotte and Prabhakar Peddikotla for help in synthetic skills and Dr. Nao H. Abe for isolating the enriched extract of Goji

I would like to thank the all the faculty of the School of Pharmacy, particularly, Drs. Daneel Ferreira, Jordan Zjawiony, Mark Hamman, Dale Nagle, Yu-Dong-Zhou, and Mark Slattery of Division of Pharmacognosy for teaching relevant course work, testing and training with seminars, comprehensive and ORP exams. Also, special thanks to professors in the Department of Medicinal Chemistry: Drs. Christopher Mc Curdy, Stephen J Cutler, and Robert Doerksen for teaching Medicinal Chemistry courses and for the warm encouragement while interacting with them. Special appreciation to the staff in the NCNPR, particularly, Ms. Jennifer Taylor, Ms. Annette Ford and Ms. Jennifer Michael, and Department of BioMolecular sciences, particularly, Ms. Casey Stauber, Ms. Sherry Gussow, Ms. Candace Lowstuter, for being supportive while in need with scheduling of seminars and documentation.

Next, I would like to thank a number my colleagues, seniors, friends and roommates within and outside the department for being with me during my-ups and downs, and making my stay memorable. To name a few, Dr. Michael Chan, Michael Cunningham, Vimal Sharma, Abhijeet Maurya, Manjeet Pimparade, Avadesh Kushwaha Murali Krishna Angamuthu Drs. Vijayshankar Raman, Zulfiqar Ali, Mallika Kumarihamy, Manal Nael, Radha Krishna Bhattar, Shuneize L. Slater, Pankaj Pandey, Rambabu Sankranthi, and Naresh Modepalli,.

I cherish being a part of Dr. Khan’s group; it has given me the opportunity to interact

with and meet a number of researchers from around the world. I would like to thank the University of Mississippi in general, and school of pharmacy in particular for giving me an opportunity to study. My time of stay here has been very enriching, and learning experience and I would cherish my stay here for the rest of my life. It has been a long tough ride with a number of ups and downs, but this has taught me to be humble, understand my own limitations, energy to face challenges and be successful.

I would like to thank all my family members, particularly my father, mother and brother, for their sacrifices, for the confidence they put upon me to pursue my Ph.D. Finally, I would like to thank my wife, Asha, for being a part of my life, for supporting and enriching me in many ways.

Best,

Chinni Yalamanchili

TABLE OF CONTENTS

LIST OF TABLES

LIST OF FIGURES

LIST OF SCHEMES

LIST OF APPENDICES

SUPPLEMENTARY INFORMATION TABLES

SUPPLEMENTARY INFORMATION SPECTAL DATA

CHAPTER 1

TRADITIONAL MEDICINE AND DRUG DISCOVERY

1. **Contribution of natural products to drug discovery**

Natural products continue to be the basis of new drugs, contributing either by acting directly as drugs or by acting as a source of new drugs. According to a review by Newmann *et al*. in 2010, over the last 30 years (1980 to 2010), natural products (including natural product-derived compounds, natural product-derived botanicals, synthetic compounds with core of natural products) contributed to the bulk of the drugs approved for clinical usage (Figures 1-1 and 1-2) [1]. Among these drugs classes, since 1940s, 75% of the small molecule anticancer drugs were other than synthetics and 48% were actually based on natural product scaffolds. Synthetic approaches were used successful to identify clinically better natural product analogues. However, combinatorial-chemistry approaches contributed to very few *de novo* drugs. Hence, drug discovery based on natural products is still relevant to identify novel agents to find treatments against health care challenges. Recently, the contribution of sources other than plants in drug discovery, especially from the microbial sources, has risen and is projected to rise with a number of them in clinical trials [1].

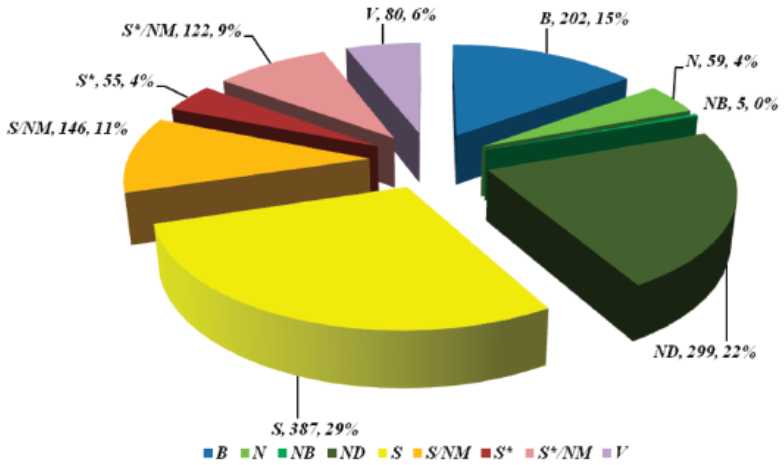

Figure 1-1. Classification of the approved drugs from 1981 to 2010.

(permitted by Newmann *et al*, 2010).

The total number of newly approved drugs from 1981 to 2010 is 1355. B = biological, N = natural product, NB = natural product botanical, ND = derived from a natural product, S = totally synthetic drug, often found by random screening/modification of an existing agent, S* = made by total synthesis, but the pharmacophore is/was from a natural product, and V = vaccine.

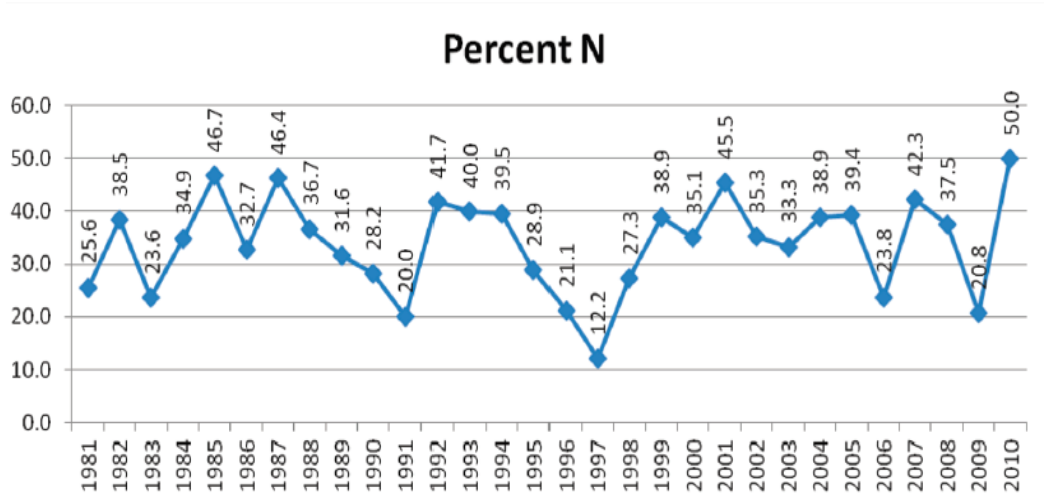

Figure 1-2. Percentage of natural products in the approved new chemical entities from 1981 to 2010 [1].

(permitted by Newmann *et al*, 2010).

The contribution of natural products to human health is significant. Two scientists,

Alexander Flemming (Medicine, 1942) and Selman Waksman (Medicine, 1952) were awarded the Nobel Prize for their discoveries of penicillin and streptomycin, from fungi and bacteria, respectively. Very recently, the significance of natural products in human health has also gained enormous publicity with the announcement of the Nobel Prize (for 2015) in medicine to three natural product scientists: Youyou Tu, Satoshi Ōmura and William Cambell (**Table 1-1**). Yougou Tu, isolated artemisinin form a plant named sweet worm wood, which was used traditionally in China for treatment of fever [2]. The antimalarial effect of sweet worm wood (*Artemisia annua*) was recorded in the compendium of Materia medica written by Shizhen Li (1518 -1593). Currently, artimisinin and its derivatives are clinically used for the treatment of malaria around the world. In 1978 Satoshi Ōmura succeeded in culturing a strain from which William Campbell purified a substance, avermectin, which, in a chemically modified form (ivermectin), proved to be active against round worm infections.

2. **Ethnomedicine/traditional medicine**

Since prehistoric periods, plants have been a major source for medical treatments across the world. In countries like Greece, Egypt, India, Tibet and China etc., there have been archeological and ancient textual references about the usage of plants for the treatment of diseases or disease symptoms [3]. Ethnomedicine is defined as the use of plants as medicine, which includes traditional forms of treatment like TCM and Ayurveda. Ethonopharmacology is "a much diversified approach to drug discovery involving observation, description and experimental investigation of indigenous drugs and their biological activities. This involves highly interrelated studies of botany, geology, biochemistry, pharmacology, and other disciplines" [4].

Table 1-1. Three natural product scientists awarded the Nobel Prize for their contribution to human health.

Youyou Tu	William C. Campbell	Satoshi Ōmura
	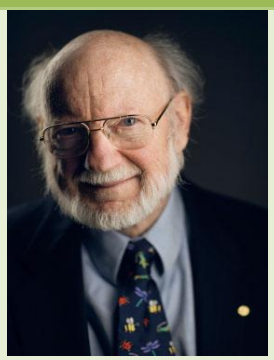	
Artemisinin 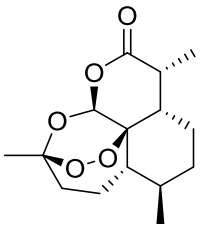 Novel therapy against Malaria Traditional Chinese medicine ○ uses sweet wormwood to treat fever ○ extracted artemisinin, which inhibits the malaria parasite.	Ivermectin chemically modified from Avermectin (isolated from bacteria) 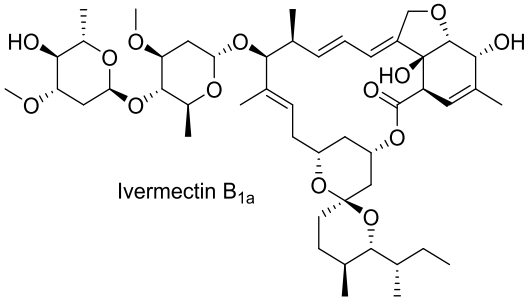 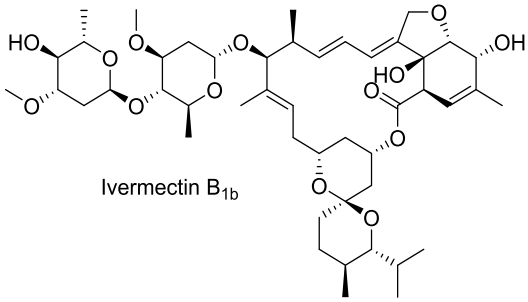 • Novel therapy against infections: Lymphatic filariasis, or elephantiasis, effective against river blindness	

Ethnomedicine contributed to the identification of a number of drugs. According to the 2001 review by Farnsworth *et al*., a total of 122 compounds were identified to be obtained from

plants used in traditional medicine, and among these 80% of the compounds were used for the same or related ethnomedical use (**Table 1-2**) [4]. Compounds from these ethnomedical plants also serve as precursors for the synthesis of new drugs like papaverine, which acted as a precursor for verapamil, galegine, which acted as a precursor for metformin (**Figure 1-3**).

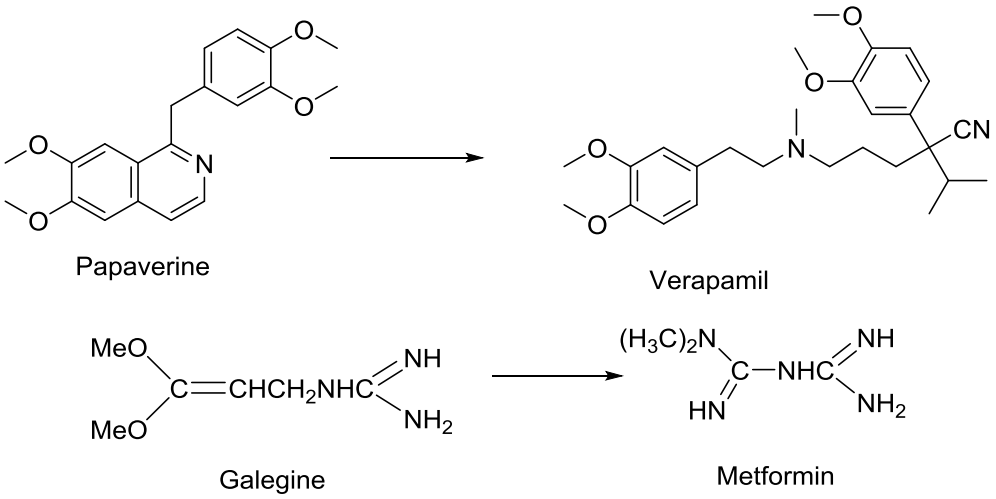

Figure 1-3. Drugs derived from natural products: verapamil from papaverine and galegine from metformin [4]

Traditional medicine is a broad term representing all forms of non-western medicine, including eastern medical systems which originated in China and India, and have been practiced for over thousands of years. Traditional Chinese medicine (TCM) and traditional Indian medicine (Ayurveda, Yoga, Siddha, Unani and Homeopathy etc.) are well documented (**Table 1-3**) for a number of centuries with a number of prescriptions mainly plant-based are used for treatment. Till today, traditional medicine is still very popular among a majority of populations of the world, with WHO estimates of 1995, indicating that 65% of the world's population continue to be treated with traditional medical treatments [4].

Table 1-2. Some examples of phytochemical drugs with similar enthomedical properties as their traditional uses. [4]

Drug	Action or clinical use	Plant source
Agrimophol	Anthelmintic	*Agrimonia eupatoria* L.
Atropine	Anticholinergic	*Atropa belladonna* L.
Cocaine	Local anesthetic	*Erythroxylum coca* Lamk.
Codeine	Analgesic; antitussive	*Papaver somniferum* L.
Cynarin	Choleretic	*Cynara scolymus* L.
Deslanoside	Cardiotonic	*Digitalis lanata* Ehrh.
Gossypol	Male contraceptive	*Gossypium* spp.
Khellin	Bronchodilator	*Ammi visnaga* (L.) Lamk.
Picrotoxin	Analeptic	*Anamirta cocculus* (L.) W.&A.
Reserpine	Antihypertensive, tranquillizer	*Rauvolfia serpentina* (L.) Benth ex. Kurz
Rotundine	Analgesic; sedative	*Stephania sinica* Diels
Scillarin A	Cardiotonic	*Urginea maritima* (L.) Baker
Theophylline	Diuretic; bronchodilator	*Camellia sinensis* (L.) Kuntze
Tubocurarine	Skeletal muscle relaxant	*Chondodendron tomentosum* R. & P.
Yohimbine	Aphrodisiac	*Pausinystalia yohimbe* (K.Schum.) Pierre

3. Ayurveda and TCM

Both TCM and *Ayurvedic* systems are based on health principles, and aim to promote both health and quality of life [5]. They mainly use plant-based formulations along with animal and other metals.

According to TCM, the world is made up of elements—water, earth, metal, wood and fire, and two relatively opposite aspects represented as *Yin* and *Yang*, which act like positive and negative opposites, and are interchangeable. The amount of *Yin* reduces while *Yang* increases and vice versa. In TCM, human body is the center of the universe with the four bodily humors (qui, blood, moisture, essence) and internal organ systems (Zang fu) playing an important role in

balancing the *Yin* and *Yang* in the body. Any disease condition is stated to be due to an imbalance of the body. TCM has contributed to a number of breakthrough drugs like ephedra (from Ma hung, isolated in 1885), artemisinin (anti-malarial) and paclitaxel (anti-cancer). The antimalarial effect of the artemisinin plant, *Artimisia annula* was recorded in the compendium of *Materia medica* written by Shizhen Li (1518-1593).

Table 1-3. Historical progress of the literature in TCM [6] and *Ayurvedic* [7].

TCM		**Ayurveda**	
Period	**Literature**	**Period**	**Literature**
~300 BC	Prescriptions for fifty-two diseases (300 BC), anonymous.	**1000 BC**	Charak Samhita
221 BC–220 AD	Shen Nong Ben Cao Jing (25 –220 AD), anonymous. Shang Han Za Bing Lun (210 AD), written by Zhang Zhong-Jing.	**100 AD**	Sushrut Samhita
581–960 AD	Xin Xiu Ben Cao (659 AD), written by Li Ji and Su Jing et al. Wai Tai Mi Yao (752 AD), written by Wang Tao.	**800 AD**	Madhav Nidan
960–1368 AD	Zheng Lei Ben Cao (1082 AD), written by Tang Shen-Wei. Sheng Ji Zong Lu (1111–1117 AD), compiled by Zhao Ji.		
1368–1643 AD	Ben Cao Gang Mu (1578 AD), written by Li Shi-Zhen. Pu Ji Fang (1406 AD), written by Zhu Di.		

According to the *Ayurvedic* system of treatment, the world is made up of five elements, akasha (ether or space), vayu (air), teja (fire), jal (water) prithvi (earth). These five elements are

coded into the human body as three forces/doshas, termed as “tridosha’ kapha, vata, pitta, each doshs consists of one or two elements, *Vata*-space and air, *Pitta* – space and air, *kapha* – water and ether. The *tridosha* is responsible for the health; any imbalances would generate disease conditions in the system [5]. Plants from *Ayurvedic* system of medicine have contributed to the discovery of a number of compounds which are useful to treat against a number of diseases and possess good bioactivities. **Table 1-4** shows some examples of compounds from *Ayurvedic* plants and their treatment target diseases. In addition, there are a number of plant formulations or whole plant parts from *Ayurveda*, which are currently used for the treatment of diseases or disease symptoms. Although *Ayurveda* has contributed to a number of pure compounds against a number of diseases, it was not able to produce any breakthrough drugs like placlitaxel or artemisinin, from TCM, and the credits were taken by the Western pharmaceutical companies for the discovery of drugs like forskolin and reserpine.

Table 1-4. List of *Ayurvedic* plants and their phytochemicals used for treatment of various disease conditions [6].

	Compound	**Plant**	**Disease**
Anti-inflammatory	Withanolides	*Withania somnifera*	Arthritis
	Curcumin	*Curcuma longa*	
	Guggul	*Commiphora mukul*	
Cardiovascular symptoms	Cardiac glycosides or cardenolides	Several plants	Potent cardiac glycosides
	Thevitin A, B, Peruvoside	Yellow oleander plant	
	Reserpine	*Rauvolfia serpentina* (L.) Benth ex. Kurz	Angina pectoris
	Colenol	*Coleus* spp	Hypotensive actionand positive ionotopic effect
Antidiabetic	Charantin with steroidal saponins in 1:1	*Momordica charantia*	Insulin-like activity, hypoglycemic activity
	Gymnemic acid	*Glymnema sylvestra*	Type-II diabetes
Anti-obesity	Guggulipid	*Commiphora mukul*	Antihyperlipidemic
Anti-malarial	Nimbolide, timonoid triterpene	*Azadirecta indica*	Anti-malarial

4. **Overall aims**

Drug discovery from plants in traditional medicine

There is an ever increasing demand to find new phytochemicals as drugs. However, the current approaches in drug discovery from plant extracts are based on mechanism-based testing of pure compounds using high-throughput screening or bioactivity-guided fractionation. Drug discovery from plants is a very laborious process with over 250 thousand known plants. In addition, the number of bioassays used for screening is ever increasing.Hence, finding the active-phytochemical principles and their disease-targets is very complex. In order to overcome these challenges, instead of random screening of plants for activities and disease treatments,

ethnomedical usage or traditional usage could be a good metric for the selection of plants to be tested for a particular bioactivity. This selection should be based on their exact or similar ethnomedical or symptomatic usage. Our aim primary aim is to identify new biological roles of the phytochemicals from plants mentioned in TCM and *Ayurveda.* Using computational/*in silico*, synthetic, *in vitro*-based approaches, TCM and *Ayurvedic* plant-based phytochemicals were tested for their anti-botulism (Chapter 2) and anti-diabetic (Chapter 3) activities.

Isoflavans are secondary metabolites of plants possessing varied biological properties. Equol **7**, an isoflavan, is a biological metabolite of the isoflavonoids commonly found in the soy based traditional foods in China, Japan and south-east Asian countries. S-Equol **7** was found to bind preferentially to estrogen receptor β (among the two nuclear estrogen receptors, estrogen receptor-α and -β). In order to further test the biological activities of equol and other isoflavonoids, a large scale general synthetic method to produce enough quantities of enantiopure material will be useful for further biological testing. In our other aim, we performed enantioselective synthesis of isoflavans, equol and sativan. The same method could be used for the synthesis of other plants (Chapter 4).

In this dissertation, three projects were performed which include testing for phytochemicals from both *Ayurveda* and TCM. They are:

1. Identification of new scaffolds from *Ayurvedic* literature against botulinum neurotoxin (Chapter 2).
2. Screening of the phytochemicals of the Traditional Chinese Medicinal plant, Goji, for the identification of small molecules with anti-diabetic activities (Chapter 3).
3 New synthetic method for enantioselective synthesis of isoflavans, equol and sativan (Chapter 4).

CHAPTER 2

IDENTIFICATION OF NOVEL PHYTOCHEMICAL INHIBITORS OF BOTULINUM NEUROTOXIN A

1. Introduction

1.1. *Ayurveda* and drug discovery

Drug discovery continues to rely on natural products which are a major source of drugs, producing 50% of all small-molecule new chemical entities from the year 2000 to 2010 [6]. Traditional systems of medicine from India and China contributed to the discovery of a number of drugs for the treatment of many diseases such as malaria (quinine, artemisinin) and cancer (vinca alkaloids, paclitaxel, camptothecin, irinotecan) [7, 8]. *Ayurveda* is a traditional system of medicine from the Indian subcontinent with a history of over 3000 years. With "*Ayur*" meaning life and "veda" meaning knowledge or science, *Ayurveda* is centered on health principles [9]. *Ayurvedic* literature such as *Charak Samhita* (1000 BC) and *Sushrut Samhita* (100 AD) provides a description of conditions and symptoms associated with a number of diseases. Over 10,000 formulations with >1,500 herbs were included in the *Ayurvedic materia medica* and over 5,000 signs and symptoms were mentioned in the diagnosis classic, Madhav Nidan (800 AD). This vast knowledge of disease symptoms and treatment procedures provides a time-tested approach for solving current challenges in drug discovery. The aim of the current study is to identify novel small-molecule leads for the treatment of botulinum neurotoxin serotype A (BoNT/A) by using

the *Ayurvedic* literature and modern *in silico* drug screening techniques.

1.2. Botulinum neurotoxins (BoNTs)

BoNTs, produced by anaerobic gram-positive bacilli such as *Clostridium botulinum*, result in a disease known as botulism which is characterized by flaccid paralysis. Symptoms arise from the inhibition of the release of acetylcholine at the peripheral neuromuscular junction (**Figure 2-1**) [10]. So far, seven identified serotypes (A to G) and numerous subtypes of BoNT have been reported. Serotypes A, B, E, and F affect humans, and among these, BoNT/A is the most potent serotype [11, 12]. The lethal dose of the crystalline form of BoNT/A is approximated as 0.09-0.15 µg intramuscularly and 0.70-0.90 µg orally for a 70 kg human being [13]. BoNTs are classified as Category A bio-warfare agents by the Centers for Disease Control and Prevention (CDC). Due to their action at the neuromuscular junction, BoNTs are used for the treatment of various muscular disorders and for various cosmetic purposes [14, 15].The currently available remedies for botulism include treatment with anti-toxins, which is limited since it is effective only for sequestering the free, circulating toxin but ineffective for treating post-infected cells [16]. Hence, the identification of small-molecule inhibitors which possess activity against the already infected cells is of immense interest to the human health and the research community.

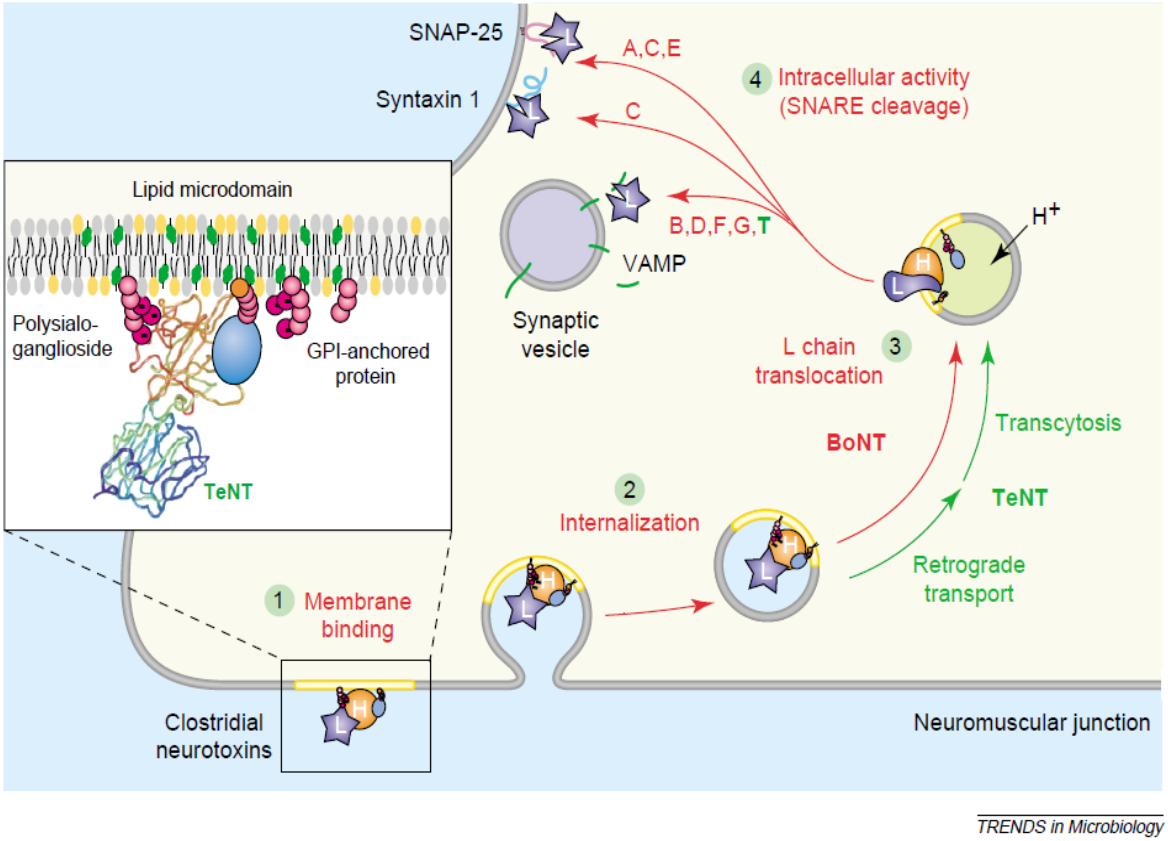

Figure 2-1. Mode of action of BoNTs [17].

BoNTs inhibit the release of acetyl choline by cleaving the proteins involved in vesicle binding to the receptor via four step mechanism (Permitted by Lalli *et al*., 2003).

1.3. BoNT/A: Structure and binding site

The structure of the BoNT/A is highly complex and consist of three domains, each of which are approximately 50 kDa in size, incorporating two peptide chains [light chain (LC) and heavy chain (HC)] connected by a disulfide bridge [18] (**Figure 2-2**). LC possesses a single catalytic domain responsible for the proteolytic activity; whereas, HC, possesses two domains: the translocation domain, and the binding domain, and is involved in neuro specific binding, uptake and translocation of LC into the neuronal cytosol. The LC, which possesses the zinc-dependent catalytic domain, cleaves one of the three proteins that are essential for synaptic

vesicle fusion, this results in the inhibition of the release of acetylcholine and leads to flaccid paralysis of the muscles [19].

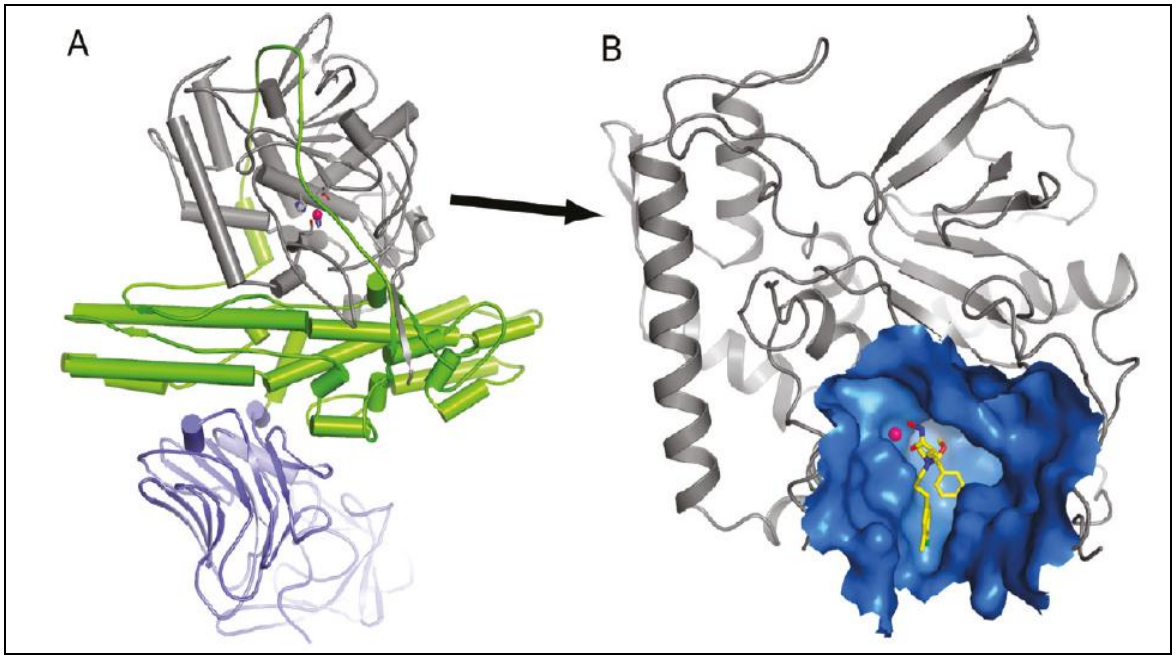

Figure 2-2 Structure of BoNT/A (PDB 3BTA).

A) BoNT/A consists of three domains, light chain (LC) domain in grey which possess the peptide cleaving pocket, heavy chain (HC) which acts as a translocation domain and receptor binding domain in violet. B) LC domain with the binding pocket possessing hydroxamate inhibitor. (permitted by Thompson *et al* [20].

The LC exerts its proteolytic action by cleaving Synaptosome Associated Protein 25kD (SNAP-25), a peptide which is involved in binding of the vesicles to the membrane, at Gln197-Arg198. SNAP -25 possesses two helices, a *C*-terminal helix and an *N*-terminal helix denoted by sn1 and sn2, respectively. The crystal structure of SNAP-25 with sn2 (PDB: 1XTG) showed extensive interface with the LC, were it was found to possess two exosites, α and β (**Figure 2-2**). These exosites are formed by the interaction of the α-helix and β-sheet of SNAP-25, in addition to the catalytic site. This extensive interface between the LC and SNAP-25 results in specificity

and efficiency of proteolytic cleavage (**Figure 2-3**) [21].

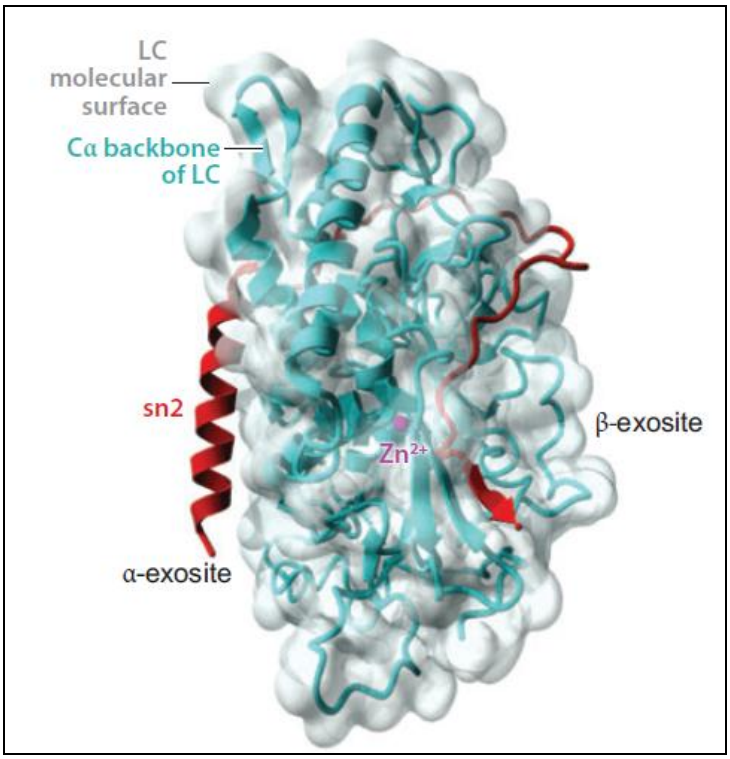

Figure 2-3. Structure of SNAP-25 (PDB 1XTG) in complex with LC of BoNT/A.

The Cα backbone of the LC is represented as cyan ribbons, and its molecular surface is in transparent gray. sn2 is depicted in red, and the catalytic Zn^{2+} at the active site as a purple sphere. [Perrmitted by Montal *et al.* [22]]

The catalytic domain (LC) consists of: Zn^{+2} ion and residues that-chelate with the zinc ion, -help in peptide cleavage, form the hydrophobic pocket, and loops surrounding the active site of BoNT/A. The LC of BoNT/A is a zinc-protease, and possess a highly conserved Zn^{+2} protease motif HEXXH. The imidazole groups of His222 and His226 and the carbonyl side chain of Glu261 coordinate with Zn^{+2} at the active site. A water molecule coordinating with Glu223 plays a crucial role in the proteolysis. They are involved in positioning the substrate to enable its cleavage. The residues that help in peptide cleavage are Tyr366 and Arg363, whereas, Ile161, Phe163, Phe194, and Phe369 make up the hydrophobic pocket [23]. Loops 360/370 (366-372)

and 60/70 (61-79) surround the catalytic site and are flexible upon inhibitor binding [20]. Kumaran *et al*. described the key interacting residues in the catalytic site of BoNT/A, by using four inhibitory substrate tetrapeptides. They showed that Tyr 366 and Arg 363 interact with the P1 and P1′ of the substrate. S1 is formed by Glu164, whereas, S1′ is formed by Phe194, Thr215, Thr220, Asp370 and Arg363, and S3′ is formed by Tyr250, Tyr251, Met253, Leu256, Phe369, Phe423, Pro206, and Leu207 [24] (**Figure 2-4**).

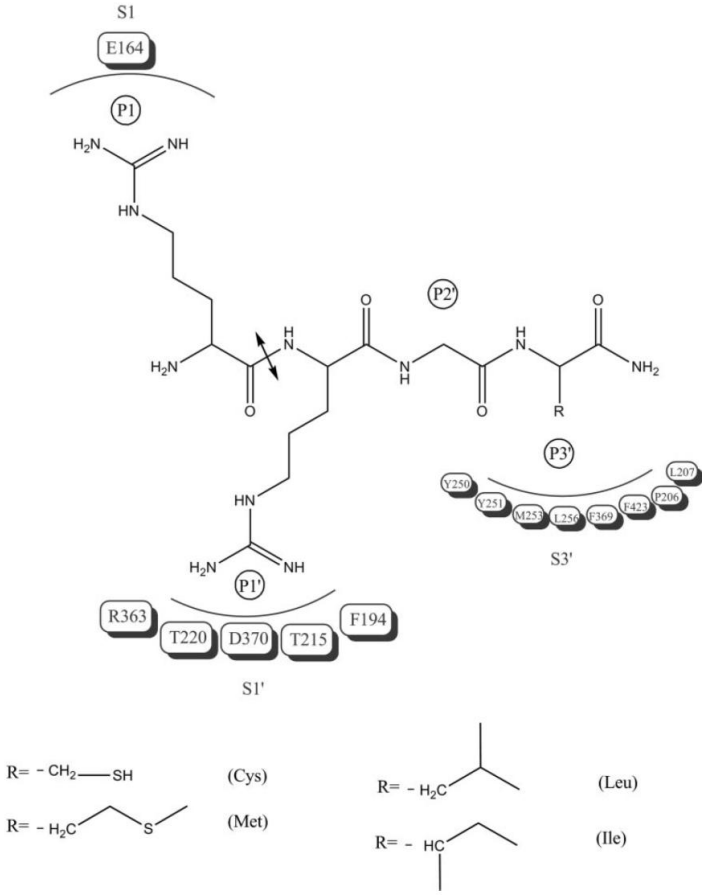

Figure 2-4. Binding site of BoNT/A representing S1, S1', and S3' sites using an inhibitor peptide [25].

"The side chain groups of the terminal peptides are shown at the bottom of the figure. Residues of the enzyme forming the subsites are shown in boxes [25]."

1.4. BoNT/A inhibitors

In general, the identification of inhibitors and modulators of BoNT is approached by targeting all three modules: the receptor-binding module, the translocation domain module, and the protease module [19, 26]. Among these three approaches, we want to target BoNT/A at its catalytic domain (LC) which is located in the protease module of the enzyme. Several inhibitors which target the catalytic domain were reported including peptide inhibitors [27] and small molecule inhibitors, including natural products.

Small molecule inhibitors: Identification of small-molecule inhibitors which target the catalytic domain of BoNT/A is a very active area of research. Several small-molecule inhibitors including natural products have been reported by various groups. However, none have reached advanced levels such as clinical trials [13, 28]. These small-molecule inhibitors include hydroxamic acid derivatives, their prodrugs [20, 29-31] (**Figure 2-5**) and quinolinol [27, 32, 33] inhibitors (**Figure 2-6**).

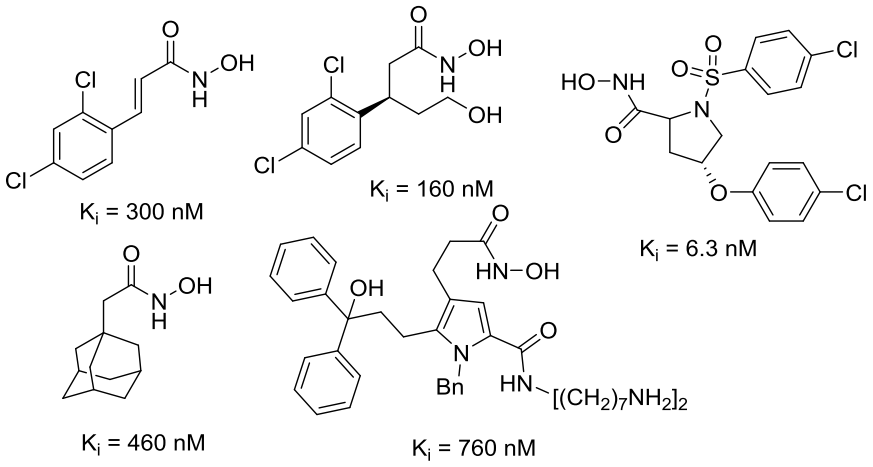

Figure 2-5. Structures of the hydroxamic acid derivatives possessing BoNT/A inhibitory activity [20].

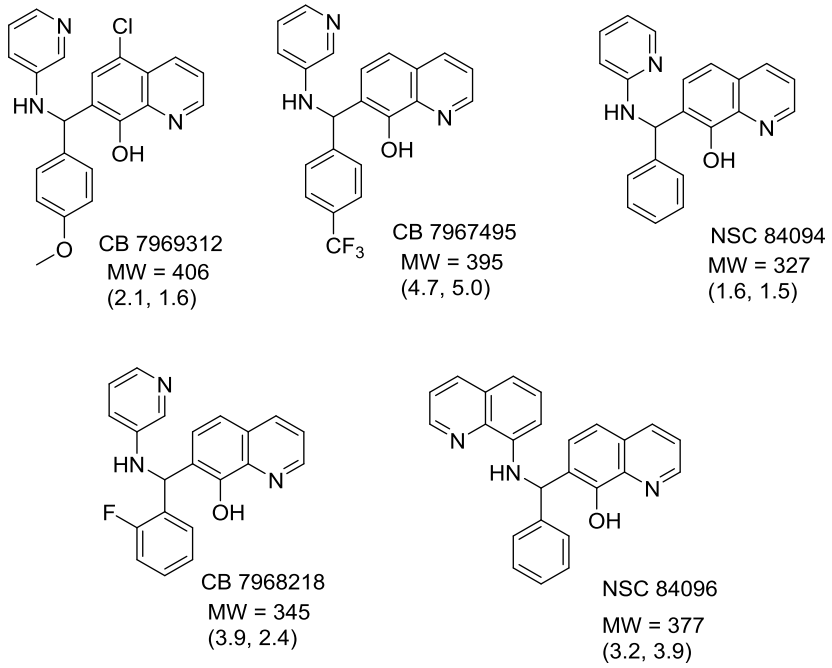

Figure 2-6. Structures of quinolinol based inhibitors of BoNT/A [32].

IC_{50} values of selected analogs against recombinant full-length BoNT/A LC (rALC) and truncated BoNT/A LC (tALC; residues 1 to 425) are given in parenthesis.

Natural products: In addition to the synthetic molecules, several natural products, including some from fungal sources, have been identified as inhibitors of BoNT/A (**Figure 2-7**). These compounds include chicoric acid [34], caftaric acid, and chlorogenic acid [35] which were found to act via exosite mechanisms. Lomofungin, a compound first isolated from fungi, was found to be an inhibitor with a K_i of 6.7 $\pm$ 0.7 μM [36]. Capsaicin was previously identified by Thyagarajan *et al.* as a potential inhibitor of BoNT [37, 38]. By *in silico* screening of the NIH Molecular Library Small-Molecule Repository (MLSMR) containing ~350,000 compounds, fungal bis-naphthopyrones, chaetochromin A, and talaroderxines A and B were identified as potent inhibitors of BoNT/A [39]. Five highly potent quinolinol inhibitors were first identified using a combination of *in silico* and *in vitro* screening of the NCI database [32].

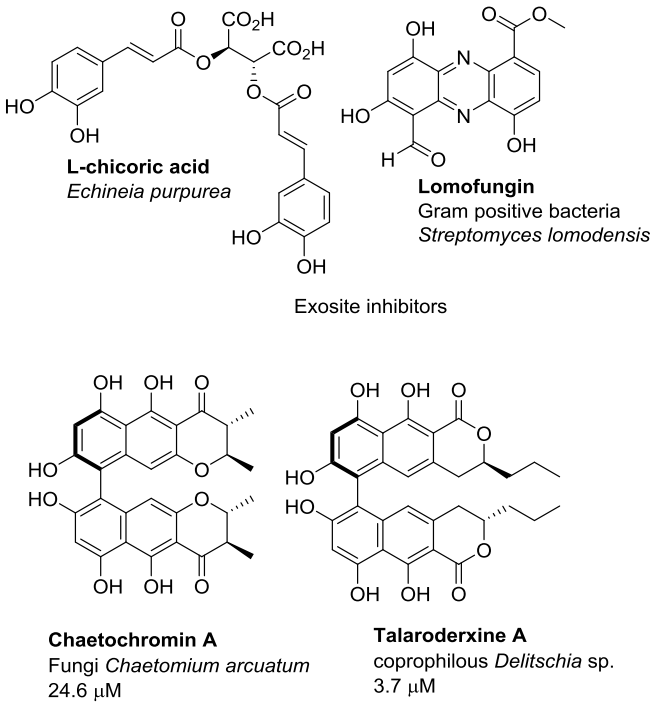

Figure 2-7. Structures of the reported natural product inhibitors of BoNT/A [34, 39].

2. Results and discussion

We hypothesized that phytochemicals obtained from *Ayurvedic* plants which are used for the treatment of diseases with symptoms closely related to that of botulism can be used as small-molecule inhibitors of BoNT/A LC protease. With the aim to identify novel natural product inhibitors of BoNT/A using symptom based-*Ayurvedic* literature in three stages: i) selection of plants from *Ayurvedic* literature, ii) *in silico* screening, iii) *in vitro* and *ex vivo* testing. Several crystal structures of BoNT/A were reported in the literature, six crystal structures were selected for computational work. All the phytochemicals from the selected *Ayurvedic* plants were first screened against six known crystal structures of BoNT/A for probing the available chemical space with *in silico* methods such as docking. The resulting hits were further investigated with

HPLC-based *in vitro* screening method.

2.1. Selection of plants from *Ayurvedic* literature

Botulinum neurotoxin causes flaccid paralysis of the muscles. The weakness of the muscles descends from the muscles of the head and upper extremities via respiratory muscles to the muscles of the lower extremities. This could become fatal when left untreated, due to the respiratory failure resulting from the arrest of the intercostal muscles and the diaphragm. Clinical symptoms of botulism include blurred vision, drooping eye lids, symptoms of the throat such as slurred speech, difficulty swallowing, dry mouth, muscle weakness, and flaccid paralysis [40] (**Table 2-1**).

Table 2-1. Clinical symptoms of Botulism [40].

Initial prodromal symptoms	Initial neurological	Muscle weakness	If untreated
Nausea Vomiting Abdominal cramps Diarrhea	Ocular cranial nerve dysfunction: Blurred vision; diplopia, ptosis, photophobia, facial weakness Bulbar nerve dysfunction) Dysarthria, dysphonia (speech) & dysphagia (swallowing)	Head control Upper extremities Respiratory muscles Lower extremities	If unrecognized and untreated, the intercostal muscles (ribs) and the diaphragm are compromised, then respiratory insufficiency occurs followed by respiratory failure.

Using clinical symptoms as a benchmark, *Ayurvedic* literature were analyzed to identify within them any discussion of diseases with neuromuscular symptoms similar to that of botulism. Interestingly**,** the neuromuscular symptoms of some of the diseases mentioned in the *Ayurvedic* text, *Ayurveda Saukhyam of Todarananda* written by Vaidya Bhagwan Dash and Lalitesh Kashyap, were similar to the clinical symptoms of botulism [40]. These diseases include *Ardita*,

Apa tänaka, *Hanu graha*, *Hanu stambha*, *Gŗdhrasi*, and *Akshepaka* (**Table 2-2**).

Table 2-2. List of the diseases with symptoms similar to botulism mentioned in the *Ayurvedic* text by Vaidya Bhagwan Dash and Lalitesh Kashyap.

Disease name (*Ayurvedic*)	**Symptoms**
Ardita	Facial paralysis
Apa tänaka	Emprosthotonos: A tetanic spasm in which the head and feet are drawn forward and the spine arches backward
Hanu graha	Lock jaw
Hanu stambha	Lock jaw
Gŗdhrasi	Sciatica: A sharp or burning pain that radiates from the lower back or hip, possibly following the path of the sciatic nerve to the foot
Aksepaka	Convulsions: Frequent spasmodic contractions of all the muscles in the body

The *Ayurvedic* text also includes formulations made up of a number of plants which can be used for the treatment of these diseases. A thorough analysis of the plants discussed in the *Ayurvedic* text revealed 325 plants mentioned in the 46 formulations used to treat the six diseases. These plants were ranked based on their utility to treat more than one disease and the frequency of their mention in the formulations. Out of the 325 plants, 14 plants belonging to 12 different families were selected based on their ranking to be studied further (**Table 2-3**). The phytochemicals of these 14 plants were further tested using docking studies.

Table 2-3. List of the 14 *Ayurvedic* plants selected based on their treatment of botulism like diseases mentioned in the *Ayurvedic* literature.

No	Plant Name	Family	Formulatios	Disease	Reference
1	*Acorus calamus* Linn.	Acoraceae	16	5	[41]
2	*Foeniculum vulgare* Mill.	Apiaceae	12	5	[42]
3	*Coriandrum sativum* Linn.	Apiaceae	7	3	[43]
4	*Pluchea lanceolata* Oliver and Hiern.	Compositae	27	6	[44]
5	*Argyreia speciosa* Linn. f.Sweet	Convolvulaceae	5	3	[45]
6	*Ricinus communis* Linn.	Euphorbiaceae	17	5	[46]
7	*Clerodendrum serratum* Moon.	Lamiaceae	6	4	[47]
8	*Phaseolus mungo* Linn.(vigna mungo)	Leguminosae	10	4	[48]
9	*Sida cordifolia* Linn.	Malvaceae	19	5	[49]
10	*Sida rhombifolia* Linn.	Malvaceae	2	2	[50]
11	*Cedrus deodara* Laud.	Pinaceae	12	4	[51]
12	*Piper chaba* Hunter.	Piperaceae	5	3	[52]
13	*Hordeum vulgare* Linn.	Poaceae	7	4	[53]
14	*Zingiber officinale* Rosc.	Zingiberaceae	23	5	[54]

2.2. Docking studies

Selection of crystal structures

An analysis of the crystal structures of BoNT/A in complex with various inhibitors was performed using a protein data bank (PDB). The search produced eighteen crystal structures containing proven BoNT/A inhibitors reported at the time of this analysis. Out of these 18, thirteen contained peptide inhibitors (PDB code: 3C88, 3C89, 3C8A, 3C8B, 3DS9, 3DSE, 3NF3, 3QW5, 3QW6, 3QW7, 3QW8, 3DDA and 3DDB) and 5 crystal structures contained small-molecule inhibitors (PDB code: 3QIY, 3QIZ, 3QJ0, 4HEV and 2ILP) [20, 23, 24, 30]. The crystal structures containing the five small-molecule and one peptide- inhibitor (PDB: 3C8B) were selected for their utilization in the docking studies. The structures of the six proven BoNT/A inhibitors from the selected crystal structures are included in the **Figure 2-8**.

Protein preparation and grid validation

All six selected ligand-BoNT/A complex crystal structures were prepared by the addition of hydrogen atoms and the removal of all the water molecules. Their grids were generated around a 12 Å radii from the centroid of the ligand and were used for docking studies in the virtual screening workflow (VSW) in the glide docking module. In order to test if water molecules can influence the docking results, a test docking run was performed using the grids with and without the water molecules. Although, water molecules were reported to facilitate in the hydrolysis of SNAP-25 [25], test docking results indicated no difference in the docking scores of the compounds docked in grids with or without water. Thus, all the water molecules were removed prior to docking.

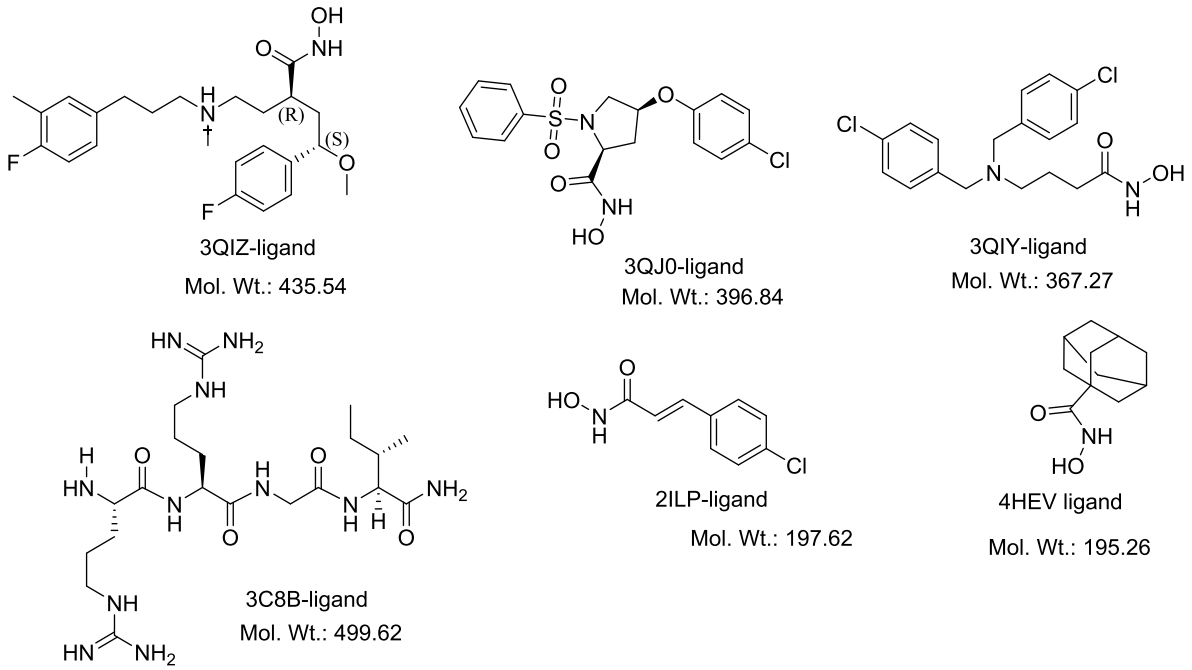

Figure 2-8. Structures of the ligands in the crystal structures selected for BoNT/A docking studies.

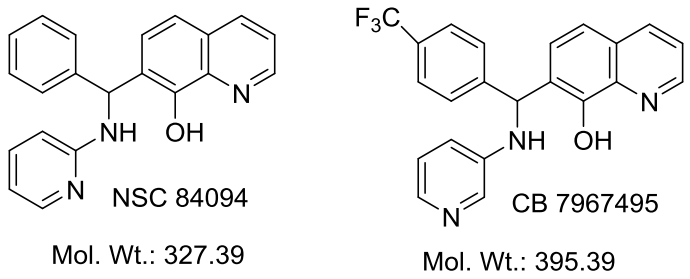

Figure 2-9. Structures of BoNT/A LC inhibitor positive controls used in *in vitro* and docking studies.

The grids were also tested by re-docking the native ligand to the grid and the RMSD of the output ligands were compared to the ligands' crystal structure conformations. Results showed an RMSD of <1 Å for the output ligands when compared to the native crystal structure conformation for all the small-molecule grids except for the protein ligand (due to its large, flexible structure). The prepared 570 ligands selected from the *Ayurveda* literature (section 3.1)

resulted in 835 structures (more than one stereoisomer for some ligands), which were then docked into the six grids using the VSW module. In addition to the phytochemicals, native ligands and known BoNT/A inhibitors were also included in the docking studies as positive controls.

Docking results and selection of compounds

Docking of the 570 compounds from Ayurvedic plants using Glide SP in the six BoNT/A grids generated 866 results. These 866 results (more than one conformer for each compound) contain 535 compounds, indicating that about 35 compounds were eliminated in the docking in the specified conditions. The docked ligands included two proven BoNT/A inhibitors, CB 7967495 and NSC 84094 [55] and the native BoNT/A crystal structure ligands (**Figures 2-8**, **9**). The docking scores of the docked compounds ranged from -11.2432 to +0.7210 kcal/mol. A compound with a more negative docking score represents more favorable binding at the binding site, hence a more negative score is desirable for a compound to act as an inhibitor. The native ligands of the crystal structures and their conformers showed good docking scores ranging from -11.074 to -7.50 kcal/mol.

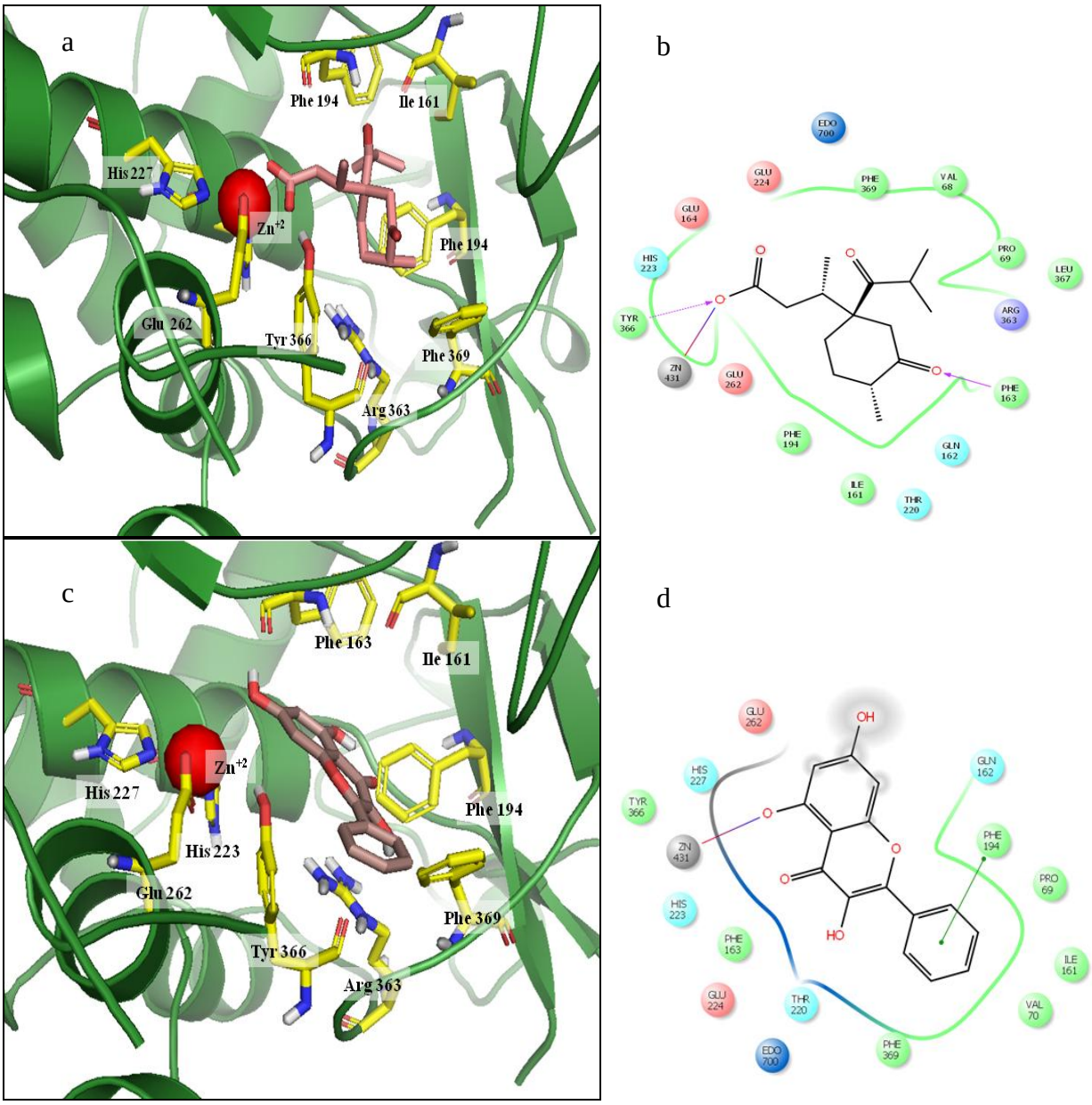

Figure 2-10. The binding poses and ligand-interaction diagrams of the two hit compounds selected from virtual screening in the BoNT/A active site of PDB 3QJ0.

a, b) acoric acid **1** (color: pinkish-orange), c, d) galangin **3** (color: pinkish-black) in the catalytic domain of the BoNT/A LC showing that both interact with Zn^{+2}. The other key residues in the catalytic site are shown as sticks in yellow.

The docking scores of the conformers of positive controls, CB 7967495 and NSC 84094,

ranged from -8.5490 to -6.51 kcal/mol. The first 250 results in the docking output include 170 compounds and show docking scores ranging from -11.2432 to -7.11989 kcal/mol (**SI table 1**). Among these, acoric acid **1**, chlorogenic acid **2**, galangin **3** and quercetin **4** possessed docking scores of -9.089, -11.094, -7.187 and -7.603 kcal/mol, respectively, and were selected for further testing *in vitro*. The ligand-interaction diagrams of these compounds showed that the carboxylic acid group of acoric acid **1** and the hydroxyl group of galangin **3** coordinate with the zinc ion in the catalytic site and also interact with other residues such as Tyr366, Phe163, Ile161, Pro69, Asp370, and Arg363 in the hydrophobic pocket around the S1′ region of the catalytic site (**Figure 2-10**).

Based on structural similarity, twenty-seven other compounds were selected and tested for their BoNT/A inhibitor activities using an HPLC-based protease assay. These compounds include seven isoflavonoids (**5** to **9**), six kavalactones (**10** to **15)**, two capsaicin derivatives (**16**, **17**), three coumarin derivatives (**18** to **20**), three gingerols (**22** to **24**), and one compound of each type such as curcumin **21**, epigallocatechingalelate (EGCG) **25**, (Z)-5-benzylidenethiazolidine-2,4-dione **26**, chicoric acid **27**, piperine **28**, pterostilbene **29**, bilobalide **30,** and ginkgolide C **31**. Capsaicin **16** was previously identified by Thyagarajan *et al* as a potential inhibitor of BoNT/A [56, 57]. Chicoric acid **27** [34] and chlorogenic acid **2** [35] were previously studied by Janda *et al.*, and were found to act as *exo*-site inhibitors of BoNT/A. Chlorogenic acid **2** was included since it was one of the docking hits and chicoric acid **27** was included to test its activity on the catalytic site. **Figure 2-11** shows the structures of all the compounds tested using *in vitro* HPLC/UPLC based bioassay.

2.3. *In vitro* studies utilizing SNAP-25 substrate

In vitro assays were performed using the isolated LC of BoNT/A and a 17-residue substrate peptide consisting of residues 187–203 of SNAP-25, which is the minimum length of SNAP25 required for light chain protease activity. The sequence of the substrate peptide is (*N*(α)-acetyl)-SNKTRIDEANQRATKML-(carboxamide), corresponding to residues 197 and 198 of SNAP-25 [58]. LC cleaves this substrate peptide between residues 11 (glutamine, Q) and 12 (arginine, R). The peak areas of the corresponding *N*-terminal and *C*-terminal cleaved peptides were measured using liquid chromatography, and test compounds were compared to that of the blank (treated only with BoNT/A). All the compounds were tested at 20 µM, and the results were reported as % inhibition compared to the blank.

In vitro bioassay results

Twenty-two compounds (**Table 2-4**) were first analyzed using HPLC, whereas nine compounds were tested using UPLC (**Table 2-5**) [59]. UPLC method was utilized since the HPLC method has several issues like long run times (~ 50 min for 1 sample), non-reproducible activities of the blank and test sample, affecting the stability of the toxin. Hence, a UPLC method was applied mainly to reduce the run times and to make it ideal for large set of compounds. The results of the HPLC BoNT/A protease activity bioassay are presented in **Tables 2-4** and **2-5.** Compounds CB 7967495 and NSC 84094 were used as positive controls [55] and showed 92% and 91% inhibition, respectively at 20 µM in the HPLC assay, whereas the activities of the same were lower 86 and 87% in UPLC runs.

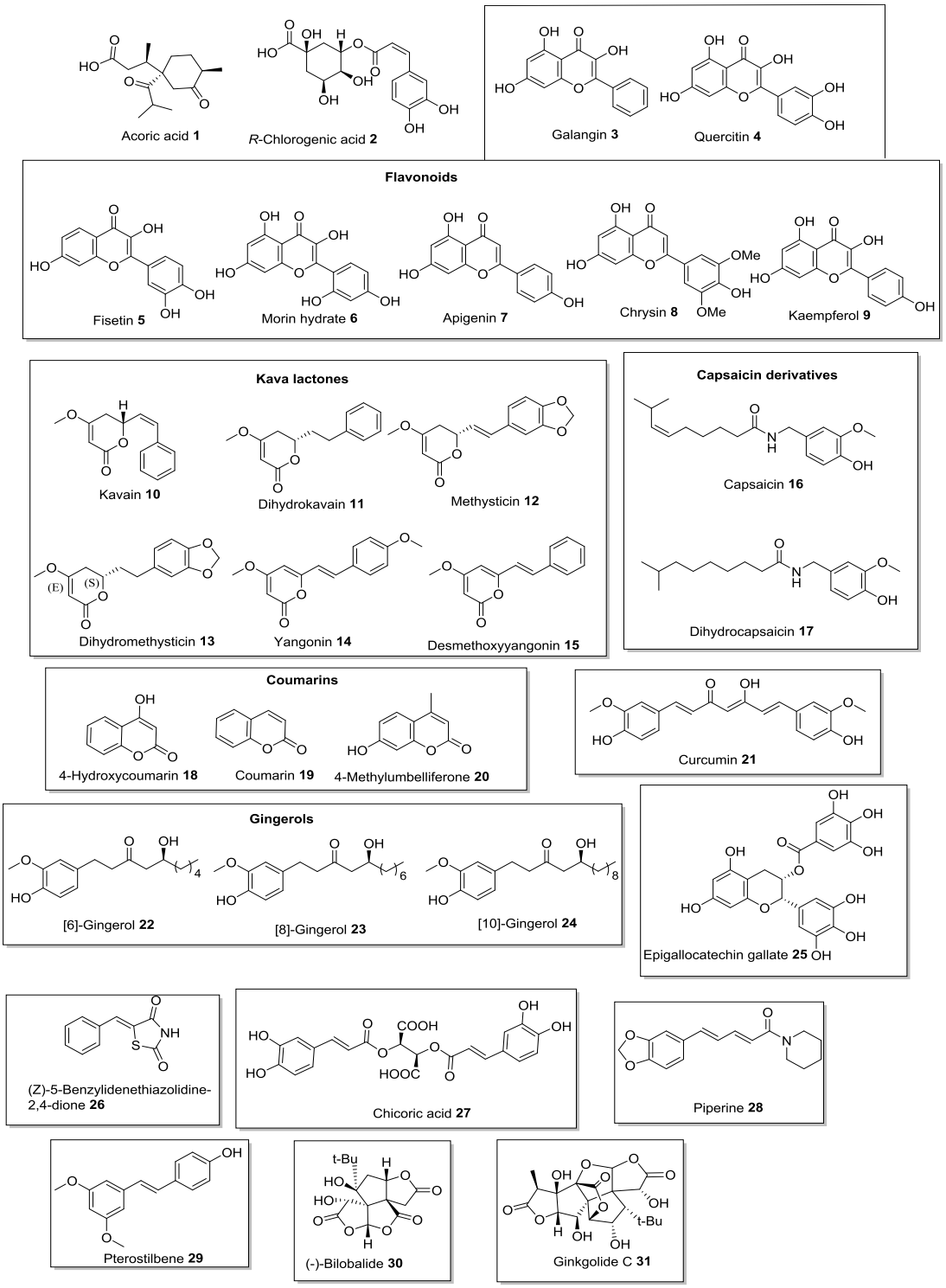

Figure 2-11. Structures of the compounds tested using HPLC-BoNT/A LC protease assay.

Testing the four hit compounds selected from virtual screening revealed acoric acid **1**, as the most active of the compounds exhibiting an inhibition of 47 ± 7% at 20 µM, followed by galangin **3** which showed 43 ± 8% inhibition. Among the five other isoflavonoid derivatives, fisetin **5** was found to be the most active, possessing inhibition of 59 ± 0.5%. Kavain **10** was the most active compound among the six kava lactones, showing 53 ± 13% inhibition, with a significant standard deviation between the results and among the three coumarins derivatives (**18** to **19**). 4-hydroxy coumarins **18** showed superior inhibition of 41 ± 8% compared to coumarin **19** and 4-methylumbelliferone **20**, with 25 ± 11 and 16 ± 1% inhibitions, respectively.

None of the three gingerols **22**–**24** were good inhibitors possessing % inhibitions ranging from 17 to 20%. Among the two capsaicin derivatives **16** and **17**, capsaicin **16** showed 38 ± 7 %. Curcumin **21** showed inhibition of 49 ± 4%. Among the seven ungrouped compounds **25-31**, none of them showed good inhibition: epigallocatechin gallate (EGCG) **25** (4 ± 1.1%), (Z)-5-benzylidenethiazolidine-2,4-dione **26 (**13 ± 1%), chicoric acid **27 (**6 ± 1.4%), piperine **28** (21 ± 1.5), pterostilbene **29** (16 ± 1.5), bilobalide **30** (13 ± 2.0%), and ginkgolide C **31** (2 ± 0). The known exosite inhibitors chlorogenic acid **2** and chicoric acid **27** also showed low inhibition (15 ± 3.0%), and 6 ± 1.4%), respectively, indicating that these compounds are not active in the catalytic site which validates the reported exosite binding of these compounds.

From the HPLC/UPLC bioassay results, seven compounds **1**, **3**, **5**, **10**, **16**, **18**, and **21** showed good inhibitions and were tested further using mouse phrenic nerve hemidiaphragm assay (MPNHDA) *ex vivo* assay (**Table 2-6**). The mouse phrenic nerve hemidiaphragm contains the myoneuronal junction that is the target of botulinum intoxication. Hence, it best replicates the *in vivo* system and can be used as an *ex vivo* method for testing BoNT/A inhibitors.

Table 2-4. HPLC-bioassay results and docking scores of the twenty-two compounds tested for BoNT/A LC protease inhibition.

Number	Compound	% Inhibition (20 µM)	Glide Docking Score
1	Acoric acid	47 ± 7	-9.089
3	Galangin	43 ± 8	-7.187
4	Quercitin	20 ± 2	-7.603
5	Fisetin	59 ± 0.5	-7.061
6	Morin hydrate	11 ± 1	-6.935
7	Apigenin	38 ± 6	-7.969
8	Chrysin	26 ± 2	-7.984
9	kaempferol	30 ± 1.5	-8.663
10	kavain	53 ± 13	-6.536
11	Dihydrokavain	23 ± 1	-6.614
12	Methysticin	12 ± 1.5	-6.614
13	Dihydromethysticin	19 ± 1.5	-6.588
14	Yangonin	27 ± 1	-5.996
15	Desmethoxyyangonin	24 ± 2	-6.16
18	4-Hydroxycoumarin	41 ± 8	-6.448
19	Coumarin	25 ± 11	-6.328
20	4-Methylumbelliferone	16 ± 1	-6.737
21	Curcumin	49 ± 4	-6.328
22	[6]-Gingerol	20 ± 2	-5.049
23	[8]-Gingerol	17 ± 2	-5.77
24	[10]-Gingerol	18 ± 2.5	-6.639
26	(Z)-5-Benzylidenethiazolidine-2,4-dione	13 ± 1	-8.302
	CB79674951	91 ± 1.3	-7.75
	NSC 84094	92 ± 0	-8.549

Table 2-5. BoNT/A LC inhibition and docking scores of the nine compounds tested using UPLC.

Number	Compound	% Inhibition (20 µM)	Glide Docking Score
2	Chlorogenic acid	15 ± 3.0	-11.094
16	Capsaicin*	38 ± 7.2	-7.983
17	Dihydrocapsaicin*	30 ± 4.8	-6.931
25	Epigallocatechin gallate (EGCG)*	4 ± 1.1	-9.431
27	Chicoric acid*	6 ± 1.4	-10.83
28	Piperine*	21 ± 1.5	-6.411
29	Pterostilbene	16 ± 1.5	-7.251
30	Bilobalide*	13 ± 2.0	-6.954
31	Ginkgolide C*	2 ± 0.8	-6.147
	CB79674951	86 ± 1.3	-7.75
	NSC 84094	87 ± 1.5	-8.549

2.4. Ex vivo assay

The MPNHDA uses a small amount of BoNT/A LC, it can be done in a non-CDC registered laboratory. It can test small molecules, peptides, and antibodies for efficacy. Its drawbacks are: it is technically difficult as takes about 6 months to 1 year to be proficient. It can test only one inhibitor per day at three concentrations. The hemidiaphragm can only run about 5 hours and the tissues become exhausted. It cannot detect subtle toxicity as well as cell culture. Small molecules require DMSO. Too much DMSO will stop intoxication of the nerve.

Figures 2-12 and **2-13** show the MPNHDA results of the seven tested compounds. Curcumin **21** was not protective against BoNT/A at 20 µM and so was not tested at any lower concentrations. Fisetin **5** was found to be marginally protective against BoNT/A at 20 µM. On retest, it was found to not be protective at 20 µM or at 2 µM against BoNT/A. 4-Hydroxy coumarin **18** showed marginal partial protection against BoNT/A at 20 µM but no protection at 2 µM. The retest of 4-hydroxy coumarin **18** indicated it was not effective against BoNT/A at either

concentrations.

Kavain **10** was tested in two individuals assays at 20 µM, little protection observed.. However, in these runs the toxin was not very “hot”, and also, it was not run out to 210-270 minutes.

Acoric acid **1**, which showed good binding poses and docking scores in the docking studies, and an *in vitro* inhibition of 47 $\pm$ 7 (**Table 2-4)**, was tested *ex vivo* in two iterations, each at 20 µM. This compound might be partially protective, but it would have to be retested to confirm this activity in different concentrarions and also using other relevant assays. Galangin **3** was found to be toxic at 20 µM. The tissues receiving the galangin **3** dropped the twitch tension faster than the toxin controls. Capsaicin **16** was found to be non-protective against BoNT/A at 20 µM and so was not tested at the lower concentrations.

Table 2-6. Results of selected seven compounds tested using MPNHA.

Compound	Concentration	Protection against BoNT/A	Notes
Acoric acid 1	20 μM	2 assays marginal protection	Note: To be retested to confirm its activity
Galangin 3	20 μM	Toxic at 20 μM	Note: The graph shows the tissues receiving the galangin dropped twitch tension faster than the toxin controls
Fisetin 5	Trial 1: 20 μM Trial 2: 20 μM and 2 μM	Trial 1: Marginal protection at 20 μM Trial 2: Not protective protective in the second trial	
Kavain 10	20 μM	2 assays at 20 μM, but neither were active	Note: Toxin was not very "hot" in this run, and it was not run up to to 210-270 minutes but there was little protection observed
Capsaicin 16	20 μM	non-protective	
4-Hydroxy coumarin 18	20 μM and 2 μM	20 μM:, marginal/partial protection 2 μM: No protection	
Curcumin 21	20 μM	Not protective	

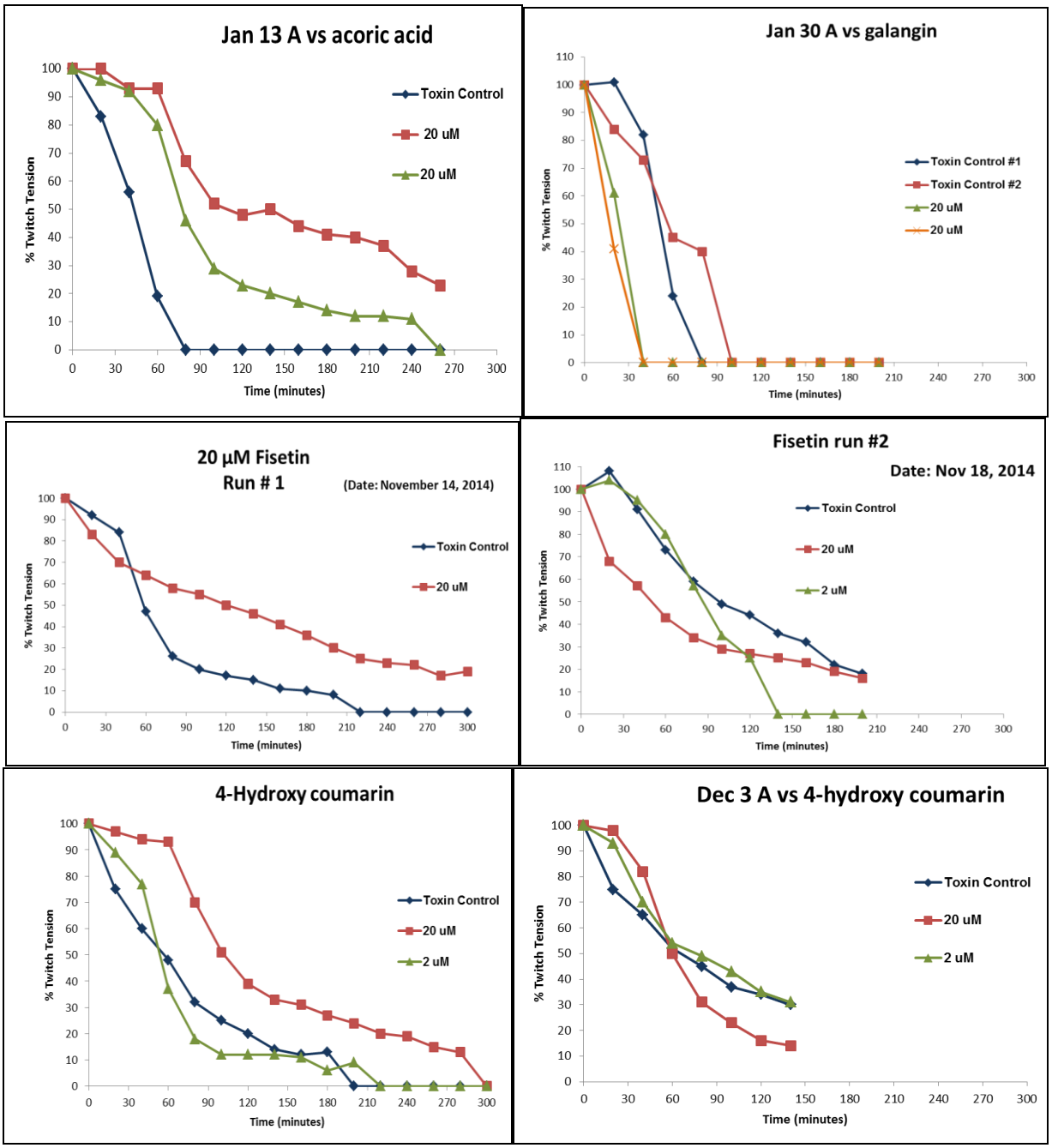

Figure 2-12. MPNHDA activities of acoric acid **1**, galangin **3,** fisetin **5**, and 4-hydroxycoumarin **18**. The percent twitch tension is measured vs time. At 20 µM Acoric acid **3** showed marginal activity, whereas galangin **4** was found to exacerbate then to BoNT/A activity.

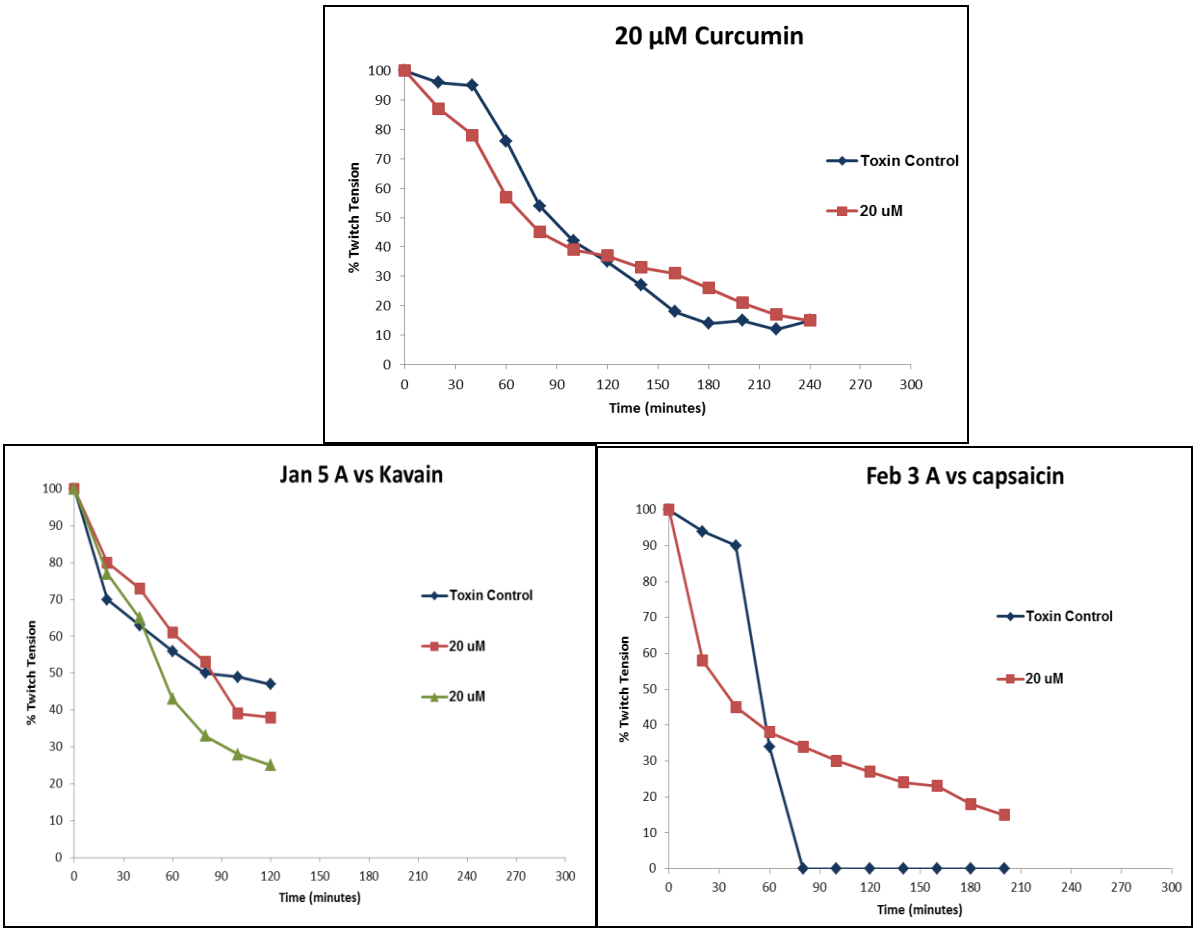

Figure 2-13. BoNT/A inhibition activities of curcumin **21**, kavain **10,** capsaicin **16** tested against LC of BoNT/A using MPNHDA.

2.5. Conclusions

Botulinum neurotoxin acts like a double edge-sword. On one side, it is a possible-bioterror threat, and on the other side, it is increasingly used for cosmetic purposes and against neurological disorders [60]. Hence, the identification of novel small molecule inhibitors of BoNT serotype A is of great significance. A number of small molecules were found to be active against the BoNT/A protease enzyme which include the zinc-binding hydroxamic acid derivatives [31]

and natural products like chicoric acid and chlorogenic acid [61] on the *exo*-sites α/β [18]. However, none of the reported compounds reached the market as drugs or to the clinical trial stage [62, 63]. In a novel approach, combining *Ayurvedic* literature, computer-based drug screening, and *in vitro* HPLC-based testing was used to identify the activities of natural products against BoNT/A.

Analysis of the *Ayurvedic* literature resulted in the identification of plants which could possess BoNT inhibition activities. The phytochemicals of the selected plants were screened using *in silico* docking in the BoNT/A inhibitor crystal structures (**SI table 2**). Based on the docking results, thirty-one compounds were tested using *in vitro* HPLC/UPLC based assay. The results indicated seven compounds showing BoNT/A inhibition of around 45-60% including acoric acid and some flavonoids (**Tables 2-4** and **2-5**). These seven compounds were evaluated further in an *ex vivo* methods such as mouse phrenic nerve-hemidiaphragm assay (MPNHDA) [55].

Based on the bioassay results, acoric acid **1**, a novel scaffold which was isolated from *Acorus calamus*, was also found to show promising activity (~50% inhibition) *in vitro* and partial protection in MPNHDA. Further confirmatory testing of these compounds using *in vivo* or *ex vivo* models could evaluate their utility as BoNT/A inhibitors. Acoric acid **1** possesses three arms similar to the reported hydroxamic acid derivativies [20] and also possesses chelating ability with zinc metal. These functional points, like the carbonyl group on the cyclohexane and isobutyryl side chain, could be explored further for structural modifications to allow them to take advantage of the unexplored region in the binding site (**Figure 2-14**). These modifications may increase the inhibitory activity and potency of acoric acid **1**.

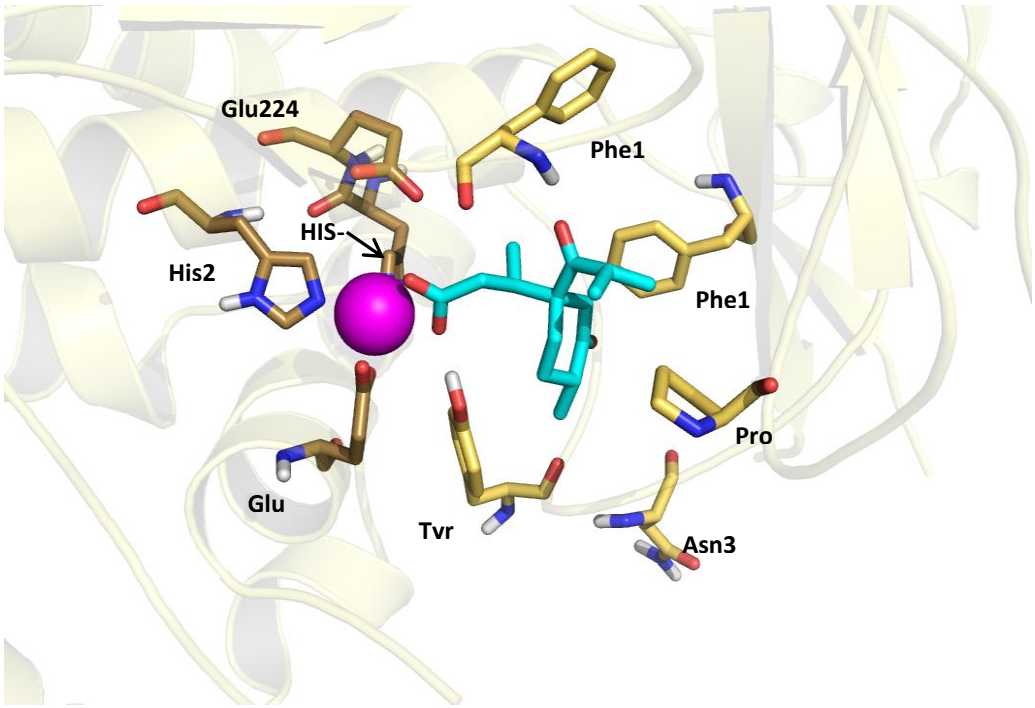

Figure 2-14. Structure of acoric acid **1** in the ligand binding domain of BoNT/A.

3. Experimental

3.1. Virtual screening for identification of BoNT/A inhibitors

System specifications

To perform virtual screening studies, a commercial version of the Schrödinger software package [64] was installed on a Windows desktop computer with Intel® Core™ Quad CUP Q6600@2.40GHz 2.40 GHz processor with a random access memory (RAM) of 4.00 GB and 32-bit operating system.

Protein Preparation and alignment of binding sites

The Protein Data Bank (PDB) structures of six BoNT/A crystal structures were downloaded (PDB codes: 3QIY, 3QIZ, 3QJ0, 4HEV, 2ILP and 3C8B) and prepared using the Protein Preparation Wizard (PPW) module of Schrödinger suite to remove errors in the

structures from the crystallographic data by adding hydrogen atoms and correcting their bond orders. The prepared proteins were minimized with Optimized Potentials for Liquid Simulations (OPLS)-2005 force field (FF) at an intermediate docking stage, and all the water molecules without contact and 5 Å or more away from the protein residues were removed. All the prepared proteins were aligned at the binding site.

Virtual screening of ligands from Ayurvedic literature

Using *Ayurvedic* literature, a total of 356 plants were identified as potential plants for treating the symptoms of botulism, and among these, 14 plants were shortlisted based on their frequency of usage in various formulations and the number of diseases they treat. To generate a structural database of the reported phytochemicals of these 14 plants, Duke's database, PubChem, SciFinderDictionary of Natural Products [65] and various online sources were searched, and their exact structures, including stereochemistry, were drawn. Chem3D (Perkin Elmer) was used to convert these structures into 3D, and Maestro [64] was used to label each compound individually and save the files in structural-data file (.sdf) format. The database from these 14 plants consisted of 570 compounds. These compounds were prepared using the Ligprep module with Epik to generate metal binding sites at pH 7.4, to include metal binding states, and to include only one stereoisomer per ligand. The binding sites of all the six selected crystal structures were overlaid to align their binding sites. For each crystal structure, grids were generated using Glide with an area of 12 Å around the native ligand and with no constraints. The prepared ligands were then docked with the Virtual Screening Workflow (VSW) option in Maestro (Schrödinger, LLC) using all the six prepared grids and using Glide standard precision (SP) with settings to generate docking results for all the compounds. The poses from the docking results were analyzed on Maestro and PyMol softwares [64].

3.2. *In vitro* studies

Experimental material

Recombinant botulinum neurotoxin type A light chain (BoNT/A LC) was prepared according to procedures previously described [66]. The substrate for the HPLC-based enzymatic assay was a 17-mer peptide consisting of residues 187 to 203 of SNAP-25 (Ac-SNKTRIDEANQRATKML-NH_2). It was custom synthesized to 98.0% purity by GenScript (Piscataway, NJ). The HPLC system consisted of Waters model 6000A pumps, U6K injector, 680 automated gradient controller, 996 PDA and Empower 2 software (Waters Corp., Milford, MA, USA). The UPLC system consisted of Waters Aquity with PDA detector. The HPLC column (Zorbax 300SB-C18, 4.6 x 150 mm) was obtained from Agilent Technologies (Santa Clara, CA) while the UPLC column (Acquity UPLC BEH C18 (2.1 x 50 mm column) was obtained from Waters Technologies (Waters, Bedford, MA).

HPLC-based BoNT/A LC protease assay

Compounds were tested in an HPLC-based BoNT/A LC enzymatic assay as previously described [67]. The assay mixture contained 50 mM HEPES pH 7.3 buffer, test compound dissolved in dimethyl sulfoxide (DMSO) at the final assay concentration (20 μM), 0.8 mM 17-mer SNAP-25, and 3.0 to 6.0 μg/ml (60 to 120 nM) BoNT/A LC. In negative control samples, the test compound was replaced by DMSO. Upon addition of the LC, the reaction mixture was briefly vortexed and incubated at 37°C for 5 min. Reactions were stopped by acidification with 90 μL of 0.7% trifluoroacetic acid (TFA). Uncleaved substrate and products were separated by reverse-phase HPLC. Solvent A was 100% water/0.1% TFA and solvent B was 70% acetonitrile/0.1% TFA. The flow rate was 1.0 ml/min. at 25°C with a gradient profile of 10% B

(2.5 min.), linear gradient to 36% B (21 min.), and 100% B (6 min.). Amounts of intact and cleaved substrate were quantified and used to calculate LC activity (μM/min/mg). Percent inhibition was determined by comparing the LC activity in control and test samples**.**

In vitro UPLC analysis

UPLC method [59] was applied to improve the sensitivity of the bioassay and reduce the run times and to make it ideal for large set of test compounds. A number of compounds were tested using UPLC method and are reported in the **Table 2-4**. The BoNT/A reaction was performed same as in the HPLC method. However, the reaction mixture was analyzed using UPLC loaded with Aquity UPLC BEH C18 column, under the similar solvent conditions as that of the HPLC method. Unlike the reported method, no bovine serum albumin was included in the reaction mixture as reported in the literature [59].

3.4 *Ex vivo* assay (MPNHDA)

The mouse phrenic nerve hemidiaphragm assay (MPNHDA) was conducted by our collaborators at the US Army Medical Research Institute for Infectious Diseases USAMRIID, similar to the reported on the procedure [32]. "Female CD-1 mice (20 to 25 g) were euthanized with CO_2, and their diaphragms with attached phrenic nerves were removed. The diaphragms were then divided into two hemidiaphragms, with each section complete with a phrenic nerve and myoneural junction. Each hemidiaphragm was attached to an isometric force transducer (Fohr Medical Instruments, Seeheim, Germany), and its phrenic nerve was secured to a stimulating electrode. The nerve-muscle preparations were immersed in separate 10-ml tissue baths containing Tyrode's buffer (1.8 μM $CaCl_2$, 1 mM $MgCl_2$, 2.7 mM KCl, 137 mM NaCl, 0.4

mM NaH_2PO_4, 12 mM $NaHCO_3$, and 6 mM glucose), pH 7.2 to 7.4 (Sigma, St. Louis, MO). A mixture of 95% O_2-5% CO_2 gas was passed through the Tyrode's buffer. The tissue baths were kept at 37°C. Each phrenic nerve was stimulated with single supramaximal pulses (SD9 Stimulators Grass Instruments, Warwick, RI) through a Powerlab/4sp and Bridge Amp relay (AD Instruments, Inc., Colorado Springs, CO) with a 0.3-ms duration at 0.03 Hz. The twitch tensions were digitally recorded by Chart software (AD Instruments, Inc., Colorado Springs, CO). After acclimation to the tissue baths, the tissue preparations were run for 20 to 30 min for baseline measurements. The inhibitor (dissolved in DMSO at 2x the final assay concentration) was mixed with 60 pM BoNT/A (Metabiologics, Madison, WI) in 5 ml of Tyrode's buffer and incubated for 15 to 20 min at 37°C. After baseline stabilization, the toxin-inhibitor mixture was added to a 10-ml bath with an additional 5 ml of Tyrode's buffer, bringing the final concentration of BoNT/A toxin to 30 pM. The concentration of BoNT/A neurotoxin was previously calibrated to induce a 50% loss of twitch tension in approximately 60 min. In all samples, including the controls, the final concentration of DMSO was 0.3%.

For each experiment, four tissue baths were used. One bath was the BoNT/A toxin-only control. A second bath was an assay control with toxin or inhibitor. The third and fourth baths contained toxin plus two different concentrations of inhibitor. Adding the toxin or the toxin/inhibitor mixture to the bath initiated the beginning of data collection, which continued for 5 h or until muscle twitch tension ceased. For all preparations, neurotoxin-induced paralysis was measured as a 50% loss of twitch tension evoked by nerve stimulation.

Procedures used to obtain mouse tissues were conducted in compliance with the Animal Welfare Act and other federal statutes and regulations relating to animals and experiments involving animals and adhered to the principles stated in the Guide for the Care and Use of

Laboratory Animals, National Research Council, 1996. The facility where this research was conducted is fully accredited by the Association for Assessment and Accreditation of Laboratory Animal Care International" [32].

.

CHAPTER 3

STUDY OF *LYCIUM SPECIES* (GOJI) FOR ANTIDIABETIC COMPOUNDS

1. Introduction

1.1. Diabetes mellitus and metabolic syndrome

Type 2 diabetes mellitus (T2D), a complication resulting from insulin resistance, has reached epidemic proportions worldwide. According to world health organization (WHO) statistics, T2D accounts to about 90% of the total diabetic populations of 382 million, which was 8.3% of the total adult population in 2012-2013, and resulted in 1.5 to 5.5 million deaths worldwide [68]. There are approximately 1.4 million new cases of diabetes each year and if the current trends continue, these numbers are projected to increase to 1 in 3 by 2050 [69] (**Figure 3-1**). T2D patients are non-responsive to insulin, have impaired glucose and lipid metabolism and could be at high risk for developing complications, such as hypertension, dislipidemia, cardiovascular disease related death, heart attack, stroke, blindness, eye problems, kidney diseases and amputations. Metabolic syndrome is a series of highly interrelated disease conditions which include hypertension, obesity and elevated blood glucose levels. Among the people affected with metabolic syndrome, the chances of occurrence of T2D are found to be high. T2D and the risk factors associated with metabolic syndrome can be treated by targeting peroxisome-proliferator activated receptors (PPARs) [70].

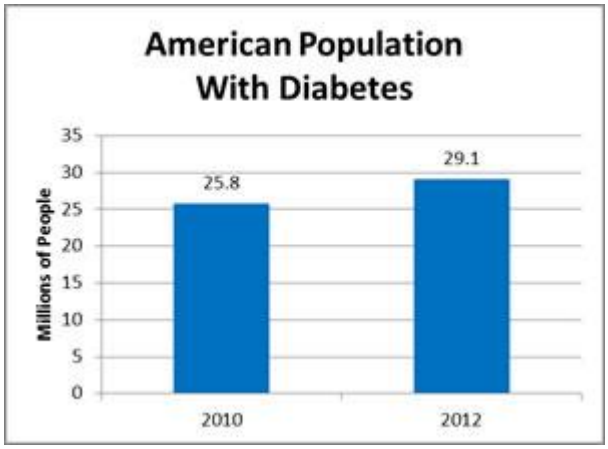

Figure 3-1. The raise in the population of Americans suffering from diabetes in 2010 (25.8 million) and 2012 (29.1 million) [69].

1.2. PPARγ role and importance

PPAR's are a family of nuclear transcription factors, expressed on various tissues and regulate key biological processes including glucose and lipid homeostasis. There are three PPAR subtypes: PPARα, PPARβ/δ and PPARγ, and these three receptors are considered as viable targets for treating metabolic syndrome [70] and diabetes [71].They exert their action in the nucleus by heterodimerization with retinoid X receptor (RXR), which are stabilized by co-repressors. Ligand binding to PPARs results in its activation by inducing changes in the receptor conformation which results in the recruitment of coactivators and removal of corepressors. The activated RXR-PPAR dimers then regulate the expression of genes in DNA by binding to the specific response elements in the promoter region of the DNA (**Figure 3-2**). PPARs have a role in the carbohydrate and lipid metabolism pathways by directly regulating their metabolism and transport, or by acting on the proliferation and differentiation of a number of cells including adipocytes [70].

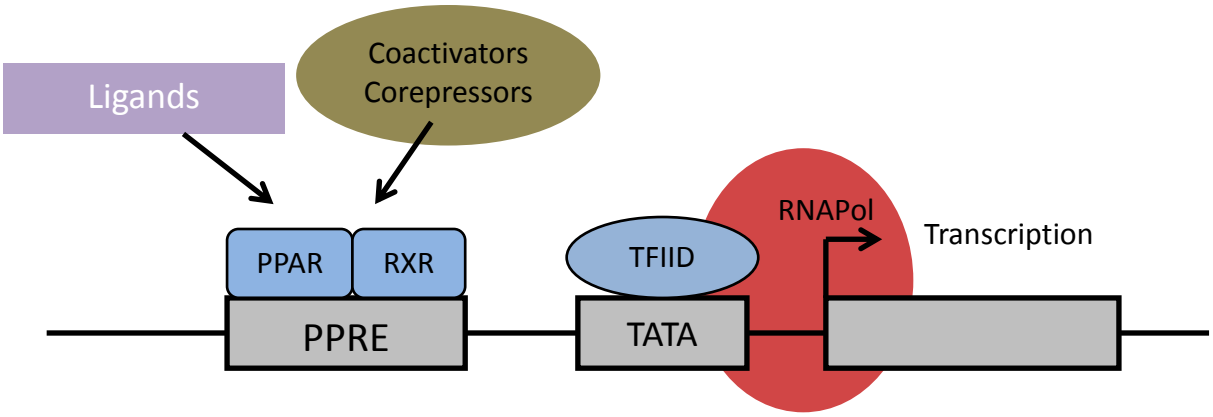

Figure 3-2. Mode of action of PPARs [70].

PPARα subtype is expressed mainly in the liver, adipose tissue, kidneys, heart, skeletal muscle and large intestine. Fibrates, a class of ampiphilic carboxylic acids, activate PPARα and are used for treating metabolic disorders mainly, hypercholesterolemia and are used as hypolipidemic or lipid-lowering agents. PPAR β/δ subtype is expressed in various tissues including the skin, gut, placenta, skeletal and heart muscles.

PPARγ is expressed mainly in adipose tissue (white and brown) and in significant amounts in intestines, kidneys, retina, immunologic system and trace amounts in muscles and is considered as a primary target for treating diabetes [72]. Hence, intense research efforts were put into identifying clinical agents targeting PPARγ [73]. Several ligands, both endogenous and synthetic agents act as PPAR ligands. The endogenous ligands targeting PPARγ include, fatty acids, oxidized lipids, prostaglandin J2 metabolites. Synthetic agents of PPARγ. include full- and partial-agonists. Phenyl acetic acids, tyrosine-based compounds, thiazolidine dione-class of compounds act as PPARγ full-agonists (**Figure 3-3**). Fmoc-*L*-leucine, FK-614, T2384 [74], INT-131 [75], MBX-102 [76], azadiole derivatives, 2-BABA-derivatives, GW0072 [77], L-764406[78], cercosporamide-derivative **VI** [79] act as PPARγ modulators or partial agonists [80]

(**Figure 3-4**).

Partial and full agonists

Thiazolidinediones (TZD) or glitazones are a class of insulin sensitizing pharmacological agents, targeting insulin resistance, and preserve β-cell function in the pancreatic islets. PPARγ agonists include TZDs like ciglitazone **I**, pioglitazone (Actos®) **II**, torglitazone (Rezulin®) **III**, rosiglitazone (Avandia®) **IV**, and a non-TZD compound, farglitazar **V** (**Figure 3-3**). Rosiglitazone **IV** and pioglitazone **II** are currently used for treating diabetes clinically. These agents are effective in improving insulin and glucose parameters, and increase whole-body insulin sensitivity [81]. Hence, they are termed insulin-sensitizing medications. They decrease hepatic glucose production and prolong pancreatic β-cell function by preventing apoptosis of β-cells [81].

Although, TZDs are effective in treating T2D, adverse events like weight-gain, edema, and anemia are seen among the patients and the treated populations have an increased risk for cardiovascular events and bone fracture [82]. In the TZD treated population, there is an increased risk for exacerbation of congestive heart failure, volume-overload, systemic edema due to fluid retention and subsequent increase in intravascular volume by approximately 15% [81]. Therefore, there is a high demand for the identification of new, safer antidiabetic agents which do not cause high fluid retention. Unlike full agonists like TZDs, which show side-effects, partial agonists or modulators of PPARγ are effective against insulin-resistance without the undesirable side-effects observed while using full agonists [79, 83]. Hence, finding new partial agonists of PPARγ could be a viable method for treating diabetes. Our aim is to identify novel natural product-based antidiabetic agents by targeting PPARγ and by screening the TCM-based anti-

diabetic plant, Goji, using *in silico*, *in vitro* and validate with *in vivo* models.

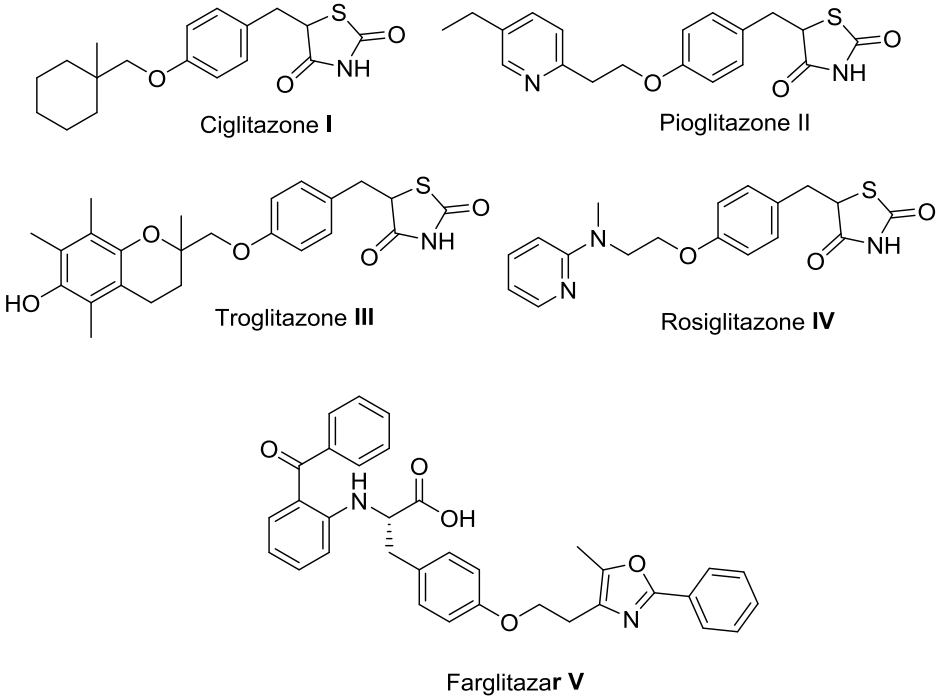

Figure 3-3. Structures of thiazolidinedione (TZD) class of compounds **I** to **IV** and farglitazar **V**, which act as PPARγ full agonists.

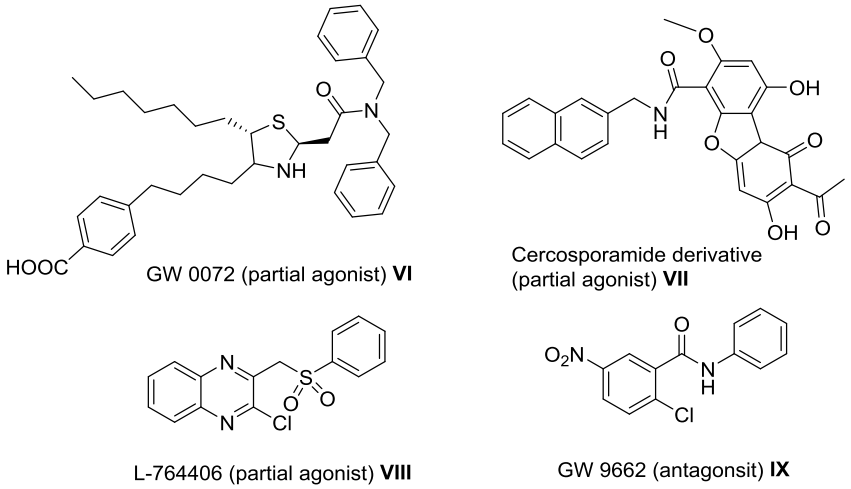

Figure 3-4. Structures of PPARγ- partial agonists: GW0072 **VI** [77], cercosporamide-derivative **VII** [79], L-764406 **VIII** [78] and antagonist GW 9662 **IX** [84].

Ligand-binding domain description and two binding modes:

The PPARγ receptor is a nuclear receptor which is comprised of four domains including 1) *N*-terminus and ligand-independent activating domain (AF1), 2) highly conserved DNA binding domain, 3) ligand-binding domain (LBD) and 4) ligand-independent domain (AF2). The structure of apo-PPARγ site along with co-activating factor SRC-1 was determined (PDB: 2PRG) [85]. The LBD is a T-shaped cavity with a total volume of 1,300 Å and is comprised of helices 3, 4, 6, 10, two β-sheets and helix 12, which belong to the AF2 domain. The binding site consists of two regions perpendicular to each other. The region between helix 3 and the β sheet (length 20 Å) is parallel to helix 3, while another region from β sheet to AF2 (length 16 Å) is perpendicular to the cavity behind helix 3 (**Figure 3-5**) [85]. It consists of an entry site which is comprised of hydrophobic amino acids, Asp243, Glu290, Arg288, Gln295. Depending on how these agents interact with the residues in the ligand binding domain, there are two binding modes of PPARγ agonists, full-agonist binding mode and partial-agonist binding mode.

Binding mode of full-agonists

The structure of rosiglitazone **IV** in the crystal structure of PPARγ (PDB 2PRG) is L-shaped, which wraps around helix 3 and occupies 40% of the ligand binding site. In general, glitazones or thiazolidinedione (TZD)-type PPARγ full agonist structures contain three subunits: an effector sub unit, a linker sub unit and a binder subunit [73].

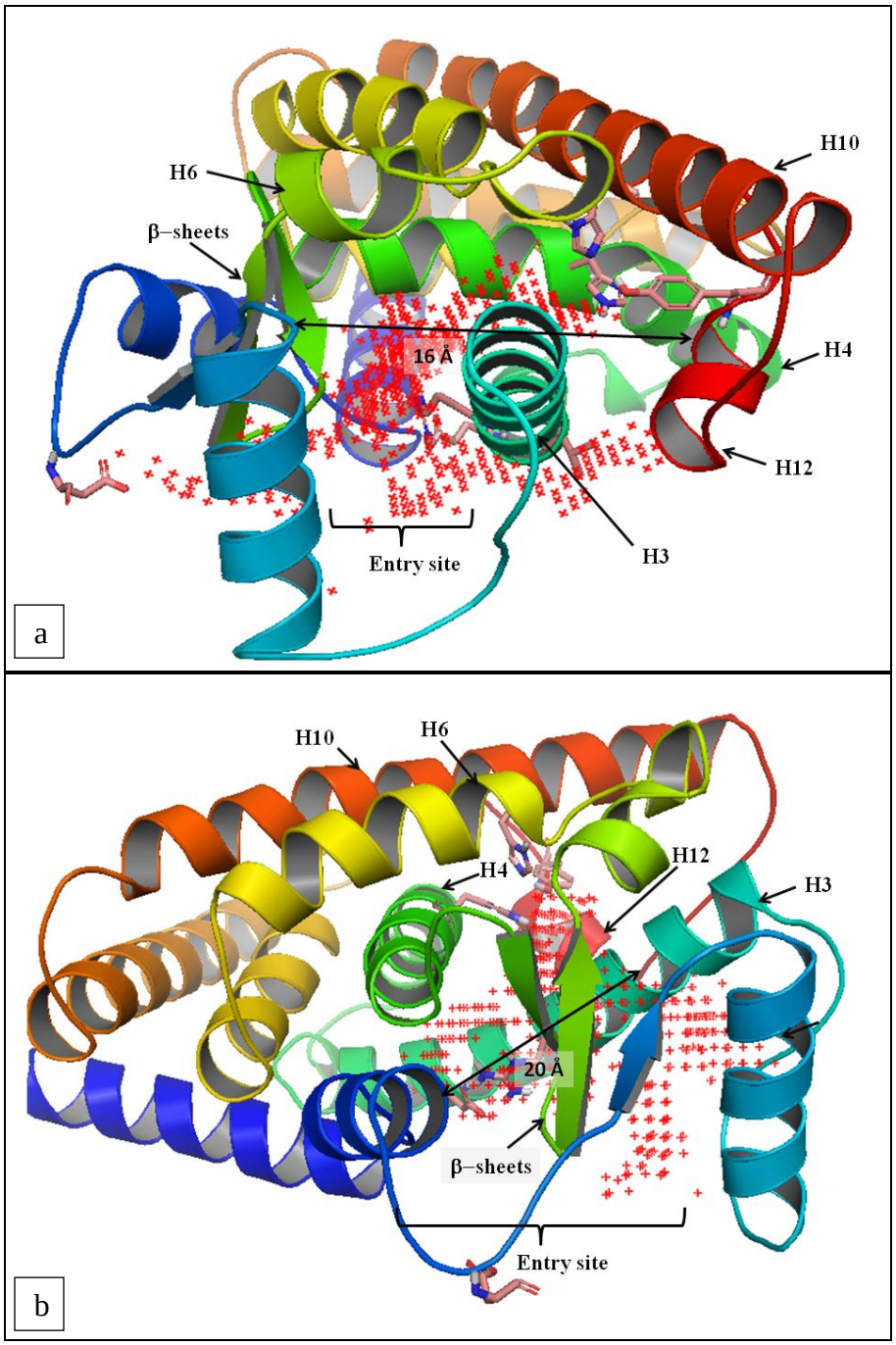

Figure 3-5. Structure of the ligand-binding domain of PPARγ.

The key helices in the ligand binding domain are labeled. The binding pocket is marked red. Figure b, is obtained by the rotation of figure a, along the z-axis.

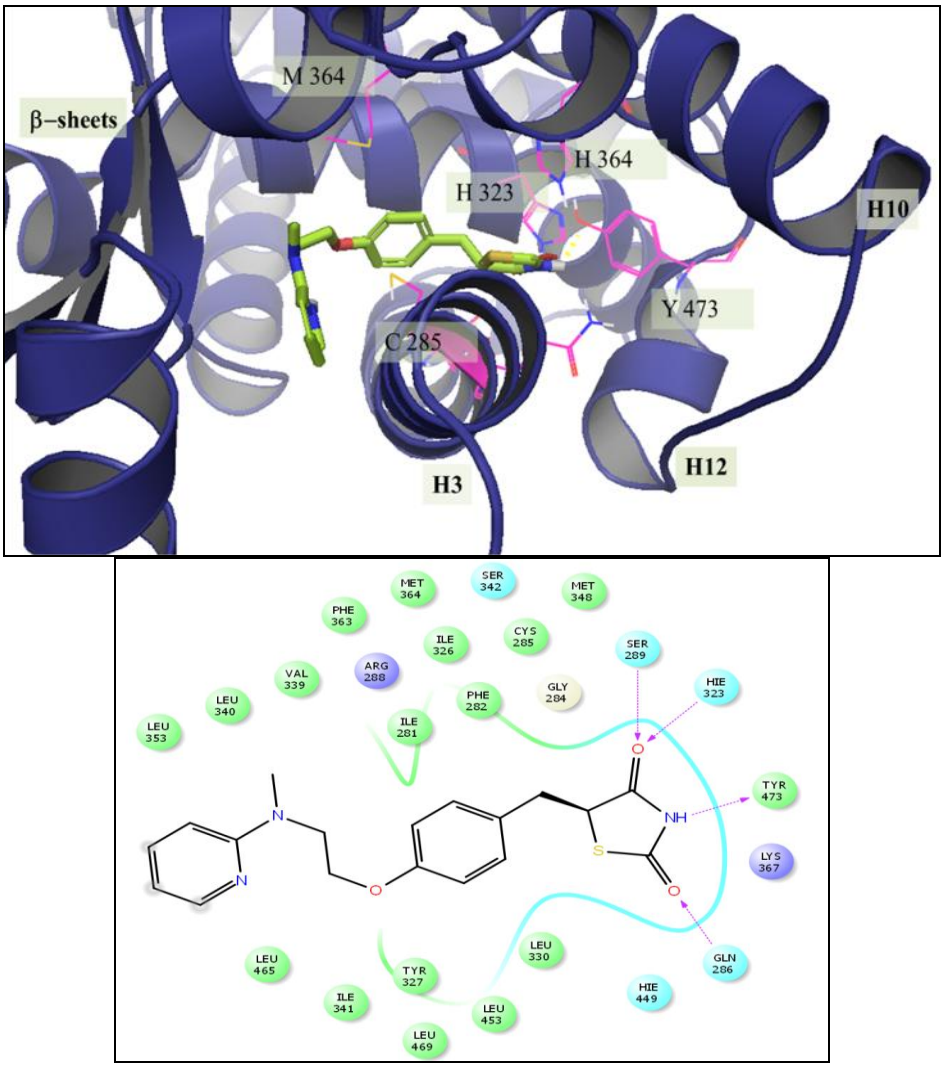

Figure 3-6. a) Binding mode of PPPARγ full-agonist, rosiglitazone **IV** (green) PDB: 2PRG; b) including its ligand-interaction diagram.

The binder subunit of rosiglitazone **IV** includes a thiazolidine (TZD) group which interacts with amino acids in the helices 3, 4, 10 and AF2. The TZD groups forms hydrogen-bonding interactions with Gln286, Ser289 on helix 3, His323 near helix 4, His449 of helix 10, and Tyr473 on helix 12 of AF2 (**Figure 3-6**). The linker is a central benzene ring, which lies behind helix 3 and forms hydrophobic interactions with residues Cys285 and Met364. The effector subunit, which is the core region, is made up of pyridine, interacts with the hydrophobic

site helix 3 and the β-sheet [73]. **Figure 3-6** shows the structures of thoazolidinedione (TZD) class of compounds.

Binding modes of partial agonists

Partial agonists or modulators of PPARγ are effective against insulin resistance without the undesirable side effects observed while using full agonists [79, 80] Hence, finding partial agonists of PPARγ could be a viable method for treating diabetes without the side-effects shown while using thiazodinedione (TZD) derivatives. Unlike full agonists, partial agonists do not interact with helix 12. PDB 3LMP [79] revealed that the cercosporamide-scaffold is located between helix 3 and β-sheet, and also makes water assisted interactions with Leu340, Ser342 consisting of helices 2, 5, β-strand-2 and helix 7 but does not interact with helix 12 (**Figures 3-7**, **3-8**).

1.3. Natural products as PPARγ agonists

Several natural products, like honokiol [86], amorfrutin 1 [87], amorfrutin B [88], amorphastilbol [89], saurufuran A [77] from *Saururus chinensis* (Saururaceae), flavonoids such as chrysin, apigenin and kaempferol, and phenolic compounds from *Glycyrrhiza uralensis* (Fabaceae) and *Glycyrrhiza glabra* [90] were found to possess PPARγ activity [91]. These natural products possessed different binding modes in the PPARγ binding pocket, compared to full agonist-binding modes, and were also found to activate PPARα or RXR and also improve the metabolic parameters with reduced side-effects compared to thiazolidinedione derivatives [91]. A careful study of more phytochemicals could result in the discovery of new anti-diabetic compounds from natural sources including traditional herbals.

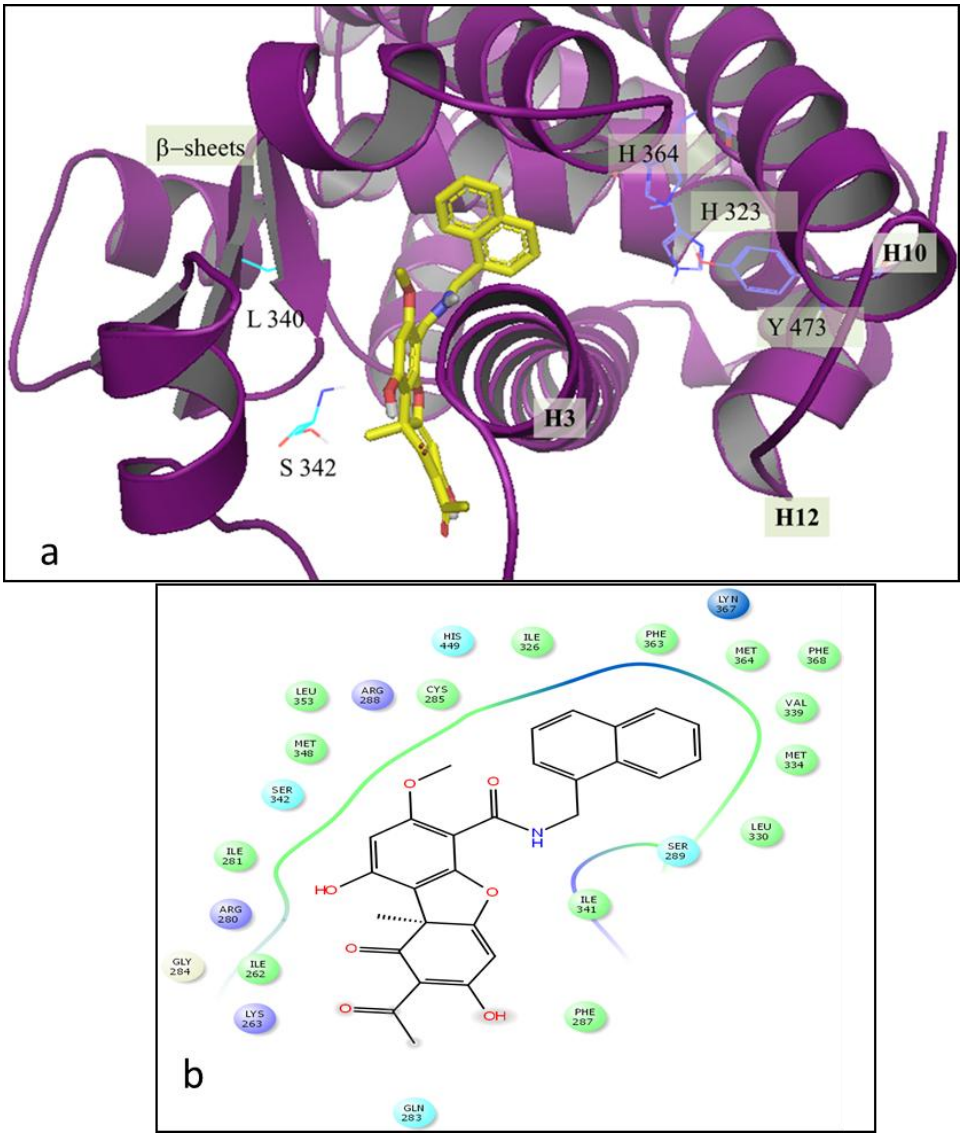

Figure 3-7. a) Binding mode of PPPARγ partial-agonist, cercosporamide-derivative **VII** (light green) PDB: 3LMP; b) including its ligand-interaction diagram.

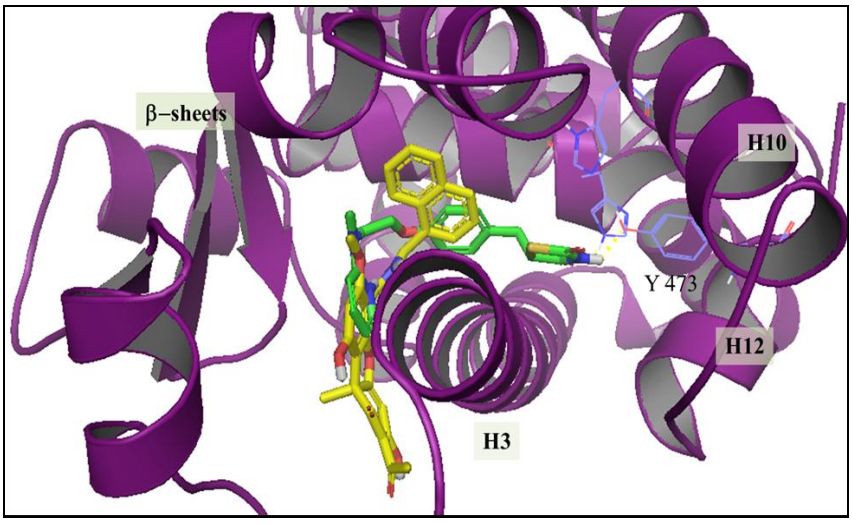

Figure 3-8. Overlap of the PPARγ-full and -partial agonists, rosiglitazone **IV** (green) and cercosporamide-derivative **VII** (light green) in 2PRG. They occupy binding sites in different binding regions.

1.4. TCM: Goji and diabetes

Natural products are important and promising sources for drug discovery. Several compounds isolated from plants used in Traditional Chinese Medicine (TCM) have been used and studied as drugs like artemisinin and paclitaxel. The root bark and fruits of two closely related medicinal plants from TCM, *Lycium barbarum* and *L. Chinense*, also known as gou qi zi or Goji, wolfberry, Chinese wolfberry, matrimony wine, have been traditionally used mainly in China, Vietnam, Korea and Japan [92]. Goji berry preparations, in the form of tinctures, powders or tablets, are used in TCM as mild *Yin*-enhancing agents, treating liver, kidneys and lungs, and are claimed to increase the longevity and reduce premature graying. The root barks of Goji are consumed as decoctions and used as cooling agents to 'clear heart' and lower consumptive fever due to *Yin* deficiency. Root barks are used in the treatment of night sweating, steaming bone sensation and chronic low grade fever, cough and against hemoptysis, hematuria, diabetes

mellitus and hypertension (**Figure 3-9**) [93].

Figure 3-9. Pictures of *L. barbarum* fruit [94].

Goji: Chemical constituents and their activities, TCM preparation

Because of the significance of Goji in traditional medicine, several investigations were performed on various parts of Goji, especially the fruit of *L. barbarum* and other parts of *L. chinense* like roots and leaves. The reported chemical constituents were reviewed in 2010 by Potterat [92]. The chemical constituents of *L. barbarum* and *L. chinense* include: carotenoids from the fruits and leaves, vitamin C precursors and glycolipids from the fruits, alkaloids and cyclopeptides from the roots, amides and other phenolic compounds from the fruits and roots of Goji. **Table 3-1** shows the different classes of chemical constituents of Goji classified based on

parts and species.

These chemical constituents were tested for activities including antioxidant, antitumor, immunomodulatory, radioprotective, antidiabetic activities and neoprotective effects [95, 96]. Proteoglycans also known as "*Lycium barbarum polysaccharides"* showed antioxidant properties and some interesting pharmacological activities in the context of age-related diseases such as atherosclerosis and diabetes [97].

Cortex Lycis Radicis (CLR) or Chinese wolfberry root bark or bark of box thorn root, which is the dried root bark of *L. barbarum* (Solanaceae family), is used to treat pneumonia, night sweats, cough, hematemesis, inflammation and diabetes mellitus [98]. The TLC analysis of CLR aqueous extracts, indicating the presence of organic acids, alkaloids, flavones, anthraquinones, polysaccharides, and saponins. These aqueous extracts of CLR were tested on Alloxan-induced diabetic mice and were shown to decrease glucose levels, increase insulin levels, and long-term hypoglycemic effects and reduced the body weight in diabetic mice [98]. *Lycii cortex radicis* (LCR) is also a traditional Chinese medication, made from the root barks of *L. chinense.* The methanolic extracts of LCR, LCR1 and LCR2 and tyramine derivatives, *tran*s-*N*-*p*-coumaroyl tyramine, *trans*-*N*-ferulolyl tyramine which were isolated from LCR were tested for hypocholestrolemic and antioxidant effects [99]. *Tran*s-*N*-feruloyl tyramine was found to possess an anti-oxidant effect by inhibiting liver microsomal HMG CoA reductase activity. Studies on LCR1 and LCR2, ginger, safflower seed using Sprague-Dawley male rats concluded that LCR possess hypocholestromeic activity.

Table 3-1. List of the chemical constituents isolated from the fruits, roots, leaves and flowers of *L. barbarum* and *L. chinense* [92].

	Class of compounds	**Examples**
Fruits of *L. barbarum*	Polysaccharides (23 %)	Termed as *Lycium barbarum* polysaccharides: Rha, Ara, Xyl, Man, Gluc, Gal in varied proportions
	Carotenoids	Zeaxanthin dipalmitate (56 % of the carotenoid content)
	Vitamins	Riboflavin, Thiamin, Ascorbic acid
	Flavonoids	Aglycone portions: Myricetin, quercetin, kaempferol
	Essential oils and fatty acids	
	Miscellaneous compounds	β-setosterol and its glycoside. scopolectin, p-coumaric acid, lyciumide A, l-monomethyl succinate
Fruits of *L. chinense*	Similar to *L.barbarum*	Polysaccharides, carotenoids, flavonoids
	Cerebrosides, pyrrole derivatives	
	Sterols	Cycloartenol, 24-ethylycloartenol, granisterol, 24-methylene cycloartenol
Roots of *L. chinenese*	Cyclic peptides	Licyumines (A-D)
	Indole glycosides, Nitrogen compounds: aurantiamide acetate, lyciumamide Tyramine derivatives	
	Alkalods	Spermine alkaloids, kukoamines A and B
	Calystegenines and N-methyl ccalysegines	
	Polyphenolic compounds	Apigenin, acaccetin, luteolin, Kaempferol
	Coumarins	Scopolecin and its glycosides: scopolin and fabiatrin
	Lignans, anthraquinonines terpenoids, fatty acids	
Roots of *L. barbarum*	Cyclopeptides	Licyumins A and B
	Betain, choline lineolic acid	
Leaves and flowers of *L. chinense*	Acyclic diterpene glycosides	Lyciumosides I - IX
	Terpenoids, Withanolides	
	Flavonoids, glycosides, carotenoids, tannins, diosgenin, β-sitosterol, lanosterol	
Leaves of *L. barbarum*	Leaves: flavonoids, damascenone, choline	Other compounds: damascenone, choline, scopoletin, vanillic acid, salicylic acid, diosgenin, β-setosterol, lanosterol

1.5. Aim:

Since Goji was used traditionally in TCM and its extracts showed anti-diabetic activities, our aim was to identify novel small molecule agonists of PPARγ from Goji, and test their antidiabetic activities. We utilized computational docking, synthesis, *in vitro* and *in vivo* approaches to achieve the desired goals.

2. Results and Discussion

Our approach to identify small molecule-antidiabetic (T2D) compounds from *Lycium* species, which are active against diabetes, using a three stepped approach: 1) *in silico* screening of the reported phytochemicals of Goji into PPAR-γ binding site to identify the best active chemical scaffolds, 2) synthesis of compounds with the desired scaffolds and, 3) validate and confirm their activities with *in vitro* and *in vivo* screening.

Several compounds were reported to be isolated from various parts of Goji (*L. barbarum* and L. *chinense*). Among these, twenty-seven compounds isolated from the fruits and roots were selected for docking studies. These included alkaloids, a cyclic peptide, licumin D, indole glycoside derivative (aglycone form), nitrogen compounds including aurantiamide acetate, lyciumamide and a series of tyramine derivatives. The roots of Goji contain alkaloids such as spermine alkaloids, kukoamines A and B. A series of calystegenines and *N*-methylcalystegines, lignin lyoniresinol aglycone, a series of anthraquinones including, physcion, emodin, 1,3,6-trihydroxy-2-methylanthraquinone (**Figure 3-10**). The glycosides of some of the reported compounds of Goji were removed to allow for binding into the small volume active site grids used in the docking studies.

2.1. Molecular docking

Full agonists of PPARγ, termed as glitazones, ex: pioglitazone **II**, troglitazone **III,** rosiglitazone **IV** are currently used for the treatment of Type 2 Diabetes. However, these compounds show undesirable side-effects in treated patients, including cardiac problems [81, 82]. Partial PPARγ agonists were shown to possess anti-diabetic activity, but with reduced activity compared to full agonists [79, 83]. Hence, targeting PPARγ using partial agonists is a viable approach for the treatment of diabetes, without the undesirable side-effects of full agonists. In the current approach, we utilized both the partial and full agonists of PPARγ. The PDB crystal structure and binding mode analysis of full agonist (rosiglitazone **IV**, PDB: 2PRG) and partial agonist (cercosporamide-derivative **VII**, PDB: 3LMP) show different binding modes and protein-ligand interactions. The binding interactions of the full and partial agonists at the active site revealed differences in the binding modes of both types of agents. While full agonists show good hydrogen bonding interactions with His343 on helix 4, His449 on helix 10, and Tyr473 on helix 12, partial agonists do not show any interactions with these residues. Partial agonists occupy the binding site, more in the region between helix 3 and the β-sheet, when compared to the full agonists which occupy the binding site, more in the region between helices 3 and 12.

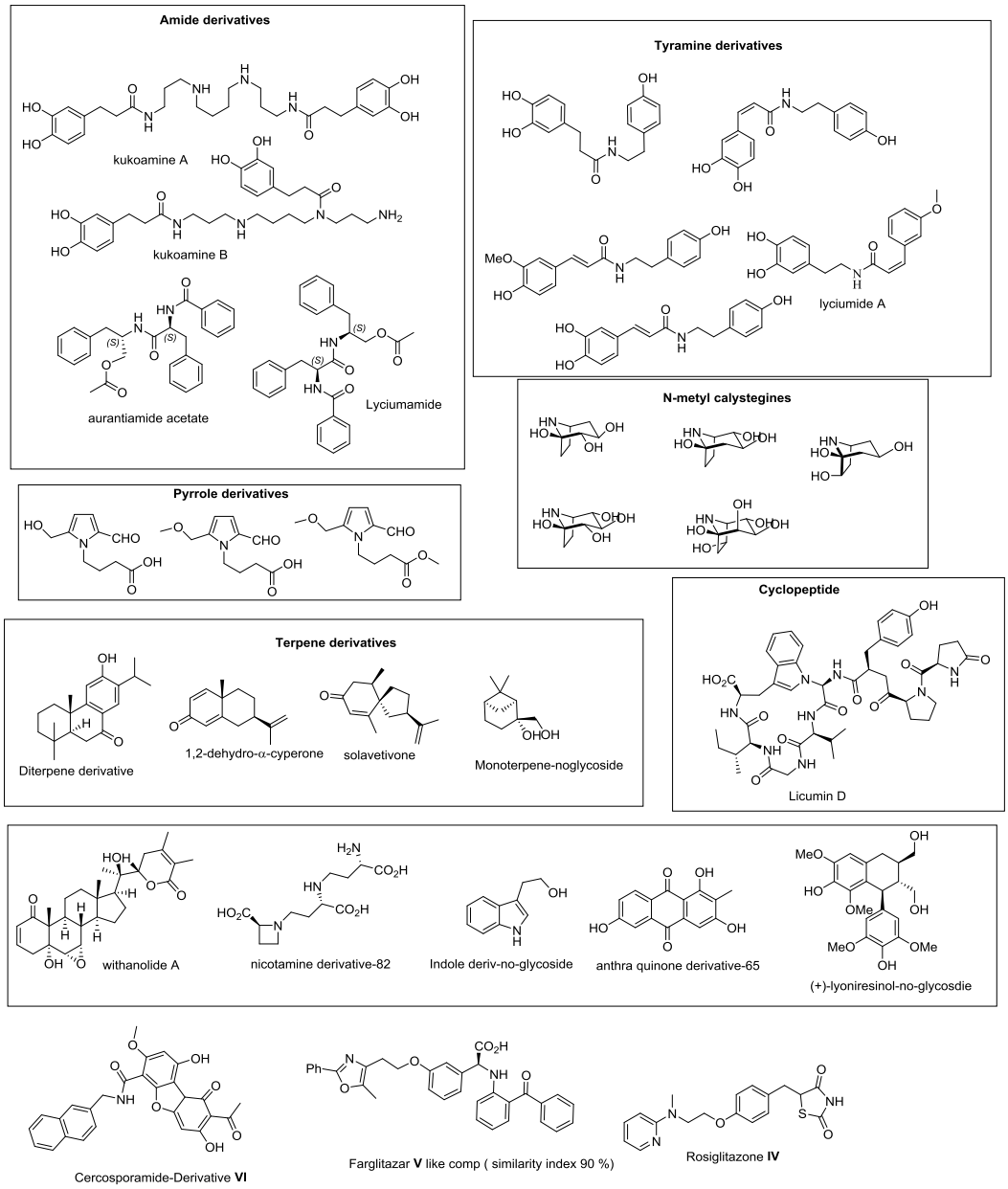

Figure 3-10. List of the compounds used for docking studies in PPAR-γ crystal structures 2PRG, 3LMP.

To identify new natural product-derived PPARγ ligands, docking of 27 reported compounds (**Figure 3-10**) isolated from various parts of both *L. barbarum* and *L. chinense* was performed inside the ligand binding domain of PPARγ using the X-ray crystal structures of full agonist rosiglitazone **IV** (PDB ID: 2PRG) and partial agonist, cercosporamide-derivative **VII** (PDB ID:

3LMP) [92]. Grid boxes were generated using Glide SP module (Schrödinger, LLC) with 12 Å radii around the native ligand generated using different hydrogen bonding constraints for full and partial agonists. For the full agonist, 2PRG, three hydrogen-bonding constraints were applied, in the partial agonist, 3LMP, no constraints were applied.

Docking output

The output for docking in both partial (3LMP) and full agonist (2PRG) binding sites was analyzed (**SI Tables 2** and **3**). Analysis of the docking results revealed that a number of compounds possessed good binding poses with favorable protein-ligand interactions. A study of the binding modes and the docking scores revealed that five compounds belonging to the cinnamomyl phenyl ethyl amide class lyciumamide A **X**, dihydro-*N*-caffeoyltyramine **XI**, *cis*-*N*-caffeoyltyramine **XII**, *trans*-*N*-caffeoyltyramine **XIII**, *trans*-*N*-feruloyloctopamine **XIV** possessed good binding poses, comparable to the native ligands (termed as tyramine derivatives hereafter for simplicity, since all of these amides are made of tyramines). These compounds displayed good hydrogen bonding interactions with the residues on the helix 3 and helix 12, similar to the full agonist, rosiglitazone **IV**. Whereas, in the partial agonist binding site, they do not show any binding near the helix 12 binding site and occupy the region more between helix 3 and β-sheet, similar to the partial agonist cercosporamide-derivative **VII**. These five tyramine-derivatives also possess good binding poses in both full and partial agonist binding sites (Table 1). This reveals that tyramine derivative-class of compounds may possess good PPARγ activity, either as a full- or partial- agonists. Hence, these simple amide derivatives were synthesized along with several analogs. All the compounds were validated using *in vitro* luciferase assays.

In general, tyramine-derivatives were reported to possess diverse biological activities like potentiation of antibiotics, inhibition of prostaglandin synthesis, anti-oxidant activities, antitubercular activity [100], bacterial efflux pump inhibitors, antihyperglycemic activites, melanin synthesis inhibitors [101], inhibitors of melanocyte-tyrosinase inhibitors [102], antifungal activities [103]. Several tyramine-derivatives were also isolated from the root barks of *L. chinense* and were found to possess anti-fungal activities [103]. Here we wanted to test the activities of these compounds against PPARα-PPARγ receptors.

Table 3-2. Docking scores of the five tyramine derivatives in full agonist and partial agonist binding sites of PPARγ.

		Glide Docking score	
Number	**Structure**	**2PRG**	**3LMP**
X	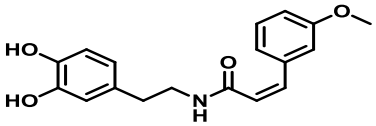 Lyciumamide A	-5.03	-7.47
XI	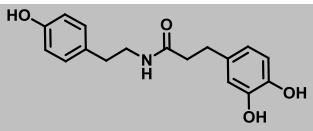 *Dihydro-N*-caffeoyltyramine	-8.82	-8.10
XII	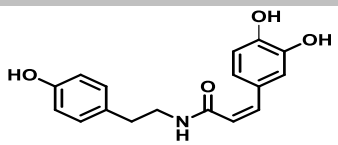 *cis-N*-caffeoyltyramine	-5.70	-6.26
XIII	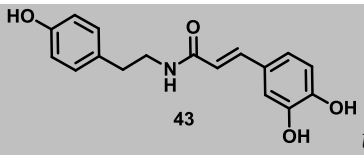 *trans-N*-caffeoyltyramine	-7.50	-6.16
XIV	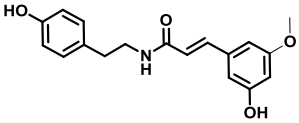 *trans-N*-feruloyloctopamine	-7.31	-8.11
	Rosiglitazone **IV**	-10.66 (native ligand)	-8.56
	Cercosporamide-derivative **VI**	No docking result obtained	-7.94 (native ligand)

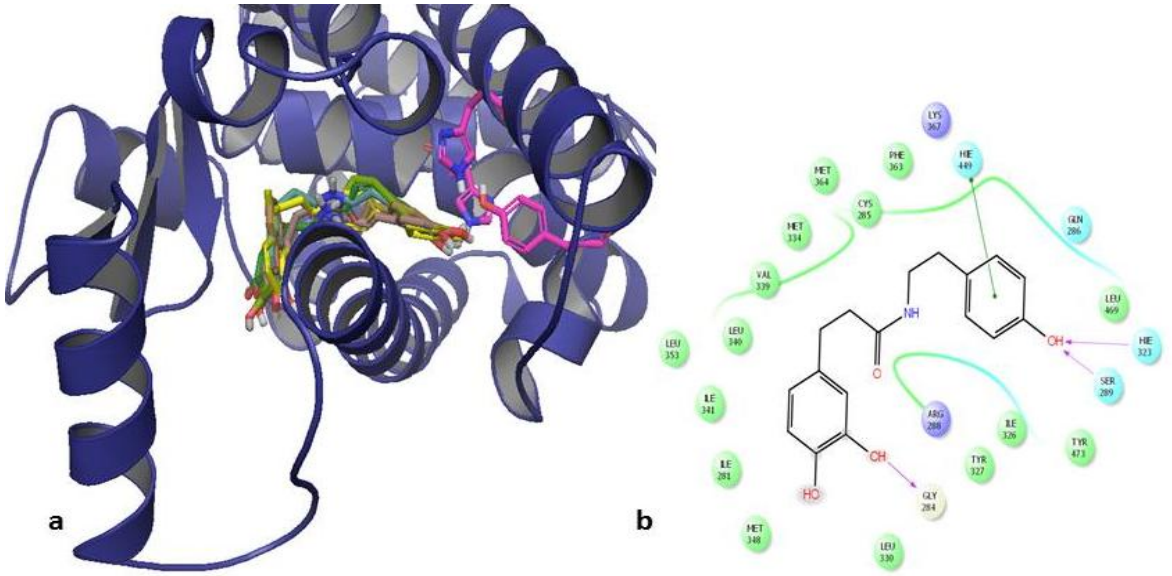

Figure 3-11. a) Binding modes of the four tyramine derivatives in the full agonist binding site and ligand-interaction diagram in the full agonist crystal structure. 2PRG-tyramine derivatives- **X** (Brown), **XI** (Blue), **XII** (dark green), **XIII** (wheat), **XIV** (light green) rosiglitazone **IV** (yellow). b) Ligand-interaction diagram of **XI** in the full agonist crystal structure (PDB: 2PRG) of
PPARγ.

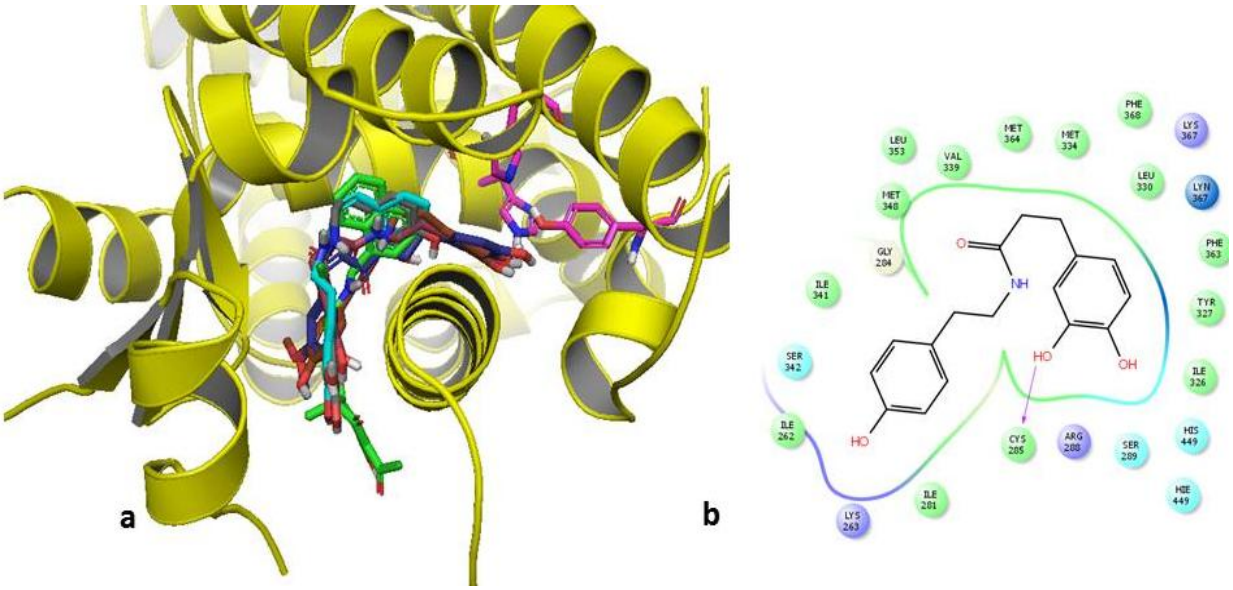

Figure 3-12. a) Binding poses of the five tyramine derivatives in the partial agonist binding site; **X** (dark blue), **XI** (brown), **XII** (light blue), **XIII** (black), **XIV** (light green), 3LMP-ligand (green). b) Ligand-interaction diagram of **X** in the partial agonist crystal structure (3LMP) of PPARγ.

2.2. Synthesis of tyramine derivatives for biological evaluation

First, a series of twelve compounds were synthesized by a coupling reaction using commercially available substituted cinnamic acid derivatives and phenyl alkylamines/tyramines, in the presence of triethyl amine and PyBOP [(Benzotriazole-1-yloxy)tripyrrolidinophosphonium hexafluorophosphate [104]. Four types of cinnamic acids (**SM1** to **SM4**) were each coupled with three types of phenylethyl amine derivatives (**SM5** to **SM7**) that resulted in amides (**1** to **12**) in 50-95% yields after flash chromatography. Moreover, the twelve-amides (**13** to **24**) were further subjected to reduction under hydrogenation conditions (Pd/H_2) and gave saturated amides in good yields (**Scheme 3-1**), (**Figure 3-13**). Among all these synthesized 24 amides, four compounds **02** (**XII**)**, 08** (**XIII**)**, 14** (**X**) were identified to possess good docking scores in our docking studies in 2PRG and 3LMP and were natural constituents of Goji [103, 105]. Along with three hits (natural products), all these twenty-one analogs (**01** to **24**) were evaluated for their activity as PPAR-γ agonists in HepG2 cells.

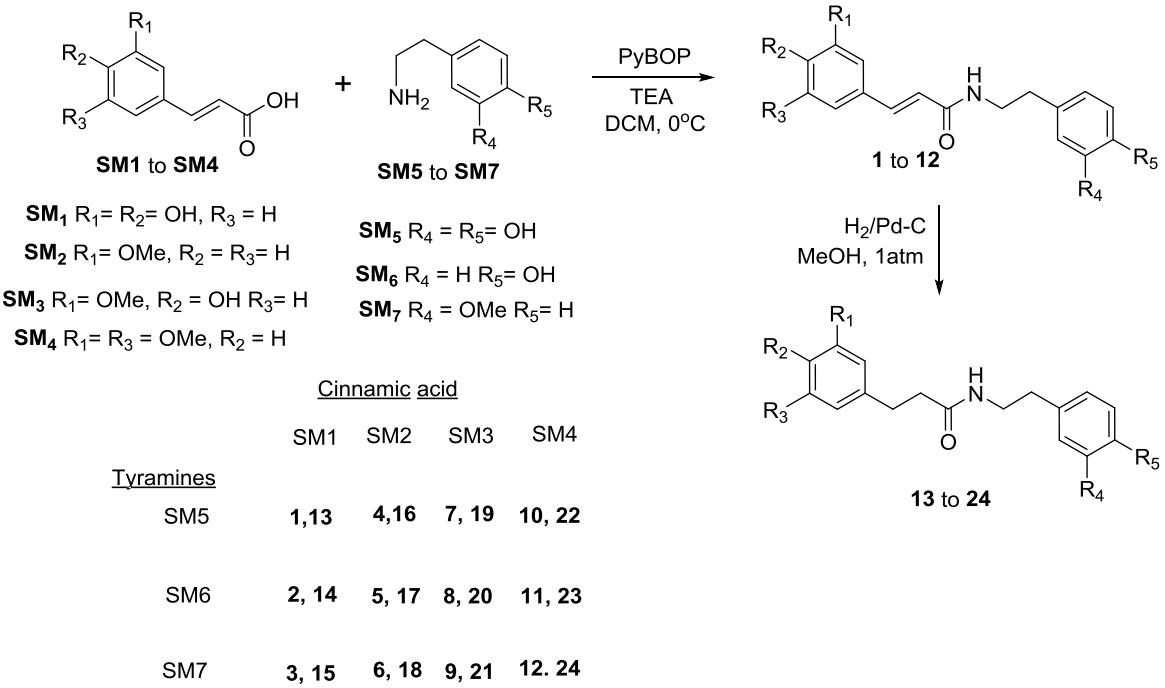

Scheme 3-1. Synthesis of twenty-four small molecule amide derivatives for *in vitro* screening using PPARγ-PPARα bioassay.

By coupling of the commercially available acids (**SM1** to **SM4**) and phenyl amines (**SM5** to **SM7**), twelve-different-amides were produced (**1** to **12**). These twelve-amides were further reduced to produce twelve-saturated compounds (**13** to **24**).

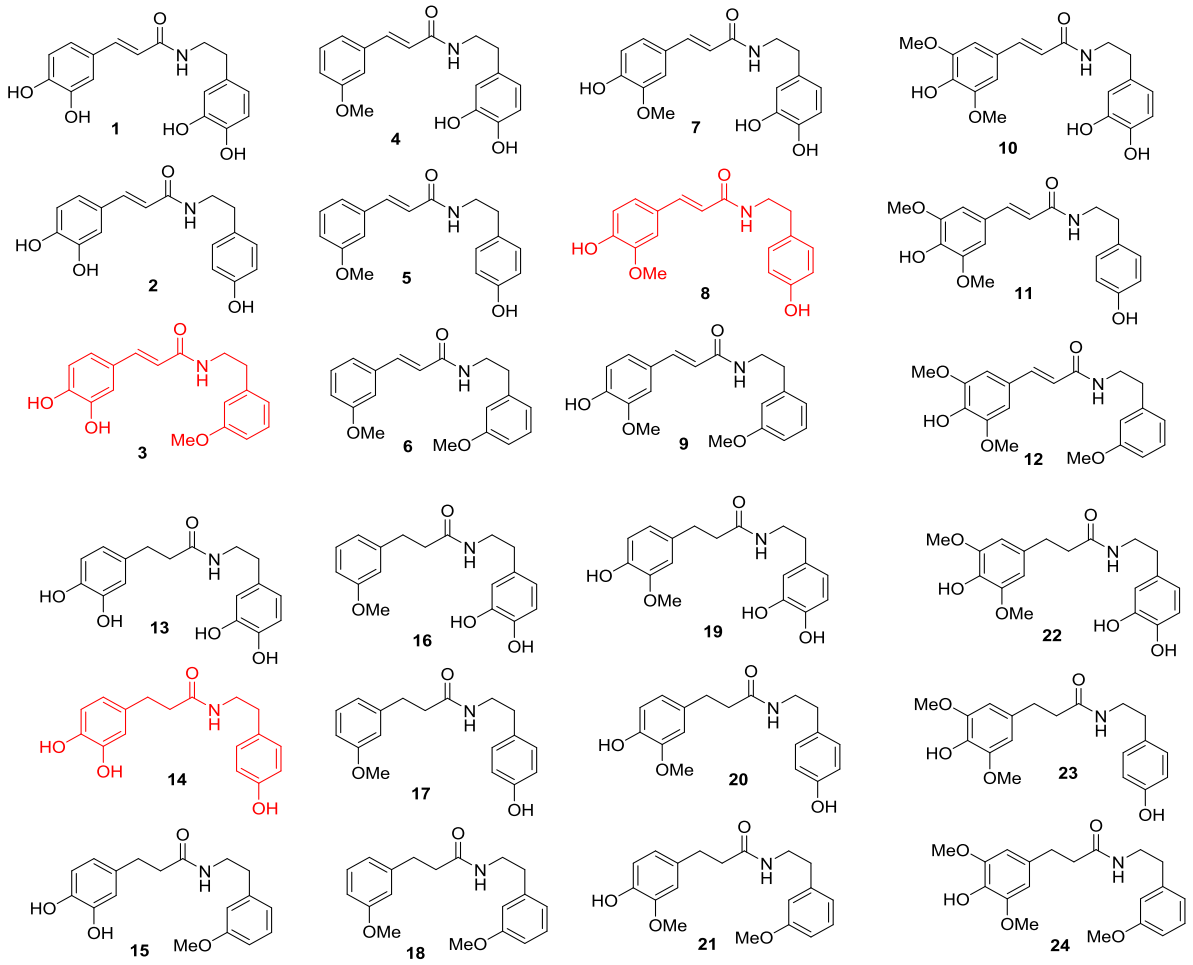

Figure 3-13. Structures of the twenty-four tyramine derivatives synthesized by coupling reaction.

2.3. *In vitro* and *in vivo* testing

In vitro luciferase assay [106] for PPARγ and PPARα induction activity was performed on all the twenty-four synthesized small molecule amide derivatives and along with the known ligands ciprofibrate (PPARα agonist) and rosiglitazone **IV**(PPAR γ agonist) as positive controls at 30, 10 and 3 μM concentrations. A two-fold induction means a 100% increase in activity compared to the DMSO control. PPARγ-selective compounds would possess a very good fold induction in PPARγ and a fold induction of 1.0 in PPARα cells (no increase in activity compared

to DMSO).

Among the twenty-four compounds, three compounds showed good PPARγ-induction compared to DMSO (**Figure 3-14**). Compound **01** showed a fold induction of 2.1, 1.4 and 1.4 at 30, 10 and 3 µM concentrations, respectively; whereas CA-G-010, showed a fold induction of 1.5, 1.8 and 1.4 at 30, 10 and 3 µM concentrations, respectively. The third compound, **08** showed best activity with a fold induction of 2.0, 1.9 and 1.4 at 30, 10 and 3 µM concentrations and this was selected for further testing using *in vivo* mouse assay.

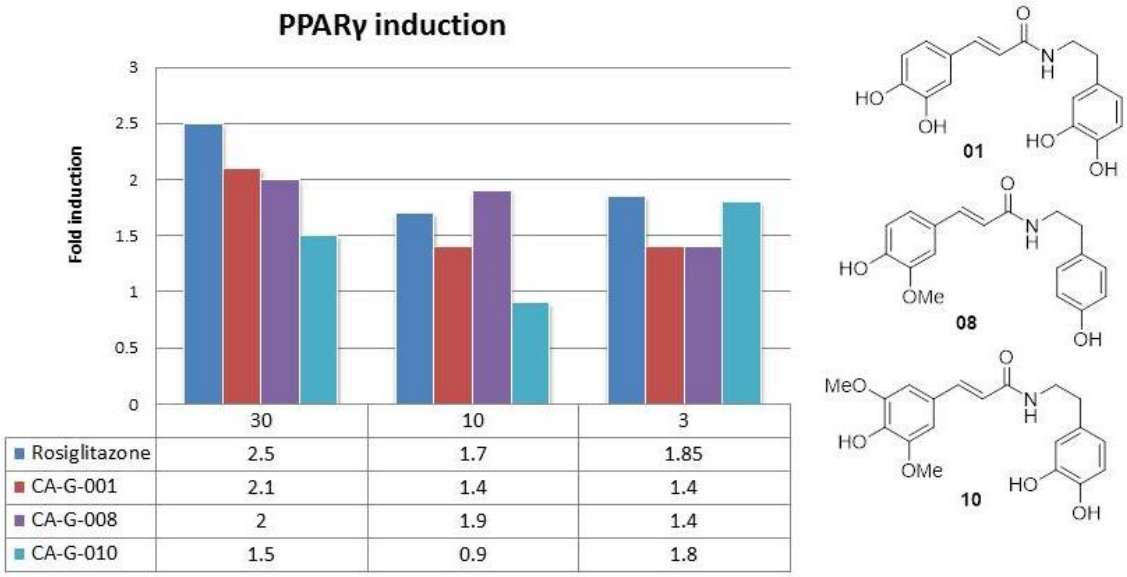

Figure 3-14. Structures and the results of the PPARγ induction-Luciferase assay in HepG2 cells for compounds **01**, **08**, **10** each studied at 3, 10 and 30 µM. These compounds did not possess much PPARα induction.

2.4. Enriched extract containing tyramine derivatives

Four phenolic amides were reported to be isolated from the root barks of *L. chinense*. [103, 105]. The root bark of *L. chinense* (0.8 Kg) extracted with ethanol yielded 137.3 g ,which was further isolated to produce four phenolic amide derivatives at 0.0187%, including *dihydro-*

N-caffeoyl tyramine **XI** (106 mg, 0.01325%), *cis*-*N*-caffeoyl tyramine **XII** (9.2 mg, 0.00115%), *trans*-*N*-caffeoyl tyramine **XIII** (14.8 mg, 0.00185), *trans*-*N*-feruloyl octopamine **XIV** (19.6 mg, 0.00245%) [103, 105]. Previous studies of the aqueous extract of Cortex Lycis Radicis (CLR) on alloxan-induced diabetic mice caused a decrease in glucose levels, increased insulin levels, and long-term hypoglycemic effects and reduce the body weight [98]. Also, studies of a methanolic extract of Lycii cortex radicis (LCR) on Sprague-Dawley male rats concluded that LCR possess hypocholestromeic activity. In order to study the antidiabetic properties of tyramines, an enriched extract of the root bark of *Lycium chinese*, was prepared and tested for *in vivo* activities along with small molecule amide derivative **08**.

2.5. *In vivo* diabetic mouse assay results

Compound **CA-G-008** and the alkaloid-enriched fraction (21% tyramine derivatives) of the Goji extract were tested *in vivo* using db/db mice model.

Body weight, food intake and glucose tolerance measurements

The body weight and food intake of both high and medium dose db/db mice groups was measured after two weeks of control period, treated either with the drug or the extract or vehicle. In the high dose groups, the mice treated with the drug showed a slight increase in the body weight, whereas as the group treated with the extract showed a slight decrease in their body weights. In contrast, the medium dose group of mice treated with extract and compound showed a slight decrease in body weight (**Figure 3-15**). The food intake of high dose groups treated with drug increased while the extract decreased slightly. In the medium dose group treated with the extract, the food intake decreased slightly, whereas the mice treated with the drug remained the same (**Figure 3-16**).

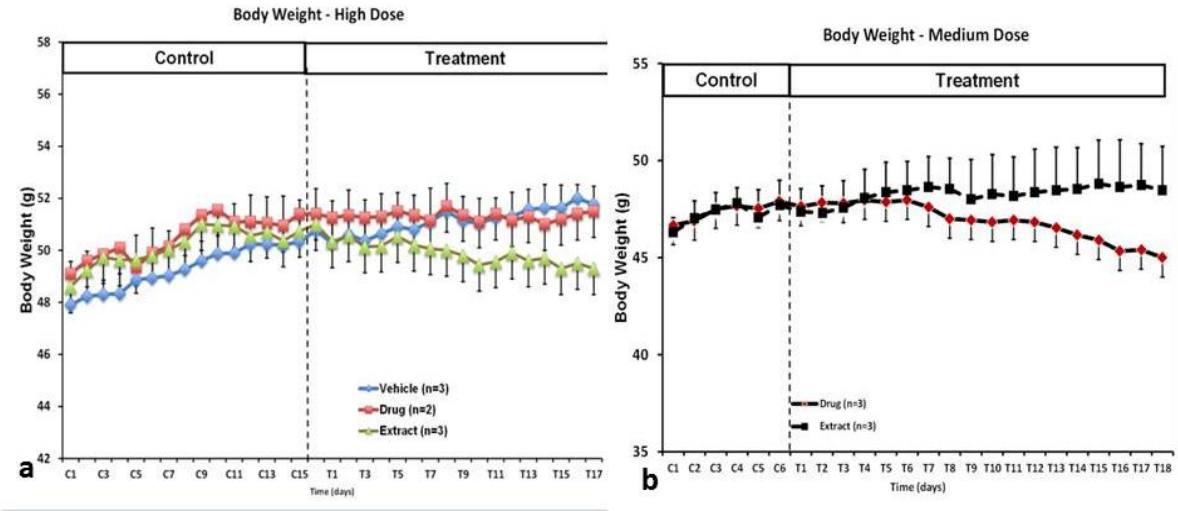

Figure 3-15. Body weight measurements of the db/db mice in both high and medium dose groups treated with both drug and extract.

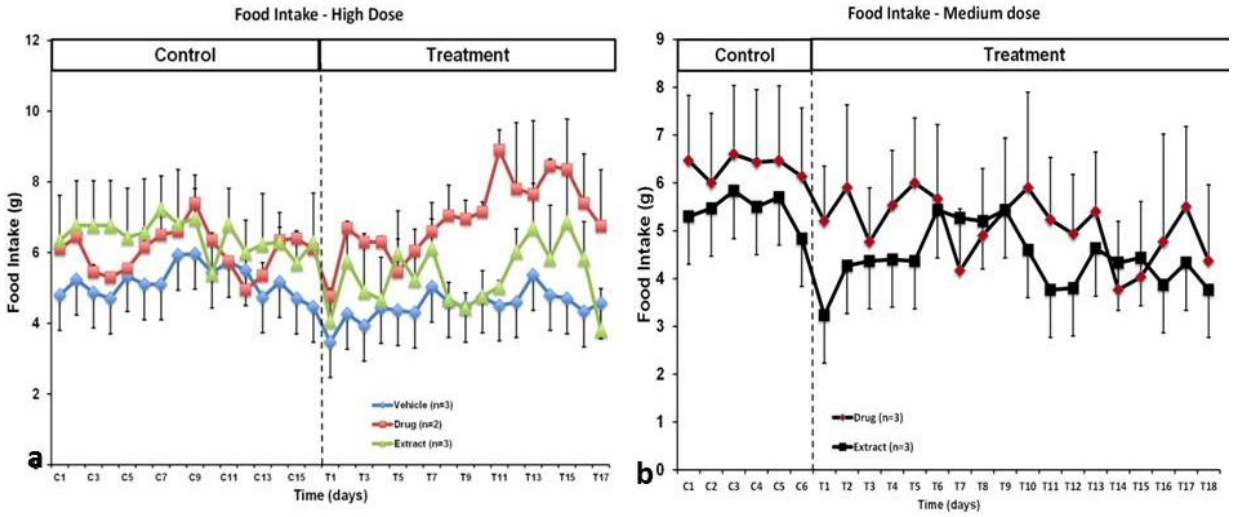

Figure 3-16. Food intake by db/db mice in both high dose group and medium dose group, treated with both drug and extract.

Glucose tolerance tests were performed by measuring the glucose concentration by treating the high and medium dose group mice with extract and the drug. In both medium and high dose treated groups, no improvements were observed in the mice treated with both drug and extract. **Figure 3-17** shows the blood glucose measurements in the medium and high dosage groups.

Metabolic Data

In both the medium- and high- dose groups (**Figures 3-18** and **3-19**), metabolic data were measured including respiratory quotient, oxygen consumption, carbon dioxide production, respiratory quotient, heat production and total movement.

In the medium dose group treated with the drug, the respiratory quotient, $VO_{2,}$ VCO_2 decreased significantly where as the heat content decreased slightly and the total movement increased slightly compared to the baseline. In the extract treated medium dose group, all the metabolic parameters decreased slightly compared to the baseline (**Figure 3-18**).

In the high dose group mice treated with the drug, compared to the baseline, the respiratory quotient, total average movement decreased compared to the drug treated group, while VO_2, VCO_2 and heat increased compared to the drug baseline group. In the extract treated high dose group, the respiratory quotient decreased slightly, total average movement increased significantly, whereas, VO_2, VCO_2 remained the same and the heat content decreased (**Figure 3-19**).

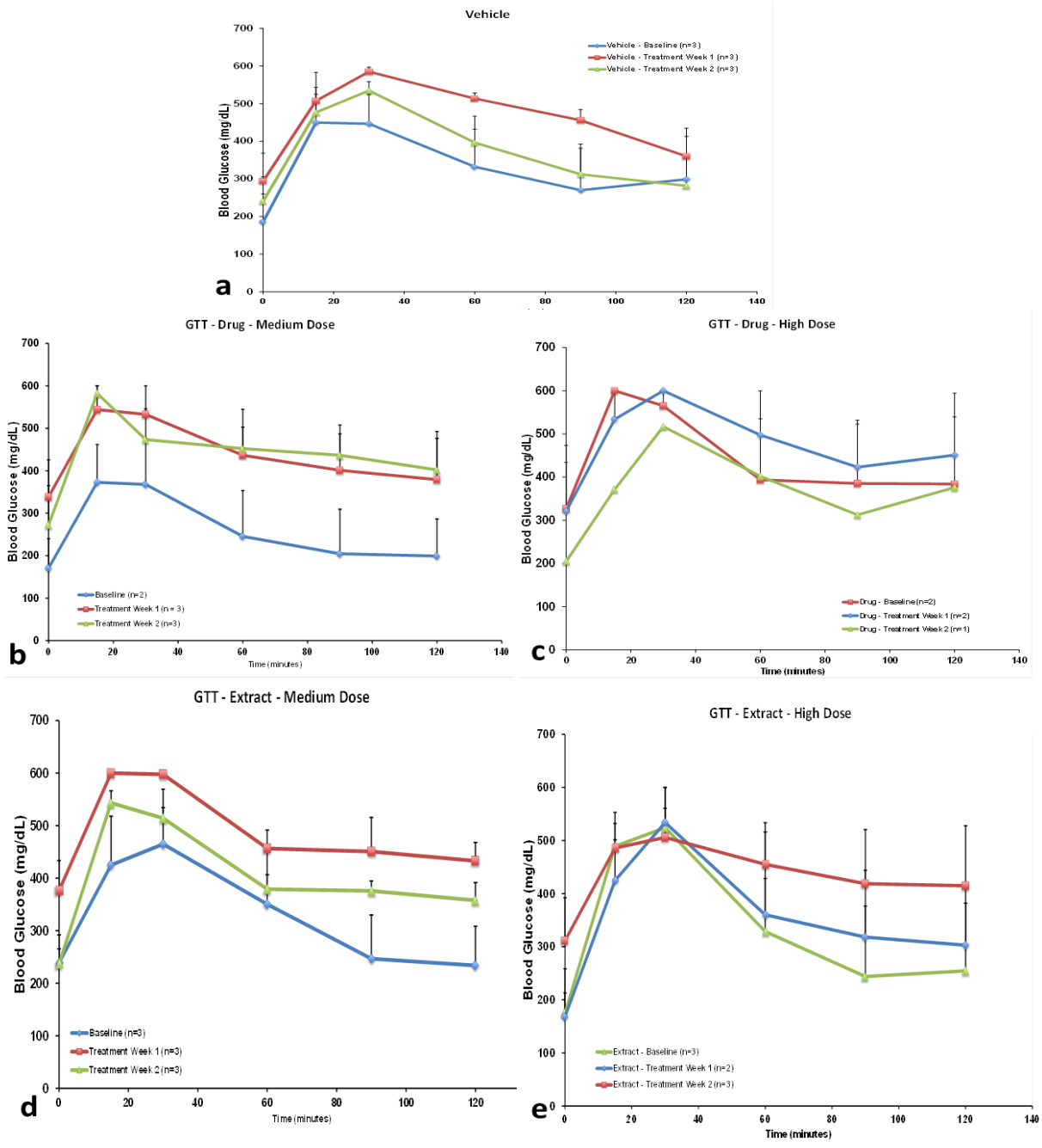

Figure 3-17. Blood glucose measurements plotted against time for drug (**08**) and extract (tyramide enriched) in medium and high dosage of the db/db mice (n=3).

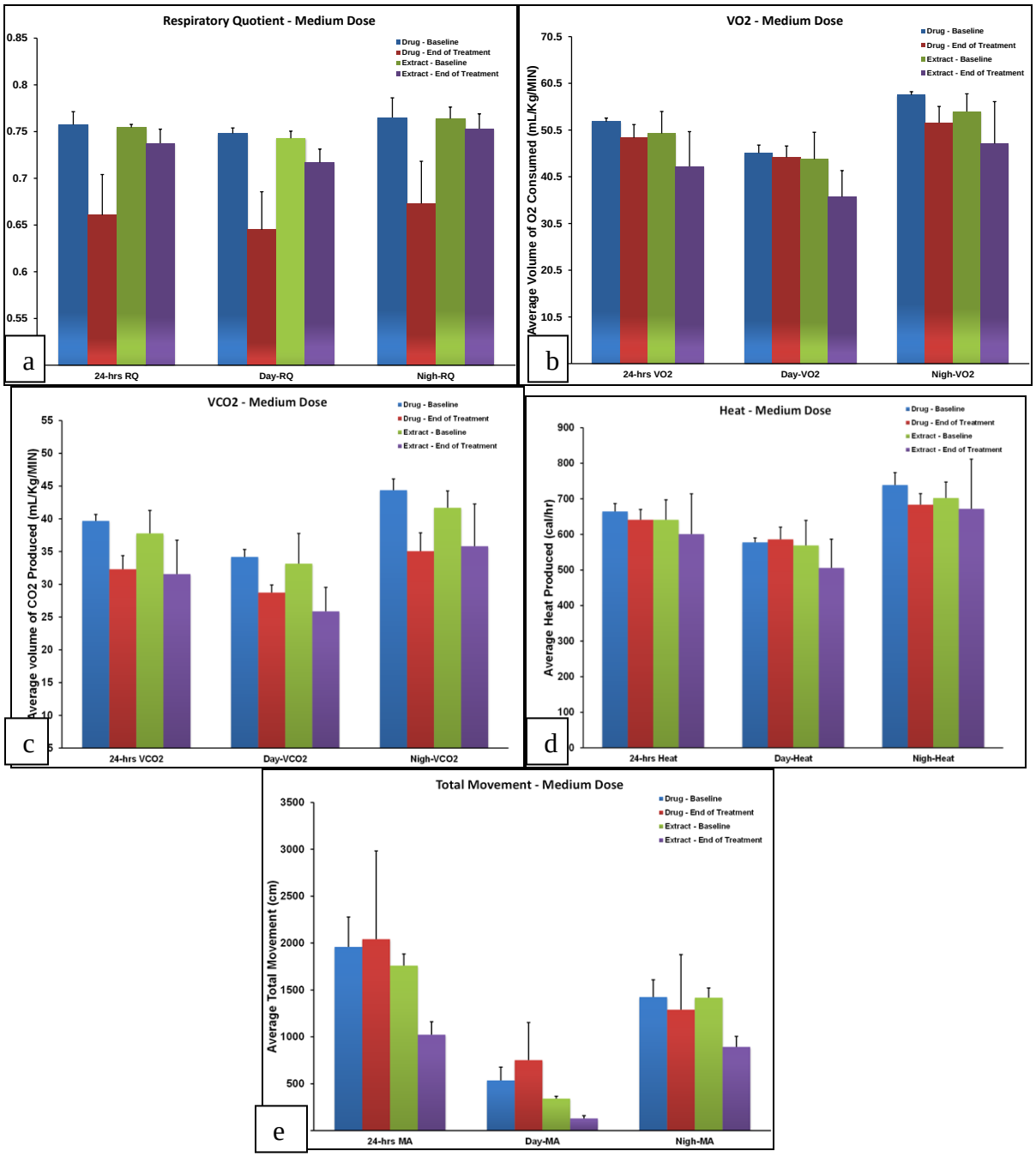

Figure 3-18. Metabolic data of the medium dose groups treated with both drug and the extract: a) respiratory quotient, b) VO_2, c) VCO_2, d) heat and e) total movement

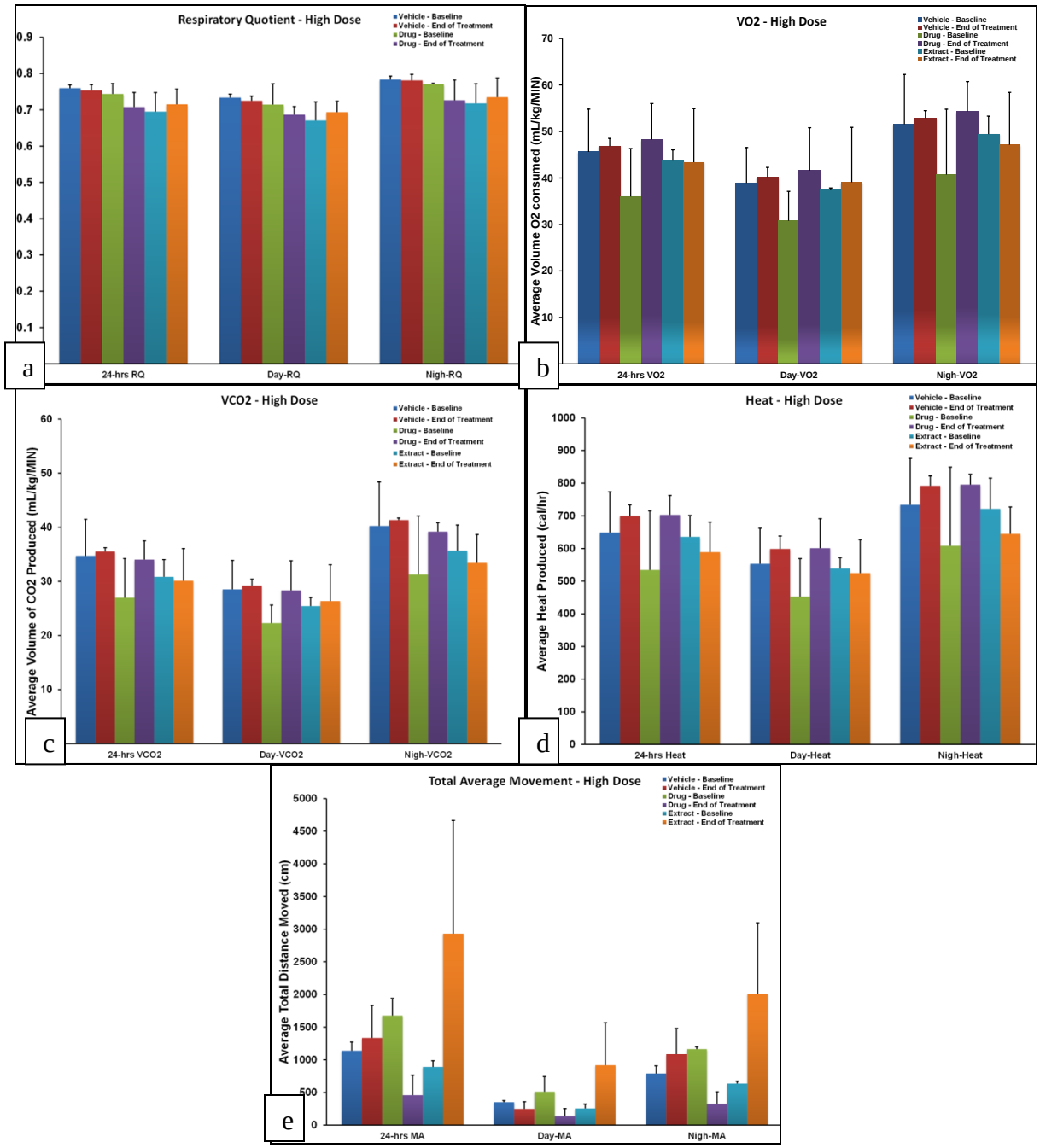

Figure 3-19. Metabolic data of the high dose groups treated with both drug and the extract: a) respiratory quotient, b) VO_2, c) VCO_2, d) heat and e) total movement.

EchoMRI body composition

The body composition was measured in the medium dose group using EchoMRI to

measure lean and fat mass, free and total water content (**Figure 3-20**). In the drug treated mice, lean mass, fat mass and total water content almost remained the same as the baseline, free-water content decreased in the first week, and it increased in the second week. In the extract-treated group, lean mass remained the same, fat mass increased slightly in the first and second weeks, and free-water content increased in the first week, and decreased in the second week.

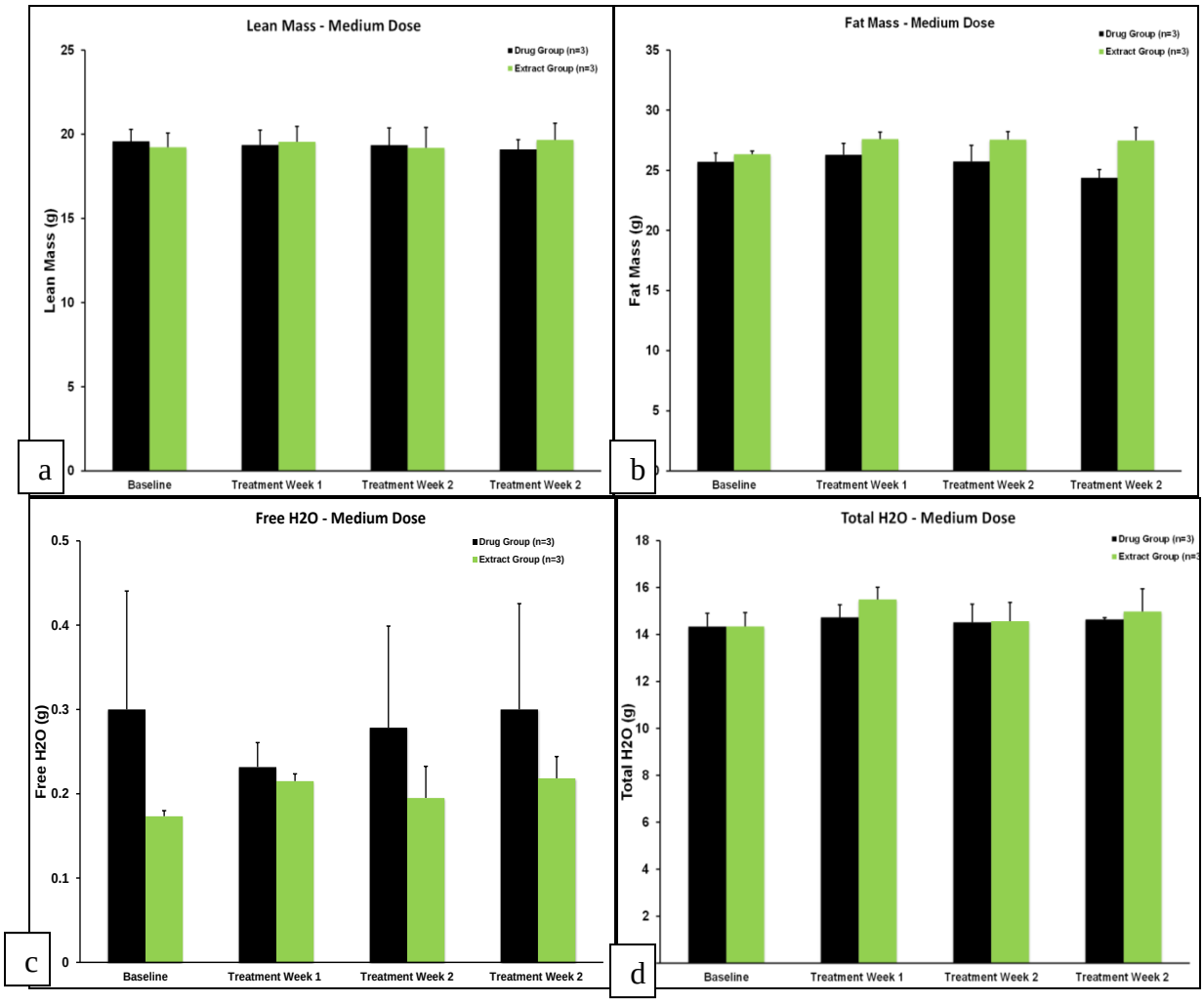

Figure 3-20. The body composition of the medium dose group mice treated with drug and the extract: a) lean mass, b) fat mass, c) free water and d) total water content.

Blood pressure and heart rate

Blood pressure and heart rate were measured in the high dose group after treatment with

extract and drug. The blood pressure in the high dose group of mice treated with the drug decreased, whereas with the extract, the blood pressure increased slightly. The heart rate of the mice increased slightly in both drug and extract treated mice.

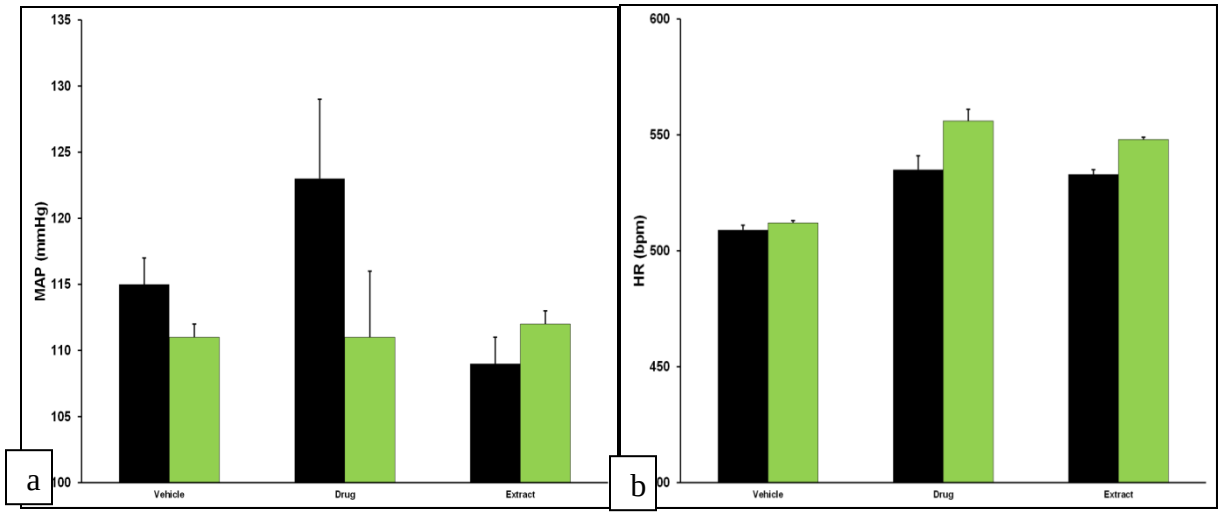

Figure 3-21. Blood pressure and heart rates of high dose group db/db mice treated with drug and extract.

2.6. **Conclusions**

Preparations containing Goji, a TCM plant, are widely used in the Eastern countries to treat various diseases including diabetes. To identify the active compounds, some of the reported phytochemicals of Goji selected and were docked into the PPARγ ligand binding domains of both full and partial agonists (2PRG and 3LMP, respectively). Docking results revealed five compounds belonging to cinnamomyl phenyl ethyl amide class **X** to **XIV** (termed as tyramine-derivatives), possess good binding poses and docking scores in both the partial and full agonist catalytic binding domains. Hence, tyramine-derivatives were selected for synthesis and further testing. An enriched extract of the root bark of *L. chinense* (calculated conc. of tyramine-derivatives, 21%) was prepared. In addition, using coupling of tyramines with cinnamic acid-

derivatives, followed by reduction, twenty-four compounds belonging to the tyramine-derivative class were synthesized and evaluated for PPARγ activity and selectivity using PPARγ- and PPARα-luciferase bioassays. Among the twenty-four compounds, three compounds (**01**, **08**, **10**) possessed a good induction compared to positive control rosiglitazone. Compound **08** and tyramine-derivative enriched extract were tested further, using *in vivo* diabetic db/db mice model to check their antidiabetic and metabolic properties. Although some tyramine derivatives possessed good activities *in vitro*, the results of the *in vivo* studies indicate no significant improvement in the biochemical parameters of the db/db mice model by both **08** and tyramine-derivative enriched Goji fraction. In conclusion, though the TCM preparations were used traditionally for their antidiabetic properties and were previously reported to possess this activity, our studies indicate that this antidiabetic property may not be due to the tyramine-derivative class of compounds either alone or in combination, at the concentrations tested *in vivo*. The phytochemicals of Goji including tyramine-analogues might be working as antidiabetic compounds via different targets or mechanisms other than PPARs.

3. Experimental

3.1. Docking studies

System specifications and software

To perform virtual screening, studies, a commercial version of the Schrödinger software package [64] was installed on a Windows desktop computer with Intel® Core™ Quad CUP Q6600@2.40GHz 2.40 GHz processor with a random access memory (RAM) of 4.00 GB and 32-bit operating system. PyMol software (Schrödinger, LLC) was utilized to perform post

docking visualization and analysis.

Ligand Preparation

Thirty one compounds, including 27 from Goji and three PPARγ agonists farglitzar, rosiglitazone **IV** and cercosporamide-derivative **VII** were prepared using LipPrep module in force field OPLS-2005, ionized at pH 7.4 $\pm$ 2, desalted and generated tautomers. The specified chirality was retained to generate at most 32 per ligand. This ligand preparation generated 81 ligands from the input of 31 compounds.

Protein preparation

Crystal structures of PPARγ with rosiglitazone **IV**, a full agonist (PDB: 2PRG) and cercosporamide-derivative **VII**, a partial agonist (PDB: 3LMP) were prepared using the protein preparation wizard. Both the proteins were preprocessed to assign bond orders, add hydrogen bonds, create zero order bonds to metals, create disulfide bonds, and delete waters beyond 5 Å from hetero groups. For 2PRG, the chains B and C were deleted, whereas, for 3LMP, chain C was deleted. The H-bond assignment was applied using sample water orientations, using PROPKA pH 7.0. Water molecules with less than three hydrogen bonding distance were removed from the protein. Restrained minimization was performed using OPLS_2005, converged the heavy atoms to RMSD 0.3 Å.

Glide Grid generation and docking

Receptor grids were generated for the prepared proteins 2PRG and 3LMP using Glide (Schrödinger, LLC). For 2PRG, three hydrogen bonding constraints to His323, 449 and Tyr473 were applied, and for 3LMP, no constraints were applied. The grids thus generated were

validated for both the native ligands to check if the RMSD of the docked output was < 1 Å from that of the crystal structure. All the prepared ligands were docked in the two generated grids. Their docking results and binding poses were analyzed using PyMol (Schrödinger, LLC).

3.2. Synthesis of tyramine-derivatives

Materials and methods.

All the reactions were performed under an atmosphere of argon with oven-dried glassware and standard syringe/septa techniques. Materials were obtained from commercial suppliers and used without further purification except when otherwise noted. All reactions were magnetically stirred with teflon stir bars, and temperatures were measured externally. Solvents were distilled under an argon atmosphere prior to use. The solvents CH_2Cl_2 was dried over P_2O_5 and triethylamine was distilled from CaH_2. Ethanol and methanol used were bottle-grade solvents. All reagents obtained commercially were used without further purification. The reaction progress was monitored on precoated silica gel TLC plates. Spots were visualized under 254 nm UV light and/or by dipping the TLC plate into a solution of 2 mL of anisaldehyde, 10 mL of glacial acetic acid, and 5 mL of H_2SO_4 in 340 mL of EtOH, followed by heating with a heat gun. Column chromatography was performed with silica gel (230−400mesh). All the solvents (hexanes, ethyl acetate, CH_2Cl_2, Et_2O) were distilled prior to use for column chromatography. ^{1}H and ^{13}C NMR spectra were measured in MeOD on 500 MHz (125 MHz) machines. Chemical shifts were reported in parts per million (ppm) downfield from tetramethylsilane (δ) as the internal standard, and coupling constants are in hertz (Hz). Assignment of proton resonances were confirmed by correlated spectroscopy. IR spectra were recorded with a universal attenuated total reflection sampling accessory (diamond ATR) on an

Agilent Cary 630 FT-IR spectrometer.

Synthesis of ***1*** *to* ***12***

General procedure: A substituted Cinnamic acid derivative (1 eq.) is dissolved in 2.5 mL of dimethylformamide (DMF) and trimethylamine (TEA) (3 eq) The solution is cooled in an ice ± water bath and substituted tyramine derivative (1.25 eq) are added followed by a solution of PyBOP (1.25 eq) in 2.5mL of CH_2Cl_2. The mixture is stirred at 0 C for 30 min and then at room temperature for 12 h. CH_2Cl_2 is removed under reduced pressure and the solution is diluted with 15mL of water. The products are extracted with ethyl acetate. The extract was washed sequentially with 1N HCl, water, 1M $NaHCO_3$ and brine, dried over $MgSO_4$, filtered and evaporated. The residue was purified on a silica gel column (eluent: ethyl acetate or petroleum ether) to obtain compounds **01** to **12**, at yields between 65 and 85%.

(*E*)-*N*-(3,4-dihydroxyphenethyl)-3-(3,4-dihydroxyphenyl)acrylamide **01**

(yield 88%) **IR** (cm^{-1}): 3313, 2939, 2487, 2073, 1648, 1579, 1513, 1463, 1439, 1360, 1280, 1203, 1164, 1122, 973, 850 and 811; **^{1}H NMR** (500 MHz, MeOD) δ 7.40 (d, *J* = 15.7 Hz, 1H), 7.02 (s, 1H), 6.94 – 6.89 (m, 1H), 6.78 (d, *J* = 8.1 Hz, 1H), 6.73 – 6.67 (m, 2H), 6.57 (d, *J* = 8.0 Hz, 1H), 6.36 (d, *J* = 15.7 Hz, 1H), 3.46 (t, *J* = 7.3 Hz, 2H), 2.71 (t, *J* = 7.3 Hz, 2H); **^{13}C NMR** (126 MHz, MeOD) δ 167.88, 147.34 , 145.31 , 144.86 , 143.39 , 140.76 , 130.72 , 126.92 , 120.70 , 119.66 , 117.03 , 115.48 , 115.03, 113.66 , 41.16 , 34.66 .

(*E*)-3-(3,4-dihydroxyphenyl)-*N*-(4-hydroxyphenethyl)acrylamide **02**

(yield 75%) **IR** (cm^{-1}): 3273, 2492 1649, 1595, 1514, 1463, 1362, 1284, 1242, 1114, 975, 850 and 815; ^{1}H NMR (500 MHz, MeOD) δ 7.41 (d, *J* = 15.6 Hz, 1H), 7.11 – 7.01 (m, 3H), 6.94 – 6.88 (m, 1H), 6.79 (d, *J* = 8.1 Hz, 1H), 6.74 (d, *J* = 8.4 Hz, 2H), 6.36 (d, *J* = 15.6 Hz, 1H), 3.52 – 3.47 (t, *J* = 7.3 Hz, 2H), 2.76(t, *J* = 7.3 Hz, 2H); ^{13}C NMR (126 MHz, MeOD) δ 167.91, 155.49,

147.35, 145.31, 140.82, 129.94, 129.37, 126.93, 120.77, 117.02, 115.10, 114.89, 113.70, 41.19, 34.42.

(*E*)-3-(3,4-dihydroxyphenyl)-*N*-(3-methoxyphenethyl)acrylamide **03**

(yield 75%) **IR** (cm^{-1}): 3170, 2944, 2491, 1651, 1585, 1514, 1456, 1362, 1284, 1260, 1203, 1154, 1116, 1039, 978, 851, 814, 783 and 696; ^{1}H NMR (500 MHz, MeOD) δ 7.41 (d, *J* = 15.6 Hz, 1H), 7.19 (t, *J* = 8.1 Hz, 1H), 7.03 (s, 1H), 6.91 (d, *J* = 8.1 Hz, 1H), 6.79 (dt, *J* = 12.5, 8.0 Hz, 5H), 6.36 (d, *J* = 15.7 Hz, 1H), 3.76 (s, 3H), 3.52 (t, *J* = 7.3 Hz, 2H), 2.83 (t, *J* = 7.3 Hz, 2H); ^{13}C NMR (126 MHz, MeOD) δ 167.91, 159.87, 147.38, 145.33, 140.87, 140.67, 129.10, 126.91, 120.75 (d, *J* = 3.1 Hz), 117.00, 115.11, 113.85 (d, *J* = 35.4 Hz), 113.50, 111.50, 54.19, 40.79, 35.28.

(*E*)-*N*-(3,4-dihydroxyphenethyl)-3-(3-methoxyphenyl)acrylamide **04**

(yield 57%) **IR** (cm^{-1}): 3245, 2488, 1655, 1598, 1520, 1489, 1456, 1361, 1280, 1256, 1197, 1116, 1047, 977, 850, 784 and 680;^{1}H NMR (500 MHz, MeOD) δ 7.50 (d, *J* = 15.7 Hz, 1H), 7.29 (t, *J* = 7.9 Hz, 1H), 7.13 (d, *J* = 7.6 Hz, 1H), 7.09 (s, 1H), 6.94 (dd, *J* = 8.1, 2.1 Hz, 1H), 6.71 (dd, *J* = 9.7, 4.9 Hz, 2H), 6.58 (dd, *J* = 8.7, 7.0 Hz, 2H), 3.81 (s, 3H), 3.48 (t, *J* = 7.3 Hz, 2H), 2.72 (t, *J* = 7.3 Hz, 2H); ^{13}C NMR (126 MHz, MeOD) δ 167.18, 160.11, 144.89, 143.43, 140.19, 136.26, 130.65, 129.53, 120.78, 119.98, 119.69, 115.50, 115.09 (d, *J* = 10.8 Hz), 112.43, 54.34, 41.18, 34.59.

(*E*)-*N*-(4-hydroxyphenethyl)-3-(3-methoxyphenyl)acrylamide **05**

(yield 88%) **IR** (cm^{-1}): 2967, 2868, 2396, 1656, 1610, 1516, 1489, 1453, 1361, 1242, 1206, 1156, 1087, 1048, 1015, 982, 831, 782 and 681; **^{1}H NMR** (500 MHz, MeOD) δ 7.50 (d, *J* = 15.7 Hz, 1H), 7.30 (t, *J* = 7.9 Hz, 1H), 7.13 (d, *J* = 7.6 Hz, 1H), 7.11 – 7.05 (m, 4H), 6.94 (dd, *J* = 8.1, 2.0 Hz, 1H), 6.74 (d, *J* = 8.3 Hz, 2H), 6.59 (d, *J* = 15.8 Hz, 1H), 3.82 (s, 4H), 3.49 (t, *J* = 7.4 Hz,

2H), 2.78 (t, *J* = 7.3 Hz, 2H); **^{13}C NMR** (126 MHz, MeOD) δ 167.14, 160.13, 155.59, 140.18, 136.27, 129.82, 129.55, 129.35, 120.78, 119.97, 115.13, 114.90, 112.44, 54.35, 41.20, 34.37.

(*E*)-*N*-(4-hydroxyphenethyl)-3-(3-methoxyphenyl)acrylamide **06**

(yield 89%) **IR** (cm^{-1}): 3277, 3070, 2935, 2835, 1655, 1602, 1582, 1546, 1488, 1454, 1433, 1367, 1315, 1209, 1217, 1153, 1039, 979, 849, 779, 695 and 677; **^{1}H NMR** (500 MHz, $CDCl_3$) δ 7.60 (d, *J* = 15.5 Hz, 1H), 7.27 (dt, *J* = 11.3, 7.8 Hz, 3H), 7.09 (d, *J* = 7.6 Hz, 1H), 7.02 (s, 1H), 6.91 (d, *J* = 8.1 Hz, 1H), 6.82 (dd, *J* = 14.7, 9.4 Hz, 3H), 6.35 (d, *J* = 15.6 Hz, 1H), 5.83 (bs, 1H), 3.83 (s, 3H), 3.81 (s, 3H), 3.68 (m, 2H), 2.89 (t, *J* = 6.8 Hz, 2H); **^{13}C NMR** (126 MHz, $CDCl_3$) δ 165.85, 159.87, 140.94, 140.51, 136.22, 129.76 (d, *J* = 12.1 Hz), 121.06 (d, *J* = 17.5 Hz), 120.42, 115.40, 114.50, 112.91, 111.94, 55.25 (d, *J* = 9.5 Hz), 40.72, 35.70.

(*E*)-*N*-(3,4-dihydroxyphenethyl)-3-(4-hydroxy-3-methoxyphenyl)acrylamide **07**

(yield 65 to 85%) **IR** (cm^{-1}): 3322, 2492, 1651, 1591, 1515, 1461, 1362, 1280, 1205, 1123, 1032, 976, 845 and 815; **^{1}H NMR** (500 MHz, MeOD) δ 7.46 (d, *J* = 15.7 Hz, 1H), 7.12 (s, 1H), 7.03 (dd, *J* = 8.1, 1.4 Hz, 1H), 6.81 (d, *J* = 8.1 Hz, 1H), 6.71 (dd, *J* = 9.4, 4.8 Hz, 2H), 6.57 (dd, *J* = 7.8, 1.5 Hz, 1H), 6.43 (d, *J* = 15.7 Hz, 1H), 3.89 (s, 3H), 3.48 (t, *J* = 7.3 Hz, 2H), 2.72 (t, *J* = 7.2 Hz, 2H); **^{13}C NMR** (126 MHz, MeOD) δ 167.79, 148.41, 147.87, 144.87, 143.40, 140.64, 130.71, 126.89, 121.84, 119.69, 117.37, 115.51, 115.05 (d, *J* = 4.3 Hz), 110.12, 54.98, 41.15, 34.65.

(*E*)-3-(4-hydroxy-3-methoxyphenyl)-*N*-(4-hydroxyphenethyl)acrylamide **08**

(yield 75%) **IR** (cm^{-1}): 3255, 2492, 1651, 1591, 1514, 1459, 1362, 1279, 1126, 1032, 977 and 819; **^{1}H NMR** (500 MHz, MeOD) δ 7.46 (d, *J* = 15.6 Hz, 1H), 7.16 – 7.01 (m, 5H), 6.81 (d, *J* = 8.1 Hz, 1H), 6.74 (d, *J* = 8.4 Hz, 2H), 6.42 (d, *J* = 15.6 Hz, 1H), 3.88 (s, 3H), 3.54 – 3.45 (m, 2H), 2.77 (t, *J* = 7.3 Hz, 2H); **^{13}C NMR** (126 MHz, MeOD) δ 167.80, 155.53, 148.44, 147.88,

140.67, 129.91, 129.37, 126.87, 121.85, 117.35, 115.09, 114.89, 110.13, 54.98, 41.17, 34.42

(*E*)-3-(4-hydroxy-3-methoxyphenyl)-*N*-(3-methoxyphenethyl)acrylamide **09**

(yield ~ 75%) **IR** (cm^{-1}): 2938, 2482, 1652, 1600, 1585, 1514, 1456, 1434, 1362, 1281, 1262, 1281, 1262, 1206, 1157, 1125, 1035, 979, 846, 818, 782 and 696; **^{1}H NMR** (500 MHz, MeOD) δ 7.46 (d, *J* = 15.7 Hz, 1H), 7.21 (t, *J* = 8.0 Hz, 1H), 7.12 (s, 1H), 7.04 (dd, *J* = 8.1, 1.3 Hz, 1H), 6.82 (t, *J* = 7.8 Hz, 2H), 6.80 – 6.75 (m, 1H), 6.42 (d, *J* = 15.6 Hz, 1H), 3.89 (s, 3H), 3.78 (s, 3H), 3.54 (t, *J* = 7.3 Hz, 2H), 2.85 (t, *J* = 7.2 Hz, 2H); **^{13}C NMR** (126 MHz, MeOD) δ 167.81, 159.90, 148.49, 147.90, 140.71, 129.09, 126.83, 121.83, 120.73, 117.28, 115.09, 114.01, 111.47, 110.13, 54.97, 54.16, 40.76, 35.26.

(*E*)-*N*-(3,4-dihydroxyphenethyl)-3-(4-hydroxy-3,5-dimethoxyphenyl)acrylamide **10**

(yield ~ 75%) **IR** (cm^{-1}): 3339, 2939, 2492, 2071, 1652, 1603, 1514, 1457, 1427, 1337, 1282, 1216, 1156, 1114, 975, 869 and 827; **^{1}H NMR** (500 MHz, MeOD) δ 7.43 (d, *J* = 15.6 Hz, 1H), 6.82 (s, 2H), 6.75 – 6.69 (m, 2H), 6.57 (d, *J* = 7.9 Hz, 1H), 6.45 (d, *J* = 15.6 Hz, 1H), 3.85 (s, 7H), 3.50 (t, *J* = 7.2 Hz, 2H), 2.72 (t, *J* = 7.2 Hz, 2H); **^{13}C NMR** (126 MHz, MeOD) δ 167.71, 148.01, 144.88, 143.41, 140.88, 137.40, 130.74, 125.86, 119.75, 117.85, 115.56, 115.09, 104.99, 55.40, 41.15, 34.63.

(*E*)-3-(4-hydroxy-3,5-dimethoxyphenyl)-*N*-(4-hydroxyphenethyl)acrylamide **11**

(yield ~ 75%) **IR** (cm^{-1}): 3339, 2939, 2493, 2071, 1652, 1603, 1514, 1457, 1427, 1337, 1282, 1216, 1156, 1114, 975, 868 and 827; **^{1}H NMR** (500 MHz, MeOD) δ 7.44 (d, *J* = 15.6 Hz, 1H), 7.06 (d, *J* = 8.2 Hz, 2H), 6.83 (s, 2H), 6.74 (d, *J* = 8.2 Hz, 2H), 6.45 (d, *J* = 15.6 Hz, 1H), 3.86 (s, 6H), 3.49 (t, *J* = 7.3 Hz, 2H), 2.77 (t, *J* = 7.2 Hz, 2H); **^{13}C NMR** (126 MHz, MeOD) δ 167.68, 155.53, 148.03, 140.87, 137.46, 129.90, 129.37, 125.84, 117.82, 114.91, 105.01, 55.39, 41.15, 34.40.

(*E*)-3-(4-hydroxy-3,5-dimethoxyphenyl)-*N*-(3-methoxyphenethyl)acrylamide **12**

(yield ~ 75%) **IR** (cm^{-1}): 3282, 2938, 2839, 2252, 1655, 1602, 1513, 1490, 1455, 1425, 1320, 1285, 1259, 1209, 1153, 1112, 1061, 1038, 976, 907, 828, 780 and 696; **^{1}H NMR** (500 MHz, $CDCl_3$) δ 7.52 (d, *J* = 15.5 Hz, 1H), 7.22 (t, *J* = 7.9 Hz, 1H), 6.79 (dd, *J* = 16.6, 6.9 Hz, 3H), 6.70 (s, 2H), 6.27 (d, *J* = 15.5 Hz, 1H), 6.09 (s, 1H), 6.02 (s, 1H), 3.84 (s, 6H), 3.77 (s, 3H), 3.69 – 3.61 (m, 2H), 2.86 (t, *J* = 6.7 Hz, 2H); **^{13}C NMR** (126 MHz, $CDCl_3$) δ 166.23, 159.79, 147.24, 141.12, 140.59, 136.63, 129.64, 126.29, 121.11, 118.66, 114.53, 111.80, 104.79, 56.26, 55.18, 40.71, 35.71.

Synthesis of **13** *to* **24**

General Procedure: The unsaturated tyramine derivative (**1** to **12**) (0.045 g, 0. 150 mmol) is dissolved in MeOH (1.5 ml) and to this solution, palladium on carbon 5% (0.010 g, 0.0944 mmol) is added and purged with hydrogen gas. The resulting solution is stirred for 12 h at room temperature under hydrogen atmosphere (with H_2 filled balloon). After 12 h, the reaction mixture is filtered using celite, washed with methanol and the combined fractions were concentrated and purified by flash column chromatography using chloroform and methanol (94:6) to yield the saturated amide derivatives (**13** to **24**) in yield (70 to 90 %)

Data **13-24**:

N-(3,4-dihydroxyphenethyl)-3-(3,4-dihydroxyphenyl)propanamide **13**

(yield 79%) **IR** (cm^{-1}): 3314, 2935, 2501, 2073, 1599, 1517, 1481, 1440, 1359, 1282, 1199, 1152, 1115, 972, 870, 811 and 783; **^{1}H NMR** (500 MHz, MeOD) δ 6.69 (dd, *J* = 8.0, 1.2 Hz, 2H), 6.65 (dd, *J* = 5.7, 1.6 Hz, 2H), 6.52 (dd, *J* = 8.0, 1.6 Hz, 1H), 6.48 (dd, *J* = 7.9, 1.6 Hz, 1H), 3.33 – 3.27 (m, 2H), 2.75 (t, *J* = 7.6 Hz, 2H), 2.57 (t, *J* = 7.7 Hz, 2H), 2.39 (t, *J* = 7.7 Hz, 2H);

^{13}C NMR (126 MHz, MeOD) δ 174.07, 144.78, 143.26 (d, *J* = 15.9 Hz), 132.44, 130.71, 119.73, 119.24, 115.45, 115.17, 114.99, 114.98, 40.90, 38.06, 34.55, 31.09.

3-(3,4-Dihydroxyphenyl)-N-(4-hydroxyphenethyl)propanamide **14**

(yield 68%) **IR** (cm^{-1}): 3282, 2499, 1610, 1515, 1449, 1361, 1284, 1242, 1115, 976 and 819; **^{1}H NMR** (500 MHz, MeOD) δ 6.97 (d, *J* = 8.3 Hz, 2H), 6.69 (dd, *J* = 20.7, 11.9 Hz, 4H), 6.53 (d, *J* = 6.5 Hz, 1H), 3.32 (dd, *J* = 12.7, 5.1 Hz, 2H), 2.75 (t, *J* = 7.5 Hz, 2H), 2.63 (t, *J* = 7.3 Hz, 2H), 2.39 (t, *J* = 7.6 Hz, 2H); **^{13}C NMR** (126 MHz, MeOD) δ 174.03, 155.43, 144.81, 132.39, 129.93, 129.34, 119.24, 115.17, 114.95, 114.82, 40.92, 38.04, 34.32, 31.06.

3-(3,4-dihydroxyphenyl)-*N*-(3-methoxyphenethyl)propanamide **15**

(yield 86%) **IR** (cm^{-1}): 3276, 2938, 2491, 1595, 1515, 1453, 1437, 1360, 1282, 1201, 1166, 1152, 1116, 1061, 1038, 869, 812, 781, 743 and 696; **^{1}H NMR** (500 MHz, MeOD) δ 7.18 (t, *J* = 8.0 Hz, 1H), 6.71 (ddd, *J* = 21.9, 13.9, 4.1 Hz, 5H), 6.55 – 6.48 (m, 1H), 3.76 (s, 3H), 3.40 – 3.32 (m, 3H), 2.72 (dt, *J* = 20.7, 7.3 Hz, 4H), 2.39 (t, *J* = 7.6 Hz, 2H); **^{13}C NMR** (126 MHz, MeOD) δ 174.08, 159.85, 144.81, 143.23, 140.67, 132.40, 129.06, 120.78, 119.23, 115.19, 114.99, 113.95, 111.45, 54.21, 40.52, 38.05, 35.21, 31.07.

N-(3,4-Dihydroxyphenethyl)-3-(3-methoxyphenyl)propanamide **16**

(yield 91%) **IR** (cm^{-1}): 3280, 2939,2507, 1627, 1602, 1519, 1485, 1465, 1455, 1440, 1359, 1278, 1260, 1197, 1152, 1116, 1049, 872, 784 and 697; **^{1}H NMR** (500 MHz, MeOD) δ 7.18 (t, *J* = 8.0 Hz, 1H), 6.81 – 6.73 (m, 3H), 6.69 (d, *J* = 8.0 Hz, 1H), 6.64 (d, *J* = 1.4 Hz, 1H), 6.47 (d, *J* = 6.4 Hz, 1H), 3.78 (s, 3H), 3.32 (t, *J* = 7.6 Hz, 2H), 2.87 (t, *J* = 7.6 Hz, 2H), 2.58 (t, *J* = 7.3 Hz, 2H), 2.45 (t, *J* = 7.3 Hz, 2H); **^{13}C NMR** (126 MHz, MeOD) δ 173.77, 159.85, 144.85, 143.36, 142.35, 130.65, 129.04, 120.32, 119.66, 115.43, 114.96, 113.66, 111.26, 54.17, 40.88, 37.53, 34.54, 31.62.

N-(4-hydroxyphenethyl)-3-(3-methoxyphenyl)propanamide **17**

(yield 95%) **IR** (cm^{-1}): 2947, 2868, 1635, 1614, 1516, 1455, 1362, 1261, 1261, 1207, 1153, 1087, 1015, 831, 780 and 697; **^{1}H NMR** (500 MHz, MeOD) δ 7.18 (t, *J* = 8.0 Hz, 1H), 6.96 (d, *J* = 8.3 Hz, 2H), 6.82 – 6.74 (m, 3H), 6.71 (d, *J* = 8.4 Hz, 2H), 3.77 (s, 3H), 3.35 – 3.29 (m, 2H), 2.87 (t, *J* = 7.6 Hz, 2H), 2.62 (t, *J* = 7.6 Hz, 2H), 2.45 (t, *J* = 7.6 Hz, 2H); **^{13}C NMR** (126 MHz, MeOD) δ 173.71, 159.86, 155.51, 142.36, 129.86, 129.33, 129.07, 120.37, 114.85, 113.70, 111.29, 54.20, 40.93, 37.50, 34.33, 31.60.

N-(3-methoxyphenethyl)-3-(3-methoxyphenyl)propanamide **18**

(yield 77%) **IR** (cm^{-1}): 3294, 2937, 1644, 1602, 1585, 1547, 1490, 1455, 1260, 1152, 1041, 874, 780 and 696; **^{1}H NMR** (500 MHz, MeOD) δ 7.18 (dd, *J* = 10.6, 5.4 Hz, 2H), 6.82 – 6.72 (m, 6H), 3.78 (s, 6H), 3.40 – 3.35 (m, 2H), 2.87 (t, *J* = 7.7 Hz, 2H), 2.71 (t, *J* = 7.3 Hz, 2H), 2.46 – 2.42 (t, *J* = 7.3 Hz, 2H); **^{13}C NMR** (126 MHz, MeOD) δ 173.76, 159.86, 142.33, 140.64, 129.03, 120.72, 120.30, 113.98, 113.67, 111.39, 111.24, 54.16, 40.49, 37.51, 35.20, 31.60.

N-(3,4-Dihydroxyphenethyl)-3-(4-hydroxy-3-methoxyphenyl)propanamide **19**

(yield 89%) **IR** (cm^{-1}): 3338, 2938, 2500, 1600, 1516, 1465, 1449, 1362, 1275, 1153, 1123, 1034, 976, 870 and 814; **^{1}H NMR** (500 MHz, MeOD) δ 6.78 (d, *J* = 1.7 Hz, 1H), 6.72 (d, *J* = 8.0 Hz, 1H), 6.69 (d, *J* = 8.0 Hz, 1H), 6.63 (dd, *J* = 5.8, 1.9 Hz, 2H), 6.46 (dd, *J* = 8.0, 1.9 Hz, 1H), 3.83 (s, 3H), 3.30 (d, *J* = 7.6 Hz, 2H), 2.81 (t, *J* = 7.6 Hz, 2H), 2.58 (t, *J* = 7.7 Hz, 2H), 2.42 (t, *J* = 7.7 Hz, 2H); **^{13}C NMR** (126 MHz, MeOD) δ 174.01, 147.48, 144.85, 144.46, 143.36, 132.37, 130.65, 120.40, 119.68, 115.42, 114.97, 114.77 111.72, 54.95, 40.88, 38.02, 34.56, 31.28.

3-(4-Hydroxy-3-methoxyphenyl)-N-(4-hydroxyphenethyl)propanamide **20**

(yield 91%) **IR** (cm^{-1}): 3279, 2938, 2499, 1627, 1613, 1596, 1515, 1465, 1452, 1436, 1363, 1236, 1153, 1125, 1034 and 822; **^{1}H NMR** (500 MHz, MeOD) δ 6.95 (d, *J* = 8.4 Hz, 2H), 6.78

(d, *J* = 1.7 Hz, 1H), 6.74 – 6.69 (m, 3H), 6.64 (dd, *J* = 8.0, 1.7 Hz, 1H), 3.84 (s, 3H), 3.33 – 3.28 (m, 2H), 2.81 (t, *J* = 7.5 Hz, 2H), 2.62 (t, *J* = 7.3 Hz, 2H), 2.42 (t, *J* = 7.5 Hz, 2H); **^{13}C NMR** (126 MHz, MeOD) δ 173.97, 155.47, 147.48, 144.50, 132.33, 129.88, 129.33, 120.44, 114.83, 114.77, 111.75, 54.95, 40.91, 37.98, 34.32, 31.23.

3-(4-Hydroxy-3-methoxyphenyl)-N-(3-methoxyphenethyl)propanamide **21**

(yield 90%) **IR** (cm^{-1}): 2937, 2488, 1631, 1600, 1516, 1465, 1433, 1363, 1260, 1153, 1125, 1037, 854, 787 and 697; **^{1}H NMR** (500 MHz, MeOD) δ 7.17 (dd, *J* = 8.8, 7.6 Hz, 1H), 6.81 – 6.74 (m, 3H), 6.72 (d, *J* = 7.9 Hz, 2H), 6.63 (dd, *J* = 8.0, 1.8 Hz, 1H), 3.83 (s, 4H), 3.78 (d, *J* = 7.9 Hz, 3H), 3.37 (t, *J* = 7.3 Hz, 2H), 2.81 (t, *J* = 7.6 Hz, 2H), 2.70 (t, *J* = 7.3 Hz, 2H), 2.42 (t, *J* = 7.6 Hz, 2H); **^{13}C NMR** (126 MHz, MeOD) δ 174.00, 159.87, 147.48, 144.51, 140.64, 132.32, 129.05, 120.74, 120.41, 114.78, 113.96, 111.73, 111.42, 54.95, 54.18, 40.50, 37.99, 35.21, 31.24.

N-(3,4-Dihydroxyphenethyl)-3-(4-hydroxy-3,5-dimethoxyphenyl)propanamide **22**

(Yield 87%) **IR** (cm^{-1}): 3348, 2939, 2499, 1611, 1519, 1461, 1345, 1282, 1215, 1114, 977 and 814; **^{1}H NMR** (500 MHz, MeOD) δ 6.68 (d, *J* = 8.0 Hz, 1H), 6.63 (d, *J* = 1.9 Hz, 1H), 6.52 – 6.47 (m, 2H), 6.45 (dd, *J* = 8.0, 1.9 Hz, 1H), 3.82 (s, 6H), 3.33 – 3.29 (m, 2H), 2.82 (t, *J* = 7.5 Hz, 2H), 2.75 (t, *J* = 7.6 Hz, 2H), 2.43 (t, *J* = 7.6 Hz, 2H); **^{13}C NMR** (126 MHz, MeOD) δ 173.96, 147.80, 144.85, 143.36, 133.50, 131.62, 130.63, 119.67, 115.41, 114.97, 105.25, 55.33, 40.90, 37.99, 34.58, 31.74.

3-(4-Hydroxy-3,5-dimethoxyphenyl)-N-(4-hydroxyphenethyl)propanamide **23**

(Yield 91%) **IR** (cm^{-1}): 2941, 2506, 2189, 2028, 1621, 1603, 1512, 1486, 1456, 1437, 1351, 1328, 1260, 1242, 1139, 1050, 969, 837 and 757; **^{1}H NMR** (500 MHz, MeOD) δ 6.94 (d, *J* = 8.4 Hz, 2H), 6.70 (d, *J* = 8.4 Hz, 2H), 6.48 (s, 2H), 3.83 (s, 7H), 3.36 – 3.30 (m, 4H), 2.82 (t, *J* = 7.5 Hz, 2H), 2.62 (t, *J* = 7.3 Hz, 2H), 2.43 (t, *J* = 7.5 Hz, 2H); **^{13}C NMR** (126 MHz, MeOD) δ

173.89, 155.36, 147.75, 133.49, 131.57, 129.87, 129.38, 114.92, 105.27, 55.51, 40.98, 38.07, 34.40, 31.80.

3-(4-Hydroxy-3,5-dimethoxyphenyl)-N-(3-methoxyphenethyl)propanamide **24**

(Yield 89%) **IR** (cm^{-1}): 3299, 2938, 2838, 2496, 1633, 1603, 1518, 1458, 1429, 1326, 1259, 1213, 1152, 1114, 1040, 908, 830, 785 and 697; **^{1}H NMR** (500 MHz, MeOD) δ 7.21 – 7.14 (m, 1H), 6.75 (d, *J* = 6.0 Hz, 2H), 6.70 (d, *J* = 7.5 Hz, 1H), 6.49 (s, 2H), 3.82 (s, 7H), 3.77 (s, 3H), 3.37 (t, *J* = 7.3 Hz, 2H), 2.82 (t, *J* = 7.5 Hz, 2H), 2.70 (t, *J* = 7.3 Hz, 2H), 2.43 (t, *J* = 7.5 Hz, 2H); **^{13}C NMR** (126 MHz, MeOD) δ 173.95, 159.87, 147.81, 140.62, 133.57, 131.57, 129.05, 120.72, 113.96, 111.41, 105.29, 55.33, 54.18, 40.52, 37.96, 35.23, 31.70.

Preparation of the tyramine-enriched extract of L. chinense

The root bark of *L. chinense* (2 Kg) was extracted with methanol (8 L) at room temperature to get the methanolic extract (345.5 g). This methanolic extract was suspended in water and successively partitioned between hexanes and ethyl acetate to obtain hexane extract and ethyl acetate extract (35.1 g). This ethyl acetate extract (33 g) was acidified with 5% HCl in water (approx. 1 L) and extracted with ethyl acetate (3x300 mL) to get ethyl acetate fraction (20.6 g). This ethyl acetate fraction (18.0 g) was subjected to Sephadex LH-20 column chromatography with $CHCl_3$:MeOH 1:1 as a solvent to get three fractions (1-3). Fraction 3 (6.49 g) was further chromatographed over Sephadex LH-20 column chromatography with MeOH to get three fractions. The tyramine derivative enriched fraction was obtained as the third fraction, identified by performing comparative TLC using a pure tyramine derivative **08**.

3.3. PPAR *in vitro* assays

Chemical reagents and plasmids

Ciprofibrate and rosiglitazone **IV** were obtained from Cayman Chemical (Ann Arbor, MI). Dulbecco's Modified Eagle's Medium (DMEM), fetal bovine serum (FBS) and phosphate-buffered saline (PBS) were from Hyclone (South Logan, Utah). Penicillin/streptomycin and trypsin were from Gibco (Grand Island, NY). Specific plasmids pSG5–PPARα (plasmid 22751) and PPRE X3-tk-luc (plasmid 1015) were obtained from Addgene (Cambridge, MA). pCMV-rPPARγ and pPPREaP2-tk-luc were provided by Dr. Dennis Feller (Department of Pharmacology, University of Mississippi).

Reporter gene assay for the activation of PPARs

Cell-based reporter gene assay for the identification of PPARα and PPARγ agonists was carried out in human hepatoma (HepG2) cells as described previously [106, 107]. Briefly, HepG2 cells were cultured in Dulbecco's Modified Eagle's Medium (DMEM) supplemented with 10% fetal bovine serum (FBS), 100 units/mL penicillin, and 100 μg/mL streptomycin in a humidified atmosphere of 5% CO2 at 37°C. HepG2 cells were transfected with either pSG5-PPARα and PPRE X3-tk-luc or pCMV-rPPARγ and pPPREaP2-tk-luc plasmid DNA (25 μg of each/1.5 mL cell suspension) by electroporation at 160 V for a single 70 msec pulse using a BTX Electro Square Porator T820 (BTX, San Diego, CA). Transfected cells were plated at a density of 5 × 104 cells/well in 96-well tissue culture plates and grown for 24 h. The cells were treated with the test compounds or ciprofibrate or rosiglitazone IV (3, 10, 30 μM). After incubation for 24 h, the cells were lysed and the luciferase activity was measured using a luciferase assay system

(Promega, Madison, WI). The fold activation of luciferase activity in treated cells was calculated in comparison to the vehicle control.

3.4 *In vivo* testing

Materials

Diabetic db/db mice were employed and measurements were made using EchoMRI to obtain the measurements of the whole body fat, lean, free water, total water masses. Transmitters were used to record the blood pressure, heart rate. *In vitro* testing was performed by our collaborators at University of Mississippi Medical Center, Jackson, MS (USA).

Methods

Diabetic db/db mice were used for *in vivo* testing of pure phenolic amide compound **8** and the amide enriched extract which contains 21% of the four amide derivatives.

Dosage calculations: The dosage for high dose group mice was given 32mg/Kg and medium dose group was 8 mg/kg. All the db/db mice were followed for one to two weeks control period before treatment was started. In the medium dose group (n=6), 3 mice received the drug, 3 mice received the extract; where as in the high dose group (n=8), 3 mice received vehicle, 3 mice received drug (1 died during treatment), 3 mice received extract. Medium dose group was monitored with EchoMRIs performed during control and experimental periods to test the body composition analysis, measuring whole body fat, lean, free water, and total water masses. High dose group was implanted with transmitters to record the blood pressure and heart rate 24-hr/day for 3 consecutive days. Animals were dosed daily by gavage.

CHAPTER 4

STEREOSELECTIVE SYNTHESES OF BIOACTIVE ISOFLAVANS: EQUOL AND SATIVAN

1. Introduction

1.1. Isoflavonoids: Structures and classes

Flavonoids are one of the main groups of phytochemicals, with a general structure with two phenyl rings and one pyran rings containing C15 (C6-C3-C6) (**Figure 4-1**). They can be further subdivided into flavonoids (general term) and isoflavonoids. Isoflavonoids are secondary metabolites of plants, mainly belonging to the subfamily *Papilionoideae* of *Leguminosae* and to a lesser extent in other families. These class of compounds act as phytoalexins and were also found to possess various biological activities [108]. Isoflavonoids contain a large class of compounds; over 2000 isoflavonoids belonging to 14 classes and 23 subclasses, based on their structural arrangements [108-113]. These classes include: isoflavones, isoflavanones, rotenoids, pterocarpans, isoflavans, isoflav-3-enes, 3-arylcoumarins, coumestans, coumaronochromones, 2-arylbenzofurans.

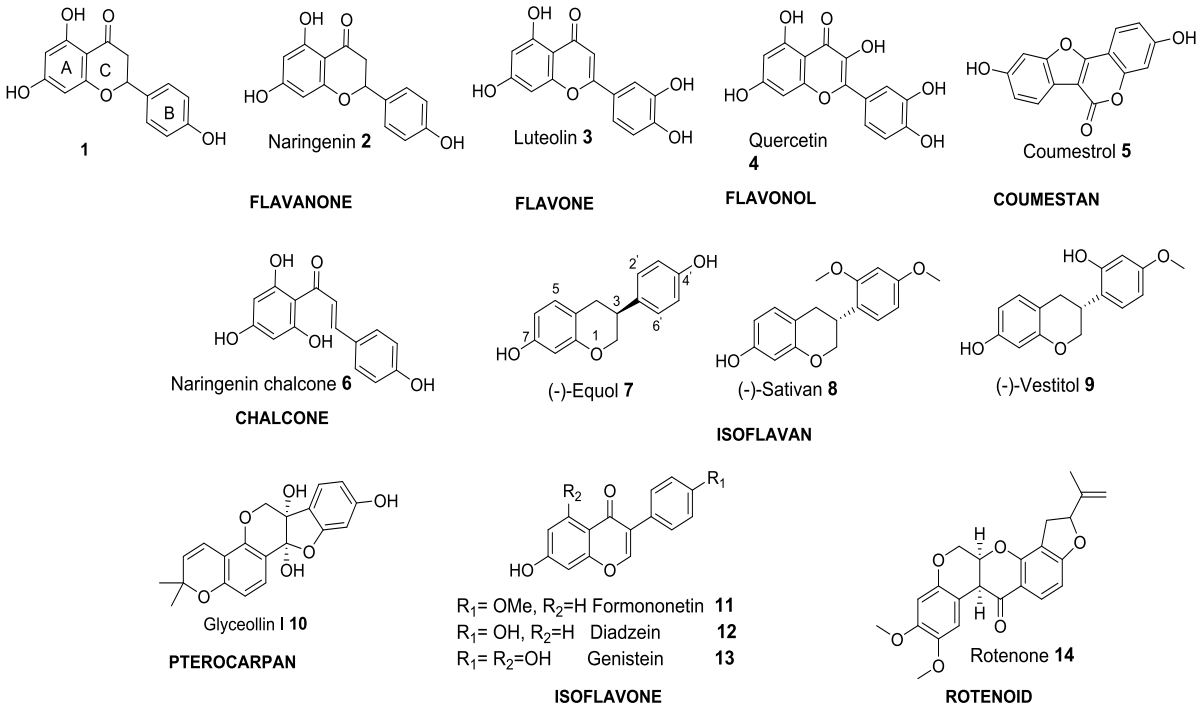

Figure 4-1. Examples of different classes of flavonoids including the isoflavonoids (isoflavans and isoflavones [102].

Among the isoflavonoid-subclasses, isoflavans are characterized by: chirality at the C-3 position of the pyran ring (C-ring). These isoflavans are produced in plants or animals upon the double reduction of isoflavanoids (eg. formonentin **11**, daidzein **12** and genistein **13**). There are a number of isoflavans, including equol **7**, sativan **8**, vestitol **9**, coluteol **15**, lespedezol G_1 **16** and lespecyrtin D_1 **17** with unique, promising biological activities are reported in the literature.

1.2. Equol **7** and Soy isoflavonoids as Phytoestrogens

Soy isoflavonoids: Historical relevance

Soy isoflavonoids were used in traditional foods in Japan and China for many millennia. Soybean (Glycine max (L.) Merr.) (**Figure 4-2**), also called “Shu” in ancient Chinese, is one of the five main plant foods in China along with rice, wheat, barley and millet. Soya bean is of

comemricial interest due to its oil and protein content [114]. Soy protein is a highly digestible protein, with a Protein Digestibility Corrected Amino Acid Score (PDCAAS) =1, highest among vegetable proteins. Since a couple of decades, soy gained a lot of interest as functional food due to its isoflavone content. Soy related food industry was given a good a great boost on October 26, 1999, when the FDA issued a ruling, based on the scientific evidences on soy protein, which states that "diet low in saturated fat and that includes 25 g of soy protein a day may reduce the risk of heart disease". In the ruling, FDA proposed that, in order to qualify for this health claim the soy food should contain 6.25 g soy protein per serving [114].

Figure 4-2. The soybean pods, soybean seeds and Tofu [115].

Note: Image obtained from He *et al* 2013 [115].

Among the legumes, soy contain largest amount of isoflavones, which act as phytoestrogens. These isoflavones are genistein **13**, daidzein **12**, glycitein, and formononetin **11** and are present in their glycosidic forms as genistin, diadzin, and glycetin with a total flavone content of 61.7 mg of diadzein (37.6 mg) and genistern (24.1 mg) per kg of dry weight [116]. These soy isoflavonoids which is present in physiologically relevant concentrations especially genestin, are found to be beneficial to treat a number of diseases including heart conditions, post-menopausal symptoms, women health and breast cancer [117].

Metabolites of isoflavones: Equol **7**

Soy isoflavonoids undergo transformation in the digestive system, especially in the colon

where these undergo transformation to other metabolites like deglucogenated products, and by the action of gut bacteria into derivatives like equol (**Figure 4-3**). Equol **7** has higher affinity to estrogen receptor (ER), than its precursor isoflavones, genistin **13** or daidzein **12**, and was found to possess varied biological activities. There are large differences in the metabolism rates of genistein **13** and daidzein **12** between the caucasian population and in Asian population. It was found that among the general population, only approximately 30–50% is able to metabolize daidzein **12** to equol **7** and among the U.S. Caucasian population, only 25–35% is capable of converting daidzein **12** to equol **7** [118]. Whereas, among the Asian people in high soy consumption areas, 40–60% are capable of converting daidzein **12** to equol **7**. Prevalence of daidzein-metabolizing phenotypes differs between Caucasian and Korean American women and girls [118]. This high variability in equol **7** production is presumably due to inter-individual differences in the composition of the intestinal microflora such as *Adlercreutzia equolifaciens* [119]. Racemate of equol **7** may not show the same activities as that of enatiomeric forms as shown in the pharmacokinetic studies on this compound [120].

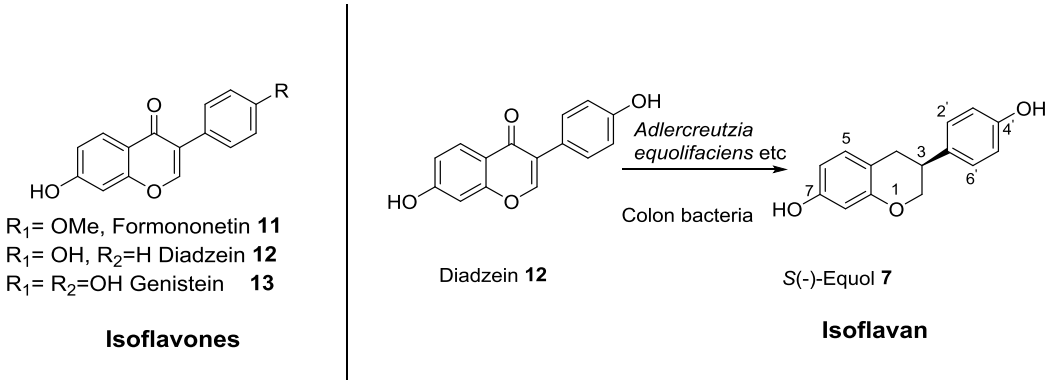

Figure 4-3. Soy isoflavonoids: Isoflavones (formonentin **11**, diadzein **12**, genistein **13**) and isoflavan (*S*-(-)-equol **7**.

History of equol **7** and isoflavans

Equol **7** was the first discovered isoflavan, isolated from equine urine [121, 122] unexpectedly (a dialcohol from equine urine, hence the name equol **7**), in an attempt to isolate estrogen, and was later isolated in the urine of other animals [123] and in humans [124], in 1980. Its absolute configuration as a *S*-isomer was assigned in 1968, after the identification of some isoflavans from plant sources [125]. It was found to be produced seteroselcetively (*S*-equol **7**) in humans, from the dietary soy isoflavonoid aglycone, daidzein **12,** by the action of gut bacteria [119]. It binds to estrogen receptors [126], immunoglobulin E (IgE) induced receptor [127], and the circulating 5α-dihydrotestosterone (DHT) [128]. Since its discovery, equol **7** was shown to possess a wide variety of biological activities such as anti-fungal [129], anti-cancer [130], anti-osteoporotic, anti-androgen [128], anti-inflammatory, anti-oxidant and anti-aging properties [131], promote brain mitochondrial function [132], inhibit prostate growth [128], and hence it is widely considered as a dietary phytoestrogen along with daidzein **12** and genistein **13** [133]. Interestingly, (*S*)-equol **7** is 13 times more selective to ERβ when compared to ERα [126, 133, 134]. Further studies of its biological and clinical properties is an area of immense interest, including our own [135, 136].

Other Isoflavans

Several other isoflavans were isolated from plant sources since the first discovery of (+)-vestitol **9**, (-)-duartin, (-)-mucronulatol in 1968 in *Dalbergia variabilis* and several *Macherium* species [125]. Isoflavans with plant origin have oxygen at C2' and almost never have oxygenation at C5 [137]. Some examples of isoflavans are sativan **8**, which was first isolated as an induced isoflavan from the leaves of *Medicago sativa* [138, 139], and later in *Lotus corniculatus [140]*, colutelol **15** from the roots of *Colutea arborescens [141]*, lespedezol G_1 **9** from the stems of *Lespedeza homoloba* [142], and lespecyrtin D_1 **17** from the root extracts of *Lespedza cyrtobotry* [143] (**Figure 4-4**).

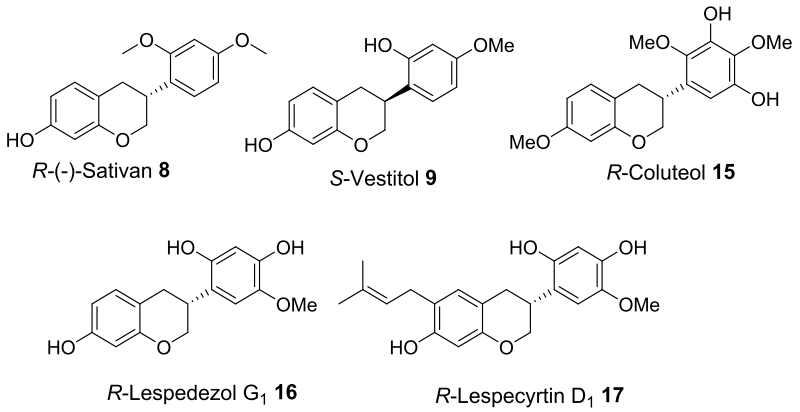

Figure 4-4. Naturally occurring phytoestrogenic isoflavans (**9**, **15-17**).

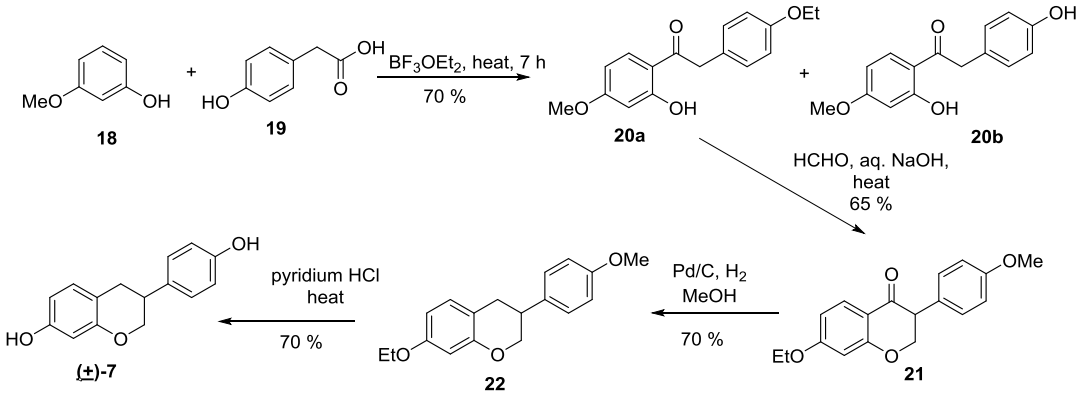

Scheme 4-1. Synthesis of racemic equol (±) **7** by Friedel-Crafts acylation of protected monomethoxy resorcinol, **18** [144].

Reported syntheses of Isoflavans

Given the desirable biological properties of isoflavans, their enantioselective large scale synthesis enables these isoflavans to study further for their biological, metabolic and pharmacokinetic studies. Several syntheses of isoflavans have been reported; majority of these produced the product in a racemic form [145-147], followed by their chiral separation. These include, catalytic hydrogenation of isoflavans using Pd catalysts at different solvent and pH conditions [148, 149]. Multistep total syntheses of racemic mixture of a number of isoflavans [150] were also reported including 5-*O*-methyllicoricidin [151], halogen substituted isoflavans and isoflavenes [152].

Racemic synthesis of equol **7**

Equol **7** was synthesized as a racemate from formononetin **11** and daidzein **12** using Pearlman's catalyst (20% $Pd(OH)_2$ on C) followed by separation using chiral HPLC [134], and by bacterial transformation [153] using bacteria isolated from human intestinal bacterium. Sie-Rong Li and co-workers [154] reported the racemic synthesis of equol **7** along with isoflavonoids; haginin E, formononetin **11** and daidzein **12** from resorcinol **18** *via* a common isoflavenene intermediate. (**Scheme 4-1**).

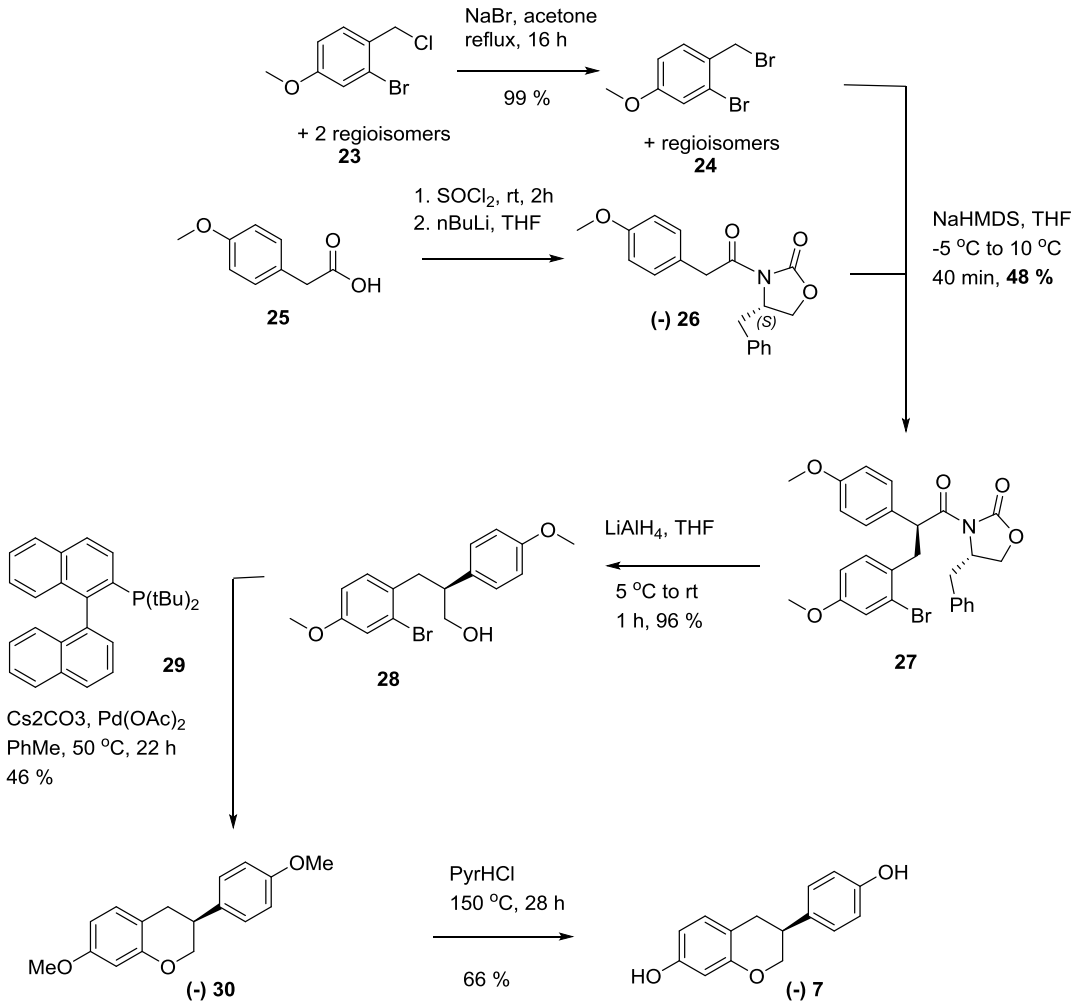

Scheme 4-2. Total synthesis of enantiopure (*S*)-equol **7** by an asymmetric Evans' alkylation [149, 155].

Enantioselective synthesis of equol **7**

Very few enantioselective syntheses of isoflavans were reported, and most of them were for the synthesis of (*S*)-equol **7**. Ferreira and co-workers [156, 157] have demonstrated the enantioselective synthesis of the dimethoxy analogue of (*S*)-equol *via* α-benzylation of *N*-acyl imidazolidinones. However, due to the unstable nature of alkoxy benzyl halide, only small quantities of dimethoxy equol was reported and the nontrivial cleavage of the methyl ethers was not attempted.

In 2006, Heemstra *et al.* [155] reported the first enantioselective total synthesis of (*S*)-

equol **7**. The described route relies on an Evans' alkylation to form the required C-3 stereocenter and an intramolecular Buchwald etherification to generate the chroman ring. However, the key transformations such as Evans' alkylation of oxazolidinone with regiomeric mixture of bromobenzyl bromide and palladium catalyzed Buchwald etherification had produced less than 50% conversion with an overall yield < 10% (**Scheme 4-2**).

Takashima *et al*. reported [158, 159] the stereoselective synthesis of three isoflavans, *S*-equol **7**, *R*-sativan **8** and *R*-vestitol **9** using allylic substitution as the chirality transfer step with the copper reagent derived form PhMgBr and CuBr.Me_2S. Mitsnobu cyclization was subsequently utilized for the formation of the chroman ring (**Scheme 4-3**). Recently, Yang S. *et al*, reported the enantioselective iridium catalyzed hydrogenation [160] of α-arylcinnamic acids and applied the same methodology for the synthesis of (*S*)-equol **7** at an overall yield of 48%.

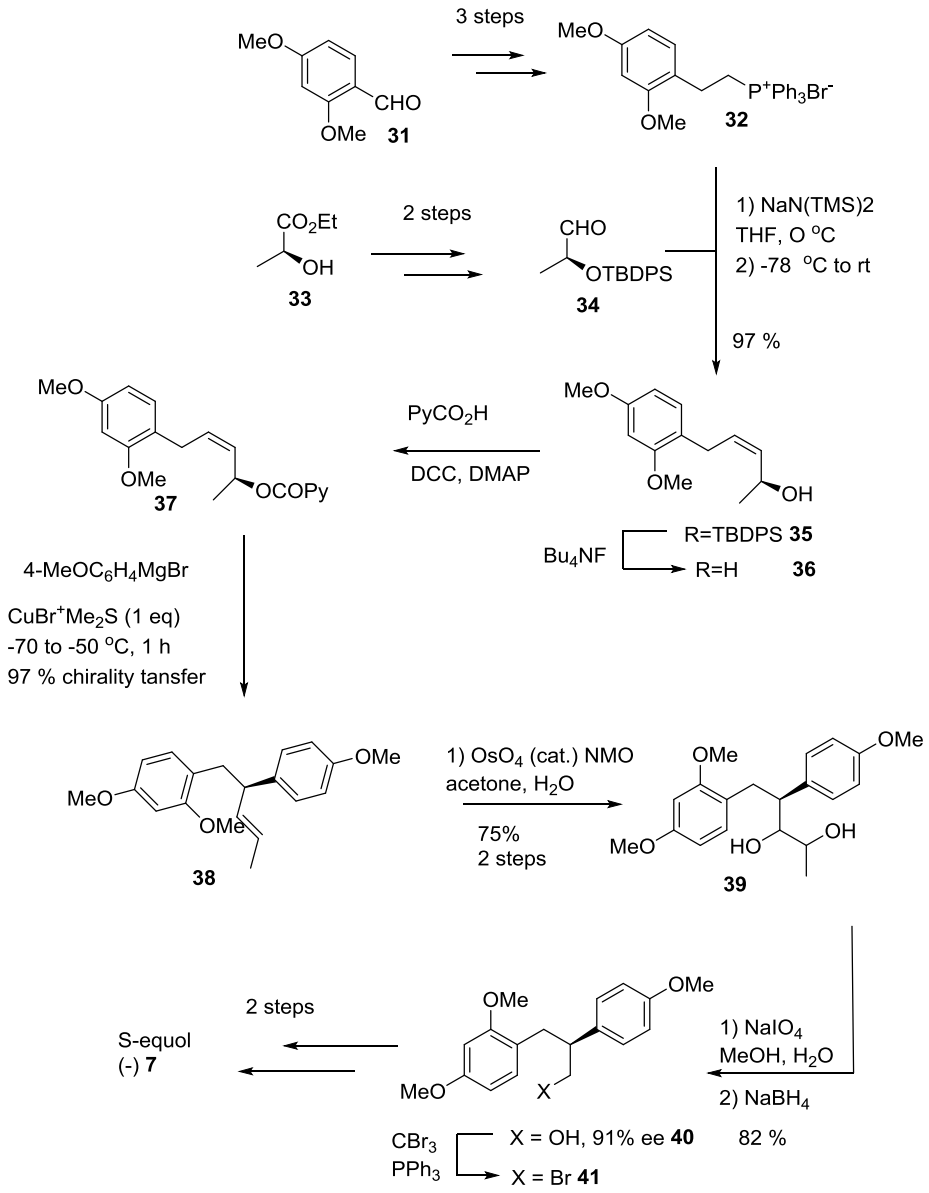

Scheme 4-3. Enantioselective total synthesis of (S)-equol **7** uisng allylic substitution as the key step with an overall yield of approximately 24% [149, 159].

1.3. Aim

In continuation of our work (for biological testing using enantiopure compounds) on phytoestrogens for women health, several grams of enantiomerically pure *S*-equol **7** and other chiral isoflavans were required. To address this need, herein, we report a scalable enantioselective synthesis of isoflavans, equol enantiomers, (-)-**7**, (+)-**7**, sativan isomers (-)-**8** and

(+)-**8** were synthesized using Evans' aldol approach (**Figure 4-5**). Unlike, the poor selectivity in Evans' alkylation [155], excellent stereoselectivity was expected with Evans' chiral imide enolate aldol condensation.

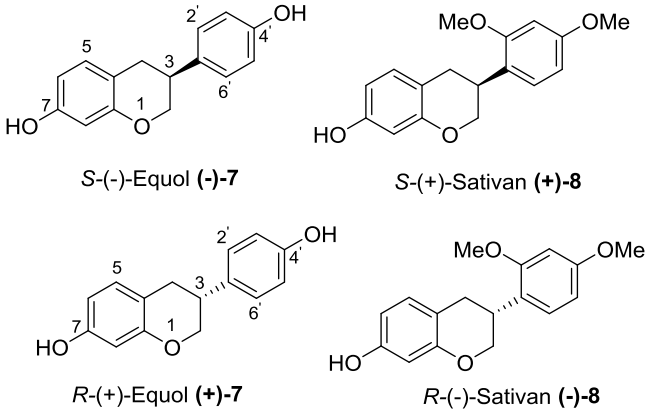

Figure 4-5. Structures of the synthesized isoflavans.

2. Results and Conclusion

2.1. Retrosynthetic scheme

Scheme 4-4 describes the retrosynthetic analysis of the chiral isoflavan scaffold. The key intermediate, *syn*-aldol product **44** (for intermediate to produce S-equol) or **45** (for intermediate to produce sativan **8)** can be obtained via Evan's aldol reaction between aldehydes (**46** or **47**) and chiral-auxiliary substituted imides (**26** or **48**). Deoxygenation of aldol product, followed by reduction would furnish hydroxy phenols **42** (for intermediate to produce equols) and **43** (intermediate to produce sativans). Cyclization under Mitsnobu conditions or base catalysis of the corresponding ditosyl derivative, followed by deprotection would produce the isoflavans, equol **7** and sativan **8**.

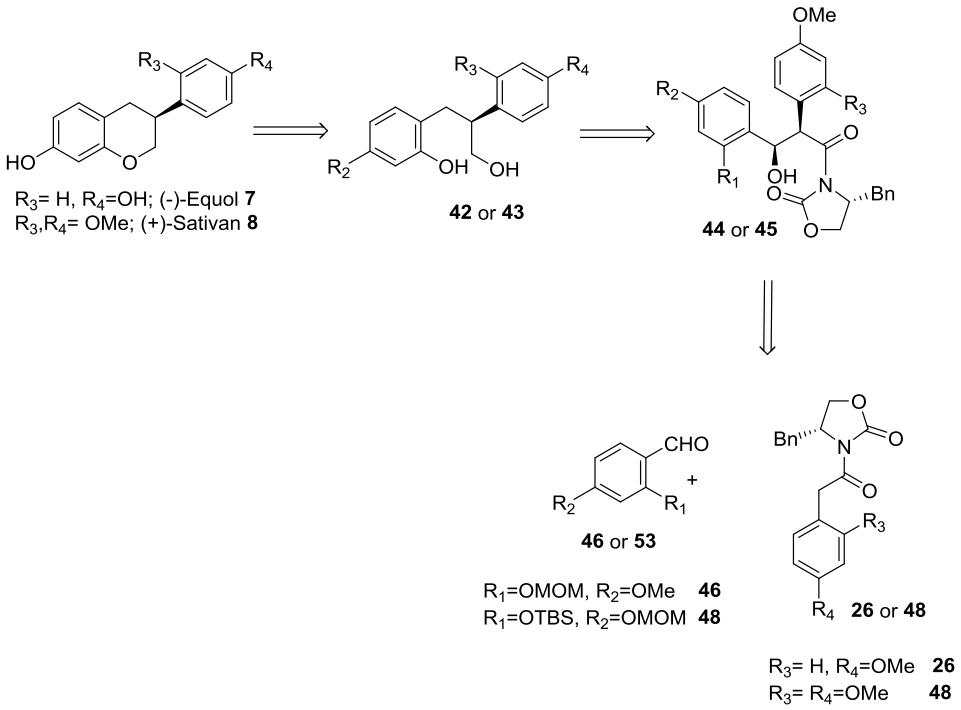

Scheme 4-4. Retro synthetic scheme for the synthesis of isoflavans, equol **7** and sativan **8** using Evans' aldol condensation to generate the chirality at C-3 position.

2.2. Synthesis of the starting materials for Evans' aldol condensation (**26**, **48**; **46**, **47**).

The crucial starting materials required for Evans' aldol reaction are benzoxazolidinone derived amides of phenyl acetic acids and oxygenated benzaldehydes. The chiral amides (-), (+)-**26** and (-), (+)-**48** were synthesized by following reported methods, in which the phenyl acetic acids were activated as acid chloride with thonyl chloride or mixed anhydride with pivolyl cholride and the resulting anhydrides were treated with respective oxazolidinone anions after treatment with BuLi. Four chiral auxiliary substituted imides (-), (+) **26** and (-), (+) **48** were synthesized according to the literature procedure [161]. The counter-part oxygenated aldehydes **46** and **47** were prepared from the commercially available starting material **51** and **52**. MOM protection of **51** at the *o*-hydroxy benzaldehyde produced **46**, while the sequential protection of **52** with MOMCl and TBSCl produced **47** (**Scheme 4-5**).

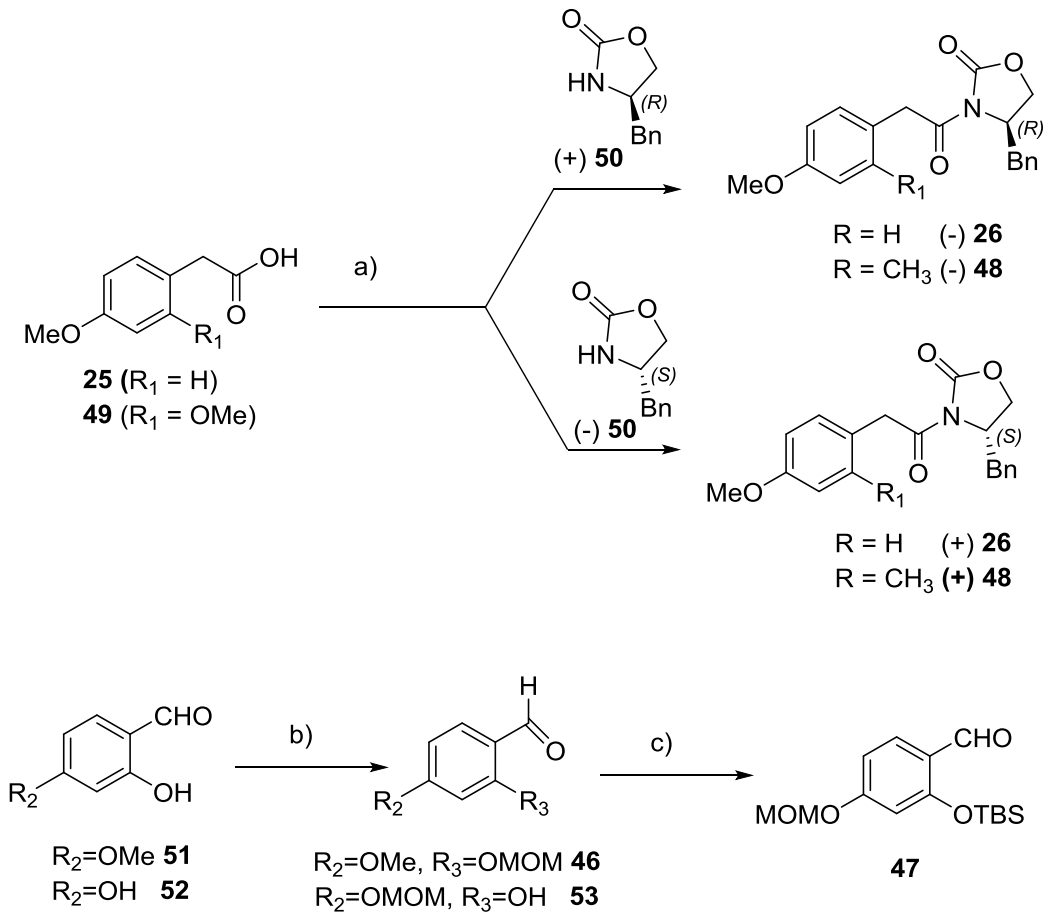

Scheme 4-5. Synthesis of the starting material for the stereo specific Evans' aldol reaction. Conditions: a) For **26** (as reported [161]) : **25**, $SOCl_2$, 2h; *n*-BuLi, -65 to -45 ^oC, **(+)** or (-) **50** in THF, 2 h, 73%; for **48**: **49**, pivolylchloride, DIPEA, THF, -78 ^oC; *n*-BuLi, (+) or (-) **50** in THF, -78 ^oC, 3 h, 91%; b) for **46**: **51**, MOMCl, DIPEA, DCM, rt, 20 h, 99%; for **53** (as reported [162]): **52**, MOMCl, K_2CO_3, acetone, rt, 24 h, 75%; c) For **47**: **53**, TBSCl, DIPEA/DCM, 0 ^oC, 1h; RT, 24 h, 99%.

2.3. Evans' aldol condensation

The synthetic venture for the synthesis of isoflavans commenced with diastereoselective Evans' aldol condensation [163-165] of benzaldehydes **46** and **47** with oxazolidinones **26** and **48**, respectively using Bu_2BOTf (**Scheme 4-6**). The generation of the enolate of the oxazolidone

derivatives were found to be affected by temperature; the enolate could not be generated below -25 °C and it decomposed above -10 °C.

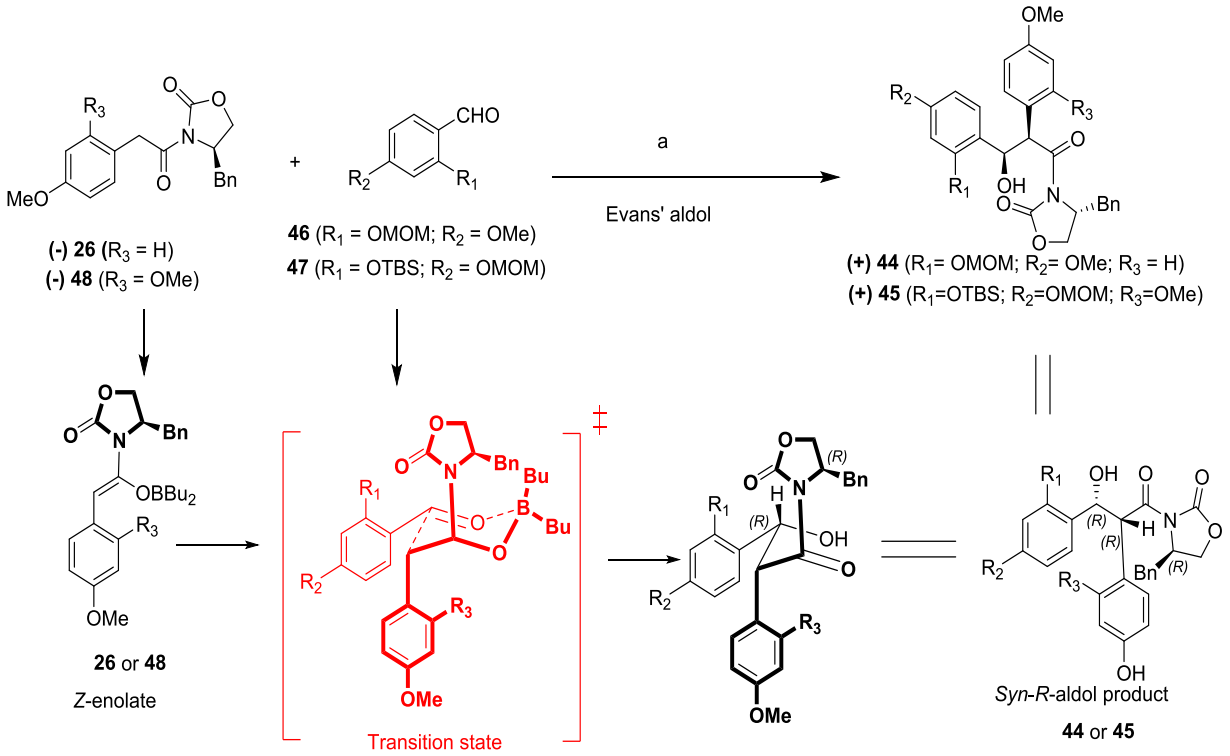

Scheme 4-6. Evans' aldol condensation to generate *R*-*syn*-aldol products (+) **44** and (+) **45** via Zimmerman-Traxler six membered chair-like transition state.

Conditions: a) DIPEA added to **26** or **48** in DCM at 0 °C; cooled to -25 °C; 1 M BBu_2OTf in DCM; -25 °C to -15 °C, 3 h/ DCM; add **46** or **47** in DCM, -25 °C to -15 °C 1.5 h, 80-90%.

The reaction of enolate from **26** with 4-methoxy-2-(methoxymethyl) benzaldehyde **46** furnished 2,3-*syn*-aldol product **44**. Similarly, the reaction of enolate from **47** with diprotected benzaldehyde **48** furnished 2,3-*syn*-aldol product **45** as a single diastereomer in 90% yield. The superior stereochemical outcome of the aldol reaction can be rationalized using a Zimmerman-Traxler six membered chair-like transition state **59** (**Scheme 4-6**). As anticipated, the facial selectivity of the aldehyde was directed by the chiral auxiliary of the enolate resulting in *re*-face attack to deliver Evans' *syn* aldol product.

2.4. Further reactions

The conversion of the aldol adducts (+) **44** and (+) **45** to natural products (-) equol **7** and (+)-sativan **8** require deoxygenation at the benzylic hydroxyl position, followed by the reduction of their chiral auxiliary to produce the dialcohols (+) **42** and (+) **43**, are further to be cyclized. The produced cyclized products, (-) **30** and (+) **57** should be deprotected in the C7 of the chroman ring to produce equol enantiomers (-)-**7** and (+)-sativan **8**, respectively (**Scheme 4-7**).

Deoxygenation

Several attempts to enable the dehydroxylation of the aldol products (+) **44** and (+) **45** in the presence of $Pd/C/H_2$ in EtOAc, $Pd/C/H_2$ in MeOH, $Pd(OH)_2/H_2$ in MeOH, $HCOONH_4$+$Pd/C/H_2$ in MeOH, NaH_2PO_2+ $Pd/C/H_2$ in THF+water and Raney Ni/H_2 in MeOH were unsuccessful or produced the required prodcuts in low quantities. Conversion of the benzylic hydroxyl group of these compounds to their corresponding tosylates were also unsuccessful. This is may be due to presence of electron rich aromatic system and possible chelation. Gratifyingly, deoxygenation of *syn*-aldol product using excess of triethylsilane in the presence of TFA, furnished the compounds in (+) **54** and (+) **56** in 75 to 80% yields, respectively. Next, the MOM group of (+) **54** was selectively deprotected using HCl in MeOH to obtain (+) **55** in 85% yield.

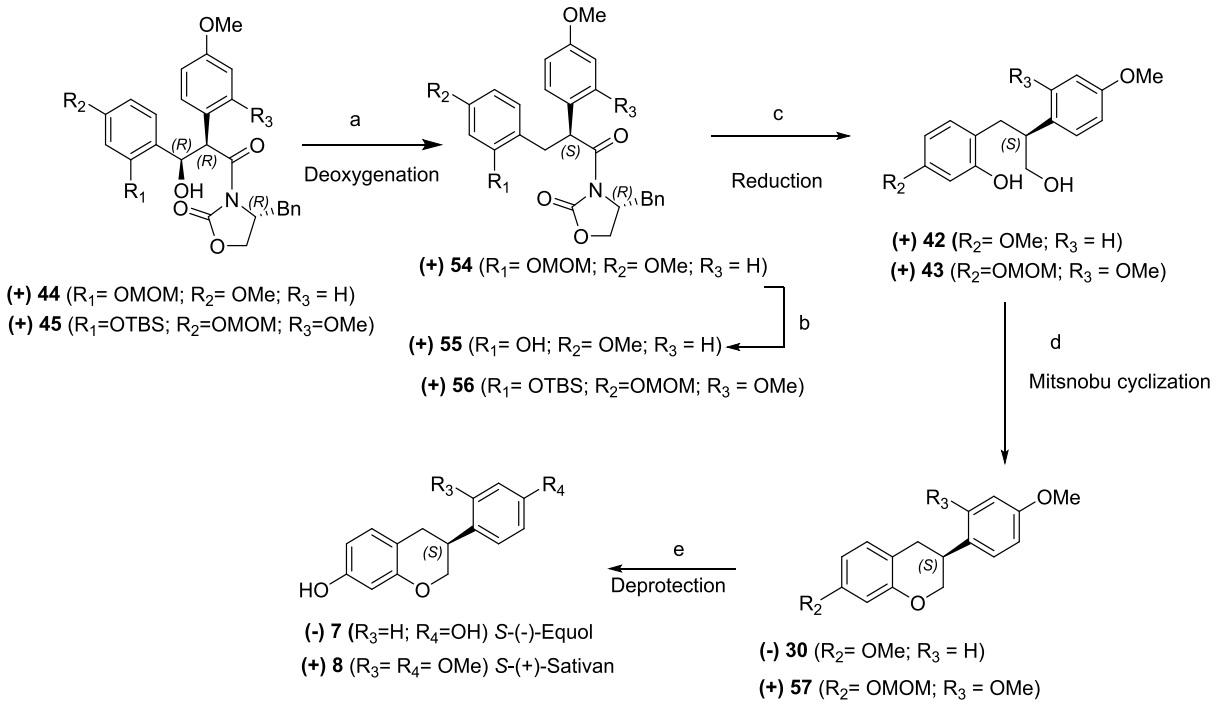

Scheme 4-7. Enantioselective synthesis of *S*-equol **7** and *S*-sativan **8** starting from Evans' aldol products **44** and **45.**

Conditions: a) TFA, Et_3SiH/DCM, 0 ^oC, 30 min (75-80%); b) 3N HCl in MeOH/reflux, 30 min, 85%; c) for **55**: $LiAlH_4$/ THF,0 ^oC to rt, 4 h, 90%; for **56**: $LiAlH_4$/THF,0 ^oC to rt, overnight, TBAF/THF, 89%; d) DEAD, TPP/THF, rt, 6 h, 86%; e). for **30**: Pyridinium.HCl/150 ^oC, overnight; for **57**: 3M HCl; rt, 0.5 to 0.75 h, 85%.

Reduction

The chiral auxialiary of the deoxygenated compound (+) **55** was reduced with LAH, to yield the diol product (+) **42** at an yield of 90%. Similarly, the chiral auxialiary of the deoxygenated compound (+) **56** was reduced with LAH, and further, the TBS group was deprotected using TBAF in THF to yield the diol (+) **43** in ~85% yield. Chiral auxiliaries were recovered further without any loss of their optical purity.

Cyclization and deprotection

The diols (+) **42** and (+) **43** were then cyclized using Mitsnobu conditions, DEAD and TPP in THF to the produce cyclic products (-) **30** and (+) **57** in ~92% and 86% yields,

respectively. The obtained dimethoxy analogues of equol (-) **30** and MOM protected analogues of sativan (+) **57** were then subjected to deprotection to yield the desired chiral products (-) **7** and (+) **8** at 86%yield.

*2.5. Synthesis of R-isomers of equol **7** and sativan **8***

Implementing the same synthetic sequences (**Scheme 4-6** and **4-7**), the stereoselective synthesis of *R*-isomers of equol (+)-**7** and sativan (-)-**8** (**Scheme 4-8**) were performed from their respective starting material, (-) **26** and (-) **48**, via aldol intermediates (-) **44** and (-) **45**, which were subjected to deoxygenation, deprotection, cyclization, and deprotection of the functional groups. The overall yield was 33% for *S*-(-) and *R*-(+)-equol (+)**7**, 34% for (+) **8** and about 25% for sativan (-) **8**, starting from their respective phenyl acetic acid-starting material.

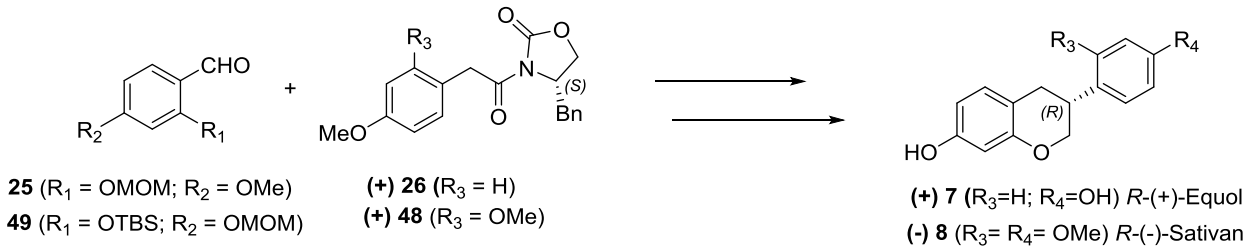

Scheme 4-8. General schemes for the synthesis of (+) equol **7** and (-) sativan **8**.

2.6. Conclusion

Chiral flavans were successfully synthesized starting for phenyl aceic acid and 4-benzyl-2-oxazolidine dinone. Reaction of boron enolates with oxygenated aldehydes resulted in *syn*-superior aldol products with excellent diastereoselectivity. This followed by deprotection, removal of chiral auxiliaries, cyclization and deprotections resulted chiral flavans in >30% overall yields This flexible synthetic approach allowed the synthesis of their antipodes by simply switching the chiral auxiliary.

3. Experimental

3.1. Materials and methods

All reactions were performed under an atmosphere of argon with oven-dried glassware and standard syringe/septa techniques. All reactions were magnetically stirred with Teflon stir bars, and temperatures were measured externally. Solvents were distilled under an argon atmosphere prior to use. The solvents tetrahydrofuran (THF) and Et_2O were distilled from sodium benzophenone, while CH_2Cl_2 and cyclohexane were dried over P_2O_5. Triethylamine and hexamethylphosphoramide (HMPA) were distilled from CaH_2. Ethanol and methanol used were bottle-grade solvents. All reagents obtained commercially were used without further purification. The reaction progress was monitored on precoated silica gel thin-layer chromatography (TLC) plates. Spots were visualized under 254 nm UV light and/or by dipping the TLC plate into a solution of 2 mL of anisaldehyde, 10 mL of glacial acetic acid, and 5 mL of H_2SO_4 in 340 mL of EtOH, followed by heating with a heat gun. Column chromatography was performed with silica gel (230−400 mesh). All the solvents (hexanes, ethyl acetate, CH_2Cl_2, Et_2O) were distilled prior to use for column chromatography. ^{1}H and ^{13}C NMR spectra were measured in $CDCl_3$ or MeOD on 400 MHz (100 MHz) or 500 MHz (125 MHz) machines. Chemical shifts were reported in parts per million (ppm) downfield from tetramethylsilane (δ) as the internal standard, and coupling constants are in hertz (Hz). Assignment of proton resonances were confirmed by correlated spectroscopy. IR spectra were recorded by use of a universal attenuated total reflection sampling accessory (diamond ATR) on an Agilent Cary 630 FT-IR spectrometer. High-resolution mass spectra were recorded on an Agilent electrospray ionization quadrupole time-of-flight (ESI-QTOF) instrument.

3.2. Synthesis

Synthesis of the aldehydes

4-methoxy-2-(methoxymethoxy)benzaldehyde **46:** 2-Hydroxy-4-methoxybenzaldehyde **51** (1g, 6.57 mmol) was dissolved in 20 mL dichloromethane and placed in an ice bath under argon atmosphere. To this solution, *N,N*-diisopropyl ethyl amine (1.27 g, 1.7 mL, 9.9 mmol) was added dropwise and stirred for 30 min after which, chloromethoxymethane (0.79 g, 0.75 mL, 9.9 mmol) was added. The reaction was stirred for 20 h. The reaction mixture was quenched with distilled water (20 mL) and the layers were separated. The aqueous layer was further extracted with (2x20 mL) DCM. The combined organic layers were dried over sodium sulfate and concentrated under vacuum to produce a pale yellow crystalline solid as MOM protected aldehyde **1046** (1.27 g, 64.7 mmol, 99%).: **IR** (cm^{-1}): 2941, 2844, 2766, 1678, 1600, 1579, 1501, 1451, 1395, 1259, 1222, 1154, 1078, 987, 925 and 815; **ESI-HRMS**: calcd. for $C_{10}H_{13}O_4$ 197.0808 $[M+H]^+$; found 197.0800.

Synthesis of the aldehyde **47**

4-Hydroxy-4-(methoxymethoxy)benzaldehyde **53**

By following the reported procedure[162]., the aldehyde **47** was prepared in two steps, first by the synthesis of **53**. 2,4-Dihydroxybenzaldehyde (1g, 7.24 mmol) and potassium carbonate (1.5 g, 13.8 mmol) dissolved in 15 mL acetone, stirred for 1 h to 0 ^{o}C. To this solution chloro(methoxy)methane (0.55 mL, 7.24 mmol) was added dropwise and allowed to heat to room temperature and stirred for 28 h. The reaction mixture was then filtered to remove potassium carbonate and concentrated the mixture with rotovap. The mixture was then separated using column chromatography to obtain mom-protected *o*-hydroxy benzaldehyde as brick colored crystals (0.99 g, 0.54 mmol, 75%). **IR** (cm^{-1}): 2961, 2848, 1628, 1579, 1503, 1250, 1225,

1156, 1078, 992, 959 and 804;**^{1}H NMR** (400 MHz, Chloroform-*d*) δ 11.34 (s, 1H), 9.71 (s, 1H), 7.42 (d, *J* = 8.6 Hz, 1H), 6.63 (dd, *J* = 8.6, 2.3 Hz, 1H), 6.58 (d, *J* = 2.3 Hz, 1H), 5.20 (s, 2H), 3.46 (s, 3H); **ESI-HRMS**: calcd. for $C_9H_{11}O_4$ 183.0652 $[M+H]^+$; found 183.0666.

TBS protection of the aldehyde intermediate **53** *to produce* **47**

2-hydroxy-4-(methoxymethoxy)benzaldehyde **53** (5.62 g, 30 mmol) and tert-butylchlorodimethylsilane (9.31 g, 61.79 mmol) were dissolved in dry dichloromethane and DIPEA (16 mL, 108 mmol) was added dropwise and allowed to stir at room temperature for 30 h. The reaction was monitored by TLC and observed for the disappearance of the starting material. The reaction was then extracted with water and dried over anhydrous $MgSO_4$ and filtered and dried to obtain brick colored crystals (9 g, 30 mmol, 99%).

2-((Tert-butyldimethylsilyl)oxy)-4-(methoxymethoxy)benzaldehyde **47***:* **IR** (cm^{-1}): 2961, 2848, 1628, 1577, 1501, 1445, 1335, 1290, 1223, 1154, 1078, 989, 959 and 806; **^{1}H NMR** (400 MHz, Chloroform-*d*) δ 10.29 (s, 1H), 7.75 (d, *J* = 8.6 Hz, 1H), 6.68 (ddd, *J* = 8.7, 2.2, 0.9 Hz, 1H), 6.52 (d, *J* = 2.2 Hz, 1H), 5.17 (s, 2H), 3.46 (s, 3H), 1.06 – 0.91 (m, 9H), 0.27 (d, *J* = 2.2 Hz, 6H); **^{13}C NMR** (101 MHz, $CDCl_3$) δ 188.7, 163.4, 160.6, 129.9, 121.9, 109.8, 107.1, 94.1, 56.2, 25.7 (3C), 18.3, -4.4 (2C); **ESI-HRMS**: calcd. for $C_{15}H_{24}O_4Si$ 297.1517 $[M+H]^+$; found: 297.1497.

Amide formation of propanoic acid with a chiral auxiliary

Coupling of (*R*)-4-benzyloxazolidin-2-one (+) **50** with phenyl acetic acid **25**, to produce (*R*)-4-Benzyl-3-(2-(4-methoxyphenyl)acetyl)oxazolidin-2-one (-) **26**

By following the procedure [155], (+) **26** and (-) **26** were prepared from the corresponding 4-benzyloxazolidin-2-ones (+) **50** and (-) **50**.

(R)-4-Benzyl-3-(2-(4-methoxyphenyl)acetyl)oxazolidin-2-one (-) **26**

MP 84-85 ^oC, $[\alpha]^D$ = -73.3 (c = 1.195, $CHCl_3$); **IR** (cm^{-1}): 3028, 2924, 1778, 1700, 1514, 1391,

1357, 1248, 1181, 1106, 1033, 793 and 706; **^{1}H NMR** (400 MHz, Chloroform-*d*) δ 7.32 – 7.22 (m, 5H), 7.17 – 7.09 (m, 2H), 6.92 – 6.85 (m, 2H), 4.72 – 4.61 (m, 1H), 4.33 – 4.11 (m, 4H), 3.80 (s, 3H), 3.26 (dd, *J* = 13.4, 3.3 Hz, 1H), 2.75 (dd, *J* = 13.4, 9.4 Hz, 1H); **^{13}C NMR** (101 MHz, $CDCl_3$) δ 171.7, 159.0, 153.5, 135.3, 131.0 (2C), 129.6 (2C), 129.1 (2C), 127.5, 125.6, 114.2 (2C), 66.3, 55.5, 55.4, 40.8, 37.9; **ESI-HRMS**: calcd. for $C_{19}H_{20}N0_4$ 326.1387 $[M+H]^+$; found 326.1367.

(R)-4-Benzyl-3-(2-(4-methoxyphenyl)acetyl)oxazolidin-2-one (+) **26**

$[\alpha]^D$ = + 70.377 (c = 1.06, $CHCl_3$); **IR** (cm^{-1}): 2935, 2996, 1780, 1758, 1700, 1615, 1514, 1359, 1249, 1181, 1108, 1033, 763, 790, and 706; **^{1}H NMR** (400 MHz, Chloroform-*d*) δ 7.32 – 7.22 (m, 5H), 7.16 – 7.11 (m, 2H), 6.92 – 6.84 (m, 2H), 4.70 – 4.61 (m, 1H), 4.31 – 4.11 (m, 4H), 3.80 (s, 2H), 3.25 (dd, *J* = 13.4, 3.4 Hz, 1H), 2.75 (dd, *J* = 13.4, 9.4 Hz, 1H).; **^{13}C NMR** (101 MHz, $CDCl_3$) δ 171.7, 158.9, 153.5, 135.3, 130.9 (2C), 129.5 (2C), 129.0, 127.4, 125.6, 114.2 (2C), 66.2, 55.4, 55.4, 40.8, 37.9; **ESI-HRMS**: calcd. for $C_{19}H_{20}NO_4$ 326.1392 $[M-H_20+H]^+$; found 326.1395.

(R)-4-Benzyl-3-(2-(2,4-dimethoxyphenyl)acetyl)oxazolidin-2-one (-) **48**

Procedure modified from that of Liu et al [161]. To a solution of 2-(2,4-dimethoxyphenyl)acetic acid **15** (3.9 g, 20 mmol) and DIPEA(2.8 g, 22 mmol) in anhydrous THF (50 mL) at -78 ^{o}C was added pivolyl chloride (3.1 g, 26 mmol) dropwise under an atmosphere of argon. The resulting mixture was stirred for 15 min at -78 ^{o}C, 1 h at 0 ^{o}C, and then recooled to –78 ^{o}C to form mixed anhydride reaction mixture. Meanwhile, in a different flask, *n*-BuLi (24 mmol; 10 mL of 2.5 M in DCM) was added dropwise to a solution of (*R*)-4-benzyl-oxazolidin-2-one (+16) (4.3 g, 24.4 mmol) in anhydrous THF at -78 ^{o}C under atmosphere of argon and the mixture was stirred for 40 min at -78 ^{o}C, it was then transferred with a cannula to

the preformed mixed anhydride reaction mixture. After stirring the reaction mixture for 15 min, it was allowed to warm up to room temperature over 2 h, then quenched with saturated aqueous NH_4Cl (50 mL) and extracted with ethyl acetate (3 x 30 mL). The combined organic layers were washed with brine, dried over anhydrous $MgSO_4$, filtered, and concentrated under reduced pressure. The residue was purified by flash chromatography on silica gel to obtain a viscous liquid (5.48 g, 18 mmol, 91%).

(R)-4-Benzyl-3-(2-(2,4-dimethoxyphenyl)acetyl)oxazolidin-2-one (-) **48**

R)-4-Benzyl-3-(2-(2,4-dimethoxyphenyl)acetyl)oxazolidin-2-one **(-) 48**: Viscous liquid $[\alpha]^D$ = -76.1 (c = 1.0, $CHCl_3$); **IR** (cm^{-1}): 2941, 2840, 2361, 1778, 1706, 1616, 1512, 1212, 1158, 1037, 886, 765 and 707; **^{1}H NMR** (400 MHz, Chloroform-*d*) δ 7.39 – 7.16 (m, 5H), 7.07 (dd, *J* = 7.9, 2.3 Hz, 1H), 6.54 – 6.42 (m, 2H), 4.68 (td, *J* = 7.7, 6.2, 3.0 Hz, 1H), 4.31 – 4.04 (m, 4H), 3.81 (s, 6H), 3.28 (dd, *J* = 13.6, 2.5 Hz, 1H), 2.81 (dd, *J* = 13.0, 9.7 Hz, 1H); **^{13}C NMR** (101 MHz, $CDCl_3$) δ 171.6, 160.5, 158.6, 153.8, 135.5, 131.6, 129.6 (2C), 129.0 (2C), 127.4, 115.1, 104.3, 98.8, 66.3, 55.6, 55.5 (2C), 37.9, 36.9; **ESI-HRMS**: calcd. for $C_{20}H_{22}NO_5$ 356.1492 $[M+H]^+$; found 356.1493.

(S)-4-Benzyl-3-(2-(2,4-dimethoxyphenyl)acetyl)oxazolidin-2-one (+) **48**

(S)-4-Benzyl-3-(2-(2,4-dimethoxyphenyl)acetyl)oxazolidin-2-one **(+13)**: $[\alpha]^D$ = + 78.8 (c = 1.0, $CHCl_3$); **IR** (cm^{-1}): 2939, 2838, 1178, 1708, 1616, 1592, 1512, 1393, 1367, 1212, 1367, 1212, 1110, 1037, 991, 838, 765 and 707; **^{1}H NMR** (400 MHz, Chloroform-d) δ 7.34 – 7.29 (m, 2H), 7.28 – 7.23 (m, 1H), 7.20 (d, J = 7.5 Hz, 2H), 7.07 (d, J = 7.9 Hz, 1H), 6.53 – 6.44 (m, 2H), 4.68 (ddtd, J = 9.0, 6.3, 3.1, 1.1 Hz, 1H), 4.29 – 4.07 (m, 4H), 3.80 (m, 6H), 3.29 (dd, J = 13.3, 3.2 Hz, 1H), 2.80 (dd, J = 13.2, 9.5 Hz, 1H); **^{13}C NMR** (101 MHz, $CDCl_3$) δ 171.7, 160.6, 158.7, 153.8, 149.2, 135.6, 131.6, 129.6 (2C), 129.1 (2C), 127.4, 115.3, 104.5, 99.0, 66.4, 55.6, 55.5,

38.0, 36.9; **ESI-HRMS**: calcd. for $C_{20}H_{22}NO$ 356.1492 $[M+H]^+$; found 356.1483.

Evans' aldol reaction of aldehydes with oxazolidinone amides to produce (+)-, (-)-**44,** (+)-, (-)-**45**

General procedure: In a 0.5 L round bottom flask, DIPEA (1 equiv.) was added drop wise to a pre-cooled solution of chiral 4-benzyl-(acetyl)oxazolidin-2-one (1 equiv.) in anhydrous DCM (200 mL) at 0 ^oC. The resulting solution was cooled to -25 ^oC, 1.0 M solution of dibutyl(((trifluoromethyl)sulfonyl)oxy)borane (1.1 equiv.) in DCM was added drop wise. The resulting orange colored solution was heated to -15 ^oC over 30 min and then stirred for 3h at -15^oC. The solution was re-cooled to -25 ^oC and a solution of 4-methoxy-2-(methoxymethoxy)benzaldehyde (1 equiv.) in DCM (50 mL) was added drop wise and continued stirring at -25 ^oC. After 20 min, the temperature of the mixture was raised to -15 ^oC over a period of 30 min and stirred further for additional 1 h. The mixture was quenched with methanol (25 mL) and phosphate buffer (15 mL, pH 7.4). Hydrogen peroxide (15 mL, 30%) in MeOH (35 mL) was added, warmed to room temperature and stirred for 1h. The whole mixture was concentrated under reduced pressure and the residue was diluted with water (150 mL) and extracted with diethyl ether (3 x 150 mL). The combined organic layers were washed with brine, dried over anhydrous $MgSO_4$, concentrated and the resulting residue was purified by column chromatography by eluting with 10-25% Ethyl acetate in hexanes to give the aldol product.

(R)-4-Benzyl-3-((2*R*,3*R)*-3-hydroxy-3-(4-methoxy-2-(methoxymethoxy)phenyl)-2-(4-methoxyphenyl)propanoyl)oxazolidin-2-one (+) **44**: Yield 90%; $[\alpha]^D$ = + 97 (c = 0.115, $CHCl_3$); **IR** (cm^{-1}): 3529, 2956, 2935, 1777, 1611, 1510, 1154, 1000, 998, 732 and 704; **^{1}H NMR** (500 MHz, Chloroform-*d*) δ 7.29 (d, *J* = 8.7 Hz, 2H), 7.22 – 7.18 (m, 3H), 7.02 (d, *J* = 8.5 Hz, 1H), 6.99 – 6.95 (m, 2H), 6.88 – 6.84 (m, 2H), 6.72 (d, *J* = 2.4 Hz, 1H), 6.42 (dd, *J* = 8.5, 2.4 Hz, 1H), 5.54 (s, 2H), 5.29 – 5.19 (m, 2H), 4.60 (ddt, *J* = 9.0, 7.1, 3.5 Hz, 1H), 4.06 – 3.97 (m, 2H), 3.80

(s, 3H), 3.76 (s, 3H), 3.54 (s, 3H), 3.09 (dd, *J* = 13.5, 3.4 Hz, 1H), 2.55 (dd, *J* = 13.5, 9.1 Hz, 1H); **^{13}C NMR** (126 MHz, $CDCl_3$) δ 173.7, 160.1, 159.1, 155.2, 152.5, 134.8, 131.1 (2C), 129.4 (2C), 129.1, 128.8 (2C), 127.2, 126.3, 121.8, 113.7 (2C), 106.0, 101.1, 94.7, 70.8, 65.7, 56.3, 55.3, 55.2, 54.7, 53.1, 37.2; **ESI-HRMS**: calcd. for $C_{29}H_{30}NO_7$ $[M-H_20+H]^+$ 504.2017; found 504.2030.

(S)-4-Benzyl-3-((2S,3*S)*-3-hydroxy-3-(4-methoxy-2-(methoxymethoxy)phenyl)-2-(4-methoxyphenyl)propanoyl)oxazolidin-2-one (-) **44**: Yield 90%,.$[\alpha]^D$ = -111.3 (c = 0.39, $CHCl_3$); **IR** (cm^{-1}): 3528, 2986, 2838, 1777, 1611, 1510, 1156, 1000, 912 and 732; ^{1}H NMR (500 MHz, Chloroform-*d*) δ 7.30 (d, *J* = 8.7 Hz, 2H), 7.23 – 7.17 (m, 3H), 7.03 (d, *J* = 8.5 Hz, 1H), 7.00 – 6.94 (m, 2H), 6.86 (d, *J* = 8.7 Hz, 2H), 6.73 (d, *J* = 2.4 Hz, 1H), 6.42 (dd, *J* = 8.5, 2.4 Hz, 1H), 5.54 (s, 2H), 5.30 – 5.21 (m, 2H), 4.60 (ddt, *J* = 8.9, 7.2, 3.6 Hz, 1H), 4.06 – 3.97 (m, 2H), 3.79 (s, 3H), 3.76 (s, 3H), 3.54 (s, 3H), 3.08 (dd, *J* = 13.5, 3.4 Hz, 1H), 2.56 (dd, *J* = 13.5, 9.0 Hz, 1H); **^{13}C NMR** (126 MHz, $CDCl_3$) δ 173.7, 160.1, 159.1, 155.2, 152.5, 134.8, 131.1 (2C), 129.4 (2C), 129.1, 128.8 (2C), 127.2, 126.3, 121.9, 113.7 (2C), 106.0, 101.1, 94.7, 70.8, 65.7, 56.3, 55.3, 55.2, 54.7, 53.1, 37.2; **ESI-HRMS**: calcd. for $C_{29}H_{30}NO_7$ 504.2017 $[M-H_20+H]^+$; found 504.1997.

(*R*)-4-Benzyl-3-((2*R*,3*R*)-3-(2-((tert-butyldimethylsilyl)oxy)-4-(methoxymethoxy)phenyl)-2-(2,4-dimethoxyphenyl)-3-hydroxypropanoyl)oxazolidin-2-one (+) **45:** viscous liquid, yield 82% $[\alpha]^D$ = + 203.5 (c = 1.0, $CHCl_3$) ; **IR** (cm^{-1}): 3542, 2931, 2857, 1791, 1674, 1613, 1588, 1508, 1389, 1212, 1160, 1121, 1017, 843, and 786; **^{1}H NMR** (400 MHz, Chloroform-*d*) δ 7.38 – 7.21 (m, 3H), 7.20 – 7.10 (m, 2H), 7.06 (d, *J* = 8.3 Hz, 1H), 6.77 (d, *J* = 8.4 Hz, 1H), 6.56 – 6.51 (m, 1H), 6.48 – 6.41 (m, 2H), 6.35 – 6.30 (m, 1H), 5.63 (d, *J* = 3.6 Hz, 1H), 5.47 (d, *J* = 4.1 Hz, 1H), 5.09 (s, 2H), 4.72 – 4.62 (m, 1H), 4.01 (d, *J* = 5.5 Hz, 2H), 3.79 (s, 3H), 3.71 (s, 1H), 3.44 (s,

3H), 3.42 (s, 3H), 3.35 (dd, *J* = 13.3, 3.5 Hz, 1H), 2.53 (dd, *J* = 13.3, 10.0 Hz, 1H), 1.00 (s, 9H), 0.34 (s, 3H), 0.32 (s, 3H); **^{13}C NMR** (101 MHz, $CDCl_3$) δ 175.1, 160.3, 159.3, 157.1, 153.2, 152.0, 135.5, 131.1, 129.5 (2C), 129.1 (2C), 128.4, 127.4, 125.4, 114.5, 108.1, 106.2, 103.8, 98.6, 94.7, 69.0, 66.0, 55.9, 55.4, 55.2 (2C), 48.2, 37.8, 25.9 (3C), 18.4, -3.9, -4.1; **ESI-HRMS**: calcd. for $C_{35}H_{44}NO_8Si$ 634.2831[M-H_2O+H]$^+$; found 634.2827.

(*R*)-4-Benzyl-3-((2R,3R)-3-(2-((tert-butyldimethylsilyl)oxy)-4-(methoxymethoxy)phenyl)-2-(2,4-dimethoxyphenyl)-3-hydroxypropanoyl)oxazolidin-2-one (-) **45**: Yield 85 %; $[\alpha]^D$ = - 203.4 (c = 1.0, $CHCl_3$) ; **IR** (cm^{-1}): 3540, 2931, 2859, 1790, 1672, 1611, 1508, 1366, 1292, 1212, 1158, 1119, 1013, 842, 784 and 704; **^{1}H NMR** (400 MHz, Chloroform-*d*) δ 7.36 – 7.19 (m, 3H), 7.20 – 7.11 (m, 2H), 7.06 (d, *J* = 8.4 Hz, 1H), 6.77 (d, *J* = 8.5 Hz, 1H), 6.53 (d, *J* = 2.2 Hz, 1H), 6.48 – 6.39 (m, 2H), 6.32 (d, *J* = 2.2 Hz, 1H), 5.63 (t, *J* = 3.4 Hz, 1H), 5.47 (d, *J* = 3.6 Hz, 1H), 5.09 (s, 2H), 4.72 – 4.61 (m, 1H), 4.01 (d, *J* = 5.4 Hz, 2H), 3.78 (s, 3H), 3.71 (d, *J* = 3.0 Hz, 1H), 3.44 (s, 3H), 3.42 (s, 3H), 3.34 (dd, *J* = 13.2, 2.8 Hz, 1H), 2.53 (dd, *J* = 13.1, 10.2 Hz, 1H), 1.00 (s, 9H), 0.34 (s, 3H), 0.32 (s, 3H); **^{13}C NMR** (101 MHz, $CDCl_3$) δ 175.1, 160.3, 159.3, 157.1, 153.2, 152.0, 135.5, 131.1, 129.5 (2C), 129.0 (2C), 128.3, 127.4, 125.4, 114.5, 108.1, 106.2, 103.8, 98.6, 94.7, 69.0, 66.0, 55.9, 55.4, 55.2 (2C), 48.2, 37.8, 25.9 (3C), 18.4, -3.9, -4.1; **ESI-HRMS**: calcd. for $C_{35}H_{44}NO_8Si$ 652.2936 [M-H_20+H]$^+$= 634.2831; found 634.2817.

Deoxygenation of the aldol products for the synthesis of (+)-, (-)- ***54****, (+)-, (-)-* ***56***

(*R*)-4-Benzyl-3-((*2R,3R*)-3-hydroxy-3-(4-methoxy-2-(methoxymethoxy)phenyl)-2-(4-methoxyphenyl)propanoyl)oxazolidin-2-one (**+) 44** (1.04 g, 2 mmol) was dissolved in 10 mL dichloromethane, cooled to O ^{o}C and triethyl silane (10 mL, 64.7 mmol) was added dropwise. After stirring for 10 min, trifluoroacetic acid (1 mL, 12.9 mmol) was added drop-wise in two installments, allowed to heat to room temperature, and the reaction was monitored using TLC.

After 30 min, the reaction was cooled to 0 ^{o}C quenched using $NaHCO_3$ (10 mL) and extracted using dichloromethane (2x15mL), dried over anhydrous $MgSO_4$, concentrated and separated using column chromatography to obtain a colorless viscous liquid (0.98 g, 1.62 mmol, 81%).

(R)-4-Benzyl-3-((S)-3-(4-methoxy-2-(methoxymethoxy)phenyl)-2-(4-methoxyphenyl)propanoyl)oxazolidin-2-one **(+) 54**: $[\alpha]^D$ = +24.0 (c = 0.15, $CHCl_3$); **IR** (cm^{-1}): 2933, 2836, 1778, 1695, 1613, 1510, 1249, 1218, 1156, 1007, 836 and 707; **^{1}H NMR** (400 MHz, Chloroform-d) δ 7.36 (d, J = 8.4 Hz, 2H), 7.22 – 7.15 (m, 3H), 7.02 – 6.92 (m, 3H), 6.87 (d, J = 8.4 Hz, 2H), 6.68 (d, J = 2.5 Hz, 1H), 6.39 (dd, J = 8.3, 2.5 Hz, 1H), 5.41 (dd, J = 8.8, 6.2 Hz, 1H), 5.18 (s, 2H), 4.63 (tt, J = 7.6, 3.5 Hz, 1H), 4.07 – 3.95 (m, 2H), 3.80 (s, 3H), 3.75 (s, 3H), 3.52 (s, 3H), 3.35 (dd, J = 13.6, 8.8 Hz, 1H), 3.13 – 2.98 (m, 2H), 2.56 (dd, J = 13.6, 8.9 Hz, 1H); **^{13}C NMR** (101 MHz, $CDCl_3$) δ 173.9, 159.4, 158.8, 156.4, 152.7, 135.1, 131.3 , 130.8, 129.8 (2C), 129.4 (2C), 128.8(2C), 127.1, 120.2, 113.9 (2C), 105.8, 101.0, 94.6, 65.6, 56.1, 55.3, 55.2, 54.9, 47.9, 37.4, 34.4; **ESI-HRMS**: calcd. for $C_{29}H_{32}NO_7$ 506.2173 $[M+H]^+$; found 506.2176.

(S)-4-Benzyl-3-((R)-3-(4-methoxy-2-(methoxymethoxy)phenyl)-2-(4-methoxyphenyl)propanoyl)oxazolidin-2-one **(-) 54**: Yield: 75%, $[\alpha]^D$ = -26.4 (c = 0.33, $CHCl_3$); **IR** (cm^{-1}): 2933, 2838, 1178, 1695, 1510, 1218, 1156 and 1007; **^{1}H NMR** (500 MHz, Chloroform-*d*) δ 7.36 (d, *J* = 8.7 Hz, 2H), 7.24 – 7.16 (m, 3H), 7.00 – 6.93 (m, 3H), 6.87 (d, *J* = 8.7 Hz, 2H), 6.68 (d, *J* = 2.4 Hz, 1H), 6.39 (dd, *J* = 8.3, 2.5 Hz, 1H), 5.41 (dd, *J* = 8.8, 6.2 Hz, 1H), 5.19 (s, 2H), 4.68 – 4.59 (m, 1H), 4.06 – 3.98 (m, 2H), 3.80 (s, 3H), 3.75 (s, 3H), 3.51 (s, 3H), 3.34 (dd, *J* = 13.4, 8.9 Hz, 1H), 3.09 – 3.01 (m, 2H), 2.56 (dd, *J* = 13.5, 9.0 Hz, 1H). **^{13}C NMR** (126 MHz, $CDCl_3$) δ 174.0, 159.6, 158.9, 156.5, 152.9, 135.2, 131.5, 130.9, 129.9 (2C), 129.6 (2C), 128.9 (2C), 127.3, 120.3, 114.1 (2C), 105.9, 101.1, 94.6, 65.7, 56.3, 55.4, 55.4, 55.0, 48.1, 37.5, 34.6; **ESI-HRMS**: calcd. for $C_{29}H_{32}NO_7$ 506.2173 $[M+H]^+$; found 506.2151.

(*R*)-4-Benzyl-3-((*S*)-3-(2-((tert-butyldimethylsilyl)oxy-4-(methoxymethoxy)phenyl)-2-(2,4-dimethoxyphenyl)propanoyl)oxazolidin-2-one **(+) 56**: Colorless crystalline solid (1.35 g, 2.12 mmol, 73%). $[\alpha]^D$ = + 11.6 (c = 1.0, $CHCl_3$) ; IR (cm^{-1}): 2954, 2931, 2859, 1784, 1698, 1611, 1506, 1292, 1210, 1156, 1015, 843 and 784; ^1H NMR (400 MHz, Chloroform-*d*) δ 7.36 – 7.21 (m, 4H), 7.19 – 7.11 (m, 2H), 6.89 (d, *J* = 8.2 Hz, 1H), 6.54 (d, *J* = 2.4 Hz, 1H), 6.50 – 6.46 (m, 2H), 6.42 (d, *J* = 2.4 Hz, 1H), 5.54 (t, *J* = 7.6 Hz, 1H), 5.15 – 5.01 (m, 2H), 4.60 (ddt, *J* = 10.7, 7.4, 3.2 Hz, 1H), 3.98 (dd, *J* = 8.9, 3.0 Hz, 1H), 3.92 (t, *J* = 8.3 Hz, 1H), 3.80 (s, 3H), 3.68 (s, 3H), 3.44 (s, 3H), 3.34 – 3.24 (m, 2H), 3.03 (dd, *J* = 13.3, 7.3 Hz, 1H), 2.55 (dd, *J* = 13.2, 10.0 Hz, 1H), 1.01 (s, 9H), 0.30 (s, 3H), 0.29 (s, 3H); ^{13}C NMR (101 MHz, $CDCl_3$) δ 174.9, 159.9, 158.3, 156.5, 154.7, 152.4, 135.7, 131.0, 129.5, 129.3 (2C), 128.9 (2C), 127.2, 123.1, 120.1, 108.1, 107.1, 104.1, 98.6, 94.6, 65.7, 55.8, 55.6, 55.4, 55.3, 42.7, 37.7, 32.5, 25.9 (3C), 18.3, -4.1, -4.2; ESI-HRMS: calcd. for $C_{35}H_{46}NO_8Si$ 636.2987 $[M+H]^+$; found 636.2995.

(*R*)-4-Benzyl-3-((S)-3-(2-((tert-butyldimethylsilyl)oxy)-4-(methoxymethoxy)phenyl)-2-(2,4-dimethoxyphenyl)propanoyl)oxazolidin-2-one **(-) 56**: Yield 68%; $[\alpha]^D$ = -10.7 (c = 1.0, $CHCl_3$) ; IR (cm^{-1}): 2957, 2857, 2361, 1788, 1698, 1613, 1508, 1292, 1212, 1158, 1018, 924, 843, 784 and 706; ^1H NMR (400 MHz, Chloroform-*d*) δ 7.32 – 7.23 (m, 4H), 7.21 – 7.13 (m, 2H), 6.88 (d, *J* = 8.3 Hz, 1H), 6.53 (d, *J* = 2.4 Hz, 1H), 6.48 (dd, *J* = 8.4, 2.4 Hz, 2H), 6.42 (d, *J* = 2.4 Hz, 1H), 5.53 (t, *J* = 7.7 Hz, 1H), 5.17 – 5.01 (m, 2H), 4.60 (ddt, *J* = 10.6, 6.7, 3.1 Hz, 1H), 3.98 (dd, *J* = 9.1, 3.1 Hz, 1H), 3.93 (t, *J* = 8.3 Hz, 1H), 3.81 (s, 3H), 3.68 (s, 3H), 3.45 (s, 3H), 3.34 – 3.23 (m, 2H), 3.02 (dd, *J* = 13.3, 7.3 Hz, 1H), 2.55 (dd, *J* = 13.3, 10.0 Hz, 1H), 1.01 (s, 9H), 0.29 (s, 3H), 0.28 (s, 3H); ^{13}C NMR (101 MHz, $CDCl_3$) δ 174.9, 159.9, 158.3, 156.5, 154.8, 152.4, 135.8, 131.0, 129.5, 129.3 (2H), 128.9 (2H), 127.2, 123.2, 120.1, 108.1, 107.1, 104.1, 98.6, 94.6, 65.7, 55.8, 55.6, 55.4, 55.3, 42.7, 37.7, 32.5, 25.9 (3H), 18.3, -4.1, -4.2; ESI-HRMS: calcd. for

$C_{35}H_{46}NO_8Si$ 636.2987 $[M+H]^+$= 636.2987; found 636.2979.

MOM deprotection of the deoxygenated aldol products **(+) 54, (-) 54** to produce **(+) 55, (-) 55**.

(+) 54 (1 g, 2 mmol) was dissolved in 3 M HCl in methanol (10 mL), refluxed and the reaction monitored by TLC. After 30 to 40 min, the reaction was cooled to 0 ^oC, quenched with saturated $NaHCO_3$ (10 mL), methanol was evaporated using roptovap and extracted using ethyl acetate (2x10 mL). The organic layer was dried over anhydrous $MgSO_4$, concentrated and isolated using column chromatography to obtain a colorless viscous liquid product (0.78 g, 1.7 mmol, 85%).

(R)-4-Benzyl-3-((*S*)-3-(2-hydroxy-4-methoxyphenyl)-2-(4-ethoxyphenyl)propanoyl)oxazolidin-2-one **(+) 55**: $[\alpha]^D$ = +37.1 (c = 0.205, $CHCl_3$); **IR** (cm^{-1}): 3401, 2929, 2838, 1777, 1510, 1164, 1181, 1106, 1033, 834 and 704; **^{1}H NMR** (400 MHz, Chloroform-d) δ 7.40 (d, J = 8.7 Hz, 2H), 7.25 – 7.15 (m, 4H), 7.03 (d, J = 8.3 Hz, 1H), 6.99 – 6.88 (m, 4H), 6.48 (d, J = 2.5 Hz, 1H), 6.45 (dd, J = 8.3, 2.6 Hz, 1H), 5.21 (dd, J = 11.0, 4.3 Hz, 1H), 4.68 (tt, J = 8.5, 3.3 Hz, 1H), 4.09 (t, J = 8.5 Hz, 1H), 4.02 (dd, J = 9.1, 3.1 Hz, 1H), 3.82 (s, 3H), 3.76 (s, 3H), 3.45 (dd, J = 14.3, 11.1 Hz, 1H), 3.07 (dd, J = 13.5, 3.5 Hz, 1H), 2.76 (dd, J = 14.4, 4.3 Hz, 1H), 2.56 (dd, J = 13.5, 8.9 Hz, 1H); **^{13}C NMR** (101 MHz, $CDCl_3$) δ 175.8, 159.7, 159.1, 155.1, 152.3, 134.6, 131.9, 130.2, 129.6 (2C), 129.4 (2C), 128.9 (2C), 127.3, 117.8, 114.3 (2C), 107.0, 102.8, 65.7, 55.3, 55.2, 54.8, 50.8, 37.1, 33.9; **ESI-HRMS**: calcd. for $C_{27}H_{28}NO_6$ 462.1911 $[M+H]^+$; found 462.1917.

(S)-4-benzyl-3-((*R)*-3-(2-hydroxy-4-methoxyphenyl)-2-(4-methoxyphenyl)propanoyl)oxazolidin-2-one **(-) 55**: $[\alpha]^D$ = -34.7 (c = 0.15, $CHCl_3$); **IR** (cm^{-1}): 3388, 2928, 1777, 1695, 1620, 1510, 1181, 1033 and 704; **^{1}H NMR** (400 MHz, Chloroform-*d*) δ 7.41 (d, *J* = 8.6 Hz, 2H), 7.26 – 7.13 (m, 4H), 7.03 (d, *J* = 8.3 Hz, 1H), 6.97 – 6.93 (m, 2H), 6.92 (d, *J* = 8.6 Hz, 2H), 6.48 (d, *J* = 2.5 Hz, 1H), 6.45 (dd, *J* = 8.3, 2.6 Hz, 1H), 5.21 (dd, *J* = 11.0, 4.3 Hz, 1H), 4.68 (tt, *J* = 8.5, 3.3 Hz,

1H), 4.09 (t, *J* = 8.5 Hz, 1H), 4.02 (dd, *J* = 9.1, 3.1 Hz, 1H), 3.82 (s, 3H), 3.76 (s, 3H), 3.45 (dd, *J* = 14.3, 11.0 Hz, 1H), 3.07 (dd, *J* = 13.5, 3.5 Hz, 1H), 2.77 (dd, *J* = 14.4, 4.3 Hz, 1H), 2.56 (dd, *J* = 13.5, 8.9 Hz, 1H); **^{13}C NMR** (101 MHz, $CDCl_3$) δ 175.9, 159.9, 159.2, 155.3, 152.5, 134.8, 132.0, 130.3 (2C), 129.8 (2C), 129.5 (2C), 129.0 (2C), 127.4, 118.0, 114.4 (2C), 107.1, 102.9, 65.9, 55.4, 55.4, 55.0, 50.9, 37.3, 34.1. **ESI-HRMS**: calcd. for $C_{27}H_{28}NO_6$ 462.1911 $[M+H]^+$; found 462.1891.

Reduction of the chiral auxiliary to produce dialcohols (+) ***42****, (-)* ***42****:*

(+) 55 (24 g, 52 mmol) was dissolved in THF (150 mL) and added dropwise to a suspension of $LiAlH_4$ (4 g, 104 mmol) in 25 mL THF at 0 ^oC and stirred overnight at room temperature. Then the reaction was cooled to 0 ^oC and quenched with a dropwise addition of saturated NaOH (50 mL), THF was evaporated and the resulting solution was extracted with ethyl acetate (3 x 50 mL) and separated, dried over anhydrous $MgSO_4$ and isolated using flash chromatography toproduce colorless liquid **(+) 42** (13.5 g, 47 mmol, 90%).

(*S)*-2-(3-Hydroxy-2-(4-methoxyphenyl)propyl)-5-methoxyphenol **(+) 42**: $[\alpha]^D$ = +31.6 (c = 0.185, $CHCl_3$); **^{1}H NMR** (400 MHz, Chloroform-*d*) δ 7.15 (d, *J* = 8.8 Hz, 2H), 6.86 (d, *J* = 8.8 Hz, 2H), 6.81 (d, *J* = 8.5 Hz, 1H), 6.44 (d, *J* = 2.5 Hz, 1H), 6.39 (dd, *J* = 8.3, 2.5 Hz, 1H), 3.80 (s, 3H), 3.74 (bs, 5H), 3.08 (dd, *J* = 13.5, 8.4 Hz, 1H), 2.98 (dq, *J* = 9.9, 4.8 Hz, 1H), 2.82 (dd, *J* = 13.5, 5.0 Hz, 1H); **^{13}C NMR** (101 MHz, $CDCl_3$) δ 159.4, 158.4, 155.5, 134.6, 131.9, 128.8 (2C), 118.0, 114.0 (2C), 106.3, 102.1, 65.1, 55.3, 55.3, 47.5, 31.5; **ESI-HRMS**: calcd. for $C_{17}H_{21}O_4$ 289.1434 $[M+H]^+$; found 289.1433.

(*R)*-2-(3-Hydroxy-2-(4-methoxyphenyl) propyl)-5-methoxyphenol (-) **42**

$[\alpha]^D$ = -33.3 (c = 0.185, $CHCl_3$); **^{1}H NMR** (400 MHz, Chloroform-*d*) δ 7.15 (d, *J* = 8.6 Hz, 2H), 6.86 (d, *J* = 8.6 Hz, 2H), 6.81 (d, *J* = 8.3 Hz, 1H), 6.44 (d, *J* = 2.5 Hz, 1H), 6.39 (dd, *J* = 8.3, 2.6

Hz, 1H), 3.80 (s, 3H), 3.75 (bs, 5H), 3.08 (dd, *J* = 13.6, 8.5 Hz, 1H), 3.04 – 2.93 (m, 1H), 2.82 (dd, *J* = 13.6, 5.0 Hz, 1H); **^{13}C NMR** (101 MHz, $CDCl_3$) δ 159.4, 158.4, 155.6, 134.6, 131.9, 128.8 (2C), 117.9, 114.0 (2C), 106.3, 102.1, 65.1, 55.3, 55.2, 47.4, 31.4; **ESI-HRMS**: calcd. for $C_{17}H_{21}O_4$ 289.1434 $[M+H]^+$; found 289.1441.

(*S*)-2-(2-(2,4-Dimethoxyphenyl)-3-hydroxypropyl)-5-(methoxymethoxy)phenol (**+) 43**

A solution of (*R*)-4-Benzyl-3-((S)-3-(2-((tert-butyldimethylsilyl)oxy-4-(methoxymethoxy)phenyl)-2-(2,4-dimethoxyphenyl)propanoyl)oxazolidin-2-one **(+) 56** (1.18 g, 1.86 mmol) in THF (50 mL) and added dropwise to a suspension of $LiAlH_4$ (0.2 g, 5.13 mmol) in 15 mL THF at 0 ^oC and stirred overnight at room temperature. Then the reaction was cooled to 0 ^oC and quenched with a dropwise addition of saturated NaOH (10 mL) and extracted with ethyl acetate (3 x 20 mL). The combined layers were dried over anhydrous $MgSO_4$. TLC indicated mixture of the expected alcohol along with the desilylated alcohol as the major products. Without further purification, the mixture was subjected to desilylation using TBAF in THF. After workup, the crude mixture was purified using flash chromatography to produce desilylated product as a colorless liquid (0.085g, 0.183 mmol, 10%) and colorless viscous liquid (+) **43** (0.575 g, 1.65 mmol, 89%).

(*S*)-2-(2-(2,4-Dimethoxyphenyl)-3-hydroxypropyl)-5-(methoxymethoxy)phenol (+) **43**:

Yield 89%; Colorless viscous liquid, $[\alpha]^D$ = + 26.9 (c = 1.0, $CHCl_3$) ; **IR** (cm^{-1}): 3362, 2939, 2954, 1615, 1588, 1508, 1467, 1292, 1210, 1156 and 1015**; ^{1}H NMR** (400 MHz, Chloroform-*d*) δ 7.14 (d, *J* = 8.3 Hz, 1H), 6.88 (d, *J* = 8.3 Hz, 1H), 6.60 (d, *J* = 2.4 Hz, 1H), 6.55 – 6.41 (m, 3H), 5.12 (s, 2H), 3.82 (s, 3H), 3.80 (s, 3H), 3.80 – 3.66 (m, 3H), 3.47 (s, 3H), 3.32 (dt, *J* = 9.6, 4.6 Hz, 1H), 3.04 (dd, *J* = 14.0, 9.6 Hz, 1H), 2.74 (dd, *J* = 14.0, 4.6 Hz, 1H); **^{13}C NMR** (101 MHz, $CDCl_3$) δ 159.5, 157.7, 156.9, 155.8, 131.7, 128.5, 123.4, 119.8, 108.3, 104.5, 104.2, 98.9,

94.4, 63.5, 55.9, 55.5, 55.4, 41.3, 30.5; **ESI-HRMS:** calcd. for $C_{19}H_{25}O_6$ 349.1646 $[M+H]^+$; found 349.1655.

(*R*)-2-(2-(2,4-Dimethoxyphenyl)-3-hydroxypropyl)-5-(methoxymethoxy)phenol **(-) 43:**

Yield 74%; $[\alpha]^D$ = - 24.4 (c = 1.0, $CHCl_3$) ; **IR** (cm^{-1}): 3391, 2939, 2934, 1615, 1588, 1506, 1290, 1210, 1154, 1015 and 836 ; **^{1}H NMR** (400 MHz, Chloroform-*d*) δ 7.15 (d, *J* = 8.3 Hz, 1H), 6.89 (d, *J* = 8.3 Hz, 1H), 6.61 (d, *J* = 2.4 Hz, 1H), 6.57 – 6.42 (m, 3H), 5.13 (s, 2H), 3.84 (s, 3H), 3.81 (s, 3H), 3.79 – 3.70 (m, 2H), 3.47 (s, 3H), 3.29 (dq, *J* = 9.3, 4.6 Hz, 1H), 3.04 (dd, *J* = 14.1, 9..3 Hz, 1H), 2.73 (dd, *J* = 14.1, 4.6 Hz, 1H); **^{13}C NMR** (101 MHz, $CDCl_3$) δ 159.7, 157.8, 157.1, 156.0, 131.8, 128.6, 123.5, 119.8, 108.5, 104.8, 104.3, 99.1, 94.6, 63.6, 56.1, 55.6, 55.5, 41.7, 30.7; **ESI-HRMS**: calcd. for $C_{19}H_{25}O_6$ 349.1646 $[M+H]^+$; found 349.1645.

Mitsnobu cyclization of the dialcohol to produce isoflavan product

(*S)*-2-(3-Hydroxy-2-(4-methoxyphenyl)propyl)-5-methoxyphenol **(+) 42** (0.1 g, 0.35 mmol) was dissolved in 5 mL THF, followed by the addition of triphenyl phosphine (0.3 g, 1.15 mmol) and dropwise addition of diethylazodicarboxylate (0.2 g, 1.15 mmol) at room temperature and allowed to stir for 2 h. Then the solvent was removed, purified using flash chromatography with 7% ether in hexanes to obtain a colorless viscous liquid (-) **30** (0.059 g, 0.17 mmol, 90 %).

(*S)*-7-methoxy-3-(4-methoxyphenyl)chromane **(-) 30** $[\alpha]^D$ = - 12.2 (c = 0.66, $CHCl_3$); **^{1}H NMR** (400 MHz, Chloroform-*d*) δ 7.17 (d, *J* = 8.5 Hz, 2H), 6.99 (d, *J* = 8.3 Hz, 1H), 6.90 (d, *J* = 8.6 Hz, 2H), 6.49 (dd, *J* = 8.3, 2.6 Hz, 1H), 6.44 (d, *J* = 2.6 Hz, 1H), 4.31 (dd, *J* = 10.6, 2.9 Hz, 1H), 3.98 (t, *J* = 10.5 Hz, 1H), 3.81 (s, 3H), 3.78 (s, 3H), 3.18 (tdd, *J* = 10.5, 7.1, 3.5 Hz, 1H), 2.99 – 2.89 (m, 2H). ^{13}C NMR (101 MHz, $CDCl_3$) δ 159.1, 158.6, 155.0, 133.4, 130.2, 128.3 (2C), 114.2 (3C), 107.3, 101.4, 71.1, 55.3, 55.3, 37.9, 31.9; **ESI-HRMS**: calcd. for $C_{17}H_{19}O_3$ 271.1329 $[M+H]^+$; found 271.1339.

(S)-3-(2,4-Dimethoxyphenyl)-7-(methoxymethoxy)chromane (+) **57**

(*S*)-2-(2-(2,4-Dimethoxyphenyl)-3-hydroxypropyl)-5-(methoxymethoxy)phenol **(+) 43** (0.07 g, 0.20 mmol) was dissolved in 2 mL THF, followed by the addition of triphenyl phosphine (0.3 g, 1.15 mmol) and dropwise addition of diethylazodicarboxylate (0.2 g, 1.15 mmol) at room temperature and allowed to stir for 6 h. Then the solvent was removed, purified using flash chromatography with 7% ether in hexanes to obtain a colorless viscous liquid (*S*)-3-(2,4-Dimethoxyphenyl)-7-(methoxymethoxy)chromane (**+) 57** (0.057 g, 0.17 mmol, 86%).

(*S*)-3-(2,4-Dimethoxyphenyl)-7-(methoxymethoxy)chromane (**+) 57**: Yield 86%; $[\alpha]^D$ = + 9.2 (c = 1.0, $CHCl_3$) ; **IR** (cm^{-1}): 2952, 2933, 1616, 1587, 1506, 1467, 1261, 1208, 1154, 1127, 1033, 925, 836, 827 and 799; **^{1}H NMR** (400 MHz, Chloroform-*d*) δ 7.03 (d, *J* = 8.3 Hz, 1H), 7.00 (d, *J* = 9.1 Hz, 1H), 6.64 – 6.54 (m, 2H), 6.54 – 6.42 (m, 2H), 5.15 (s, 2H), 4.32 (ddd, *J* = 10.4, 3.4, 2.0 Hz, 1H), 4.01 (t, *J* = 10.2 Hz, 1H), 3.82 (s, 3H), 3.81 (s, 3H), 3.65 – 3.49 (m, 1H), 3.49 (s, 3H), 3.00 (dd, *J* = 15.8, 10.8 Hz, 1H), 2.89 (dd, *J* = 15.7, 3.9 Hz, 1H); **^{13}C NMR** (101 MHz, $CDCl_3$) δ 159.7, 158.3, 156.6, 155.1, 130.2, 127.6, 121.8, 116.1, 108.8, 104.4, 104.1, 98.7, 94.6, 70.2, 55.9, 55.4 (2C), 31.6, 30.5. **ESI-HRMS**: calcd. for $C_{19}H_{23}O_5$ 331.1545 $[M+H]^+$; found 331.1543.

(*R*)-3-(2,4-Dimethoxyphenyl)-7-(methoxymethoxy)chromane (**-) 57**: Yield 83%$[\alpha]^D$ = - 10.6 (c = 1.0, $CHCl_3$) ; **IR** (cm^{-1}): 2933, 2838, 1618, 1587, 1467, 1384, 1261, 1208, 1154, 1127, 1033, 1009 and 925; **^{1}H NMR** (400 MHz, Chloroform-*d*) δ 7.02 (d, *J* = 8.2 Hz, 1H), 6.99 (d, *J* = 9.1 Hz, 1H), 6.62 – 6.55 (m, 2H), 6.52 – 6.42 (m, 2H), 5.14 (s, 2H), 4.31 (ddd, *J* = 10.4, 3.5, 2.0 Hz, 1H), 4.00 (t, *J* = 10.1 Hz, 1H), 3.81 (s, 3H), 3.80 (s, 3H), 3.63 – 3.49 (m, 1H), 3.48 (s, 3H), 2.99 (dd, *J* = 15.7, 10.6 Hz, 1H), 2.88 (dd, *J* = 15.7, 4.2 Hz, 1H); **^{13}C NMR** (101 MHz, $CDCl_3$) δ 159.8, 158.4, 156.7, 155.2, 130.3, 127.7, 122.0, 116.2, 109.0, 104.5, 104.3, 98.9, 94.7, 70.3, 56.1,

55.5, 55.5, 31.7, 30.6; **ESI-HRMS**: calcd. for $C_{19}H_{23}O_5$ 331.1545 $[M+H]^+$; found 331.1392.

Deprotection of the isoflavan ***(-), (+) 30*** *and* ***(+), (-) 57*** *product to yield* ***(-), (+) 7****, (+), (-)* ***8.***

(-) **30** (18 g, 66 mmol) was dissolved in pyridine hydrochloride (192 g, 148 mL, 1.66 mol) and refluxed overnight (at 150 ^oC) and the reaction mixture was cooled to the room temperature. After neutralized with excessive $NaHCO_3$ (aq) and extracted by dichloromethane, the crude product was further purified by column chromatography (using 7% ether in hexanes) and dried to produce a colorless crystalline powder (*S*-equol **7**)

(S)-3-(4-Hydroxyphenyl)chroman-7-ol (**S**)-(-)-Equol **(-) 7**

(-) 4 (14 g, 58.08 mmol, 88%). $[\alpha]^D$ = - 19.5 (c = 1.05, MeOH), reported, $[\alpha]^D$ = - 13 (c = 0.21, EtOH) [159]; ^{1}H NMR (400 MHz, Methanol-*d*4) δ 7.09 (d, *J* = 8.5 Hz, 2H), 6.88 (d, *J* = 8.2 Hz, 1H), 6.76 (d, *J* = 8.5 Hz, 2H), 6.33 (dd, *J* = 8.2, 2.5 Hz, 1H), 6.25 (d, *J* = 2.5 Hz, 1H), 4.20 (ddd, *J* = 10.5, 3.6, 1.8 Hz, 1H), 3.91 (t, *J* = 10.5 Hz, 1H), 3.05 (tdd, *J* = 10.2, 6.0, 3.6 Hz, 1H), 2.93 – 2.77 (m, 2H).^{13}C NMR (101 MHz, MeOD) δ 157.6, 157.3, 156.3, 133.8, 131.2, 129.3 (2C), 116.4 (2C), 114.6, 109.1, 103.8, 72.2, 39.4, 33.0; **ESI-HRMS**: calcd. for $C_{15}H_{15}O_3$ 243.1016 $[M+H]^+$; found 243.1017.

(*S*)-3-(2,4-Dimethoxyphenyl)chroman-7-ol (+) **8**

(*S*)-3-(2,4-Dimethoxyphenyl)-7-(methoxymethoxy)chromane (+) **57** (0.034 g, 0.103 mmol) was dissolved in freshly prepared 3 M HCl in methanol (2 mL). After stirring for 30 min, the initial suspension turned into clear solution and continued stirring for additional 15 min at room temperature. The reaction was cooled to 0 ^oC, carefully quenched with saturated $NaHCO_3$ solution. The whole mixture was concentrated under reduced pressure and the resulting mixture was purified by flash chromatography with 10-15% ethyl acetate in hexanes to obtain brown-red crystalline solid (25 mg, 0.087 mmol, 89%).

(*S*)-3-(2,4-Dimethoxyphenyl)chroman-7-ol (+) **8**: $[\alpha]^D$ = + 8.5 (c = 1.0, $CHCl_3$); **IR** (cm^{-1}): 3363, 2928, 2840, 1508, 1460, 1300, 1210, 1158, 1117, 1033, 840, 799 and 739; **^{1}H NMR** (400 MHz, Chloroform-*d*) δ 7.03 (d, *J* = 8.3 Hz, 1H), 6.94 (d, *J* = 8.1 Hz, 1H), 6.55 – 6.43 (m, 2H), 6.43 – 6.30 (m, 2H), 5.18 (bs, 1H), 4.30 (ddd, *J* = 10.2, 3.2, 1.9 Hz, 1H), 4.00 (t, *J* = 10.1 Hz, 1H), 3.82 (s, 3H), 3.81 (s, 3H), 3.57 (tt, *J* = 9.8, 5.1 Hz, 1H), 2.97 (dd, *J* = 15.6, 10.7 Hz, 1H), 2.86 (dd, *J* = 15.6, 5.2 Hz, 1H); **^{13}C NMR** (101 MHz, $CDCl_3$) δ 159.6, 158.3, 155.1, 154.9, 130.4, 127.5, 121.8, 114.8, 107.9, 104.1, 103.2, 98.7, 70.1, 55.4, 55.3, 31.5, 30.3; **ESI-HRMS**: calcd. for $C_{17}H_{19}O_4$ 287.1278 $[M+H]^+$; found 287.1290.

(*S*)-3-(2,4-Dimethoxyphenyl)chroman-7-ol, (*R*)-Sativan (-) **8**: Yield: 88%; $[\alpha]^D$ = - 9.5 (c = 1.0, $CHCl_3$) Reported= -9.9 (c 0.33, MeOH), MP: 128-129 ^oC [159] ; **IR** (cm^{-1}):3404, 2935, 2838, 1618, 1460, 1262, 1210, 1158, 1117, 1033 and 838 ; **^{1}H NMR** (400 MHz, Chloroform-*d*) δ 7.02 (d, *J* = 8.2 Hz, 1H), 6.94 (d, *J* = 8.1 Hz, 1H), 6.53 – 6.43 (m, 2H), 6.43 – 6.33 (m, 2H), 5.06 (bs, 1H), 4.30 (dd, *J* = 10.3, 1.4 Hz, 1H), 4.00 (t, *J* = 10.1 Hz, 1H), 3.81 (s, 3H), 3.81 (s, 3H), 3.56 (tt, *J* = 9.8, 4.5 Hz, 1H), 2.97 (dd, *J* = 15.7, 10.5 Hz, 1H), 2.86 (dd, *J* = 15.6, 4.5 Hz, 1H); **^{13}C NMR** (101 MHz, $CDCl_3$) δ 159.8, 158.4, 155.3, 155.0, 130.5, 127.7, 122.0, 114.9, 108.0, 104.3, 103.3, 98.8, 70.2, 55.5, 55.5, 31.7, 30.5; **ESI-HRMS**: calcd. for $C_{17}H_{19}O_4$ 287.1278 $[M+H]^+$; found 287.1290.

CHAPTER 5

OVERALL CONCLUSIONS

Plants used in the traditional medical systems could beserved as excellent sources to identify new chemical entities. With an aim of identifying new bioactive compounds from traditional medical systems like *Ayurveda*, Traditional Chinese Medicine (TCM), three projects were completed:

1. Identification of small molecule phytochemical inhibitors of BoNT/A using *Ayurvedic* literature (Chapter 2).
2. Identifying the antidiabetic phytochemicals from the TCM plant, Goji (*Lycium* species) (Chapter 3).
3. Enantioselective synthesis of four bioactive isoflavanas: equol and sativan (Chapter 4).

By utilizing a symptom-based *Ayurvedic* literature search, the phytochemicals of fourteen plants were tested for their BoNT/A inhibition activities. *In silico* screening of the 570 phytochemicals was performed using six reported BoNT/A crystal structures. From the docking output, four compounds were selected and 27 other structurally related compounds were screened *in vitro* using HPLC/UPLC-based bioassay. Seven compounds were further tested *ex vivo* using mouse phrenic nerve hemidiaphragm assay (MPNHDA). Initial results of the MPNHDA showed that among the seven compounds, acoric acid possessed marginal protection again BoNT/A. Modification of the structure of the side arms of acoric acid using rational drug-design approaches by utilizing the catalytic binding site of BoNT/A could pave the way for the

identification of more active compounds

To identify new antidiabetic compounds, Goji plant (*L. barbarum* and *L. chinense*) was used. Preparations made of the root bark of Goji were used traditionally for their antidiabetic applications. We screened twenty-seven of the reported phytochemicals *in silico* using partial and full agonist crystal structures (PDB: 2PRG and 3LMP). Docking score and binding pose analysis shortlisted five compounds belonging to the tyramine derivative class of compounds possessed good binding poses. Twenty-four tyramine derivatives were synthesized and tested using PPARγ and PPARα-based luciferase assay. Among the twenty-four tested compounds, three compounds posed good PPARγ selectivity when compared to the positive control Rosiglitazone. A tyramine derivative enriched extract (21 %) was also prepared using the root bark of *L. chinense*. Compound 8 and the enriched extract were tested *in vivo* using diabetic db/db mice models of BoNT/A. Results indicated none of these compounds reduced the post-prandial glucose concentrations. Based on the *in vivo* results, it is concluded that tyramine derivatives may not possess antidiabetic activities and their reported antidiabetic activities (TCM uses) could be due to other chemical constituents of the extracts, or acting on targets other than PPAR.

Soy is commonly used in the traditional foods of the eastern countries especially, Japan, where the incidence of breast cancer is very low compared to the eastern countries like the USA. Isoflavans like *S*-equol are produced *in vivo* upon the oxidation of the soy isoflavonoids like diadzein, by the gut bacteria. The biological properties of equol and other isoflavans like sativan, and vestitol are not yet fully understood, making it necessary to have good amounts of enantio pure compounds. Enantioselective synthesis of these isoflavonoids could be useful to produce enough quantities for further testing. Using simple five synthetic steps, which utilized Evan's

aldol as the chiral center generating step, *R*- and *S*- equol were synthesized at >99% ee with overall yields of 33% ,and 27% for (-), (+) equol, and (+), (-) sativan, respectively.

LIST OF REFERENCES

[1] D.J. Newman, G.M. Cragg, Natural products as sources of new drugs over the 30 years from 1981 to 2010, Journal of Natural Products, 75 (2012) 311-335.
[2] E.D. Lephart, Review: anti-oxidant and anti-aging properties of equol in prostate health (BPH), Open Journal of Endocrine and Metabolic Diseases, 2014 (2014).
[3] W.E. Sneader, Drug Discovery (The History), Wiley Online Library, 2005.
[4] D.S. Fabricant, N.R. Farnsworth, The value of plants used in traditional medicine for drug discovery, Environmental health perspectives, 109 (2001) 69-75.
[5] B. Patwardhan, D. Warude, P. Pushpangadan, N. Bhatt, Ayurveda and traditional Chinese medicine: a comparative overview, Evidence-Based Complementary and Alternative Medicine, 2 (2005) 465-473.
[6] D.J. Newman, G.M. Cragg, Natural Products As Sources of New Drugs over the 30 Years from 1981 to 2010, J. Nat. Prod., 75 (2012) 311-335.
[7] G.M. Cragg, D.J. Newman, Natural products: A continuing source of novel drug leads, Biochim. Biophys. Acta., 1830 (2013) 3670-3695.
[8] D.S. Fabricant, N.R. Farnsworth, The value of plants used in traditional medicine for drug discovery, Environ. Health Perspect., 109 (2001) 69.
[9] B. Patwardhan, R.A. Mashelkar, Traditional medicine-inspired approaches to drug discovery: can Ayurveda show the way forward?, Drug Discovery Today, 14 (2009) 804-811.
[10] S. Koussoulakos, Botulinum neurotoxin: the ugly duckling, Eur. Neurol., 61 (2009) 331-342.
[11] R.K. Dhaked, M.K. Singh, P. Singh, P. Gupta, Botulinum toxin: Bioweapon & magic drug, Indian J. Med. Res., 132 (2010) 489.
[12] G. Schiavo, M. Matteoli, C. Montecucco, Neurotoxins affecting neuroexocytosis, Physiol. Rev., 80 (2000) 717-766.
[13] G. Kumar, S. Swaminathan, Recent Developments with Metalloprotease Inhibitor Class of Drug Candidates for Botulinum Neurotoxins, Curr. Top. Med. Chem., 15 (2015) 685-695.
[14] R. Mazzocchio, M. Caleo, More than at the Neuromuscular Synapse: Actions of Botulinum Neurotoxin A in the Central Nervous System, The Neuroscientist, (2014).
[15] J.J. Chen, K. Dashtipour, Abo-, Inco-, Ona-, and Rima-Botulinum Toxins in Clinical Therapy: A Primer, Pharmacotherapy, 33 (2013) 304-318.
[16] J. Sobel, Botulism, Clin. Infect. Dis., 41 (2005) 1167-1173.
[17] G. Lalli, S. Bohnert, K. Deinhardt, C. Verastegui, G. Schiavo, The journey of tetanus and botulinum neurotoxins in neurons, Trends in microbiology, 11 (2003) 431-437.
[18] D.B. Lacy, W. Tepp, A.C. Cohen, B.R. DasGupta, R.C. Stevens, Crystal structure of botulinum neurotoxin type A and implications for toxicity, Nat. Struct. Mol. Biol., 5 (1998) 898-902.
[19] M. Montal, Botulinum Neurotoxin: A Marvel of Protein Design, Annu. Rev. Biochem., 79 (2010) 591-617.
[20] A.A. Thompson, G.-S. Jiao, S. Kim, A. Thai, L. Cregar-Hernandez, S.A. Margosiak, A.T. Johnson, G.W. Han, S. O'Malley, R.C. Stevens, Structural characterization of three novel hydroxamate-based zinc chelating inhibitors of the Clostridium botulinum serotype A neurotoxin light chain metalloprotease reveals a compact binding site resulting from 60/70 loop flexibility, Biochemistry, 50 (2011) 4019-4028.

[21] M.A. Breidenbach, A.T. Brunger, Substrate recognition strategy for botulinum neurotoxin serotype A, Nature, 432 (2004) 925-929.
[22] M. Montal, Botulinum Neurotoxin: A Marvel of Protein Design, Annual Review of Biochemistry, 79 (2010) 591-617.
[23] P. Silhar, N.R. Silvaggi, S. Pellett, K. Capkova, E.A. Johnson, K.N. Allen, K.D. Janda, Evaluation of adamantane hydroxamates as botulinum neurotoxin inhibitors: Synthesis, crystallography, modeling, kinetic and cellular based studies, Bioorg. Med. Chem., 21 (2013) 1344-1348.
[24] D. Kumaran, R. Rawat, M.L. Ludivico, S.A. Ahmed, S. Swaminathan, Structure- and Substrate-based Inhibitor Design for Clostridium botulinum Neurotoxin Serotype A, J. Biol. Chem., 283 (2008) 18883-18891.
[25] D. Kumaran, R. Rawat, M.L. Ludivico, S.A. Ahmed, S. Swaminathan, Structure- and Substrate-based Inhibitor Design for Clostridium botulinum Neurotoxin Serotype A, Journal of Biological Chemistry, 283 (2008) 18883-18891.
[26] B. Li, N.P. Peet, M.M. Butler, J.C. Burnett, D.T. Moir, T.L. Bowlin, Small molecule inhibitors as countermeasures for botulinum neurotoxin intoxication, Molecules, 16 (2010) 202-220.
[27] H. Lai, M. Feng, V. Roxas-Duncan, S. Dakshanamurthy, L.A. Smith, D.C. Yang, Quinolinol and peptide inhibitors of zinc protease in botulinum neurotoxin A: effects of zinc ion and peptides on inhibition, Archives of biochemistry and biophysics, 491 (2009) 75-84.
[28] J.C. Larsen, US Army botulinum neurotoxin (BoNT) medical therapeutics research program: past accomplishments and future directions, Drug. Dev. Res., 70 (2009) 266-278.
[29] H. Seki, S. Pellett, P. Å ilhÃ¡r, G.N. Stowe, B. Blanco, M.A. Lardy, E.A. Johnson, K.D. Janda, Synthesis/biological evaluation of hydroxamic acids and their prodrugs as inhibitors for Botulinum neurotoxin A light chain, Bioorganic & Medicinal Chemistry, 22 (2014) 1208-1217.
[30] N.R. Silvaggi, G.E. Boldt, M.S. Hixon, J.P. Kennedy, S. Tzipori, K.D. Janda, K.N. Allen, Structures of Clostridium botulinum neurotoxin serotype A light chain complexed with small-molecule inhibitors highlight active-site flexibility, Chemistry & Biology, 14 (2007) 533-542.
[31] B. Thyagarajan, J.G. Potian, C.C. Garcia, K. Hognason, K. Capkova, S.T. Moe, A.R. Jacobson, K.D. Janda, J.J. McArdle, Effects of hydroxamate metalloendoprotease inhibitors on botulinum neurotoxin A poisoned mouse neuromuscular junctions, Neuropharmacology, 58 (2010) 1189-1198.
[32] V. Roxas-Duncan, I. Enyedy, V.A. Montgomery, V.S. Eccard, M.A. Carrington, H. Lai, N. Gul, D.C.H. Yang, L.A. Smith, Identification and biochemical characterization of small-molecule inhibitors of Clostridium botulinum neurotoxin serotype A, Antimicrobial Agents and Chemotherapy, 53 (2009) 3478-3486.
[33] D. Caglic, M.C. Krutein, K.M. Bompiani, D.J. Barlow, G. Benoni, J.C. Pelletier, A.B. Reitz, L.L. Lairson, K.L. Houseknecht, G.R. Smith, Identification of clinically viable quinolinol inhibitors of botulinum neurotoxin A light chain, Journal of Medicinal Chemistry, 57 (2014) 669-676.

[34] N.T. Salzameda, L.M. Eubanks, J.S. Zakhari, K. Tsuchikama, N.J. DeNunzio, K.N. Allen, M.S. Hixon, K.D. Janda, A cross-over inhibitor of the botulinum neurotoxin light chain B: a natural product implicating an exosite mechanism of action, Chem. Commun., 47 (2011) 1713-1715.
[35] P. Silhar, K. Capkova, N.T. Salzameda, J.T. Barbieri, M.S. Hixon, K.D. Janda, Botulinum neurotoxin A protease: discovery of natural product exosite inhibitors, Journal of the American Chemical Society, 132 (2010) 2868-2869.
[36] L.M. Eubanks, P. Šilhár, N.T. Salzameda, J.S. Zakhari, F. Xiaochuan, J.T. Barbieri, C.B. Shoemaker, M.S. Hixon, K.D. Janda, Identification of a natural product antagonist against the botulinum neurotoxin light chain protease, ACS Medicinal Chemistry Letters, 1 (2012) 268-272.
[37] B. Thyagarajan, N. Krivitskaya, J.G. Potian, K. Hognason, C.C. Garcia, J.J. McArdle, Capsaicin protects mouse neuromuscular junctions from the neuroparalytic effects of botulinum neurotoxin a, J. Pharm. Exp. Ther., 331 (2009) 361-371.
[38] B. Thyagarajan, S. Schreiner, P. Baskaran, 3. Capsaicin: A Novel Antidote against Botulinum Neurotoxin A, Toxicon, 60 98.
[39] J.H. Cardellina, V.I. Roxas-Duncan, V. Montgomery, V. Eccard, Y. Campbell, X. Hu, I. Khavrutskii, G.J. Tawa, A. Wallqvist, J.B. Gloer, Fungal bis-naphthopyrones as inhibitors of botulinum neurotoxin serotype A, ACS Medicinal Chemistry Letters, 3 (2012) 387-391.
[40] J.-C. Zhang, L. Sun, Q.-H. Nie, Botulism, where are we now?, Clinical Toxicology, 48 (2010) 867-879.
[41] R. Balakumbahan, K. Rajamani, K. Kumanan, Acorus calamus: An overview, Journal of Medicinal Plants Research, 4 (2010) 2740-2745.
[42] P. Anubhuti, S. Rahul, K.C. Kant, Standardization of Fennel (Foeniculum vulgare), its oleoresin and marketed Ayurvedic dosage forms, Int J Pharm Sci Drug Res, 3 (2011) 265-269.
[43] S. Sreelatha, P.R. Padma, M. Umadevi, Protective effects of Coriandrum sativum extracts on carbon tetrachloride-induced hepatotoxicity in rats, Food and Chemical Toxicology, 47 (2009) 702-708.
[44] D. Bhagwat, M. Kharya, S. Bani, A. Kaul, K. Kour, P.S. Chauhan, K. Suri, N. Satti, Immunosuppressive properties of Pluchea lanceolata leaves, Indian journal of pharmacology, 42 (2010) 21.
[45] A.B. Gokhale, A.S. Damre, M.N. Saraf, Investigations into the immunomodulatory activity of Argyreia speciosa, Journal of Ethnopharmacology, 84 (2003) 109-114.
[46] M. Rana, H. Dhamija, B. Prashar, S. Sharma, Ricinus communis L.—a review, International Journal of PharmTech Research, 4 (2012) 1706-1711.
[47] M.K. Singh, G. Khare, S.K. Iyer, G. Sharwan, D. Tripathi, Clerodendrum serratum: A clinical approach, (2012).
[48] Y.B. Solanki, S.M. Jain, Antihyperlipidemic activity of Clitoria ternatea and Vigna mungo in rats, Pharmaceutical biology, 48 (2010) 915-923.
[49] A. Jain, S. Choubey, P. Singour, H. Rajak, R. Pawar, Sida cordifolia (Linn)–An overview, (2011).
[50] K. Dhalwal, Y.S. Deshpande, A.P. Purohit, Evaluation of in vitro antioxidant activity of Sida rhombifolia (L.) ssp. retusa (L.), Journal of medicinal food, 10 (2007) 683-688.

[51] A. Kumar, V. Singh, A.K. Chaudhary, Gastric antisecretory and antiulcer activities of Cedrus deodara (Roxb.) Loud. in Wistar rats, Journal of ethnopharmacology, 134 (2011) 294-297.
[52] M. Taufiq-Ur-Rahman, J.A. Shilpi, M. Ahmed, C.F. Hossain, Preliminary pharmacological studies on Piper chaba stem bark, Journal of ethnopharmacology, 99 (2005) 203-209.
[53] J.G. Shah, B.G. Patel, S.B. Patel, R.K. Patel, Antiurolithiatic and antioxidant activity of Hordeum vulgare seeds on ethylene glycol-induced urolithiasis in rats, Indian journal of pharmacology, 44 (2012) 672.
[54] H. Joshi, M. Parle, Zingiber officinale: Evaluation of its nootropic effect in mice, (2006).
[55] V. Roxas-Duncan, I. Enyedy, V.A. Montgomery, V.S. Eccard, M.A. Carrington, H. Lai, N. Gul, D.C.H. Yang, L.A. Smith, Identification and biochemical characterization of small-molecule inhibitors of Clostridium botulinum neurotoxin serotype A, Antimicrob. Agents Chemother., 53 (2009) 3478-3486.
[56] B. Thyagarajan, N. Krivitskaya, J.G. Potian, K. Hognason, C.C. Garcia, J.J. McArdle, Capsaicin protects mouse neuromuscular junctions from the neuroparalytic effects of botulinum neurotoxin a, Journal of Pharmacology and Experimental Therapeutics, 331 (2009) 361-371.
[57] B. Thyagarajan, S. Schreiner, P. Baskaran, Capsaicin: A Novel Antidote against Botulinum Neurotoxin A, Toxicon, 60 (2012) 98.
[58] J.J. Schmidt, K.A. Bostian, Endoproteinase activity of type A botulinum neurotoxin: substrate requirements and activation by serum albumin, Journal of Protein Chemistry, 16 (1997) 19-26.
[59] B. Rowe, J.J. Schmidt, L.A. Smith, S.A. Ahmed, Rapid product analysis and increased sensitivity for quantitative determinations of botulinum neurotoxin proteolytic activity, Analytical Biochemistry, 396 (2010) 188-193.
[60] B. Willis, L.M. Eubanks, T.J. Dickerson, K.D. Janda, The strange case of the botulinum neurotoxin: using chemistry and biology to modulate the most deadly poison, Angew. Chem. Int. Ed., 47 (2008) 8360-8379.
[61] X. Hu, P. Legler, N. Southall, D. Maloney, A. Simeonov, A. Jadhav, Structural insight into exosite binding and discovery of novel exosite inhibitors of botulinum neurotoxin serotype A through in silico screening, J. Comput.-Aided Mol. Des., 7 (2014) 765-778.
[62] K. Patel, S. Cai, B.R. Singh, Current strategies for designing antidotes against botulinum neurotoxins, Expert Opinion on Drug Discovery, 9 (2014) 319-333.
[63] J.-C. Zhang, L. Sun, Q.-H. Nie, Botulism, where are we now?, Clin. Toxicol., 48 (2010) 867-879.
[64] Schrödinger, Release 2015-2: Maestro, version 10.3, Schrödinger, LLC, , 2015., in, New York, NY, 2015.
[65] CRCPress, Dictionary of Natural Products on DVD in, 2012.
[66] M. Jensen, T. Smith, S. Ahmed, L. Smith, Expression, purification, and efficacy of the type A botulinum neurotoxin catalytic domain fused to two translocation domain variants, Toxicon, 41 (2003) 691-701.
[67] H. Lai, M. Feng, V. Roxas-Duncan, S. Dakshanamurthy, L.A. Smith, D.C.H. Yang, Quinolinol and peptide inhibitors of zinc protease in botulinum neurotoxin A: Effects of zinc ion and peptides on inhibition, Arch. Biochem. Biophys., 1 (2009) 75-84.

[68] Z. Tao, A. Shi, J. Zhao, Epidemiological perspectives of diabetes, Cell Biochemistry and Biophysics, 73 (2015) 181-185.
[69] B. Li, S.C. Cardinale, M.M. Butler, R. Pai, J.E. Nuss, N.P. Peet, S. Bavari, T.L. Bowlin, Time-dependent botulinum neurotoxin serotype A metalloprotease inhibitors, Bioorganic & Medicinal Chemistry, 19 (2011) 7338-7348.
[70] F.A. Monsalve, R.D. Pyarasani, F. Delgado-Lopez, R. Moore-Carrasco, Peroxisome Proliferator-Activated Receptor Targets for the Treatment of Metabolic Diseases, Mediators of Inflammation, 2013 (2013) 18.
[71] T.M. Willson, P.J. Brown, D.D. Sternbach, B.R. Henke, The PPARs: from orphan receptors to drug discovery, Journal of Medicinal Chemistry, 43 (2000) 527.
[72] B. Grygiel-Górniak, Peroxisome proliferator-activated receptors and their ligands: nutritional and clinical implications - a review, Nutrition Journal, 13 (2014) 17.
[73] A. Farce, N. Renault, P. Chavatte, Structural insight into PPARγ ligands binding, Current Medicinal Chemistry, 16 (2009) 1768-1789.
[74] Y. Li, Z. Wang, N. Furukawa, P. Escaron, J. Weiszmann, G. Lee, M. Lindstrom, J. Liu, X. Liu, H. Xu, T2384, a novel antidiabetic agent with unique peroxisome proliferator-activated receptor γ binding properties, Journal of Biological Chemistry, 283 (2008) 9168-9176.
[75] U. Kintscher, M. Goebel, INT-131, a PPARgamma agonist for the treatment of type 2 diabetes, Current Opinion in Investigational Drugs, 10 (2009) 381-387.
[76] F.M. Gregoire, F. Zhang, H.J. Clarke, T.A. Gustafson, D.D. Sears, S. Favelyukis, J. Lenhard, D. Rentzeperis, L.E. Clemens, Y. Mu, MBX-102/JNJ39659100, a novel peroxisome proliferator-activated receptor-ligand with weak transactivation activity retains antidiabetic properties in the absence of weight gain and edema, Molecular Endocrinology, 23 (2009) 975-988.
[77] B.Y. Hwang, J.-H. Lee, J.B. Nam, H.S. Kim, Y.S. Hong, J.J. Lee, Two New Furanoditerpenes from Saururus c hinenesis and Their Effects on the Activation of Peroxisome Proliferator-Activated Receptor γ, Journal of Natural Products, 65 (2002) 616-617.
[78] A. Elbrecht, Y. Chen, A. Adams, J. Berger, P. Griffin, T. Klatt, B. Zhang, J. Menke, G. Zhou, R.G. Smith, L-764406 is a partial agonist of human peroxisome proliferator-activated receptor gamma. The role of Cys313 in ligand binding, The Journal of Biological Chemistry, 274 (1999) 7913-7922.
[79] A. Furukawa, T. Arita, S. Satoh, K. Wakabayashi, S. Hayashi, Y. Matsui, K. Araki, M. Kuroha, J. Ohsumi, Discovery of a novel selective PPARγ modulator from (–)-Cercosporamide derivatives, Bioorganic & Medicinal Chemistry Letters, 20 (2010) 2095-2098.
[80] A. Furukawa, T. Arita, T. Fukuzaki, S. Satoh, M. Mori, T. Honda, Y. Matsui, K. Wakabayashi, S. Hayashi, K. Araki, Substituents at the naphthalene C3 position of (−)-cercosporamide derivatives significantly affect the maximal efficacy as PPARγ partial agonists, Bioorganic & Medicinal Chemistry Letters, 22 (2012) 1348-1351.
[81] A.R. Vasudevan, A. Balasubramanyam, Thiazolidinediones: a review of their mechanisms of insulin sensitization, therapeutic potential, clinical efficacy, and tolerability, Diabetes Technology & Therapeutics, 6 (2004) 850-863.

[82] C.V. Rizos, M. Elisaf, D.P. Mikhailidis, E.N. Liberopoulos, How safe is the use of thiazolidinediones in clinical practice?, Expert Opinion on Drug Safety, 8 (2009) 15-32.
[83] F. Chang, L.A. Jaber, H.D. Berlie, M.B. O'Connell, Evolution of peroxisome proliferator-activated receptor agonists, Annals of Pharmacotherapy, 41 (2007) 973-983.
[84] J.M. Seargent, E.A. Yates, J.H. Gill, GW9662, a potent antagonist of PPARγ, inhibits growth of breast tumour cells and promotes the anticancer effects of the PPARγ agonist rosiglitazone, independently of PPARγ activation, British Journal of Pharmacology, 143 (2004) 933-937.
[85] R.T. Nolte, G.B. Wisely, S. Westin, J.E. Cobb, M.H. Lambert, R. Kurokawa, M.G. Rosenfeld, T.M. Willson, C.K. Glass, M.V. Milburn, Ligand binding and co-activator assembly of the peroxisome proliferator-activated receptor-γ, Nature, 395 (1998) 137-143.
[86] A.G. Atanasov, J.N. Wang, S.P. Gu, J. Bu, M.P. Kramer, L. Baumgartner, N. Fakhrudin, A. Ladurner, C. Malainer, A. Vuorinen, Honokiol: a non-adipogenic PPARγ agonist from nature, Biochimica et Biophysica Acta (BBA)-General Subjects, 1830 (2013) 4813-4819.
[87] C. Weidner, J.C. de Groot, A. Prasad, A. Freiwald, C. Quedenau, M. Kliem, A. Witzke, V. Kodelja, C.-T. Han, S. Giegold, Amorfrutins are potent antidiabetic dietary natural products, Proceedings of the National Academy of Sciences, 109 (2012) 7257-7262.
[88] C. Weidner, S.J. Wowro, A. Freiwald, K. Kawamoto, A. Witzke, M. Kliem, K. Siems, L. Müller-Kuhrt, F.C. Schroeder, S. Sauer, Amorfrutin B is an efficient natural peroxisome proliferator-activated receptor gamma (PPARγ) agonist with potent glucose-lowering properties, Diabetologia, 56 (2013) 1802-1812.
[89] W. Lee, J. Ham, H.C. Kwon, Y.K. Kim, S.-N. Kim, Anti-diabetic effect of amorphastilbol through PPARα/γ dual activation in db/db mice, Biochemical and Biophysical Research Communications, 432 (2013) 73-79.
[90] M. Kuroda, Y. Mimaki, S. Honda, H. Tanaka, S. Yokota, T. Mae, Phenolics from Glycyrrhiza glabra roots and their PPAR-γ ligand-binding activity, Bioorganic & Medicinal Chemistry, 18 (2010) 962-970.
[91] L. Wang, B. Waltenberger, E.-M. Pferschy-Wenzig, M. Blunder, X. Liu, C. Malainer, T. Blazevic, S. Schwaiger, J.M. Rollinger, E.H. Heiss, Natural product agonists of peroxisome proliferator-activated receptor gamma (PPARγ): a review, Biochemical Pharmacology, 92 (2014) 73-89.
[92] O. Potterat, Goji (Lycium barbarum and L. chinense): phytochemistry, pharmacology and safety in the perspective of traditional uses and recent popularity, Planta Medica, 76 (2010) 7-19.
[93] Committee of National Pharmacopoeia. China Pharmacopoeia (Part 1) Beijing, in, Chemical Industry Press 2010.
[94] H. Amagase, N.R. Farnsworth, A review of botanical characteristics, phytochemistry, clinical relevance in efficacy and safety of Lycium barbarum fruit (Goji), Food Research International, 44 (2011) 1702-1717.
[95] M. Jin, Q. Huang, K. Zhao, P. Shang, Biological activities and potential health benefit effects of polysaccharides isolated from Lycium barbarum L, International Journal of Biological Macromolecules, 54 (2013) 16-23.
[96] R.C.-C. Chang, K.-F. So, Lycium Barbarum and Human Health, Springer, 2015.

[97] R.-f. Yang, C. Zhao, X. Chen, S.-w. Chan, J.-y. Wu, Chemical properties and bioactivities of Goji (Lycium barbarum) polysaccharides extracted by different methods, Journal of Functional Foods, 17 (2014) 903-909.
[98] D. Gao, Q. Li, Z. Liu, Y. Li, Z. Liu, Y. Fan, K. Li, Z. Han, J. Li, Hypoglycemic effects and mechanisms of action of Cortex Lycii Radicis on alloxan-induced diabetic mice, The Pharmaceutical Society of Japan, 127 (2007) 1715-1721.
[99] S.-H. Cho, E.-J. Park, E.-O. Kim, S.-W. Choi, Study on the hypochlolesterolemic and antioxidative effects of tyramine derivatives from the root bark of Lycium chenese Miller, Nutrition Research and Practice, 5 (2011) 412-420.
[100] P.-C. Pan, M.-J. Cheng, C.-F. Peng, H.-Y. Huang, J.-J. Chen, I.-S. Chen, Secondary metabolites from the roots of Litsea hypophaea and their antitubercular activity, Journal of Natural Products, 73 (2010) 890-896.
[101] M. Efdi, K. Ohguchi, Y. Akao, Y. Nozawa, M. Koketsu, H. Ishihara, N-trans-feruloyltyramine as a melanin biosynthesis inhibitor, Biological and Pharmaceutical Bulletin, 30 (2007) 1972-1974.
[102] S. Okombi, D. Rival, S. Bonnet, A.-M. Mariotte, E. Perrier, A. Boumendjel, Analogues of N-hydroxycinnamoylphenalkylamides as inhibitors of human melanocyte-tyrosinase, Bioorganic & Medicinal Chemistry Letters, 16 (2006) 2252-2255.
[103] D.G. Lee, Y. Park, M.-R. Kim, H.J. Jung, Y.B. Seu, K.-S. Hahm, E.-R. Woo, Anti-fungal effects of phenolic amides isolated from the root bark of Lycium chinense, Biotechnology Letters, 26 (2004) 1125-1130.
[104] D. Seebach, T.L. Sommerfeld, Q. Jiang, L.M. Venanzi, Preparation of Oxazolidine-Containing Peptides: Unusual effects in RhIII-catalyzed acetalizations of aldehydes with urethane-protected serine and threonine esters and with dipeptides containing serine or threonine residues at the N-terminus, Helvetica Chimica Acta, 77 (1994) 1313-1330.
[105] S.-H. Han, H.-H. Lee, I.-S. Lee, Y.-H. Moon, E.-R. Woo, A new phenolic amide from Lycium chinense Miller, Archives of Pharmacal Research, 25 (2002) 433-437.
[106] M.H. Yang, Y. Vasquez, Z. Ali, I.A. Khan, S.I. Khan, Constituents from Terminalia species increase PPARα and PPARγ levels and stimulate glucose uptake without enhancing adipocyte differentiation, Journal of Ethnopharmacology, 149 (2013) 490-498.
[107] J. Zhao, S.I. Khan, M. Wang, Y. Vasquez, M.H. Yang, B. Avula, Y.-H. Wang, C. Avonto, T.J. Smillie, I.A. Khan, Octulosonic acid derivatives from roman chamomile (Chamaemelum Nobile) with activities against inflammation and metabolic disorder, Journal of Natural Products, 77 (2014) 509-515.
[108] N.C. Veitch, Isoflavonoids of the Leguminosae, Natural Product Reports, 24 (2007) 417-464.
[109] D.M.X. Donnelly, G.M. Boland, Isoflavonoids and neoflavonoids: naturally occurring O-heterocycles, Natural Product Reports, 12 (1995) 321-338.
[110] A.L. Ososki, E.J. Kennelly, Phytoestrogens: a review of the present state of research, Phytotherapy Research, 17 (2003) 845-869.
[111] N.C. Veitch, Isoflavonoids of the Leguminosae, Natural Product Reports, 26 (2009) 776-802.
[112] N.C. Veitch, Isoflavonoids of the Leguminosae, Natural product reports, 30 (2013) 988-1027.

[113] S. Tahara, R.K. Ibrahim, Prenylated isoflavonoids−an update, Phytochemistry, 38 (1995) 1073-1094.
[114] Food, D. Administration, Food labeling health claims; soy protein and coronary heart disease, Fed Regist, 64 (1999) 57699-57733.
[115] F.-J. He, J.-Q. Chen, Consumption of soybean, soy foods, soy isoflavones and breast cancer incidence: Differences between Chinese women and women in Western countries and possible mechanisms, Food Science and Human Wellness, 2 (2013) 146-161.
[116] P.B. Kaufman, J.A. Duke, H. Brielmann, J. Boik, J.E. Hoyt, A comparative survey of leguminous plants as sources of the isoflavones, genistein and daidzein: implications for human nutrition and health, The Journal of Alternative and Complementary Medicine, 3 (1997) 7-12.
[117] M. Messina, Soy foods, isoflavones, and the health of postmenopausal women, The American Journal of Clinical Nutrition, 100 (2014) 423S-430S.
[118] K.B. Song, C. Atkinson, C.L. Frankenfeld, T. Jokela, K. Wähälä, W.K. Thomas, J.W. Lampe, Prevalence of daidzein-metabolizing phenotypes differs between Caucasian and Korean American women and girls, The Journal of Nutrition, 136 (2006) 1347-1351.
[119] K.D.R. Setchell, C. Clerici, Equol: history, chemistry, and formation, The Journal of Nutrition, 140 (2010) 1355S-1362S.
[120] K.D. Setchell, C. Clerici, Equol: pharmacokinetics and biological actions, The Journal of Nutrition, 140 (2010) 1363S-1368S.
[121] G.F. Marrian, G.A.D. Haslewood, Equol, a new inactive phenol isolated from the ketohydroxyoestrin fraction of mares' urine, Biochemical Journal, 26 (1932) 1227.
[122] G.F. Marrian, D. Beall, The constitution of equol, Biochemical Journal, 29 (1935) 1586.
[123] M.C. Nottle, Composition of some urinary calculi of ruminants in Western Australia, Research in veterinary science, 21 (1976) 309-317.
[124] K.D.R. Setchell, A.M. Lawson, F.L. Mitchell, H. Adlercreutz, D.N. Kirk, M. Axelson, Lignans in man and in animal species, (1980).
[125] K. Kurosawa, W.D. Ollis, B.T. Redman, I.O. Sutherland, O.R. Gottlieb, H.M.e. Alves, The absolute configurations of the animal metabolite, equol, three naturally occurring isoflavans, and one natural isoflavanquinone, Chemical Communications (London), (1968) 1265-1267.
[126] K. Morito, T. Hirose, J. Kinjo, T. Hirakawa, M. Okawa, T. Nohara, S. Ogawa, S. Inoue, M. Muramatsu, Y. Masamune, Interaction of Phytoestrogens with Estrogen Receptors α and β, Biological and Pharmaceutical Bulletin, 24 (2001) 351-356.
[127] S. Yamashita, S. Tsukamoto, M. Kumazoe, Y.-h. Kim, K. Yamada, H. Tachibana, Isoflavones Suppress the Expression of the Fc∈RI High-Affinity Immunoglobulin E Receptor Independent of the Estrogen Receptor, Journal of Agricultural and Food Chemistry, 60 (2012) 8379-8385.
[128] T.D. Lund, D.J. Munson, M.E. Haldy, K.D.R. Setchell, E.D. Lephart, R.J. Handa, Equol Is a Novel Anti-Androgen that Inhibits Prostate Growth and Hormone Feedback, Biology of Reproduction, 70 (2004) 1188-1195.
[129] H.D. VanEtten, Antifungal activity of pterocarpans and other selected isoflavonoids, Phytochemistry, 15 (1976) 655-659.
[130] Y.H. Ju, J. Fultz, K.F. Allred, D.R. Doerge, W.G. Helferich, Effects of dietary daidzein and its metabolite, equol, at physiological concentrations on the growth of estrogen-

dependent human breast cancer (MCF-7) tumors implanted in ovariectomized athymic mice, Carcinogenesis, 27 (2006) 856-863.
[131] E.D. Lephart, Review: Anti-Oxidant and Anti-Aging Properties of Equol in Prostate Health (BPH), Open Journal of Endocrine and Metabolic Diseases, 4 (2014) 1-12.
[132] J. Yao, L. Zhao, Z. Mao, S. Chen, K.C. Wong, J. To, R.D. Brinton, Potentiation of brain mitochondrial function by S-equol and R/S-equol estrogen receptor Î²-selective phytoSERM treatments, Brain Research, 1514 (2013) 128-141.
[133] G.G.J.M. Kuiper, J.G. Lemmen, B.O. Carlsson, J.C. Corton, S.H. Safe, P.T. van der Saag, B. van der Burg, J.-A. Gustafsson, Interaction of estrogenic chemicals and phytoestrogens with estrogen receptor β Endocrinology, 139 (1998) 4252-4263.
[134] R.S. Muthyala, Y.H. Ju, S. Sheng, L.D. Williams, D.R. Doerge, B.S. Katzenellenbogen, W.G. Helferich, J.A. Katzenellenbogen, Equol, a natural estrogenic metabolite from soy isoflavones: convenient preparation and resolution of R-and S-equols and their differing binding and biological activity through estrogen receptors alpha and beta, Bioorganic & Medicinal Chemistry, 12 (2004) 1559-1567.
[135] S.L. Neese, S.L. Pisani, D.R. Doerge, W.G. Helferich, E. Sepehr, A.G. Chittiboyina, S.C. Rotte, T.J. Smillie, I.A. Khan, D.L. Korol, S.L. Schantz, The effects of dietary treatment with S-equol on learning and memory processes in middle-aged ovariectomized rats, Neurotoxicol Teratol, 41 (2014) 80-88.
[136] Y. Jiang, P. Gong, Z. Madak-Erdogan, T. Martin, M. Jeyakumar, K. Carlson, I. Khan, T.J. Smillie, A.G. Chittiboyina, S.C. Rotte, W.G. Helferich, J.A. Katzenellenbogen, B.S. Katzenellenbogen, Mechanisms enforcing the estrogen receptor beta selectivity of botanical estrogens, FASEB J, 27 (2013) 4406-4418.
[137] D. Slade, D. Ferreira, J.P.J. Marais, Circular dichroism, a powerful tool for the assessment of absolute configuration of flavonoids, Phytochemistry, 66 (2005) 2177-2215.
[138] J.L. Ingham, R.L. Millar, Sativin: an Induced Isoflavan from the Leaves of Medicago sativa L, Nature, 242 (1973) 125-126.
[139] R.W. Miller, G.F. Spencer, A.R. Putnam, (-)-5'-Methoxysativan, a New Isoflavan from Alfalfa, Journal of Natural Products, 52 (1989) 634-636.
[140] M.R. Bonde, R.L. Millar, J.L. Ingham, Induction and identification of sativan and vestitol as two phytoalexins from Lotus corniculatus, Phytochemistry, 12 (1973) 2957-2959.
[141] P.W. Grosvenor, D.O. Gray, Coluteol and colutequinone B, more antifungal isoflavonoids from Colutea arborescens, Journal of Natural Products, 61 (1998) 99-101.
[142] T. Miyase, M. Sano, H. Nakai, M. Muraoka, M. Nakazawa, M. Suzuki, K. Yoshino, Y. Nishihara, J. Tanai, Antioxidants from *Lespedeza homoloba*, Phytochemistry, 52 (1999) 303-310.
[143] M. Mori-Hongo, H. Takimoto, T. Katagiri, M. Kimura, Y. Ikeda, T. Miyase, Melanin synthesis inhibitors from Lespedeza floribunda, Journal of Natural Products, 72 (2009) 194-203.
[144] A. Gupta, S. Ray, Simple and Efficient Synthesis of (±)-Equol and Related Derivatives, Synthesis, (2008) 3783-3786.
[145] F. Wessely, F. Prillinger, Die Konstitution des Equols, Berichte der deutschen chemischen Gesellschaft (A and B Series), 72 (1939) 629-633.

[146] J.A. Lamberton, H. Suares, K. Watson, Catalytic hydrogenation of isoflavones. The preparation of (±)-equol and related isoflavans, Australian Journal of Chemistry, 31 (1978) 455-457.
[147] S.J. Gharpure, A.M. Sathiyanarayanan, P. Jonnalagadda, *o*-Quinone methide based approach to isoflavans: application to the total syntheses of equol, 3′-hydroxyequol and vestitol, Tetrahedron Letters, 49 (2008) 2974-2978.
[148] S.p. Usse, G.r. Guillaumet, M.-C. Viaud, A new route to 3,4-dihydro-2H-1-benzopyrans substituted at 3-position via palladium-catalysed reactions, Tetrahedron Letters, 38 (1997) 5501-5502.
[149] T. Jokela, Synthesis of Reduced Metabolites of Isoflavonoids, and their Enantiomeric Forms., in, Ph.D. Dissertation, University of Helsinki, 2011.
[150] C. Deschamps-Vallet, J.-B. Ilotse, M.l. Meyer-Dayan, Transformation du cation isoflavylium en pheny-3 coumarines, isoflavenes-3 et isoflavannes, Tetrahedron Letters, 24 (1983) 3993-3996.
[151] T.L. Shih, M.J. Wyvratt, H. Mrozik, Total synthesis of (±)-5-*O*-methyllicoricidin, The Journal of Organic Chemistry, 52 (1987) 2029-2033.
[152] C. Burali, N. Desideri, M.L. Stein, C. Conti, N. Orsi, Synthesis and anti-rhinovirus activity of halogen-substituted isoflavenes and isoflavans, European Journal of Medicinal Chemistry, 22 (1987) 119-123.
[153] X.-L. Wang, H.-G. Hur, J.H. Lee, K.T. Kim, S.-I. Kim, Enantioselective synthesis of S-equol from dihydrodaidzein by a newly isolated anaerobic human intestinal bacterium, Applied and Environmental Microbiology, 71 (2005) 214-219.
[154] S.-R. Li, P.-Y. Chen, L.-Y. Chen, Y.-F. Lo, I.-L. Tsai, E.-C. Wang, Synthesis of haginin E, equol, daidzein, and formononetin from resorcinol via an isoflavene intermediate, Tetrahedron Letters, 50 (2009) 2121-2123.
[155] J.M. Heemstra, S.A. Kerrigan, D.R. Doerge, W.G. Helferich, W.A. Boulanger, Total synthesis of (S)-equol, Organic Letters, 8 (2006) 5441-5443.
[156] C. Barend, The first enantioselective synthesis of isoflavonoids:(R)-and (S)-isoflavans, Journal of the Chemical Society, Chemical Communications, (1995) 1317-1318.
[157] M. Versteeg, B.C. Bezuidenhoudt, D. Ferreira, Stereoselective synthesis of isoflavonoids.(*R*)-and (*S*)-isoflavens, Tetrahedron, 55 (1999) 3365-3376.
[158] Y. Takashima, Y. Kobayashi, New synthetic route to (S)-(−)-equol through allylic substitution, Tetrahedron Letters, 49 (2008) 5156-5158.
[159] Y. Takashima, Y. Kaneko, Y. Kobayashi, Synthetic access to optically active isoflavans by using allylic substitution, Tetrahedron, 66 (2010) 197-207.
[160] S. Yang, S.-F. Zhu, C.-M. Zhang, S. Song, Y.-B. Yu, S. Li, Q.-L. Zhou, Enantioselective iridium-catalyzed hydrogenation of α-arylcinnamic acids and synthesis of (*S*)-equol, Tetrahedron, 68 (2012) 5172-5178.
[161] Z. Liu, Z. Wang, G. Yoon, S.H. Cheon, Stereoselective total synthesis of (+)-licochalcone E, Archives of Pharmacal Research, 34 (2011) 1269-1276.
[162] R.S. Khupse, J.G. Sarver, J.A. Trendel, N.R. Bearss, M.D. Reese, T.E. Wiese, S.M. Boue, M.E. Burow, T.E. Cleveland, D. Bhatnagar, P.W. Erhardt, Biomimetic Syntheses and Antiproliferative Activities of Racemic, Natural (-), and Unnnatural (+) Glyceollin I, Journal of Medicinal Chemistry, 54 (2011) 3506-3523.

[163] J.R. Gage, D.A. Evans, Diastereoselective Aldol Condensation Using a Chiral Oxazolidinone Auxiliary: (2S*, 3S*)-3-Hydroxy-3-phenyl-2-methylpropanoic acid, Organic Syntheses, 68 (1990) 83-91.
[164] D.A. Evans, J. Bartroli, T.L. Shih, Enantioselective aldol condensations. 2. Erythro-selective chiral aldol condensations via boron enolates, Journal of the American Chemical Society, 103 (1981) 2127-2129.
[165] D.A. Evans, J.V. Nelson, E. Vogel, T.R. Taber, Stereoselective aldol condensations via boron enolates, Journal of the American Chemical Society, 103 (1981) 3099-3111.

LIST OF APPENDICES

APPENDIX 1. SUPPLEMENTARY INFORMATION-CHAPTER 2

SI Table 1. Docking results of the *Ayurvedic* compounds docked into BoNT/A catalytic site. This table shows the first 250 hits including the native ligands and positive controls.

No	Title	glide grid file	docking score	glide gscore	glide emodel	glide energy
1	RC1_ 1095321-15-5	glide-grid_31_3QIY-new-10-23-2015	-11.2432	-11.265	-145.008	-86.886
2	RC1_ 1095321-15-5	glide-grid_31_3QIY-new-10-23-2015	-11.2432	-11.265	-145.008	-86.886
3	**3QIZ-prepared-new-10-22-2015_ligand**	glide-grid_36-3qj0-correct-10-23-2015	-11.0441	-11.074	-117.043	-54.42
4	HV1-CKG41-C.cdx	glide-grid_31_3QIY-new-10-23-2015	-10.9741	-10.974	-126.739	-73.128
5	**3QIZ-prepared-new-10-22-2015_ligand**	glide-grid_36-3qj0-correct-10-23-2015	-10.8408	-10.87	-111.494	-53.148
6	**3QIZ-prepared-new-10-22-2015_ligand**	glide-grid_32-3qiz-newGrid-10-23-2015	-10.7229	-10.752	-104.403	-50.243
7	RC1_ 1095321-15-5	glide-grid_31_3QIY-new-10-23-2015	-10.6787	-12.65	-122.393	-67.337
8	RC1_ 1095321-15-5	glide-grid_31_3QIY-new-10-23-2015	-10.6787	-12.65	-122.393	-67.337
9	HV1-135972-64-4.cdx	glide-grid_32-3qiz-newGrid-10-23-2015	-10.594	-10.61	-98.482	-62.068
10	**3QIZ-prepared-new-10-22-2015_ligand**	glide-grid_32-3qiz-newGrid-10-23-2015	-10.5035	-10.533	-112.814	-53.415
11	**3QJ0-prepared-new_ligand**	glide-grid_36-3qj0-correct-10-23-2015	-10.4994	-10.509	-94.618	-50.245
12	HV1-44257976	glide-grid_31_3QIY-new-10-23-2015	-10.4386	-10.46	-118.669	-72.251
13	RC1_ 1095321-14-4	glide-grid_31_3QIY-new-10-23-2015	-10.3886	-10.41	-109.798	-70.235
14	RC1_ 1095321-14-4	glide-grid_31_3QIY-new-10-23-2015	-10.3886	-10.41	-109.798	-70.235
15	**3QJ0-prepared-new_ligand**	glide-grid_36-3qj0-correct-10-23-2015	-10.3869	-10.396	-96.373	-49.141
16	**4HEV-prepared-new-10-22-2015_ligand**	glide-grid_34-4hev-correct-new-10-23-2015	-10.3421	-10.388	-75.257	-30.455
17	**3QJ0-prepared-new_ligand**	glide-grid_36-3qj0-correct-10-23-2015	-10.2474	-10.257	-95.749	-50.508
18	**3QIZ-prepared-new-10-22-2015_ligand**	glide-grid_31_3QIY-new-10-23-2015	-10.201	-10.23	-102.728	-51.701
19	**3QJ0-prepared-new_ligand**	glide-grid_36-3qj0-correct-10-23-2015	-10.1707	-10.18	-96.71	-51.322
20	**3QIZ-prepared-new-10-22-2015_ligand**	glide-grid_32-3qiz-newGrid-10-23-2015	-10.1043	-10.134	-107.397	-53.079
21	HV1-74235-23-7.cdx	glide-grid_31_3QIY-new-10-23-2015	-10.0462	-10.11	-98.982	-45.701
22	HV1-212271-12-0.cdx	glide-grid_31_3QIY-new-10-23-2015	-10.0287	-10.05	-91.96	-64.533
23	PC1_PL2_1213780-74-5	glide-grid_36-3qj0-correct-10-23-2015	-10.0136	-10.014	-99.532	-53.989
24	**3QIZ-prepared-new-10-22-2015_ligand**	glide-grid_36-3qj0-correct-10-23-2015	-9.84512	-9.875	-100.731	-48.286
25	**3QIZ-prepared-new-10-22-2015_ligand**	glide-grid_32-3qiz-newGrid-10-23-2015	-9.77159	-9.801	-98.711	-49.574
26	ZO1_44256715	glide-grid_31_3QIY-new-10-23-2015	-9.75884	-9.801	-106.67	-69.326
27	CS2-272441-52-8.cdx	glide-grid_36-3qj0-correct-10-23-2015	-9.68586	-9.686	-130.262	-80.1
28	HV1-9799386	glide-grid_36-3qj0-correct-10-23-2015	-9.53581	-9.538	-80.303	-46.685

29	ZO1_MYM60-L	glide-grid_32-3qiz-newGrid-10-23-2015	-9.52553	-9.526	-87.822	-51.141
30	HV1-212271-12-0.cdx	glide-grid_36-3qj0-correct-10-23-2015	-9.46834	-11.46	-107.016	-76.528
31	CD1-75775-36-9.cdx	glide-grid_31_3QIY-new-10-23-2015	-9.41986	-9.42	-83.239	-52.036
32	HV1_7073-64-5.cdx	glide-grid_30-3c8b_new-10-23-2015	-9.39539	-9.395	-140.947	-76.395
33	FV1_1794427 (Chlorogenic acid)	glide-grid_36-3qj0-correct-10-23-2015	-9.32865	-9.336	-89.614	-50.985
34	HV1-162350	glide-grid_31_3QIY-new-10-23-2015	-9.322	-9.346	-89.676	-54.663
35	3QIZ-prepared-new-10-22-2015_ligand	glide-grid_32-3qiz-newGrid-10-23-2015	-9.24961	-9.267	-95.618	-60.003
36	HV1-JTP73-Q.cdx	glide-grid_31_3QIY-new-10-23-2015	-9.24475	-9.269	-88.619	-59.293
37	ZO1_Duke_05	glide-grid_31_3QIY-new-10-23-2015	-9.20203	-9.202	-84.212	-54.626
38	ZO1_1794427	glide-grid_36-3qj0-correct-10-23-2015	-9.19684	-9.204	-88.523	-50.94
39	FV1_44259215	glide-grid_31_3QIY-new-10-23-2015	-9.16344	-9.181	-91.865	-60.744
40	CD1-CRC-JNB98-T.cdx	glide-grid_34-4hev-correct-new-10-23-2015	-9.13141	-9.133	-54.857	-28.523
41	AS1-150226-16-7.cdx	glide-grid_31_3QIY-new-10-23-2015	-9.10403	-9.139	-101.617	-63.518
42	CD1-27200-12-0.cdx	glide-grid_31_3QIY-new-10-23-2015	-9.06912	-9.132	-77.958	-47.426
43	FV1_5490064	glide-grid_31_3QIY-new-10-23-2015	-9.05461	-9.073	-99.97	-64.471
44	RC1_195702-53-5	glide-grid_31_3QIY-new-10-23-2015	-9.03342	-9.051	-79.714	-68.85
45	RC1_195702-53-5	glide-grid_31_3QIY-new-10-23-2015	-9.03342	-9.051	-79.714	-68.85
46	PL1_BJR89-H	glide-grid_36-3qj0-correct-10-23-2015	-8.9887	-8.989	-60.276	-28.416
47	HV1-54680783	glide-grid_32-3qiz-newGrid-10-23-2015	-8.91963	-8.92	-56.144	-29.913
48	HV1-212271-11-9.cdx	glide-grid_32-3qiz-newGrid-10-23-2015	-8.9165	-8.937	-104.207	-70.571
49	ZO1_Duke_19	glide-grid_31_3QIY-new-10-23-2015	-8.91471	-8.915	-88.996	-61.818
50	CD1-344363-33-3.cdx	glide-grid_31_3QIY-new-10-23-2015	-8.86445	-8.865	-43.962	-25.133
51	SC1_SR1_905833-45-6	glide-grid_31_3QIY-new-10-23-2015	-8.85517	-8.864	-84.354	-64.922
52	AC1-42607660	glide-grid_34-4hev-correct-new-10-23-2015	-8.85461	-8.855	-59.237	-33.138
53	HV1-35450-86-3.cdx	glide-grid_31_3QIY-new-10-23-2015	-8.85296	-8.874	-105.304	-66.627
54	HV1-496788-49-9.cdx	glide-grid_31_3QIY-new-10-23-2015	-8.79074	-8.812	-100.955	-70.674
55	ZO1_182227-92-5	glide-grid_31_3QIY-new-10-23-2015	-8.78204	-8.782	-92.598	-62.458
56	PC1_PL2_ONF51-X	glide-grid_31_3QIY-new-10-23-2015	-8.73471	-8.735	-67.807	-34.564
57	PC1_PL2_25173-72-2	glide-grid_36-3qj0-correct-10-23-2015	-8.72686	-8.727	-65.679	-36.79
58	FV1_6508	glide-grid_36-3qj0-correct-10-23-2015	-8.70238	-8.702	-64.527	-34.591
59	RC1_5280863	glide-grid_31_3QIY-new-10-23-2015	-8.68964	-8.719	-62.335	-41.522

60	RC1_5280863	glide-grid_31_3QIY-new-10-23-2015	-8.68964	-8.719	-62.335	-41.522
61	CS2-288094-92-8.cdx	glide-grid_31_3QIY-new-10-23-2015	-8.68299	-9.152	-79.967	-45.115
62	HV1-6466	glide-grid_36-3qj0-correct-10-23-2015	-8.68123	-8.681	-76.024	-40.945
63	FV1_5318717	glide-grid_31_3QIY-new-10-23-2015	-8.637	-8.655	-91.155	-59.905
64	FV1_3469	glide-grid_31_3QIY-new-10-23-2015	-8.62922	-8.63	-55.863	-27.582
65	CD1-83728-85-2.cdx	glide-grid_31_3QIY-new-10-23-2015	-8.61079	-8.612	-81.024	-50.93
66	**3QIZ-prepared-new-10-22-2015_ligand**	glide-grid_36-3qj0-correct-10-23-2015	-8.56064	-8.578	-96.987	-60.085
67	CS2-529-53-3.cdx	glide-grid_31_3QIY-new-10-23-2015	-8.55945	-8.6	-73.116	-51.567
68	**3QIZ-prepared-new-10-22-2015_ligand**	glide-grid_36-3qj0-correct-10-23-2015	-8.55482	-8.572	-97.405	-60.24
69	**NSC 84094**	glide-grid_31_3QIY-new-10-23-2015	-8.54905	-8.688	-64.319	-46.057
70	ZO1_44256715	glide-grid_31_3QIY-new-10-23-2015	-8.54783	-10.336	-104.421	-65.432
71	3QIZ-prepared-new-10-22-2015_ligand	glide-grid_32-3qiz-newGrid-10-23-2015	-8.53056	-8.548	-105.331	-62.737
72	3QIZ-prepared-new-10-22-2015_ligand	glide-grid_32-3qiz-newGrid-10-23-2015	-8.52118	-8.539	-73.889	-54.986
73	FV1_5280863	glide-grid_31_3QIY-new-10-23-2015	-8.44933	-8.478	-61.83	-40.947
74	FV1_441476	glide-grid_32-3qiz-newGrid-10-23-2015	-8.44049	-8.44	-68.221	-35.004
75	3QJ0-prepared-new_ligand	glide-grid_36-3qj0-correct-10-23-2015	-8.43637	-8.472	-85.894	-54.693
76	HV1-445858	glide-grid_31_3QIY-new-10-23-2015	-8.42794	-8.428	-51.512	-26.218
77	FV1_445858	glide-grid_31_3QIY-new-10-23-2015	-8.42794	-8.428	-51.512	-26.218
78	CD1-120019-19-4.cdx	glide-grid_32-3qiz-newGrid-10-23-2015	-8.40488	-8.407	-57.871	-33.493
79	PC1_PL2_41917-45-7	glide-grid_31_3QIY-new-10-23-2015	-8.38556	-8.387	-59.86	-29.046
80	CS1-5280805	glide-grid_31_3QIY-new-10-23-2015	-8.35134	-8.369	-90.343	-60.368
81	CS1-441476	glide-grid_34-4hev-correct-new-10-23-2015	-8.33235	-8.332	-65.801	-31.527
82	CS2-529-53-3	glide-grid_31_3QIY-new-10-23-2015	-8.29473	-8.335	-72.264	-51.932
83	CS1-72	glide-grid_32-3qiz-newGrid-10-23-2015	-8.28371	-8.284	-59.565	-28.494
84	HV1-442530	glide-grid_29-2ILP_new-10-23-2015	-8.25516	-8.403	-57.271	-36.1
85	SC1_SR1_960198-74-7	glide-grid_29-2ILP_new-10-23-2015	-8.2547	-8.255	-96.291	-63.032
86	CS2-288094-92-8.cdx	glide-grid_31_3QIY-new-10-23-2015	-8.25284	-8.615	-73.279	-39.086
87	CS2-529-53-3.cdx	glide-grid_31_3QIY-new-10-23-2015	-8.25234	-10.384	-83.13	-40.869
88	CS2-529-53-3	glide-grid_31_3QIY-new-10-23-2015	-8.25071	-10.383	-83.972	-40.828
89	3C8B-prepared-new-10-22-2015_ligand	glide-grid_29-2ILP_new-10-23-2015	-8.25041	-9.317	-141.523	-70.128
90	HV1-44257976	glide-grid_31_3QIY-new-10-23-2015	-8.23377	-10.201	-112.868	-69.291

91	HV1-69199-37-7.cdx	glide-grid_34-4hev-correct-new-10-23-2015	-8.23139	-8.372	-81.208	-40.3
92	AS1-150226-15-6.cdx	glide-grid_31_3QIY-new-10-23-2015	-8.22387	-8.259	-90.883	-60.416
93	RC1_445858	glide-grid_31_3QIY-new-10-23-2015	-8.21507	-8.215	-50.47	-25.965
94	RC1_445858	glide-grid_31_3QIY-new-10-23-2015	-8.21507	-8.215	-50.47	-25.965
95	HV1-74281-81-5.cdx	glide-grid_31_3QIY-new-10-23-2015	-8.20757	-8.348	-70.736	-35.429
96	HV1-79136-97-3.cdx	glide-grid_32-3qiz-newGrid-10-23-2015	-8.20699	-9.031	-73.031	-66.421
97	HV1-79136-97-3.cdx	glide-grid_32-3qiz-newGrid-10-23-2015	-8.20328	-8.738	-64.722	-55.424
98	SC1_SR1_1068148-58-2	glide-grid_31_3QIY-new-10-23-2015	-8.19353	-8.222	-63.159	-43.486
99	3QJ0-prepared-new_ligand	glide-grid_36-3qj0-correct-10-23-2015	-8.18619	-8.222	-91.457	-59.538
100	FV1_44258918	glide-grid_32-3qiz-newGrid-10-23-2015	-8.18618	-8.211	-84.072	-57.09
101	HV1-5280896	glide-grid_36-3qj0-correct-10-23-2015	-8.17129	-8.174	-61.142	-33.716
102	CS2-284486-60-8.cdx	glide-grid_32-3qiz-newGrid-10-23-2015	-8.17014	-8.17	-85.187	-60.944
103	HV1-5165850	glide-grid_36-3qj0-correct-10-23-2015	-8.16119	-8.161	-59.115	-30.495
104	AC1-286957-98-0.cdx	glide-grid_31_3QIY-new-10-23-2015	-8.14587	-8.146	-71.456	-51.697
105	3QIZ-prepared-new-10-22-2015_ligand	glide-grid_36-3qj0-correct-10-23-2015	-8.13628	-8.154	-86.549	-56.917
106	CS2-272441-52-8	glide-grid_31_3QIY-new-10-23-2015	-8.10422	-8.104	-73.319	-68.551
107	SC1_SR1_130690-19-6	glide-grid_31_3QIY-new-10-23-2015	-8.09622	-8.096	-67.62	-55.512
108	3C8B-prepared-new-10-22-2015_ligand	glide-grid_36-3qj0-correct-10-23-2015	-8.09366	-8.553	-104.929	-60.201
109	SC1_SR1_6159-55-3	glide-grid_31_3QIY-new-10-23-2015	-8.08566	-8.115	-50.348	-33.487
110	3C8B-prepared-new-10-22-2015_ligand	glide-grid_31_3QIY-new-10-23-2015	-8.07643	-8.442	-97.001	-58.326
111	FV1_7478	glide-grid_34-4hev-correct-new-10-23-2015	-8.07231	-8.073	-46.702	-22.218
112	HV1-135972-64-4.cdx	glide-grid_31_3QIY-new-10-23-2015	-8.06785	-10.574	-95.074	-64.129
113	AC1-5956-06-9.cdx (acoric acid)	glide-grid_34-4hev-correct-new-10-23-2015	-8.06577	-8.066	-56.819	-30.785
114	PC1_PL2_94-53-1	glide-grid_34-4hev-correct-new-10-23-2015	-8.06479	-8.065	-49.172	-24.087
115	HV1-73607-09-7.cdx	glide-grid_32-3qiz-newGrid-10-23-2015	-8.04973	-8.05	-73.803	-41.945
116	SC1_SR1_PSS18-Z	glide-grid_31_3QIY-new-10-23-2015	-8.0208	-8.037	-58.143	-39.551
117	RC1_ 1095321-14-4	glide-grid_31_3QIY-new-10-23-2015	-8.01734	-9.989	-113.579	-76.323
118	RC1_ 1095321-14-4	glide-grid_31_3QIY-new-10-23-2015	-8.01734	-9.989	-113.579	-76.323
119	3QIZ-prepared-new-10-22-2015_ligand	glide-grid_31_3QIY-new-10-23-2015	-8.00863	-8.026	-86.604	-56.043
120	3C8B-prepared-new-10-22-2015_ligand	glide-grid_29-2ILP_new-10-23-2015	-8.00109	-8.367	-141.341	-70.601
121	CD1-439533	glide-grid_32-3qiz-newGrid-10-23-2015	-7.98639	-9.463	-85.785	-47.874

122	CD1-27200-12-0.cdx	glide-grid_32-3qiz-newGrid-10-23-2015	-7.98507	-9.468	-88.835	-49.799
123	3C8B-prepared-new-10-22-2015_ligand	glide-grid_31_3QIY-new-10-23-2015	-7.97301	-8.339	-90.159	-57.871
124	3C8B-prepared-new-10-22-2015_ligand	glide-grid_31_3QIY-new-10-23-2015	-7.96955	-8.429	-99.983	-62.285
125	CD1-31106-05-5.cdx	glide-grid_30-3c8b_new-10-23-2015	-7.96223	-9.439	-106.593	-58.448
126	AS1-12309749	glide-grid_31_3QIY-new-10-23-2015	-7.95861	-8.094	-58.823	-39.139
127	HV1-439258	glide-grid_34-4hev-correct-new-10-23-2015	-7.93694	-7.937	-63.681	-29.858
128	ZO1_5280863	glide-grid_31_3QIY-new-10-23-2015	-7.93111	-7.96	-61.759	-41.336
129	3C8B-prepared-new-10-22-2015_ligand	glide-grid_30-3c8b_new-10-23-2015	-7.91267	-8.979	-143.322	-68.554
130	ZO1_6431302	glide-grid_36-3qj0-correct-10-23-2015	-7.90271	-7.903	-42.573	-26.885
131	FV1_5280804	glide-grid_31_3QIY-new-10-23-2015	-7.8918	-7.91	-83.984	-55.566
132	HV1-189811	glide-grid_31_3QIY-new-10-23-2015	-7.87601	-8.009	-67.83	-34.508
133	ZO1_Duke_10	glide-grid_31_3QIY-new-10-23-2015	-7.85581	-7.856	-78.683	-52.668
134	SC1_SR1_1000152-08-8	glide-grid_31_3QIY-new-10-23-2015	-7.83612	-8.175	-49.352	-30.393
135	CD1-51373-21-8.cdx	glide-grid_34-4hev-correct-new-10-23-2015	-7.82712	-7.827	-50.848	-25.28
136	SC1_SR1_32164-04-8	glide-grid_36-3qj0-correct-10-23-2015	-7.8132	-7.828	-56.462	-37.7
137	3C8B-prepared-new-10-22-2015_ligand	glide-grid_31_3QIY-new-10-23-2015	-7.79753	-8.164	-101.644	-64.931
138	FV1_637540	glide-grid_36-3qj0-correct-10-23-2015	-7.79307	-7.795	-47.058	-24.344
139	PM1-5281810	glide-grid_31_3QIY-new-10-23-2015	-7.77438	-7.801	-81.597	-55.442
140	3QIZ-prepared-new-10-22-2015_ligand	glide-grid_31_3QIY-new-10-23-2015	-7.77143	-7.789	-83.49	-55.379
141	3C8B-prepared-new-10-22-2015_ligand	glide-grid_31_3QIY-new-10-23-2015	-7.77082	-8.23	-95.606	-58.337
142	**NSC 84094**	glide-grid_31_3QIY-new-10-23-2015	-7.76001	-8.76	-69.837	-46.236
143	CD1-57308-24-4.cdx	glide-grid_34-4hev-correct-new-10-23-2015	-7.75705	-7.757	-56.145	-38.158
144	HV1-212271-11-9.cdx	glide-grid_36-3qj0-correct-10-23-2015	-7.75119	-9.743	-106.109	-64.814
145	**CB 7967495**	glide-grid_31_3QIY-new-10-23-2015	-7.74581	-7.784	-70.275	-45.745
146	PM2-611-40-5.cdx	glide-grid_31_3QIY-new-10-23-2015	-7.73667	-7.764	-81.84	-55.491
147	SC1_SR1_1040198-26-2	glide-grid_36-3qj0-correct-10-23-2015	-7.73586	-7.736	-54.522	-33.441
148	ZO1_Duke_14	glide-grid_36-3qj0-correct-10-23-2015	-7.72124	-7.721	-87.276	-58.247
149	3C8B-prepared-new-10-22-2015_ligand	glide-grid_36-3qj0-correct-10-23-2015	-7.71896	-8.085	-92.678	-55.083
150	AS1-442072	glide-grid_31_3QIY-new-10-23-2015	-7.71	-7.835	-48.88	-31.977
151	PL1_HBY78-W	glide-grid_34-4hev-correct-new-10-23-2015	-7.70495	-8.26	-57.136	-28.786
152	HV1-5281166	glide-grid_34-4hev-correct-new-10-23-2015	-7.7035	-7.704	-57.337	-28.569

153	FV1_5281166	glide-grid_34-4hev-correct-new-10-23-2015	-7.7035	-7.704	-57.337	-28.569
154	CS1-938	glide-grid_34-4hev-correct-new-10-23-2015	-7.70288	-7.706	-43.452	-21.828
155	CB 7969312	glide-grid_31_3QIY-new-10-23-2015	-7.70063	-7.949	-65.856	-44.916
156	CS2-267892-26-2.cdx	glide-grid_32-3qiz-newGrid-10-23-2015	-7.69216	-7.696	-80.666	-59.48
157	HV1- 10502-21-3.cdx	glide-grid_29-2ILP_new-10-23-2015	-7.68666	-7.689	-98.953	-61.552
158	3QJ0-prepared-new_ligand	glide-grid_29-2ILP_new-10-23-2015	-7.68472	-7.72	-83.402	-55.483
159	SC1_SR1_934476-88-7	glide-grid_34-4hev-correct-new-10-23-2015	-7.68442	-7.78	-69.427	-46.199
160	SC1_SR1_960198-73-6	glide-grid_29-2ILP_new-10-23-2015	-7.68328	-7.683	-98.095	-68.566
161	CD1-CRC-OQM82-L.cdx	glide-grid_31_3QIY-new-10-23-2015	-7.67989	-7.687	-88.492	-62.704
162	CD1-57759-55-4.cdx	glide-grid_32-3qiz-newGrid-10-23-2015	-7.66694	-7.667	-70.221	-47.153
163	HV1-189811	glide-grid_31_3QIY-new-10-23-2015	-7.6577	-8.863	-80.853	-37.841
164	CD1-31076-39-8.cdx	glide-grid_34-4hev-correct-new-10-23-2015	-7.64576	-9.117	-80.871	-43.807
165	3C8B-prepared-new-10-22-2015_ligand	glide-grid_31_3QIY-new-10-23-2015	-7.64391	-8.103	-99.552	-63.591
166	PM1-Glutamylmethioninsulfoxide.cdx	glide-grid_31_3QIY-new-10-23-2015	-7.63204	-7.632	-69.69	-38.724
167	SC1_SR1_905833-45-6	glide-grid_30-3c8b_new-10-23-2015	-7.63177	-10.122	-114.91	-63.132
168	CS2-267892-28-4	glide-grid_30-3c8b_new-10-23-2015	-7.62415	-7.624	-87.605	-62.862
169	3C8B-prepared-new-10-22-2015_ligand	glide-grid_31_3QIY-new-10-23-2015	-7.60088	-7.967	-96.712	-62.428
170	3C8B-prepared-new-10-22-2015_ligand	glide-grid_32-3qiz-newGrid-10-23-2015	-7.59863	-8.058	-98.565	-58.904
171	ZO1_Duke_02	glide-grid_31_3QIY-new-10-23-2015	-7.59316	-7.593	-86.915	-60.931
172	CS2-222853-11-4.cdx	glide-grid_30-3c8b_new-10-23-2015	-7.57271	-7.573	-92.737	-65.754
173	CD1-33788-39-5.cdx	glide-grid_32-3qiz-newGrid-10-23-2015	-7.57142	-9.043	-82.388	-45.792
174	3QJ0-prepared-new_ligand	glide-grid_29-2ILP_new-10-23-2015	-7.57002	-7.606	-82.036	-54.357
175	3C8B-prepared-new-10-22-2015_ligand	glide-grid_31_3QIY-new-10-23-2015	-7.56556	-8.025	-85.111	-55.27
176	ZO1_5280343 (Quercetin dihydrate)	glide-grid_31_3QIY-new-10-23-2015	-7.56261	-7.592	-70.068	-44.723
177	3C8B-prepared-new-10-22-2015_ligand	glide-grid_32-3qiz-newGrid-10-23-2015	-7.55793	-7.924	-97.439	-54.328
178	4HEV-prepared-new-10-22-2015_ligand	glide-grid_36-3qj0-correct-10-23-2015	-7.55311	-7.559	-56.123	-33.615
179	HV1-69199-37-7.cdx	glide-grid_31_3QIY-new-10-23-2015	-7.54671	-8.634	-75.502	-38.19
180	3C8B-prepared-new-10-22-2015_ligand	glide-grid_30-3c8b_new-10-23-2015	-7.53896	-7.905	-156.051	-83.623
181	CD1-26294-59-7.cdx	glide-grid_31_3QIY-new-10-23-2015	-7.53739	-7.537	-47.301	-33.109
182	CD1-75513-81-4.cdx	glide-grid_32-3qiz-newGrid-10-23-2015	-7.5256	-9.003	-84.885	-47.566
183	AC1-71609-04-6.cdx	glide-grid_36-3qj0-correct-10-23-2015	-7.51927	-7.519	-35.808	-25.371

184	CS2-267892-26-2	glide-grid_31_3QIY-new-10-23-2015	-7.51605	-7.518	-71.167	-53.491
185	CD1-33788-39-5.cdx	glide-grid_31_3QIY-new-10-23-2015	-7.50014	-7.552	-67.87	-45.758
186	CD1-65373	glide-grid_31_3QIY-new-10-23-2015	-7.49389	-7.494	-73.68	-48.888
187	CD1-5280343	glide-grid_31_3QIY-new-10-23-2015	-7.49252	-7.522	-69.334	-44.168
188	ZO1_SID_135265111	glide-grid_36-3qj0-correct-10-23-2015	-7.49039	-7.49	-85.796	-61.011
189	FV1_5280343	glide-grid_31_3QIY-new-10-23-2015	-7.48647	-7.515	-69.255	-44.132
190	CD1-26920-04-7.cdx	glide-grid_31_3QIY-new-10-23-2015	-7.47956	-7.48	-42.002	-31.598
191	AS1-442072	glide-grid_36-3qj0-correct-10-23-2015	-7.46396	-10.429	-79.902	-38.06
192	CS1-NJP14.cdx	glide-grid_31_3QIY-new-10-23-2015	-7.44958	-7.45	-81.08	-58.72
193	AS1-12309749	glide-grid_29-2ILP_new-10-23-2015	-7.44936	-10.415	-82.953	-38.52
194	CS1_104154-37-2.cdx	glide-grid_36-3qj0-correct-10-23-2015	-7.4484	-7.448	-63.246	-41.307
195	3C8B-prepared-new-10-22-2015_ligand	glide-grid_32-3qiz-newGrid-10-23-2015	-7.42853	-7.795	-99.151	-57.533
196	CB 7969312	glide-grid_34-4hev-correct-new-10-23-2015	-7.42567	-8.125	-73.631	-41.92
197	ZO1_65575	glide-grid_34-4hev-correct-new-10-23-2015	-7.42033	-7.42	-50.006	-34.143
198	HV1-442530	glide-grid_32-3qiz-newGrid-10-23-2015	-7.41913	-8.315	-81.904	-43.858
199	3C8B-prepared-new-10-22-2015_ligand	glide-grid_32-3qiz-newGrid-10-23-2015	-7.41033	-7.869	-96.496	-57.929
200	PC1_PL2_23477-80-7	glide-grid_31_3QIY-new-10-23-2015	-7.40943	-7.409	-62.883	-42.691
201	HV1_28608-75-5.cdx	glide-grid_32-3qiz-newGrid-10-23-2015	-7.39769	-7.42	-86.853	-58.531
202	HV1- LBD65-H.cdx	glide-grid_34-4hev-correct-new-10-23-2015	-7.39035	-7.395	-43.814	-28.062
203	CS1-5280804	glide-grid_32-3qiz-newGrid-10-23-2015	-7.36838	-7.386	-77.506	-51.991
204	ZO1_5317588	glide-grid_36-3qj0-correct-10-23-2015	-7.35953	-7.36	-60.058	-43.338
205	ZO1_Duke_06	glide-grid_34-4hev-correct-new-10-23-2015	-7.35903	-7.359	-70.854	-48.902
206	CS1-5280343	glide-grid_31_3QIY-new-10-23-2015	-7.34859	-7.378	-68.037	-44.868
207	PC1_PL2_20069-09-4	glide-grid_31_3QIY-new-10-23-2015	-7.34639	-7.346	-59.144	-42.682
208	AC1-71305-89-0.cdx	glide-grid_31_3QIY-new-10-23-2015	-7.33951	-7.34	-41.588	-27.508
209	AC1-258885-35-7.cdx	glide-grid_29-2ILP_new-10-23-2015	-7.33828	-7.338	-81.747	-59.637
210	ZO1_12306047	glide-grid_31_3QIY-new-10-23-2015	-7.33565	-7.336	-34.168	-24.852
211	AS1-442072	glide-grid_30-3c8b_new-10-23-2015	-7.31776	-8.301	-78.627	-45.855
212	ZO1_44256715	glide-grid_31_3QIY-new-10-23-2015	-7.31524	-9.647	-104.97	-66.721
213	CD1-31106-05-5.cdx	glide-grid_32-3qiz-newGrid-10-23-2015	-7.30513	-7.362	-87.95	-59.447
214	ZO1_Duke_04	glide-grid_31_3QIY-new-10-23-2015	-7.29093	-7.291	-71.354	-50.276

215	3C8B-prepared-new-10-22-2015_ligand	glide-grid_32-3qiz-newGrid-10-23-2015	-7.28832	-10.245	-114.446	-61.456
216	SC1_SR1_957477-44-0	glide-grid_34-4hev-correct-new-10-23-2015	-7.2812	-7.29	-95.951	-69.376
217	ZO1_Duke_13	glide-grid_31_3QIY-new-10-23-2015	-7.27511	-7.275	-81.067	-58.981
218	HV1-69199-37-7.cdx	glide-grid_34-4hev-correct-new-10-23-2015	-7.26854	-9.033	-84.306	-41.123
219	CD1-3853-83-6.cdx	glide-grid_36-3qj0-correct-10-23-2015	-7.265	-7.265	-43.556	-30.396
220	SC1_SR1_486-64-6	glide-grid_31_3QIY-new-10-23-2015	-7.25897	-7.259	-47.286	-31.44
221	CD1-85317-74-4.cdx	glide-grid_34-4hev-correct-new-10-23-2015	-7.25295	-7.253	-82.265	-53.77
222	PC1_PL2_109771-09-7	glide-grid_31_3QIY-new-10-23-2015	-7.24451	-7.348	-56.281	-40.261
223	HV1-74235-23-7.cdx	glide-grid_32-3qiz-newGrid-10-23-2015	-7.24358	-8.636	-82.144	-43.369
224	AC1-211944-25-1.cdx	glide-grid_29-2ILP_new-10-23-2015	-7.23863	-7.239	-77.399	-59.931
225	ZO1_SID_135229712	glide-grid_31_3QIY-new-10-23-2015	-7.22721	-7.234	-86.543	-64.413
226	ZO1_Duke_11	glide-grid_31_3QIY-new-10-23-2015	-7.20988	-7.21	-86.296	-61.527
227	ZO1_120163-17-9	glide-grid_34-4hev-correct-new-10-23-2015	-7.20538	-7.205	-76.205	-52.29
228	HV1-JTP73-Q.cdx	glide-grid_31_3QIY-new-10-23-2015	-7.19416	-9.527	-87.959	-57.417
229	3C8B-prepared-new-10-22-2015_ligand	glide-grid_36-3qj0-correct-10-23-2015	-7.18911	-7.648	-91.556	-56.44
230	AC1-5281616 (Galangin)	glide-grid_31_3QIY-new-10-23-2015	-7.18884	-7.227	-56.136	-38.383
231	CS1-116408-80-1.cdx	glide-grid_36-3qj0-correct-10-23-2015	-7.18839	-7.188	-46.282	-30.332
232	RC1_5281855	glide-grid_30-3c8b_new-10-23-2015	-7.18382	-7.249	-75.944	-49.662
233	RC1_5281855	glide-grid_30-3c8b_new-10-23-2015	-7.18382	-7.249	-75.944	-49.662
234	CS2- 288094-92-8	glide-grid_31_3QIY-new-10-23-2015	-7.17828	-7.647	-62.085	-39.414
235	PC1_PL2_23434-88-0	glide-grid_31_3QIY-new-10-23-2015	-7.17633	-7.176	-54.653	-38.793
236	CS2- 288094-92-8	glide-grid_32-3qiz-newGrid-10-23-2015	-7.17419	-7.536	-69.84	-41.625
237	UP2-942486-48-8.cdx	glide-grid_29-2ILP_new-10-23-2015	-7.1741	-9.002	-101.773	-56.528
238	HV1-10153	glide-grid_29-2ILP_new-10-23-2015	-7.16243	-7.2	-64.324	-42.213
239	ZO1_5352470	glide-grid_34-4hev-correct-new-10-23-2015	-7.14286	-7.143	-42.518	-31.973
240	ZO1_5281775	glide-grid_32-3qiz-newGrid-10-23-2015	-7.14149	-7.141	-70.84	-48.643
241	HV1-74281-81-5.cdx	glide-grid_32-3qiz-newGrid-10-23-2015	-7.13648	-8.223	-80.517	-40.845
242	CD1-75423-03-9.cdx	glide-grid_34-4hev-correct-new-10-23-2015	-7.13568	-7.192	-94.231	-65.944
243	ZO1_86609	glide-grid_36-3qj0-correct-10-23-2015	-7.13529	-7.135	-32.058	-22.96
244	CD1-439533	glide-grid_30-3c8b_new-10-23-2015	-7.13312	-7.19	-75.414	-50.498
245	CS2-284486-60-8	glide-grid_31_3QIY-new-10-23-2015	-7.12842	-7.128	-78.768	-59.748

246	FV1_5388319	glide-grid_30-3c8b_new-10-23-2015	-7.12331	-7.123	-87.383	-57.243
247	CD1-31076-39-8.cdx	glide-grid_32-3qiz-newGrid-10-23-2015	-7.12236	-7.174	-67.05	-47.796
248	PC1_PL2_ 42438-80-2	glide-grid_36-3qj0-correct-10-23-2015	-7.12227	-7.122	-63.608	-45.602
249	3C8B-prepared-new-10-22-2015_ligand	glide-grid_32-3qiz-newGrid-10-23-2015	-7.12006	-7.486	-101.269	-61.89
250	FV1_10212	glide-grid_36-3qj0-correct-10-23-2015	-7.11989	-7.12	-56.403	-38.473

APPENDIX 2. SUPPLEMENTARY INFORMATION-CHAPTER 3

SI Table 2. Docking output of ligands docked in 2PRG with three H-bonding constraints.

S.No.	Title	docking score	glide gscore	glide emodel	glide energy
	2PRG-Prepared_final-Aligned				
1	Rosiglitazone	-10.658	-10.976	-94.121	-57.727
2	2,4-Thiazolidiinedione_derivative_2PRG	-10.534	-10.853	-91.928	-57.731
3	2,4-Thiazolidiinedione_derivative_2PRG	-10.483	-11.03	-97.989	-60.693
4	Rosiglitazone	-9.985	-10.532	-95.823	-60.972
5	Rosiglitazone	-8.992	-11.682	-103.617	-57.688
6	2,4-Thiazolidiinedione_derivative_2PRG	-8.889	-11.58	-101.555	-57.225
7	Tyramine derivative-44	-8.455	-8.617	-67.754	-49.105
8	Lyciumide A 24	-8.364	-8.366	-70.924	-50.202
9	Tyramine derivative-41	-8.182	-8.183	-70.163	-48.207
10	Anthra quinone derivative-65	-8.034	-8.143	-52.155	-36.113
11	Kavatin	-7.948	-7.948	-50.223	-34.688
12	Indole deriv-no-glycoside 38	-7.609	-7.609	-45.101	-31.943
13	Tyramine derivative-43	-7.491	-7.683	-67.43	-50.284
14	Tyramine derivative-44	-7.311	-8.159	-66.122	-46.477
15	Pyrrole derivative-27	-7.3	-7.3	-54.497	-34.977
16	Kukoamine B 46	-7.289	-7.297	-79.353	-63.487
17	Calystegines-54	-7.12	-7.325	-30.606	-25.299
18	Pyrrole derivative-28	-6.932	-6.933	-54.151	-35.868
19	Calystegines-57	-6.893	-7.569	-40.9	-32.298
20	Calystegines-57	-6.863	-7.095	-36.405	-27.462
21	Calystegine-47	-6.856	-6.908	-30.046	-24.197
22	Nicotamine derivative-82	-6.792	-6.824	-52.318	-34.911
23	Nicotamine derivative-82	-6.575	-6.607	-49.748	-34.99
24	Calystegines-54	-6.51	-7.245	-28.592	-22.977
25	1,2-dehydro-a-cyperone 33	-6.485	-6.485	-15.356	-9.433
26	calystegines-49-related	-6.476	-6.585	-35.989	-28.419
27	Calystegines-48	-6.453	-6.504	-30.421	-25.18
28	Tyramine derivative-42	-6.221	-6.413	-65.5	-47.974
29	Tyramine derivative-43	-6.148	-6.911	-63.821	-45.113
30	Pyrrole derivative-29	-6.112	-6.112	-47.861	-35.934
31	Solavetivone 32	-5.997	-5.997	-23.107	-13.545
32	Monoterpene-noglycoside-69	-5.988	-5.988	-20.95	-18.882
33	Anthra quinone derivative-65	-5.891	-7.805	-49.656	-32.038
34	Calystegines-48	-5.809	-7.304	-33.827	-25.601
35	Tyramine derivative-42	-5.699	-6.461	-67.616	-45.641

36	Calystegine-47	-5.533	-7.029	-27.796	-20.78
37	calystegines-49-related	-5.398	-6.465	-35.902	-26.825
38	Nicotamine derivative-82	-5.128	-7.207	-60.306	-34.797
39	Nicotamine derivative-82	-5.096	-7.174	-57.651	-35.834
40	Lyciumide A 24	-5.03	-8.546	-71.352	-44.458
41	Nicotamine derivative-82	-4.592	-6.845	-52.179	-34.085
42	Nicotamine derivative-82	-4.032	-6.285	-54.502	-34.385
43	Pyrrole derivative-27	-3.792	-7.914	-53.041	-38.26
44	Kukoamine B 46	-3.742	-7.178	-73.408	-64.157
45	Pyrrole derivative-28	-3.501	-7.624	-53.522	-38.736
46	Kukoamine B 46	-1.696	-9.114	-102.072	-71.699
47	Nicotamine derivative-82	8.801	-7.313	-64.823	-45.822
48	Nicotamine derivative-82	9.178	-6.936	-60.687	-42.312
49	Nicotamine derivative-82	19.772	-7.513	-63.329	-43.463
50	Nicotamine derivative-82	19.821	-7.464	-62.939	-40.961
51	Nicotamine derivative-82	19.997	-7.288	-60.272	-48.342
52	Nicotamine derivative-82	20.188	-7.097	-62.333	-47.989
53	Nicotamine derivative-82	20.236	-7.049	-67.836	-46.529
54	Nicotamine derivative-82	20.408	-6.877	-62.016	-48.43
55	Nicotamine derivative-82	20.658	-6.627	-61.007	-44.181

SI Table 3. Docking output of ligands docked in 3LMP without hydrogen-bonding constraints.

S. No	**Title**	**Potential Energy-OPLS-2005**	**docking score**	**glide gscore**	**glide emodel**	**glide energy**
	3LMP_Partial-agonist					
1	Farglitazar-like-90percent_SI	154.152	-9.085	-9.085	-81.369	-51.252
2	Rosiglitazone	81.414	-8.561	-9.107	-71.857	-49.164
3	2,4-Thiazolidiinedione_derivative_2PRG	82.787	-8.555	-9.101	-71.822	-49.165
4	Kavatin	112.682	-8.191	-8.191	-53.522	-35.611
5	Tyramine derivative-44	62.657	-8.114	-8.276	-64.076	-44.977
6	Tyramine derivative-41	28.923	-8.091	-8.093	-71.852	-49.177
7	2,4-Thiazolidiinedione_derivative_2PRG	102.485	-8.079	-8.398	-68.35	-47.17
8	Rosiglitazone	101.803	-8.07	-8.388	-68.837	-46.928
9	Cercosporamide-Der_3LMP	199.69	-7.944	-10.112	-83.195	-55.686
10	Kukoamine B 46	99.934	-7.574	-7.583	-89.978	-63.05
11	Lyciumamide 40	65.832	-7.519	-7.519	-64.014	-48.271
12	Lyciumide A 24	90.259	-7.473	-7.476	-67.361	-46.465

13	Tyramine derivative-44	61.248	-7.341	-8.19	-63.752	-43.398
14	Indole deriv-no-glycoside 38	21.648	-7.142	-7.142	-39.614	-28.758
15	1,2-dehydro-a-cyperone 33	14.267	-7.122	-7.122	-33.679	-24.423
16	Anthra quinone derivative-65	94.547	-7.016	-7.125	-59.105	-40.397
17	Cercosporamide-Der_3LMP	203.596	-6.945	-7.489	-84.496	-58.348
18	Aurantiamide acetate 39	23.176	-6.808	-6.808	-67.431	-49.977
19	Tyramine derivative-43	46.325	-6.735	-6.927	-61.788	-45.728
20	Diterpene derivative 67	156.715	-6.507	-6.508	-47.194	-34.57
21	Solavetivone 32	138.913	-6.495	-6.495	-19.482	-20.286
22	Pyrrole derivative-27	28.095	-6.494	-6.494	-44.757	-30.597
23	Cercosporamide-Der_3LMP	265.536	-6.442	-6.9	-73.552	-53.71
24	Withanolide A 79	447.515	-6.407	-6.407	-70.408	-53.321
25	Pyrrole derivative-28	38.307	-6.262	-6.262	-44.334	-32.087
26	Tyramine derivative-42	72.069	-6.256	-7.019	-61.38	-42.015
27	Cercosporamide-Der_3LMP	284.258	-6.182	-7.849	-89.223	-57.884
28	Tyramine derivative-43	44.393	-6.16	-6.923	-61.658	-43.241
29	Rosiglitazone	83.12	-6.137	-8.827	-71.533	-49.353
30	Cercosporamide-Der_3LMP	217.183	-6.032	-7.782	-86.791	-57.928
31	2,4-Thiazolidiinedione_derivative_2PRG	83.684	-5.981	-8.672	-73.469	-48
32	Tyramine derivative-42	72.22	-5.888	-6.08	-51.389	-38.236
33	(+)-Lyoniresinol-no-glycoside 64	183.871	-5.879	-5.879	-27.237	-28.014
34	Kukoamine B 46	90.116	-5.621	-9.566	-113.219	-70.39
35	Anthra quinone derivative-65	90.116	-5.583	-6.827	-57.507	-38.897
36	Calystegines-54	230.398	-5.561	-5.766	-44.546	-26.331
37	Pyrrole derivative-29	42.866	-5.56	-5.56	-45.763	-34.545
38	Cercosporamide-Der_3LMP	196.413	-5.548	-7.716	-75.865	-53.098
39	Calystegine-47	206.388	-5.545	-5.597	-40.628	-24.421
40	Calystegines-48	179.715	-5.506	-5.557	-41.498	-24.895
41	Nicotamine derivative-82	24.442	-5.401	-5.432	-53.906	-32.157
42	Monoterpene-noglycoside-69	172.531	-5.339	-5.339	-17.608	-15.559
43	Calystegines-57	269.287	-5.311	-5.542	-40.137	-29.592
44	Nicotamine derivative-82	-2.895	-5.301	-5.333	-49.652	-31.565
45	calystegines-49-related	188.191	-5.284	-5.393	-39.125	-23.091
46	Calystegines-57	251.591	-5.279	-5.955	-47.279	-27.663
47	Cercosporamide-Der_3LMP	220.414	-5.159	-9.282	-87.688	-57.373
48	Anthra quinone derivative-65	89.261	-5.114	-7.028	-54.893	-37.069
49	Calystegines-54	213.208	-5.004	-5.74	-36.941	-26.063
50	calystegines-49-related	186.285	-4.567	-5.635	-34.569	-24.404
51	Lyciumide A 24	87.747	-4.399	-7.915	-65.857	-43.813

52	Calystegines-48	160.11	-4.349	-5.845	-33.259	-23.722
53	Calystegine-47	190.735	-4.312	-5.808	-34.313	-23.953
54	Farglitazar-like-90percent_SI	156.246	-4.122	-8.653	-84.647	-55.607
55	Kukoamine B 46	94.605	-3.962	-7.399	-90.461	-57.009
56	Nicotamine derivative-82	35.633	-3.206	-5.46	-49.428	-33.102
57	Nicotamine derivative-82	9.387	-3.183	-5.261	-42.291	-30.267
58	Nicotamine derivative-82	7.553	-3.162	-5.415	-47.839	-32.93
59	Kukoamine B 46	78.431	-3.082	-6.54	-92.368	-58.114
60	Nicotamine derivative-82	36.938	-2.694	-4.773	-39.723	-28.689
61	Kukoamine A 45	56.277	-2.319	-5.548	-81.743	-58.802
62	Pyrrole derivative-27	38.238	-2.145	-6.267	-45.946	-33.383
63	Pyrrole derivative-28	48.293	-1.741	-5.864	-47.519	-35.828
64	Kukoamine B 46	85.33	-1.654	-9.072	-109.676	-73.565
65	Kukoamine B 46	74.725	-0.595	-7.711	-105.945	-65.928
66	Kukoamine A 45	50.74	-0.387	-7.082	-87.283	-61.037
67	Kukoamine B 46	75.023	3.109	-7.868	-84.237	-60.106
68	Kukoamine B 46	76.882	7.322	-7.098	-81.495	-55.485
69	Nicotamine derivative-82	83.197	10.577	-5.537	-65.668	-41.656
70	Nicotamine derivative-82	59.037	10.983	-5.131	-66.049	-43.525
71	Nicotamine derivative-82	80.449	20.723	-6.562	-59.62	-46.428
72	Nicotamine derivative-82	88.587	20.992	-6.293	-72.712	-46.947
73	Nicotamine derivative-82	75.886	21.336	-5.949	-64.208	-43.364
74	Nicotamine derivative-82	53.819	21.509	-5.776	-65.083	-43.568
75	Nicotamine derivative-82	81.133	21.637	-5.648	-61.017	-42.467
76	Nicotamine derivative-82	66.503	21.919	-5.366	-66.506	-44.407
77	Nicotamine derivative-82	78.958	22.048	-5.237	-58.91	-39.809

SI Spectral Data 1. Spectral data of tryaminederivatives **01**, **08**, **10**.

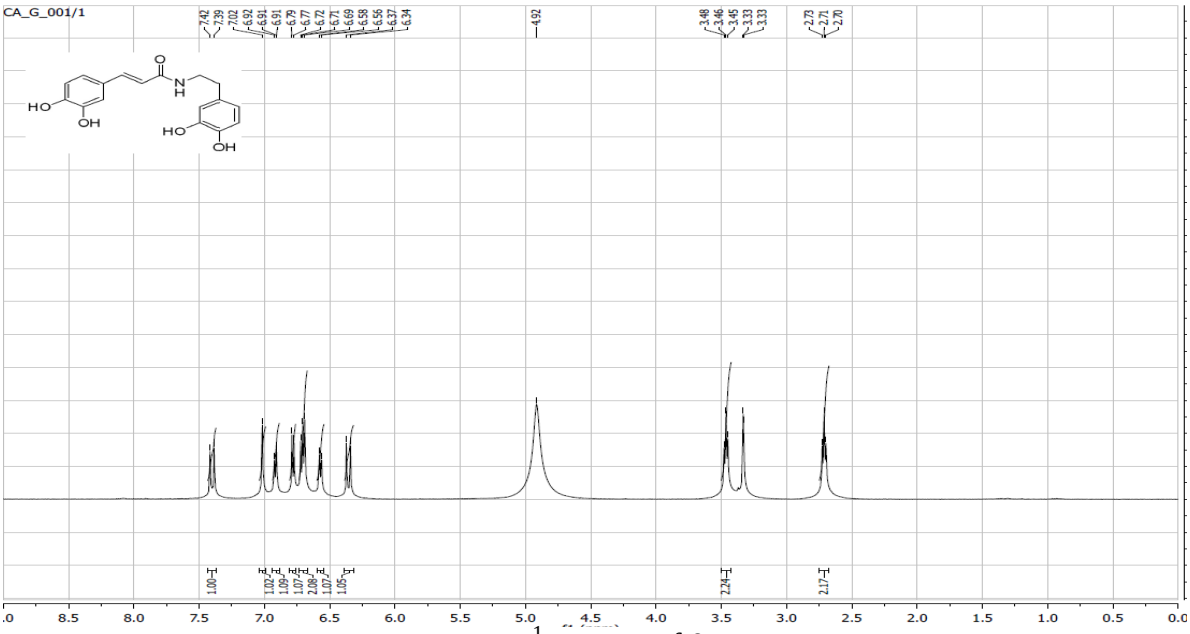

^{1}H NMR of **01**

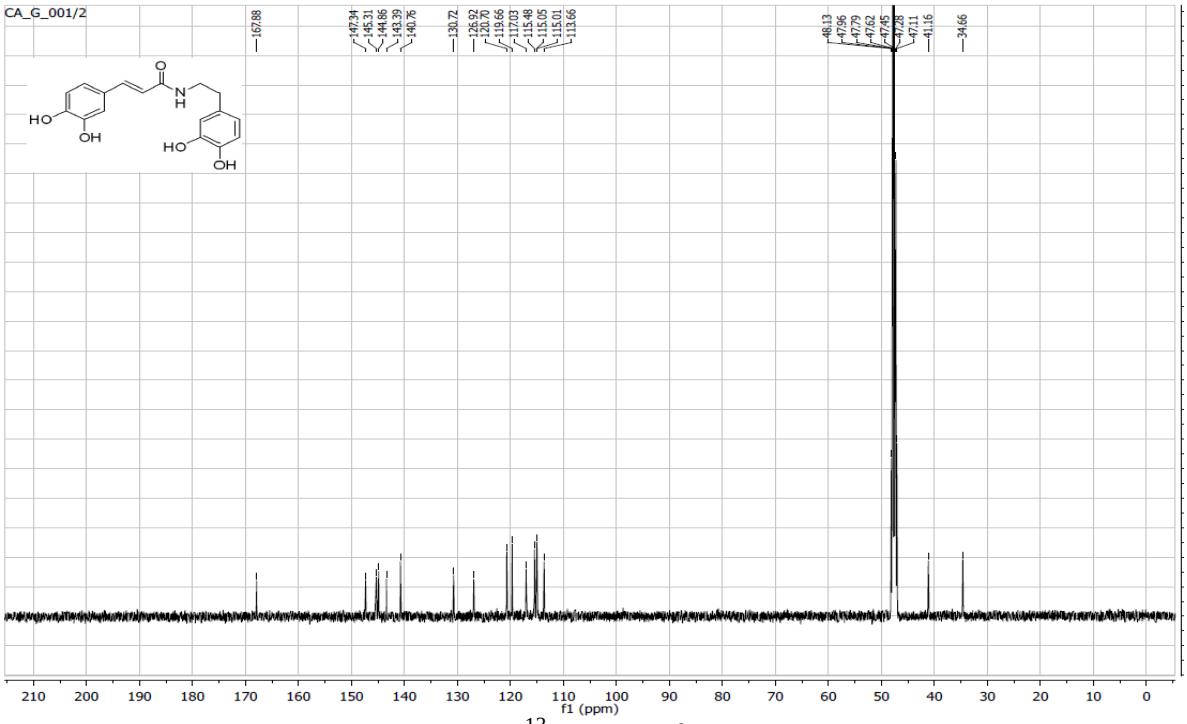

^{13}C NMR of **01**

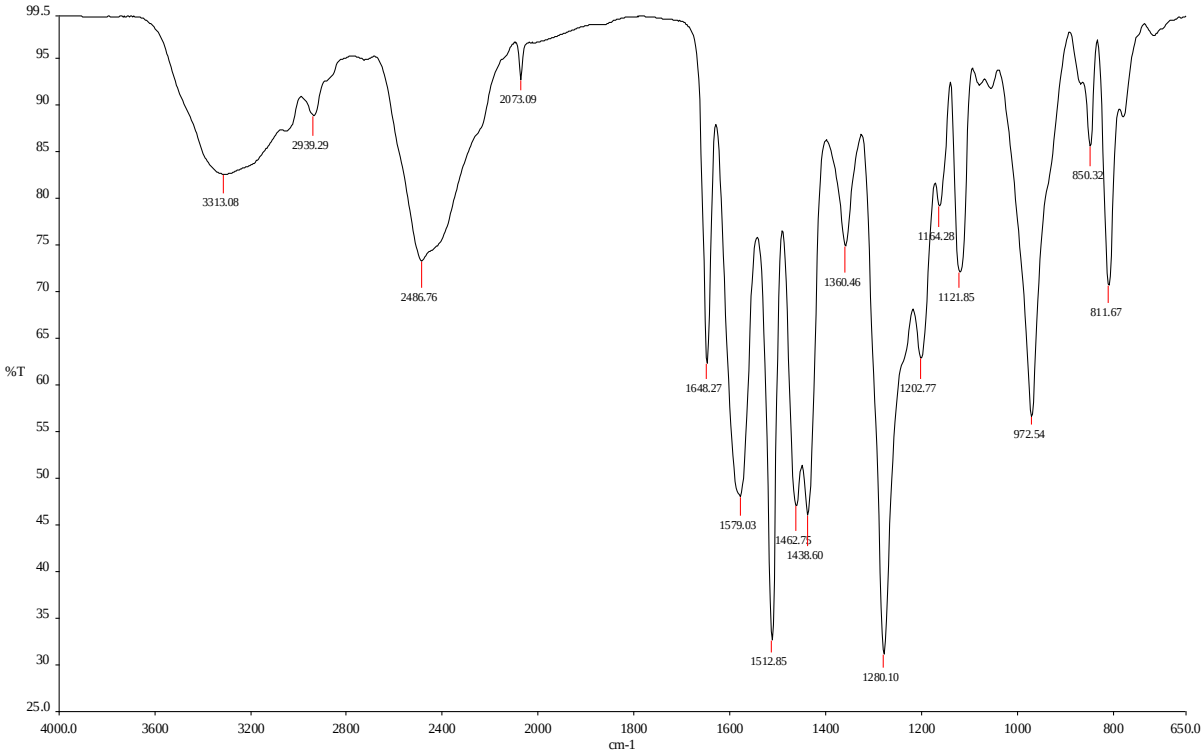
99.5
95
90
85
80
75
70
65
60
55
50
45
40
35
30
25.0
%T
4000.0
3600
3200
2800
2400
2000
1800
1600
1400
1200
1000
800
650.0
cm-1
3313.08
2939.29
2486.76
2073.09
1648.27
1579.03
1512.85
1462.75
1438.60
1360.46
1280.10
1202.77
1164.28
1121.85
972.54
850.32
811.67

FT-IR of 01

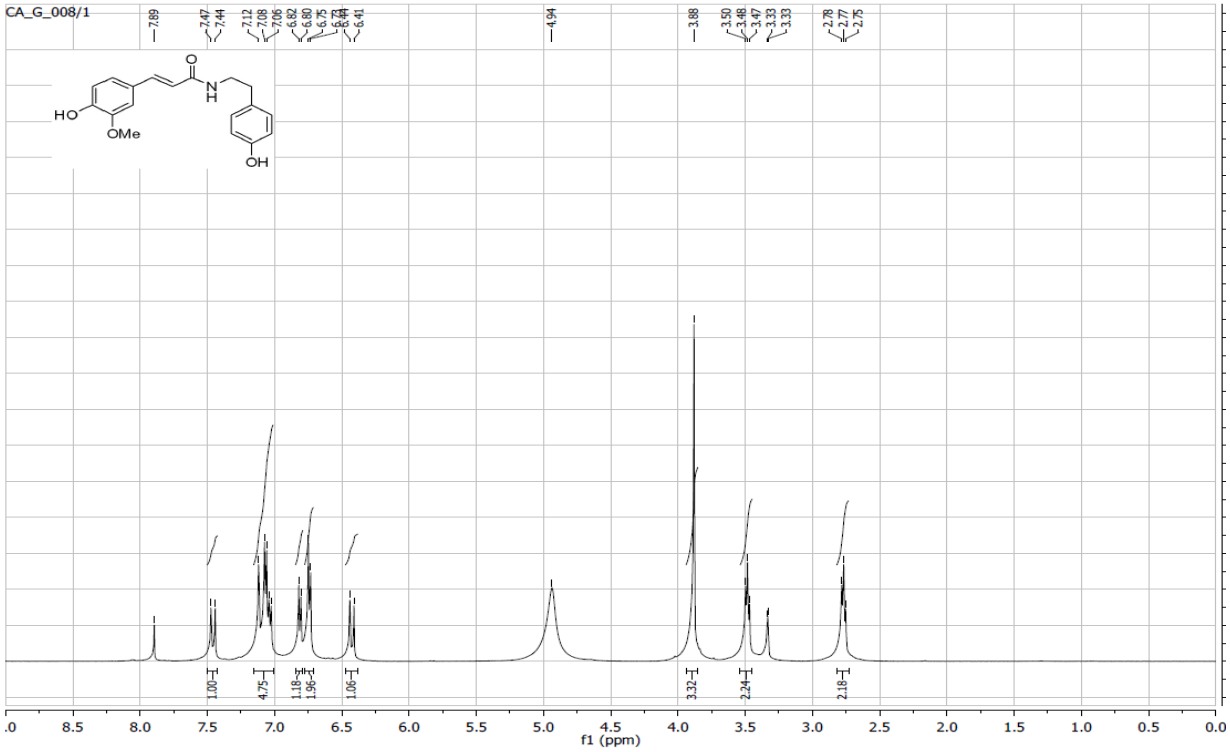

^{1}H NMR of **08**

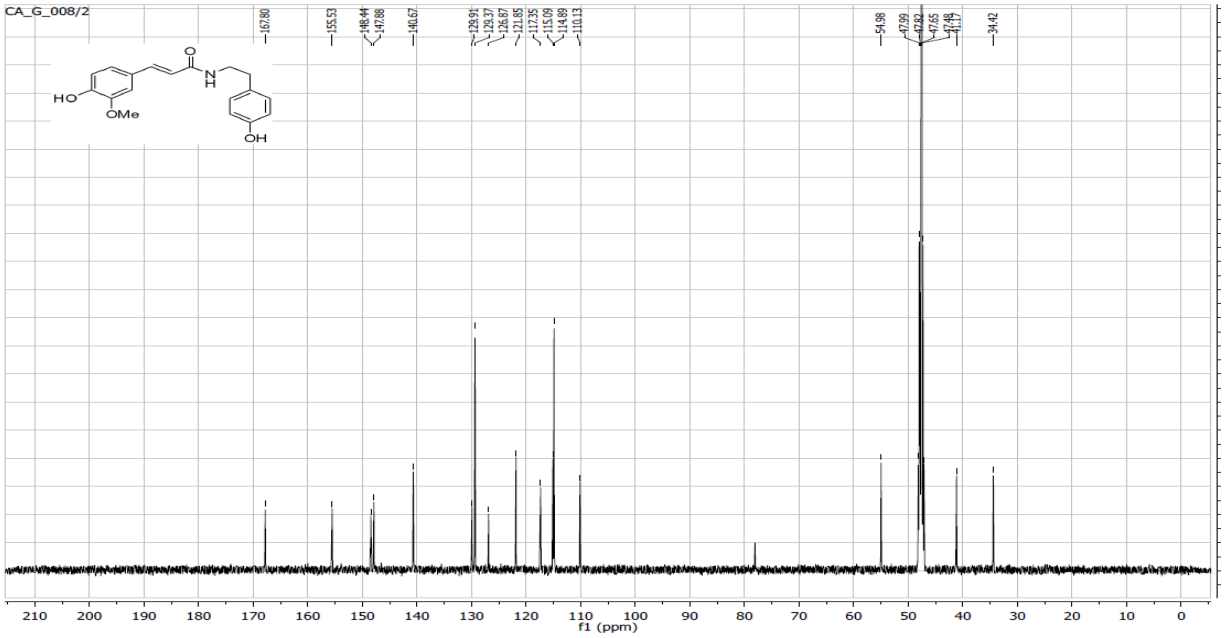

^{13}C NMR of **08**

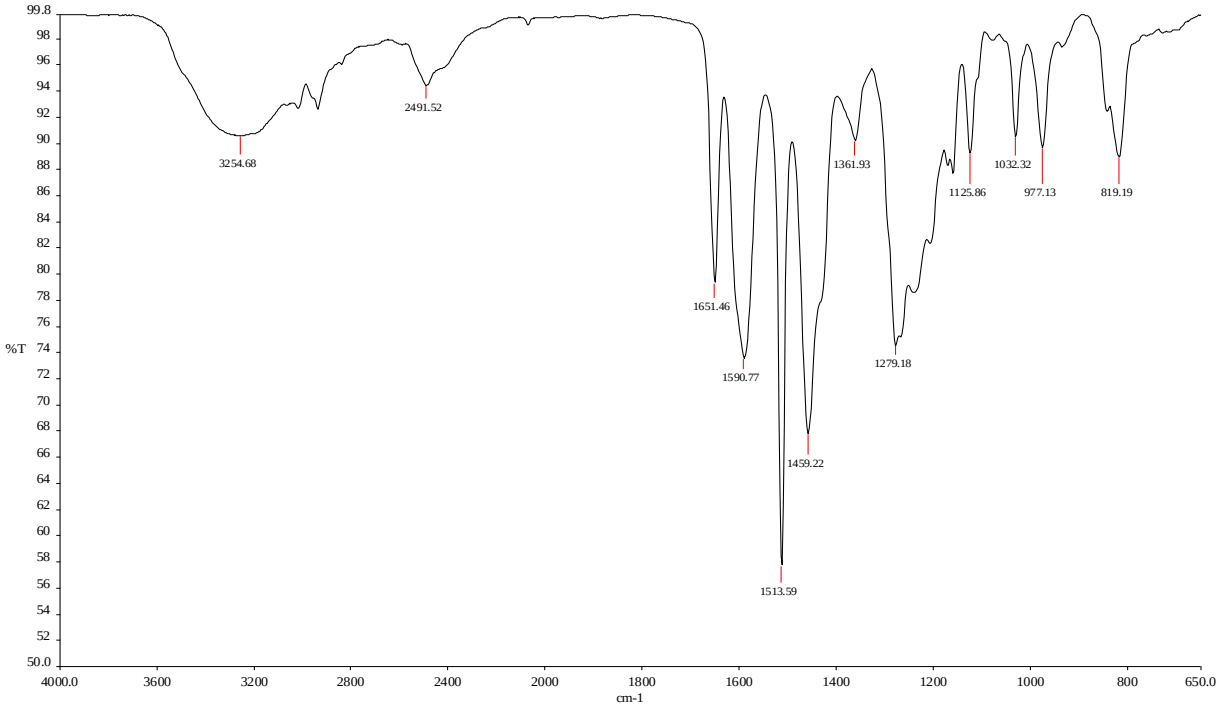

FT-IR of CA-G-008

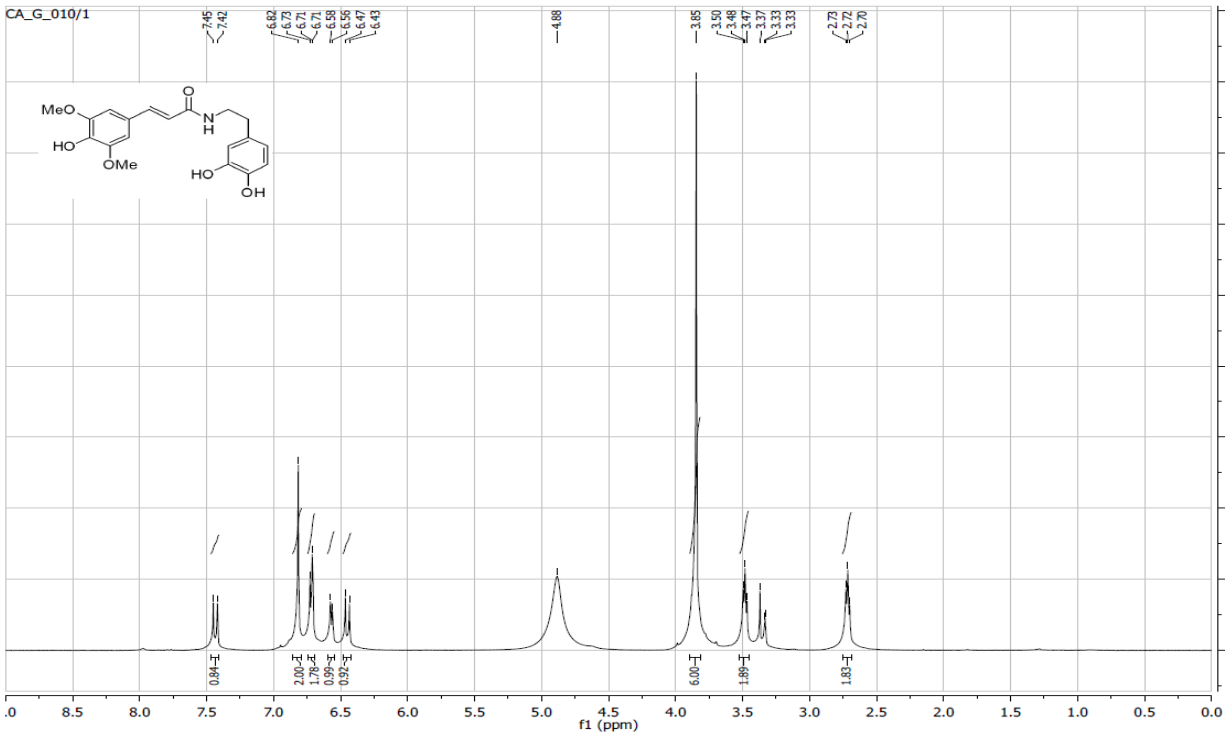

^{1}H NMR of **10**

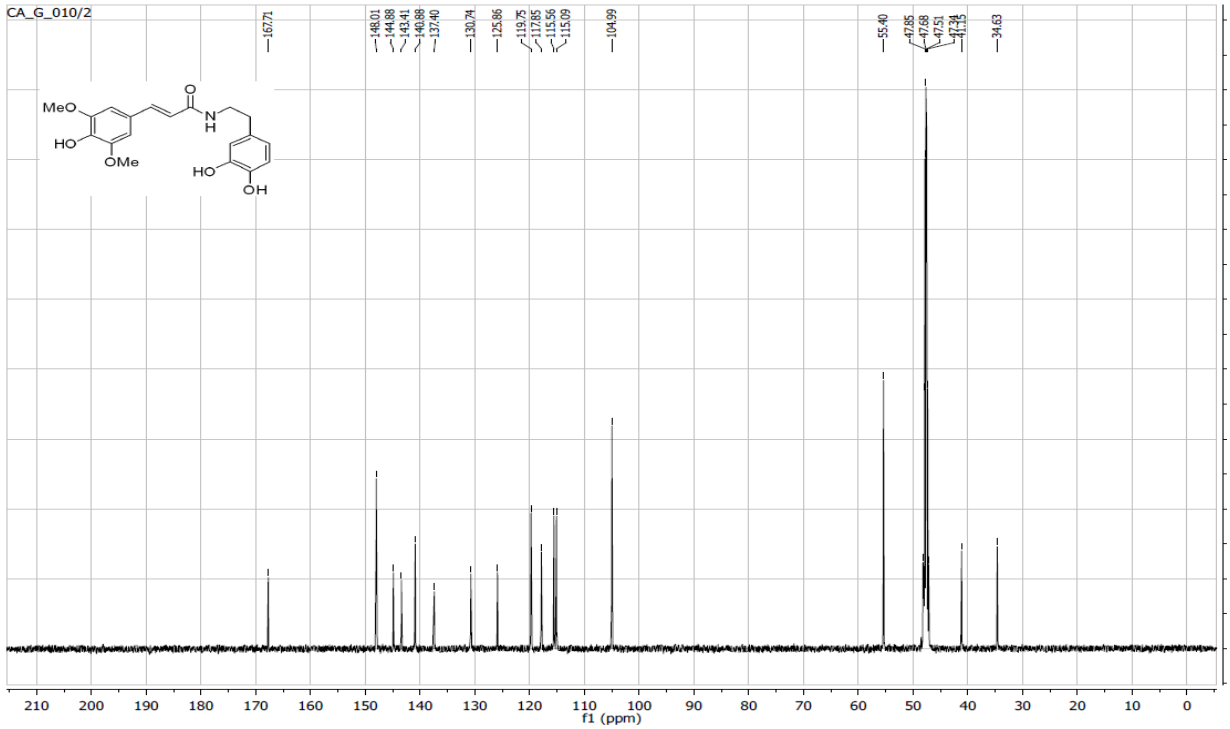

^{13}C NMR of **10**

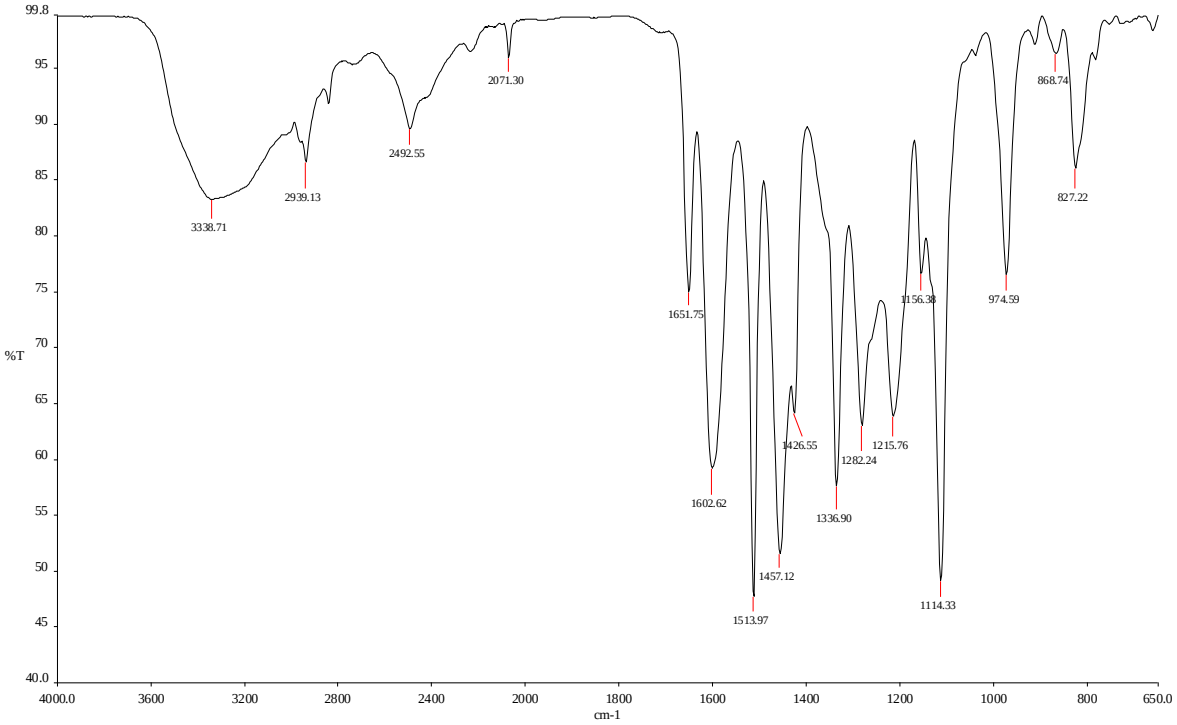
99.8
95
90
85
80
75
70
65
60
55
50
45
40.0
%T
4000.0
3600
3200
2800
2400
2000
1800
1600
1400
1200
1000
800
650.0
cm-1
3338.71
2939.13
2492.55
2071.30
1651.75
1602.62
1513.97
1457.12
1426.55
1336.90
1282.24
1215.76
1156.38
1114.33
974.59
868.74
827.22

FT-IR of **10**

APPENDIX 3. SUPPLEMENTARY INFORMATION-CHAPTER 4

SI Spectral Data 2. Synthesis of the starting material-aldehydes: **46**, **47** and **53**.

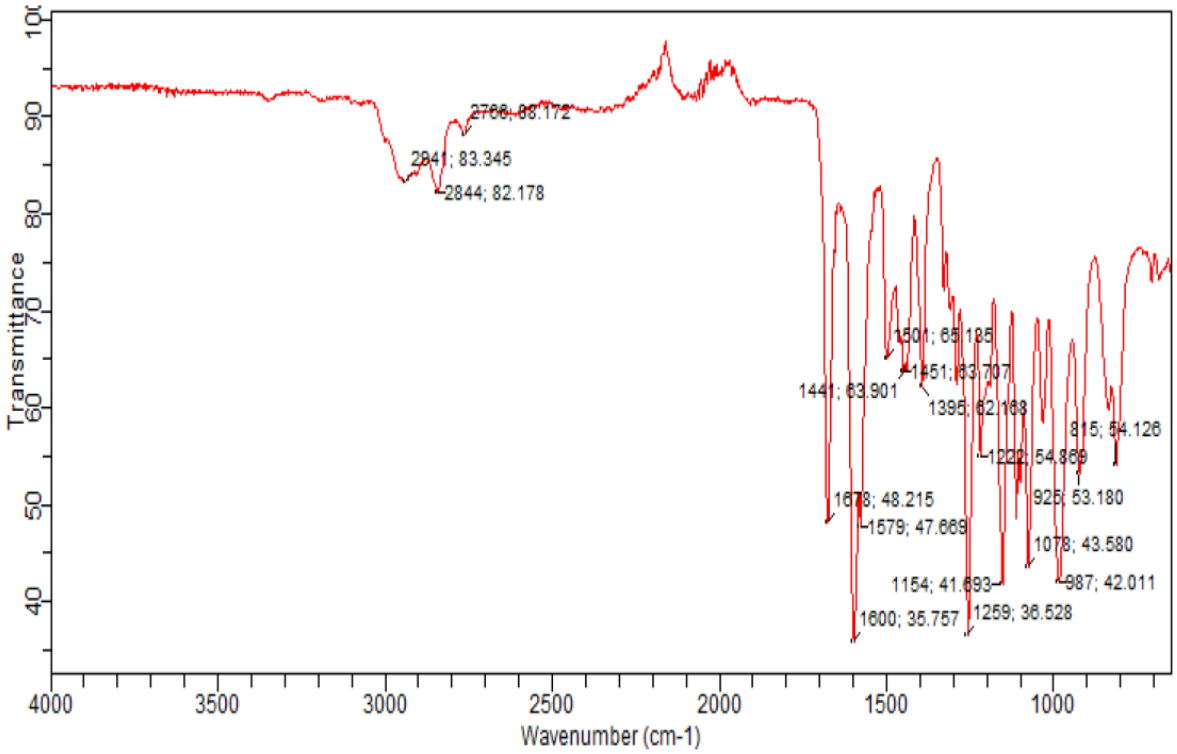

IR spectrum of compound 46

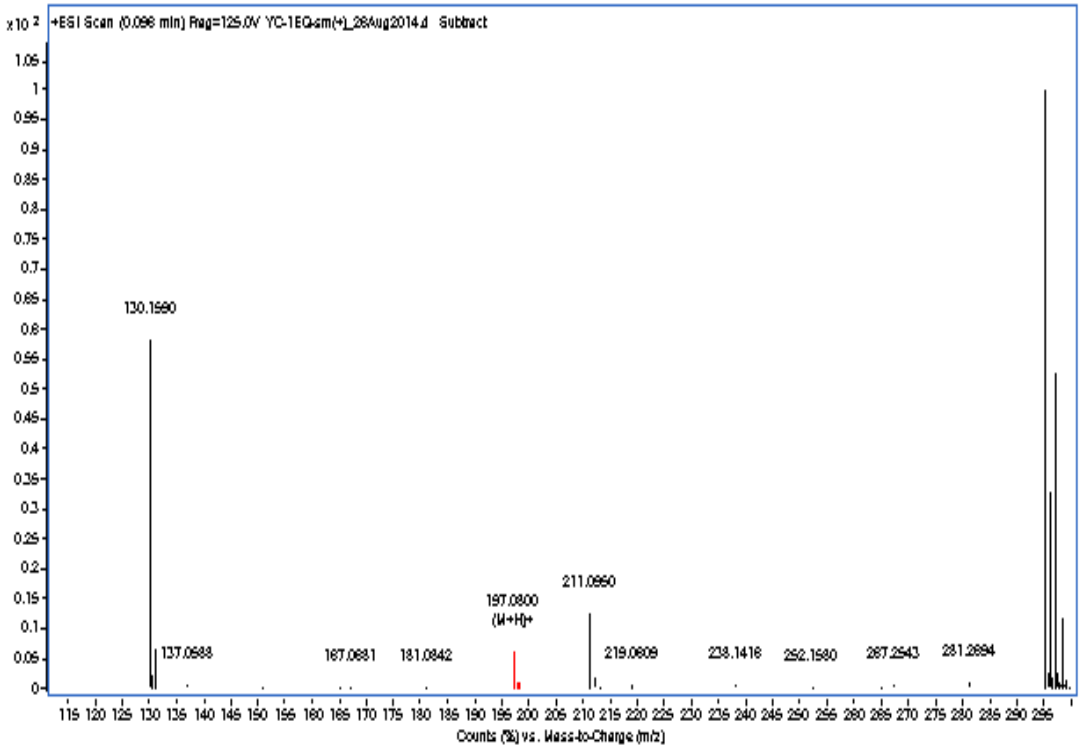

ESI-HRMS of compound 46

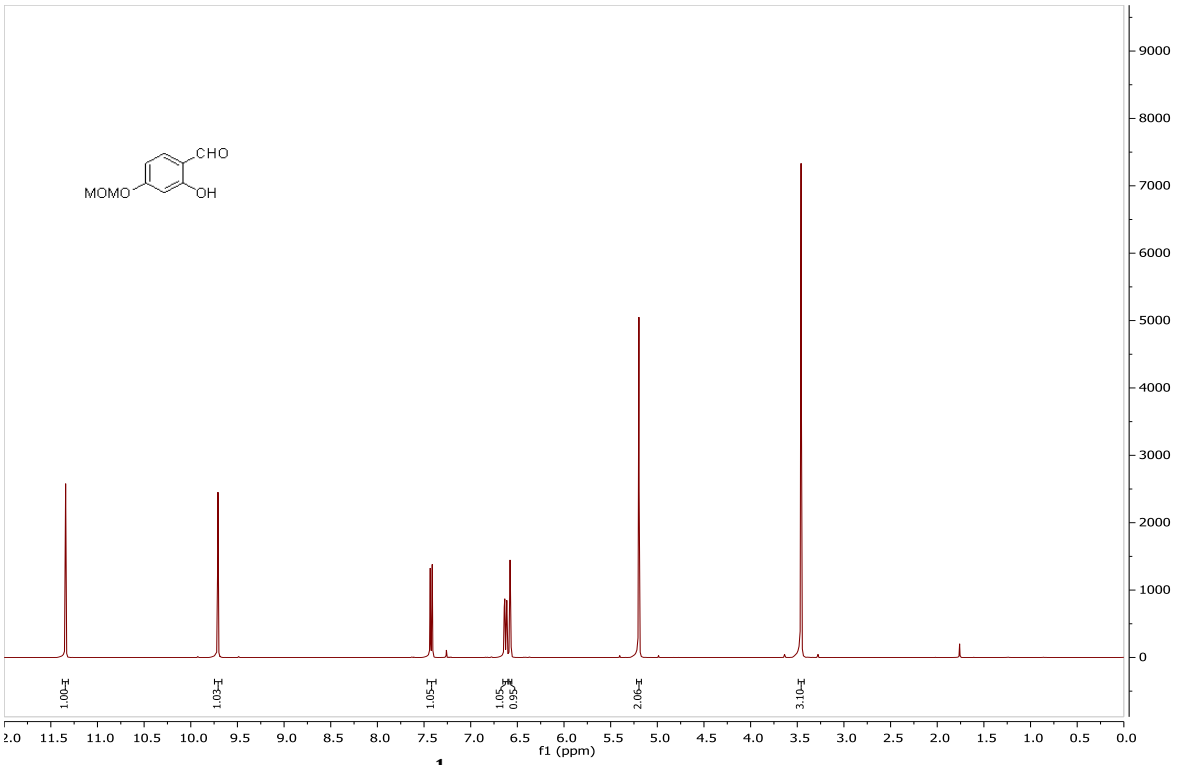

^{1}H NMR spectrum of 53.

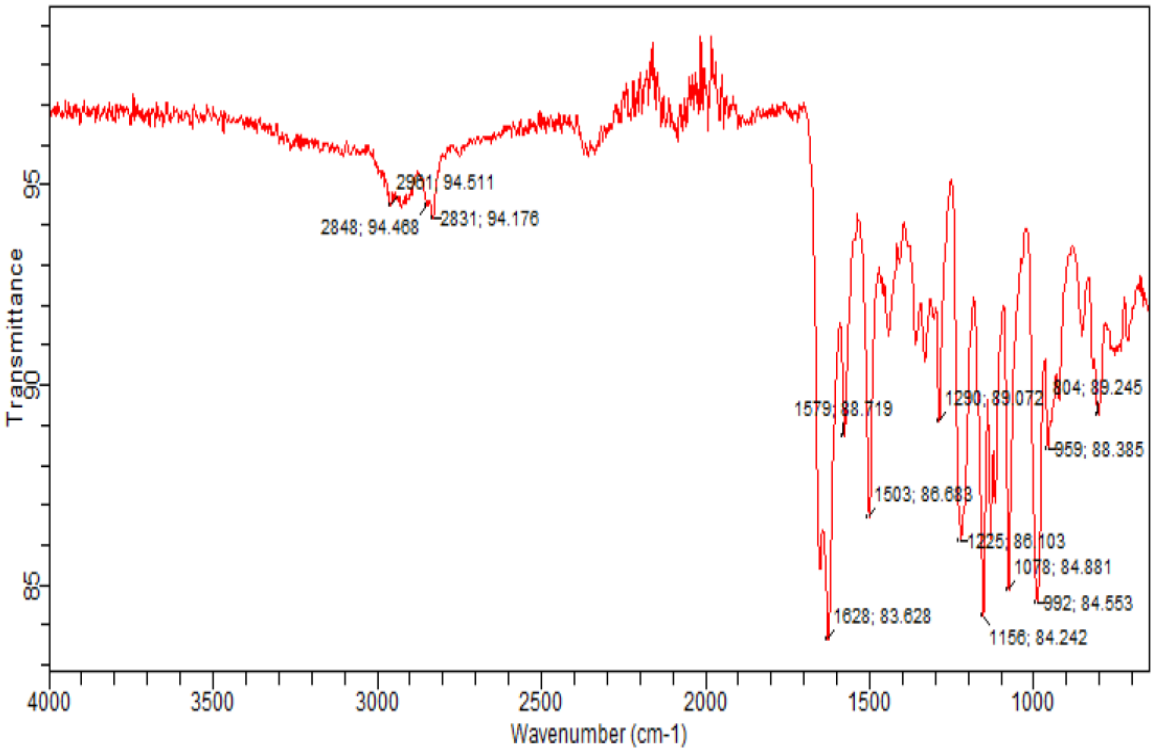

IR spectrum of compound 53

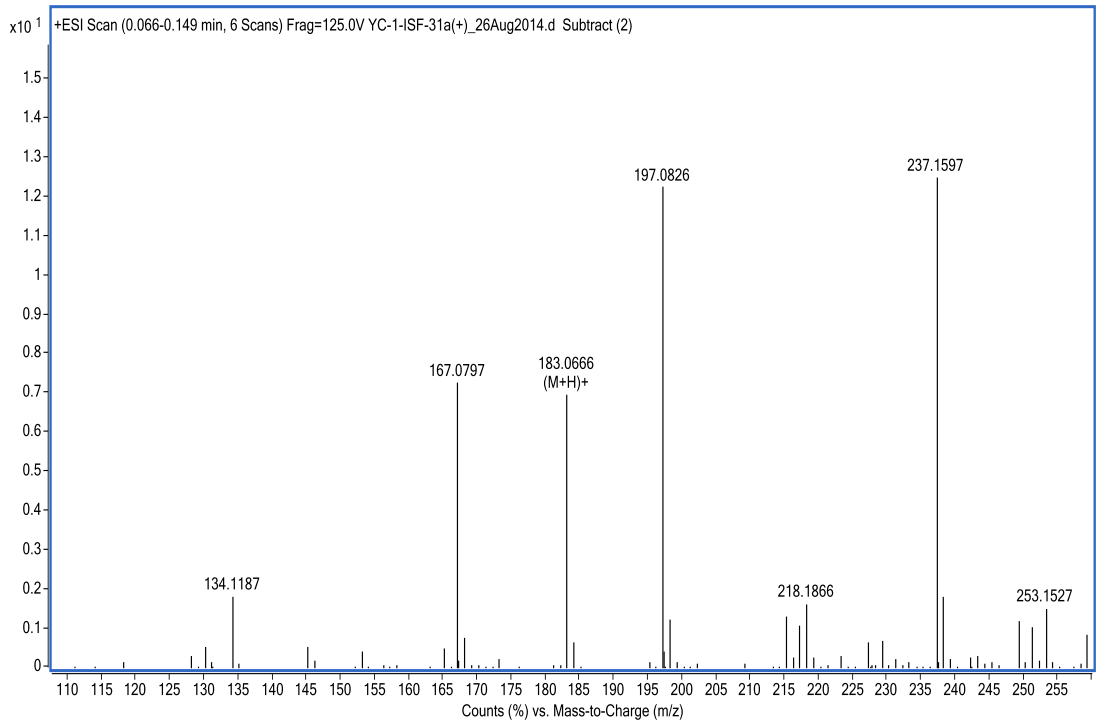

ESI-HRMS of 53

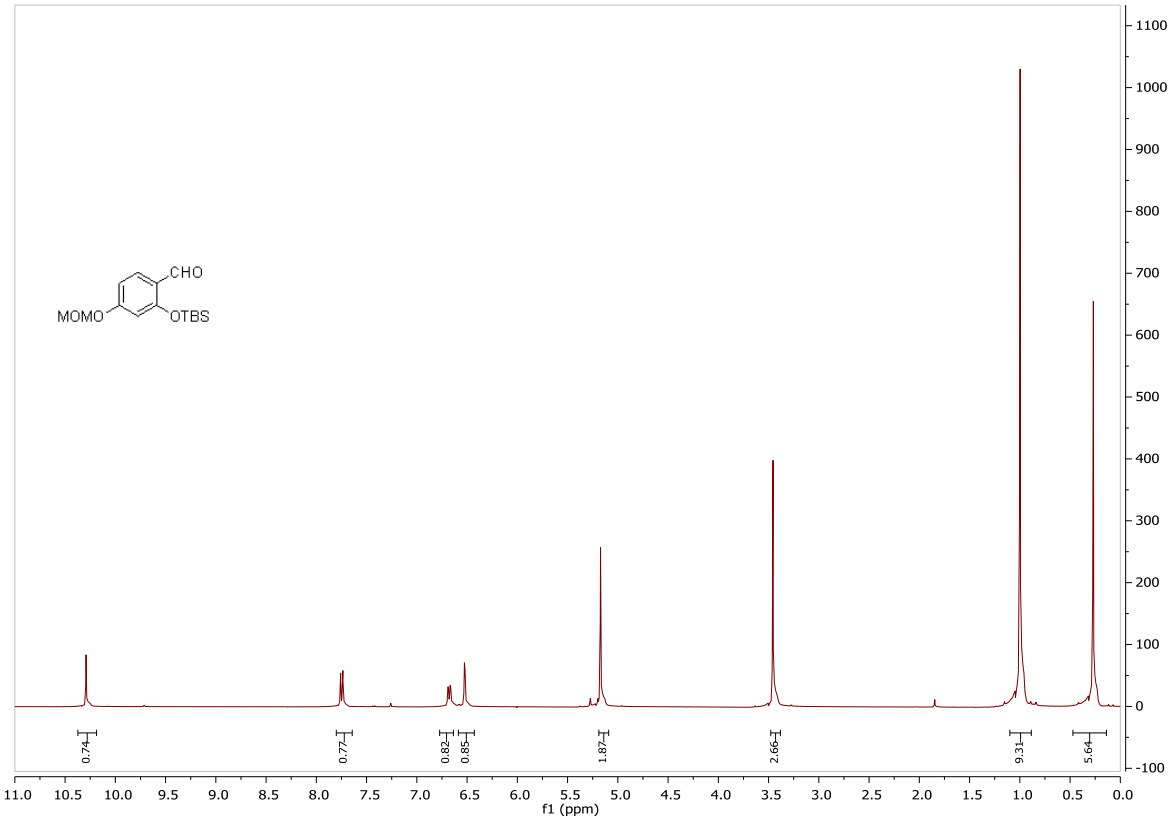

^{1}H NMR spectrum of compound 47

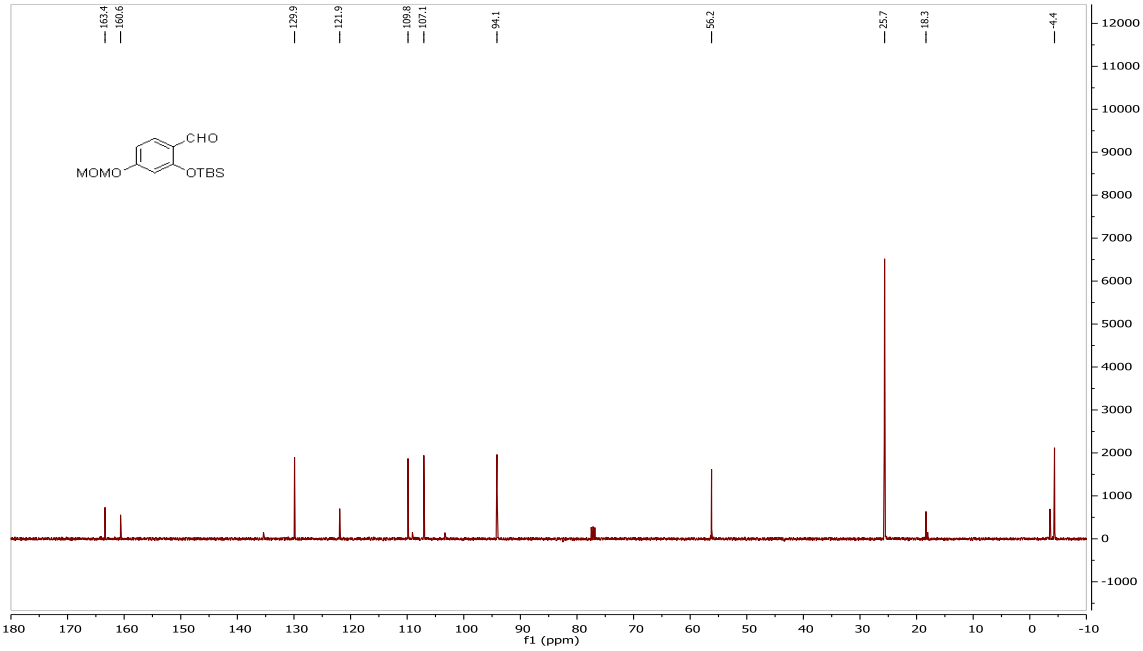

^{13}C NMR spectrum of compound 47

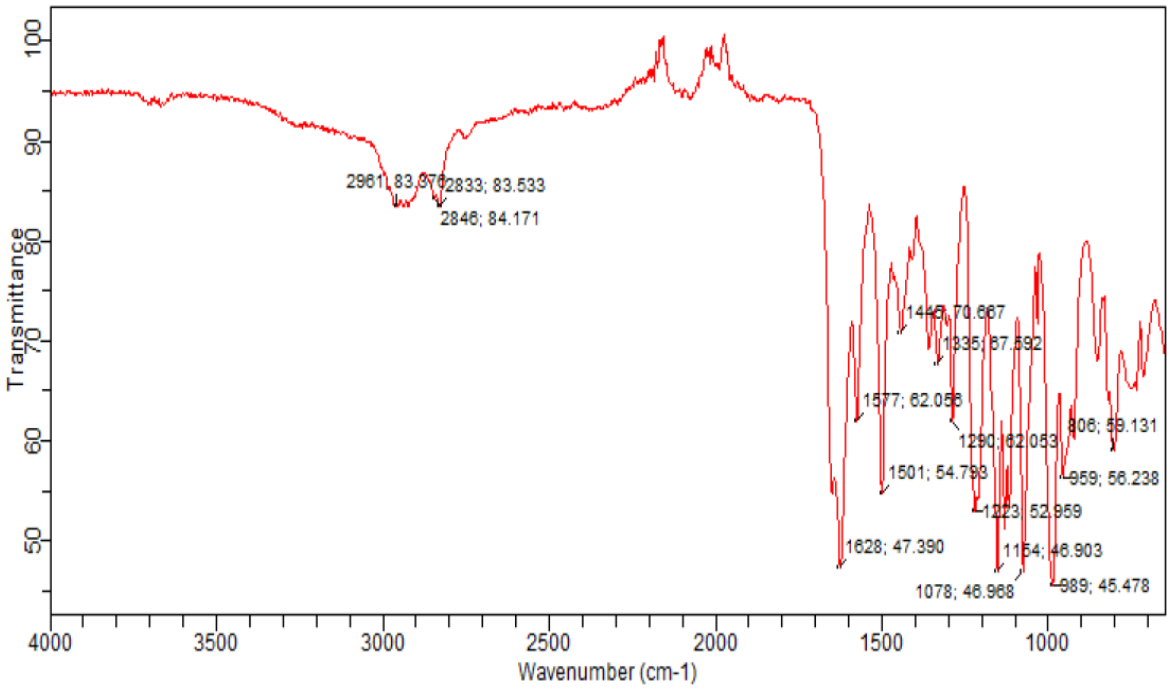

IR spectrum of compound 47

SI Spectral Data 3. Spectral data of the compounds for synthesis of *S*-(-)-Equol **7**.

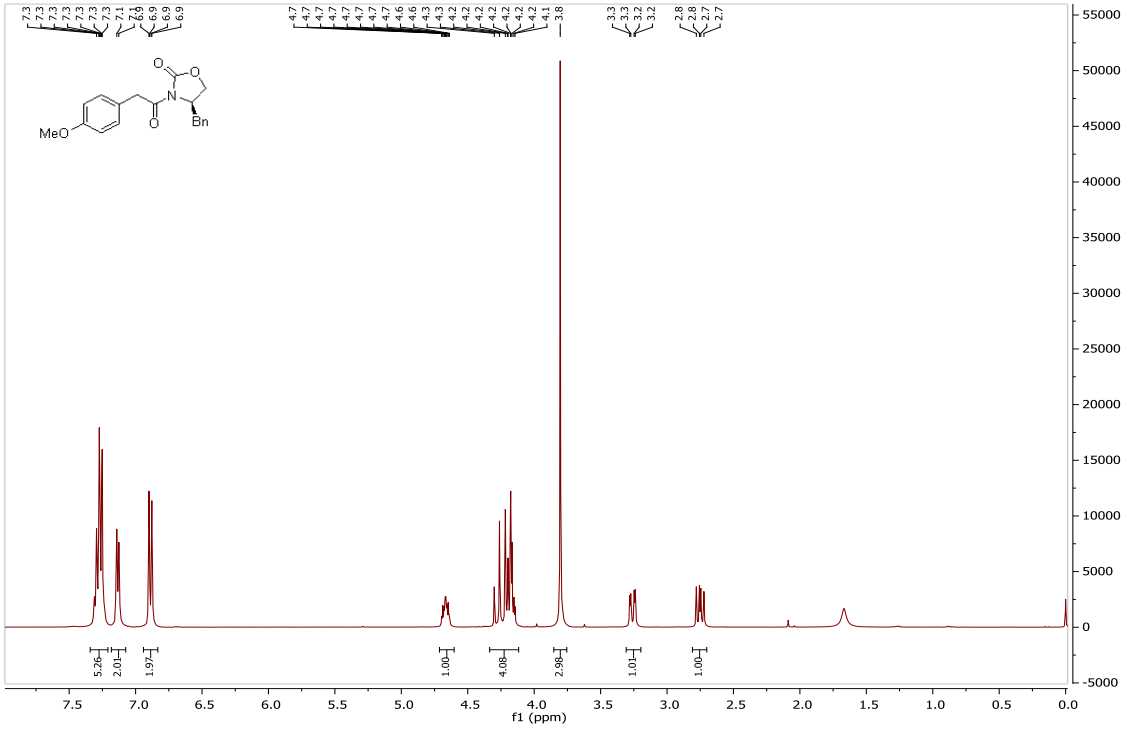

^{1}H NMR spectrum of compound (-) 26

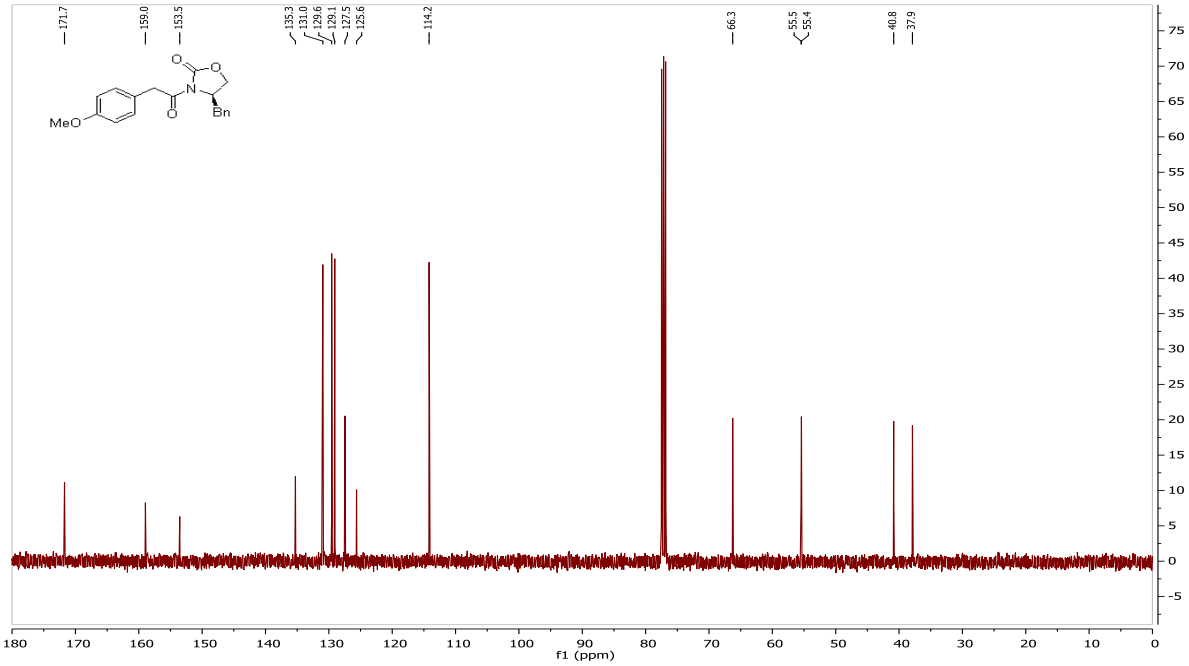

^{13}C NMR spectrum of compound (-) 26

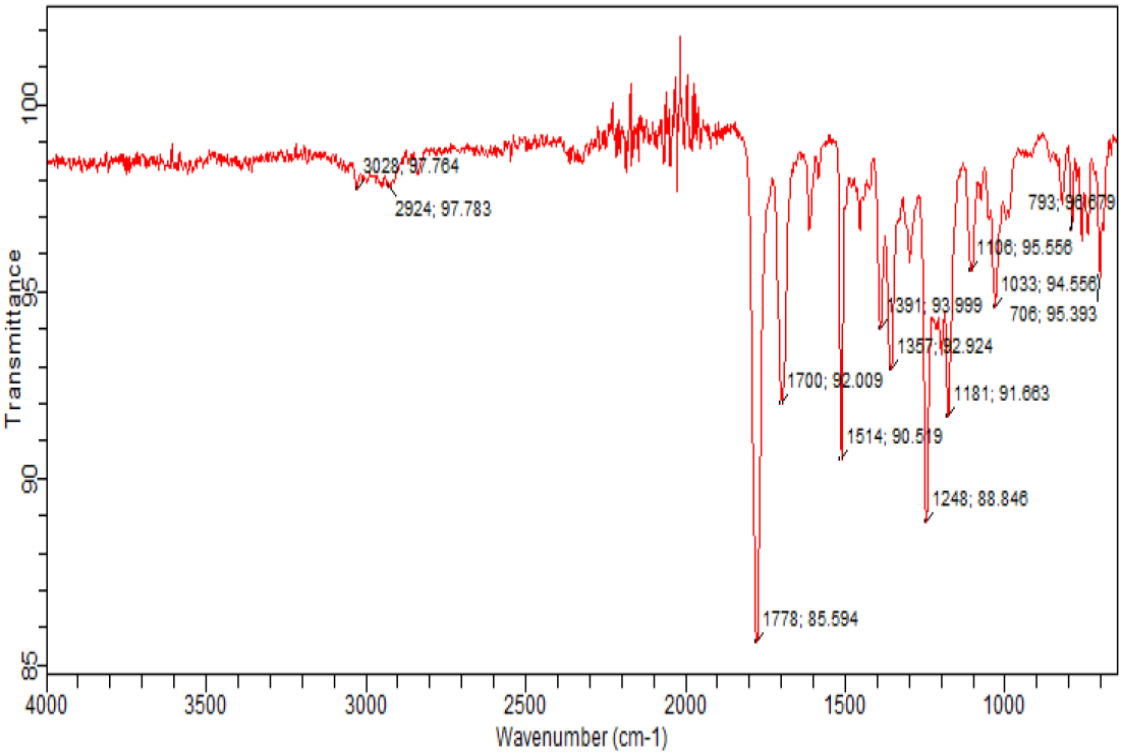

IR spectrum of compound (-) 26

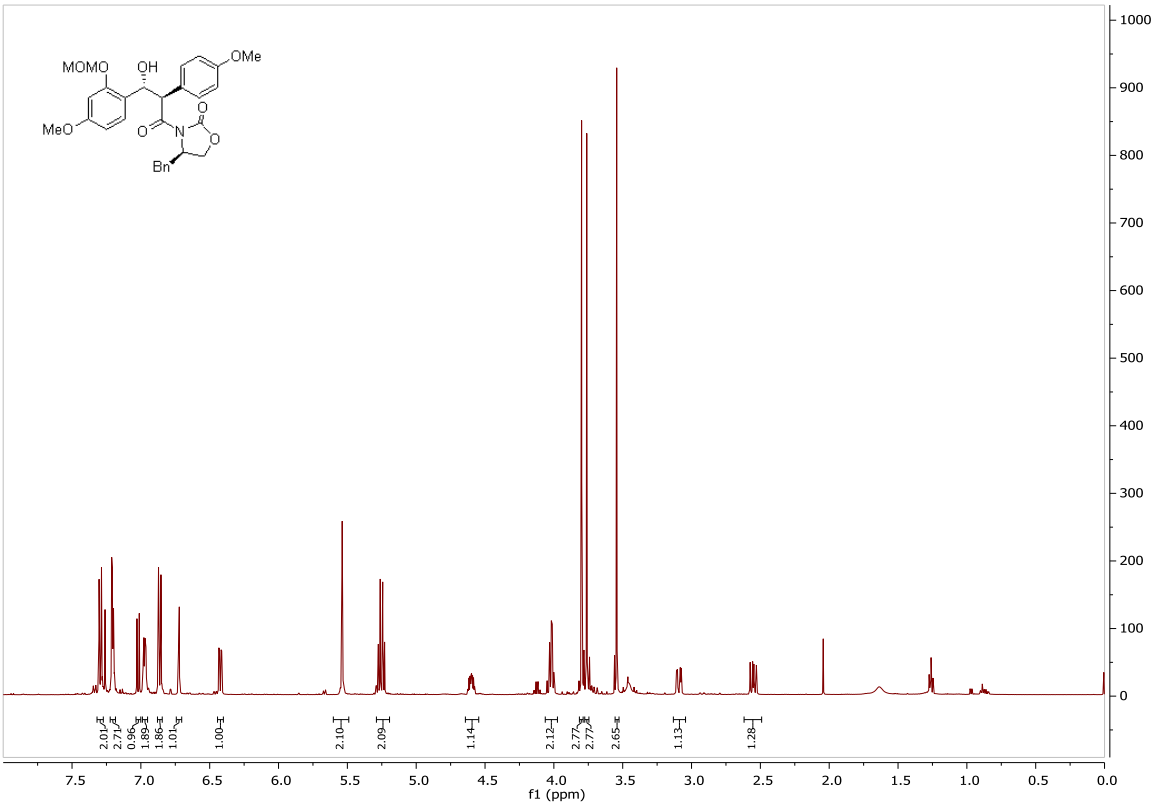

^{1}H

NMR spectrum of compound (+) 44

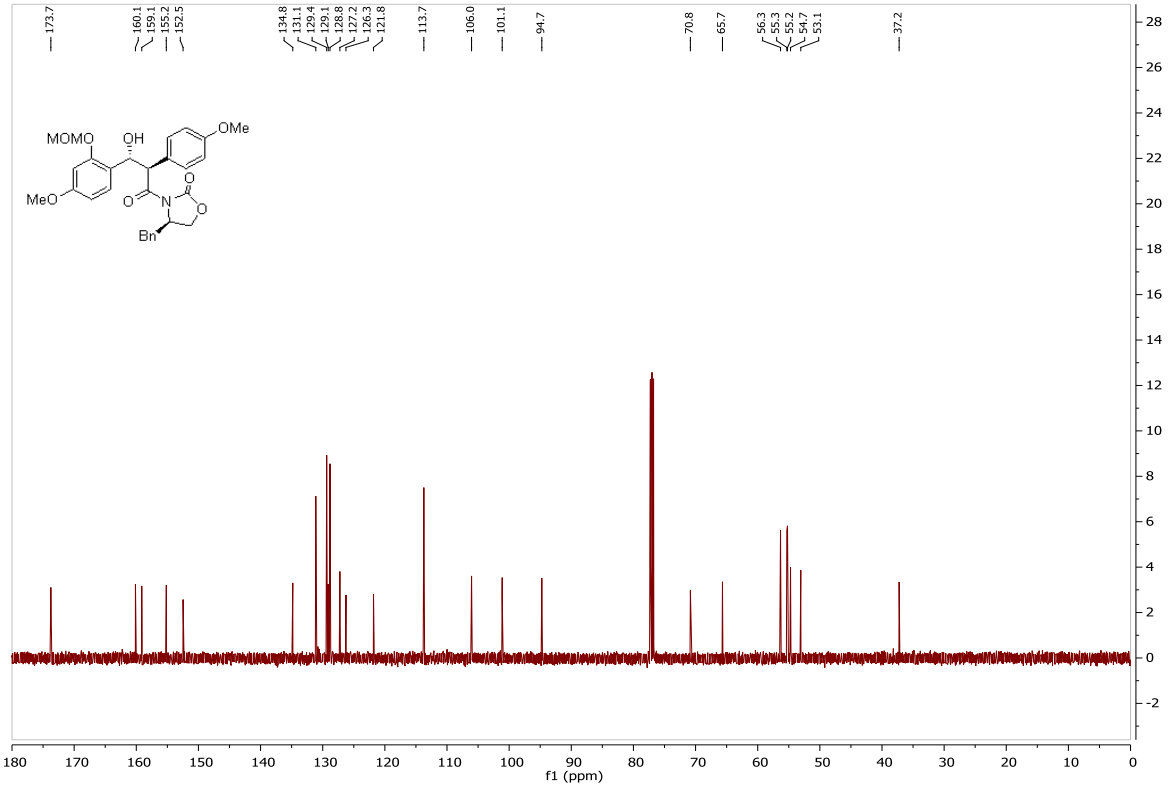

^{13}C NMR spectrum of compound (+) 44

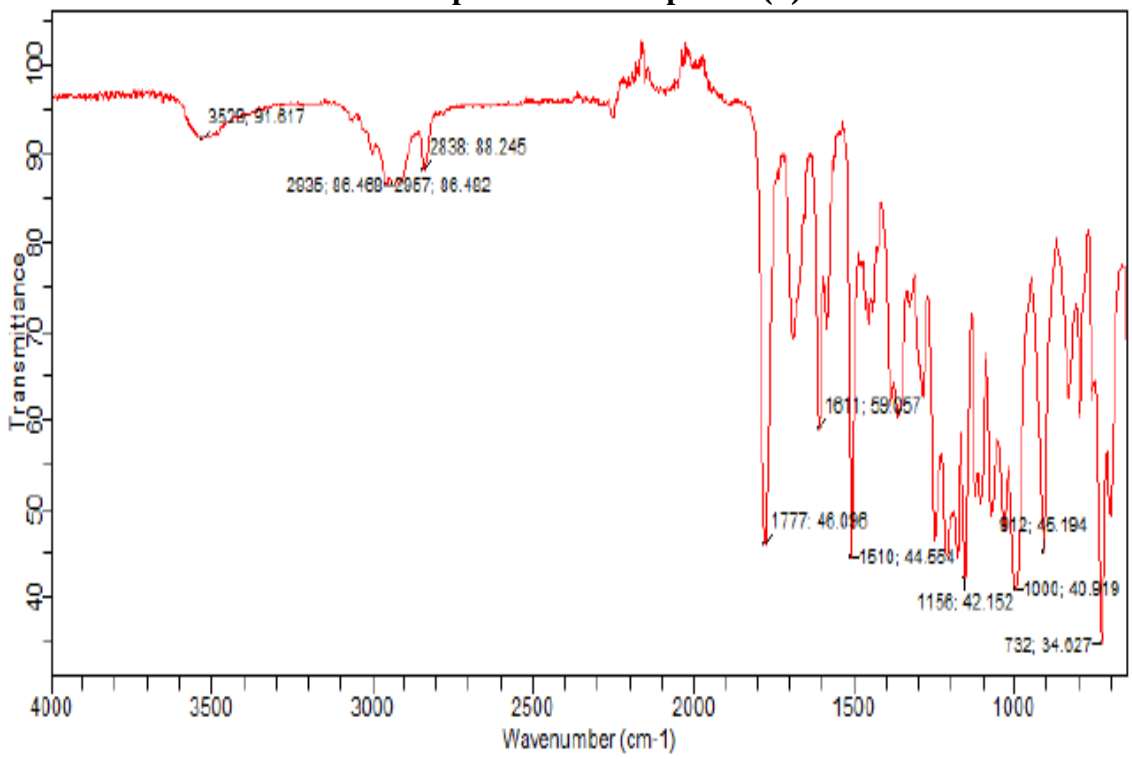

IR spectrum of compound (+) 44

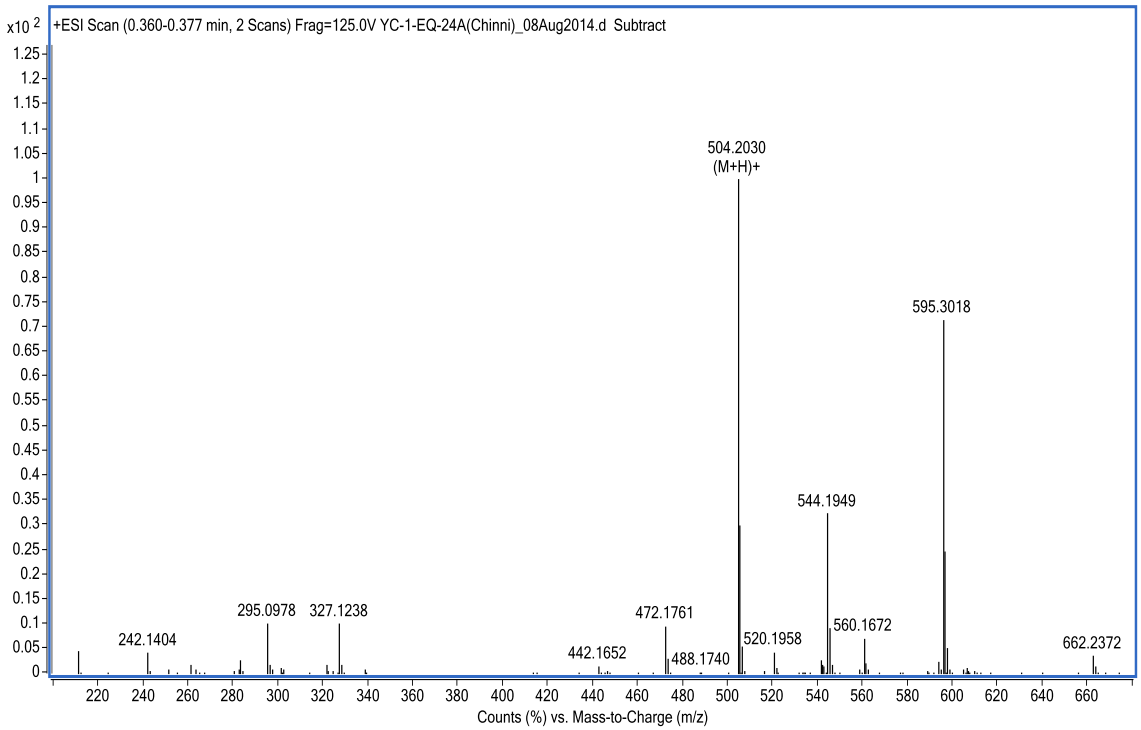

ESI-HRMS of compound (+) 44

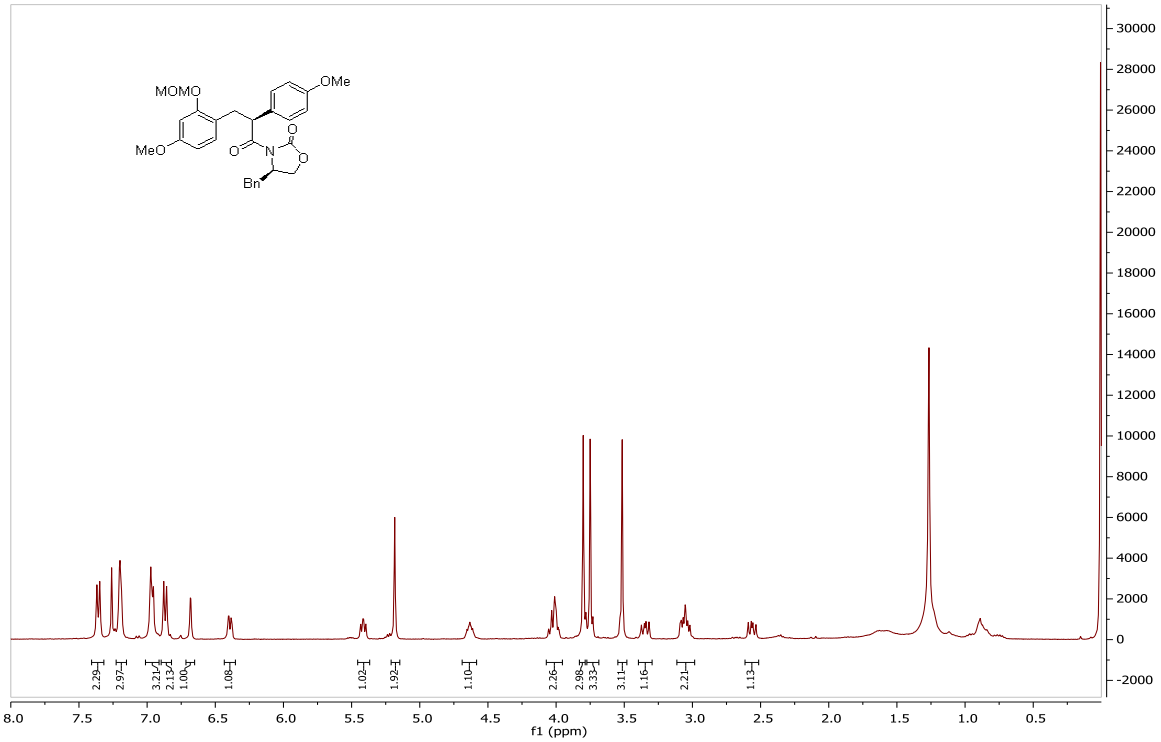

^{1}H NMR spectrum of compound (+) 54

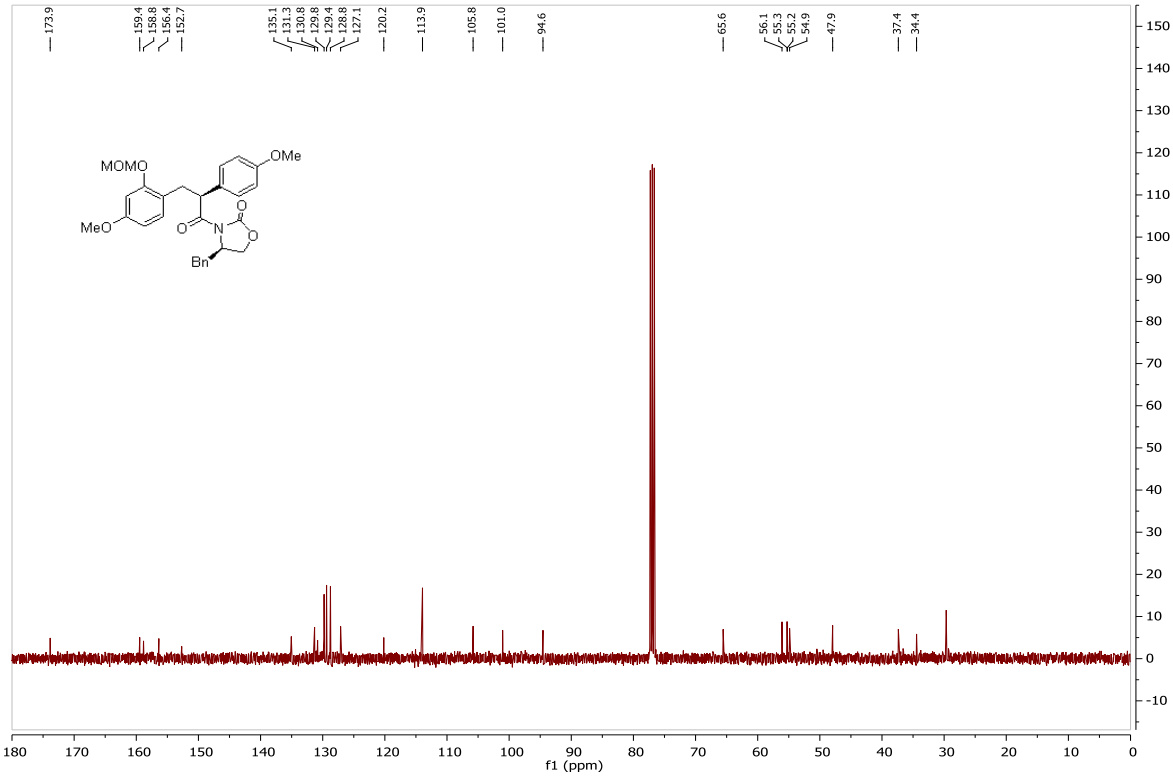

^{13}C NMR spectrum of compound (+) 54

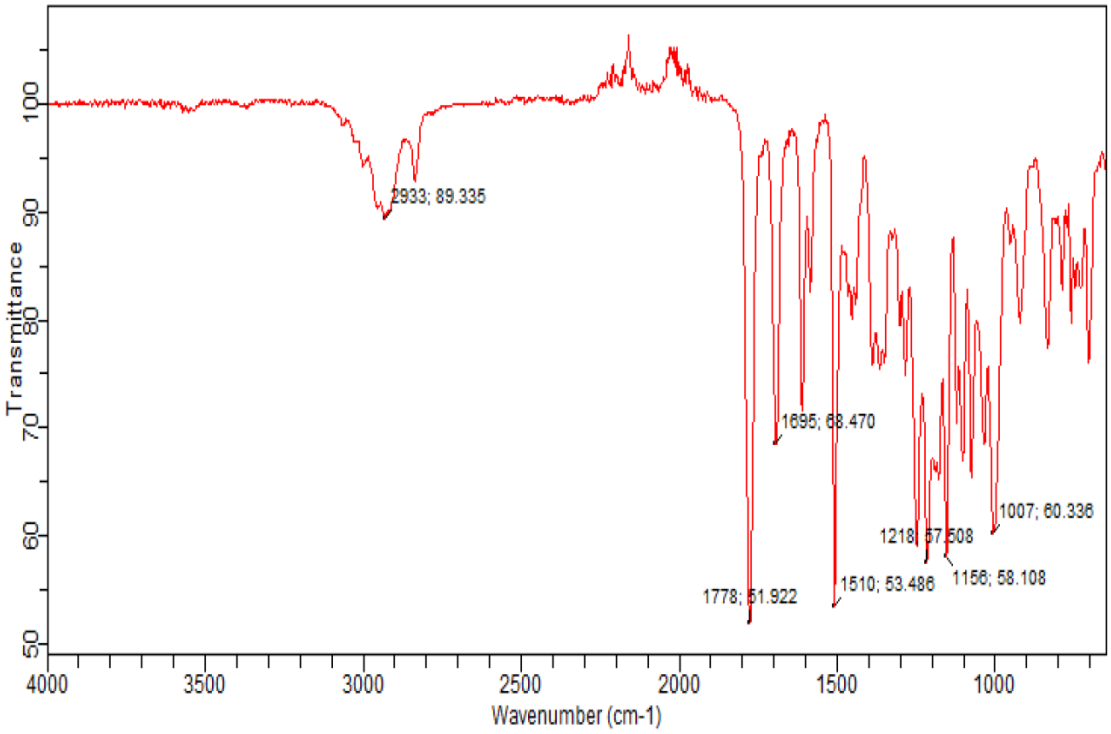

IR spectrum of compound (+) 54

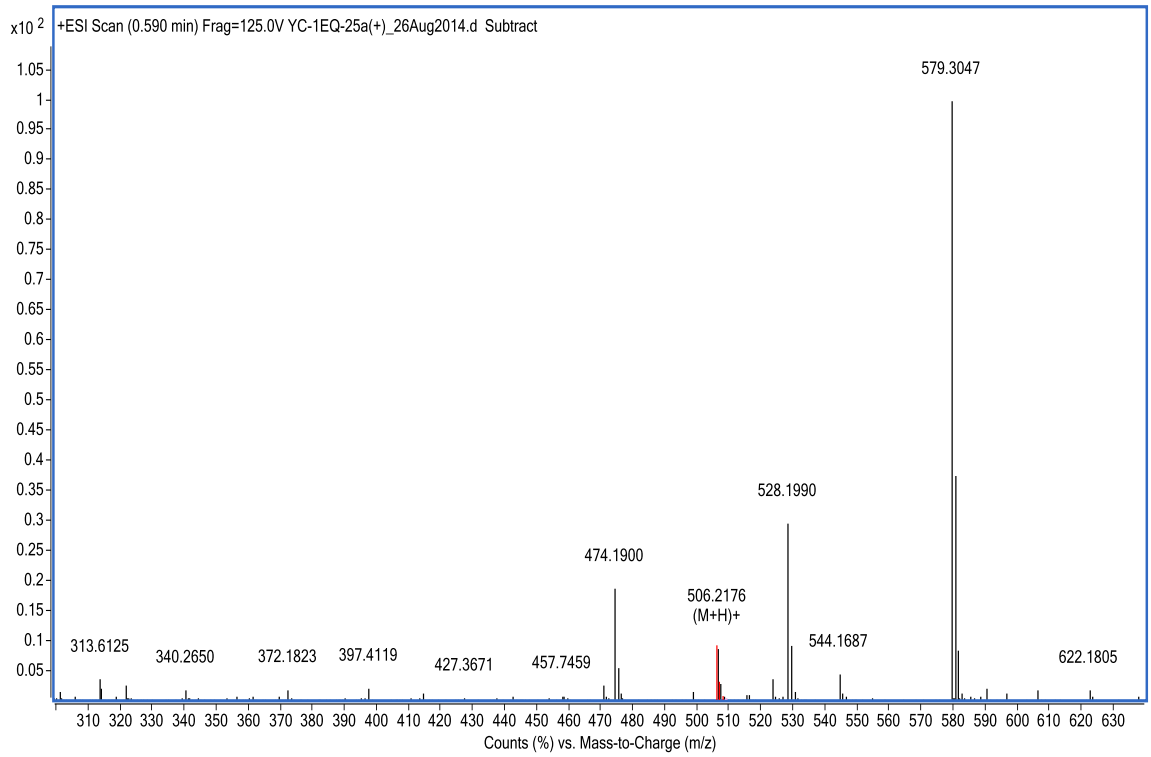

ESI-HRMS of compound (+) 54

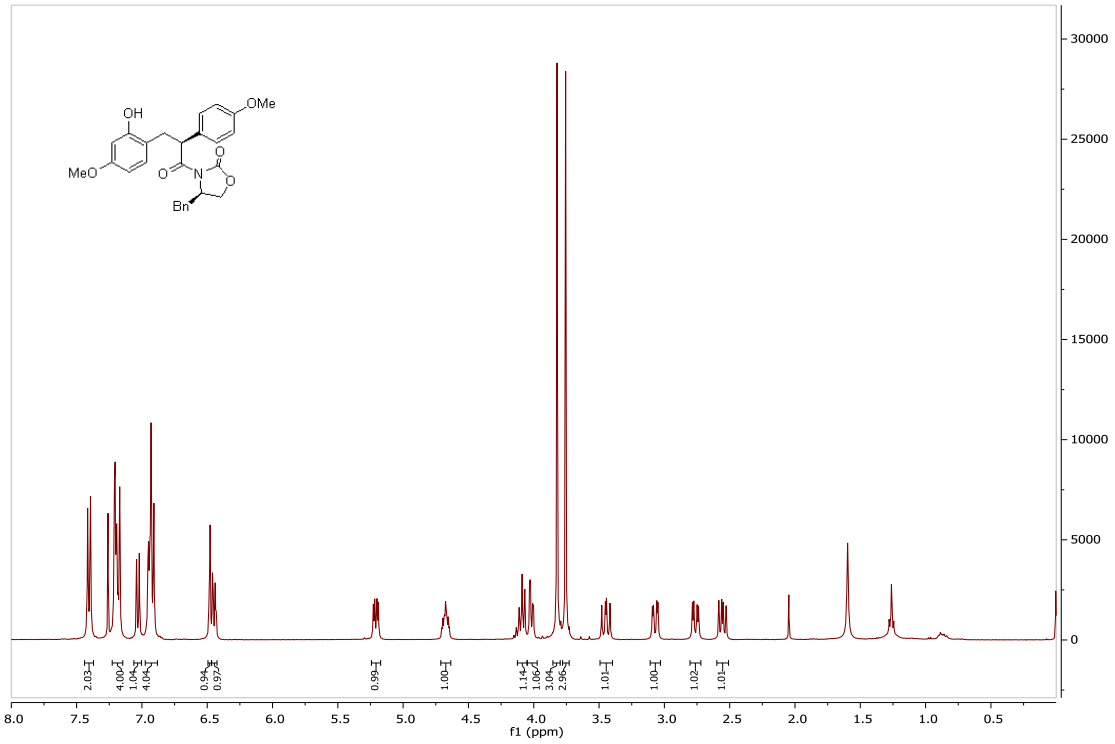

^{1}H NMR spectrum of compound (+) 55

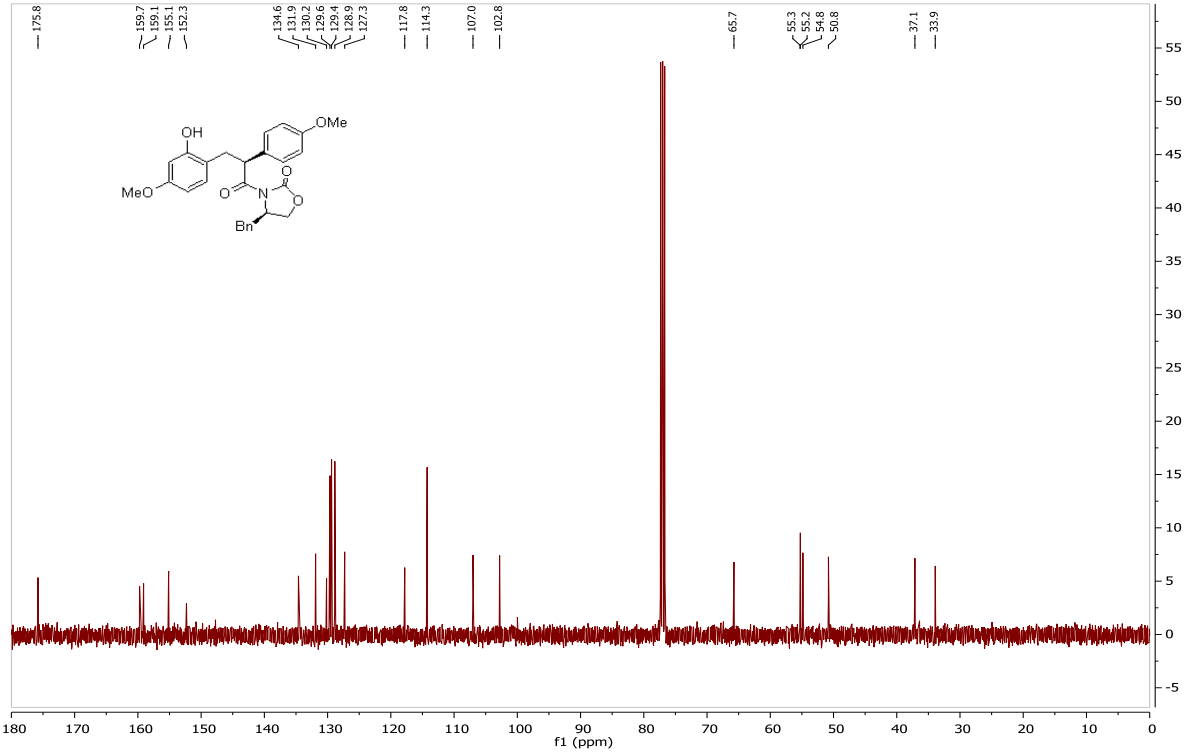

^{13}C NMR spectrum of compound (+) 55

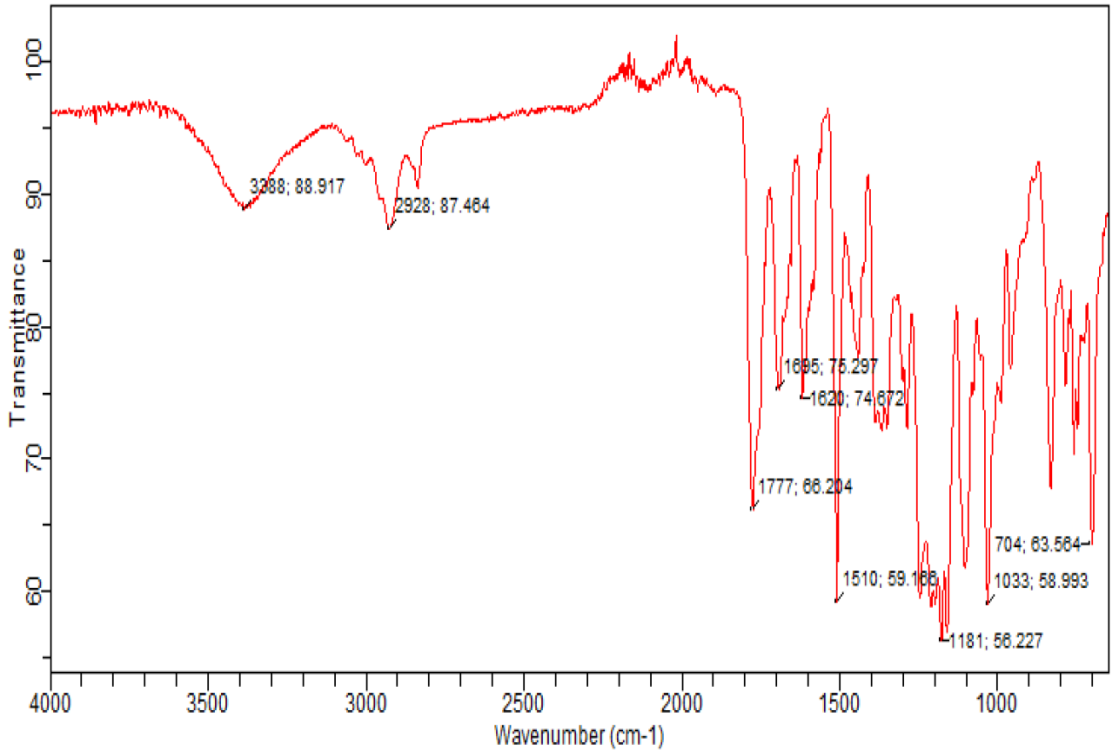

IR spectrum of compound (+) 55

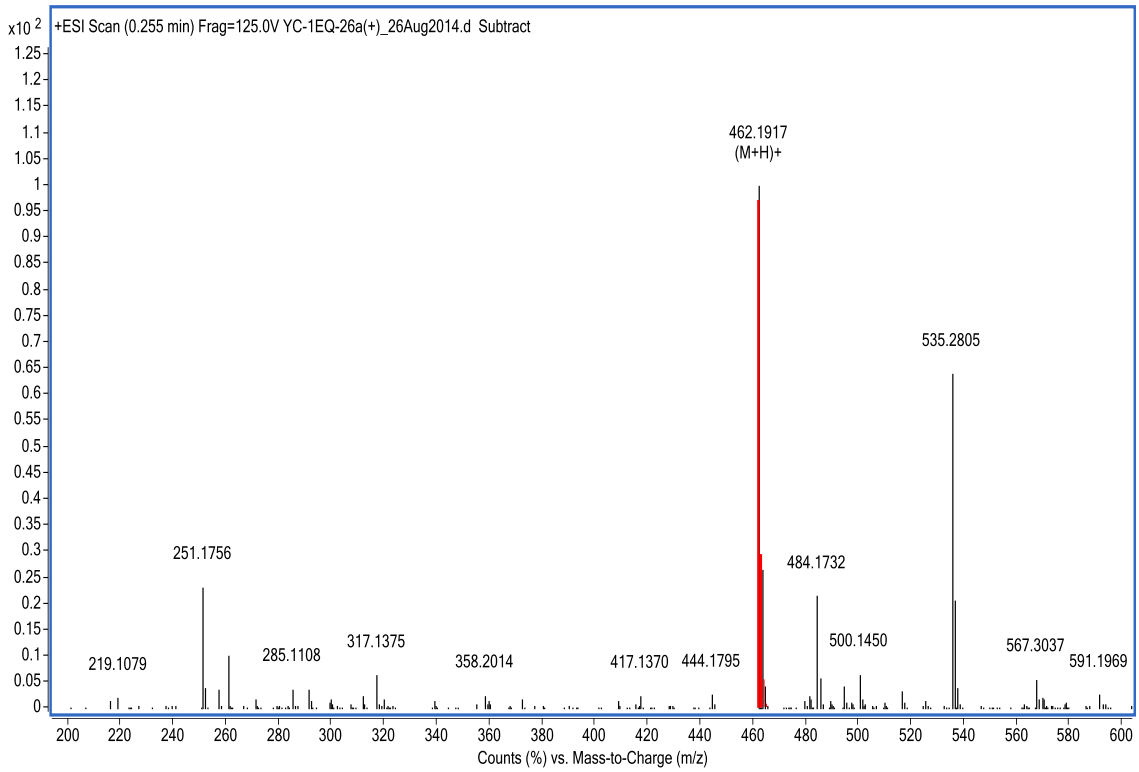

ESI-HRMS of compound (+) 55

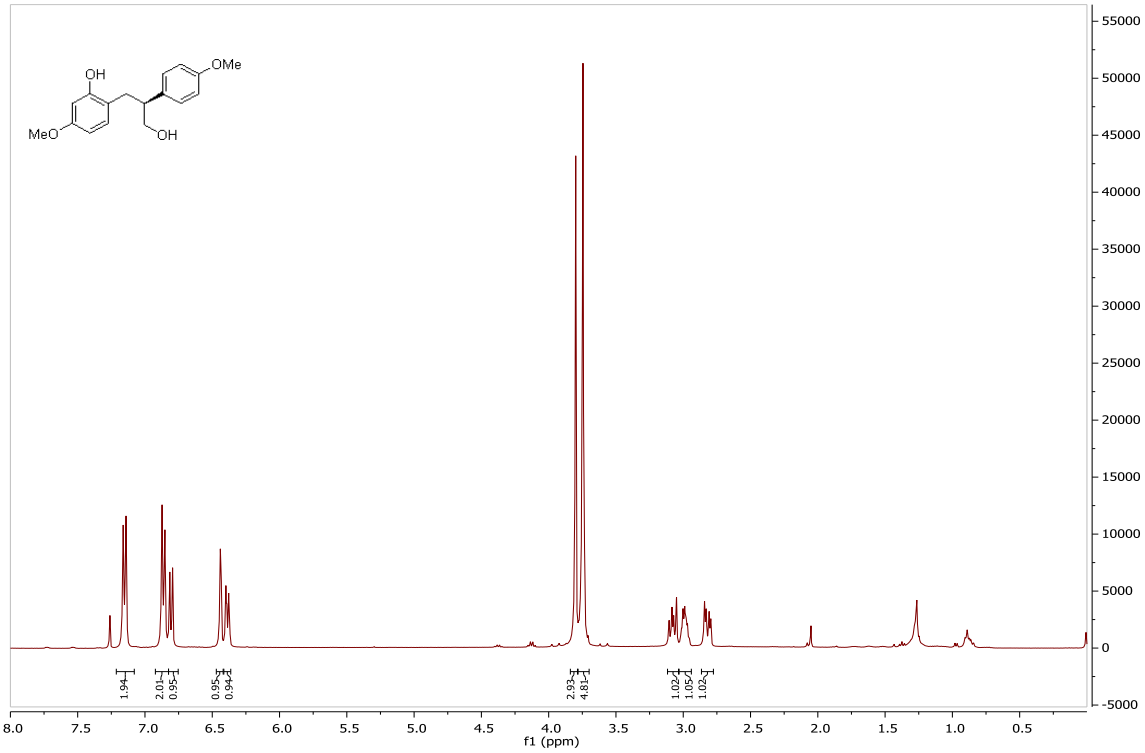

^{1}H NMR spectrum of compound (+) 42

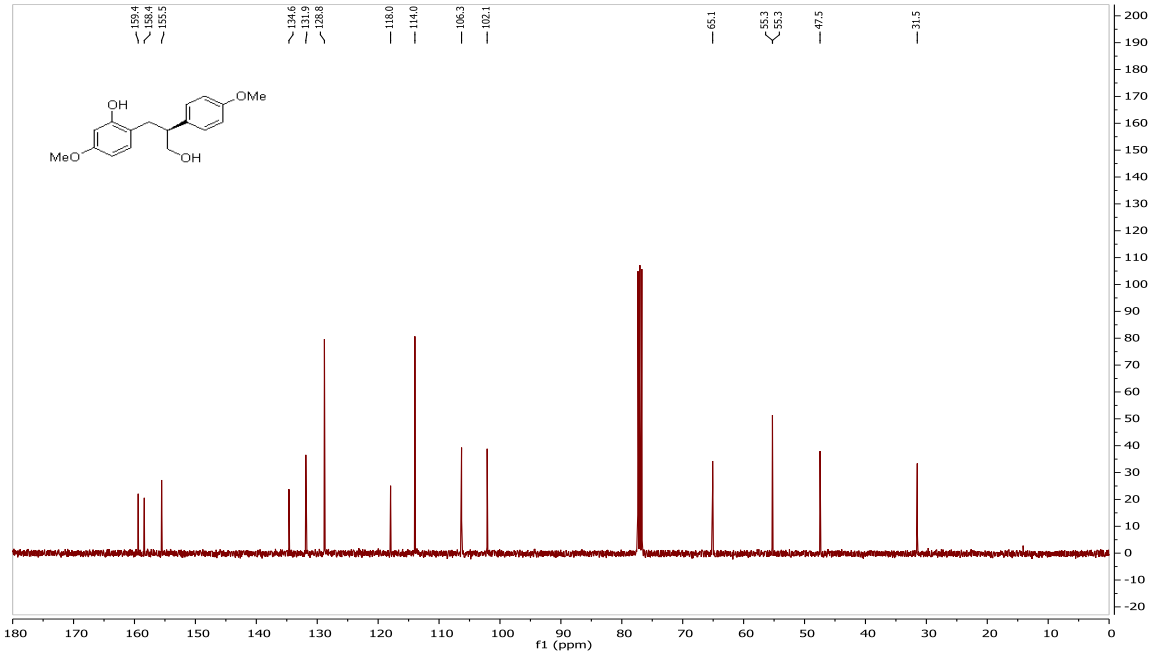

^{13}C NMR spectrum of compound (+) 42

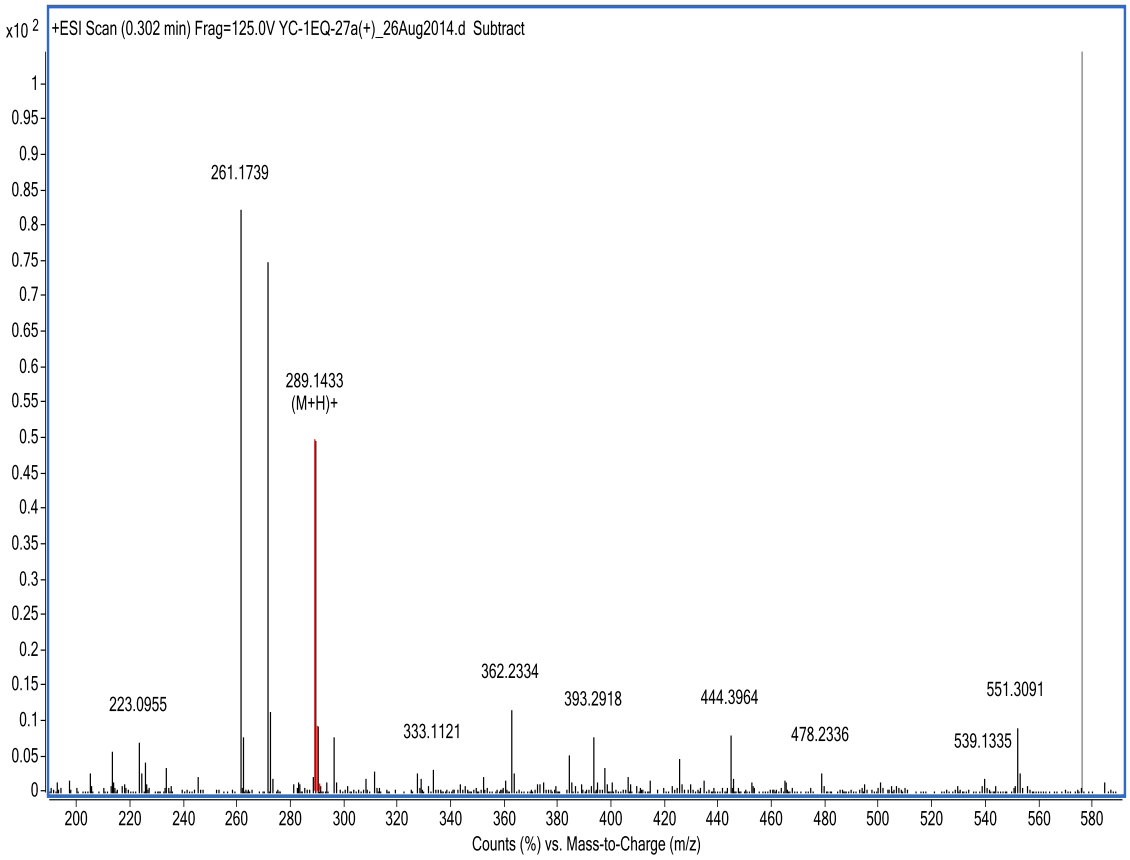

ESI-HRMS of compound (+) 42

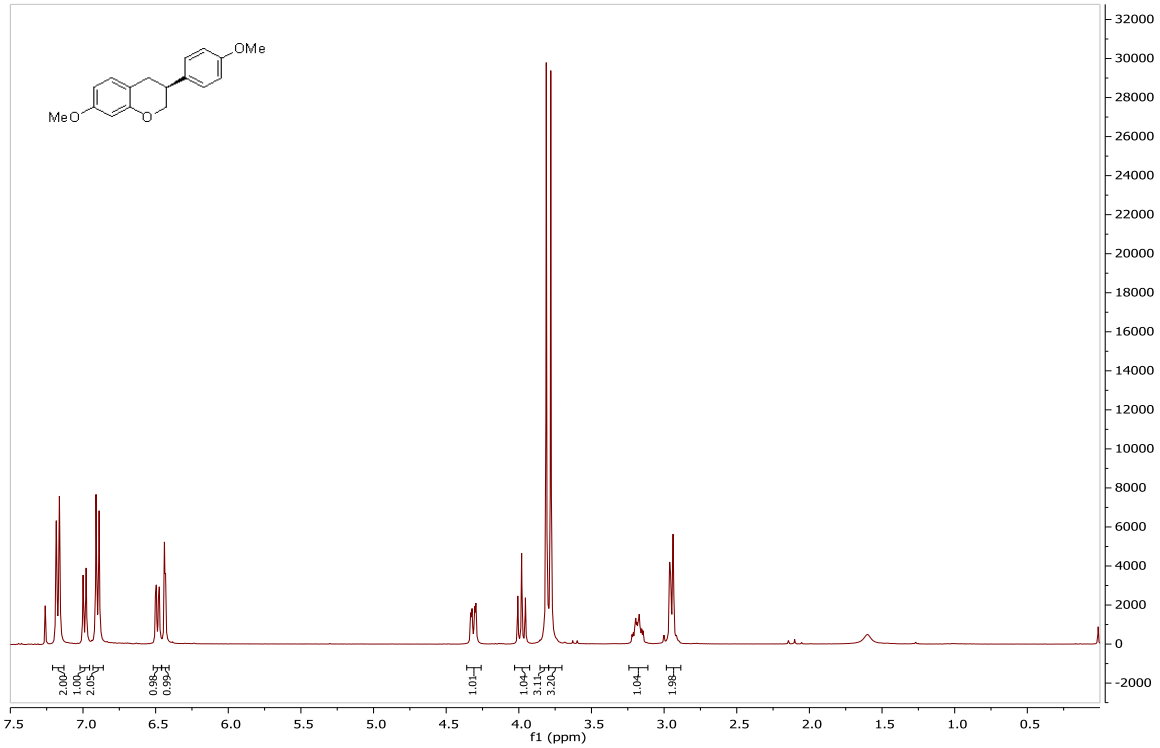

^{1}H NMR spectrum of compound (-) 30

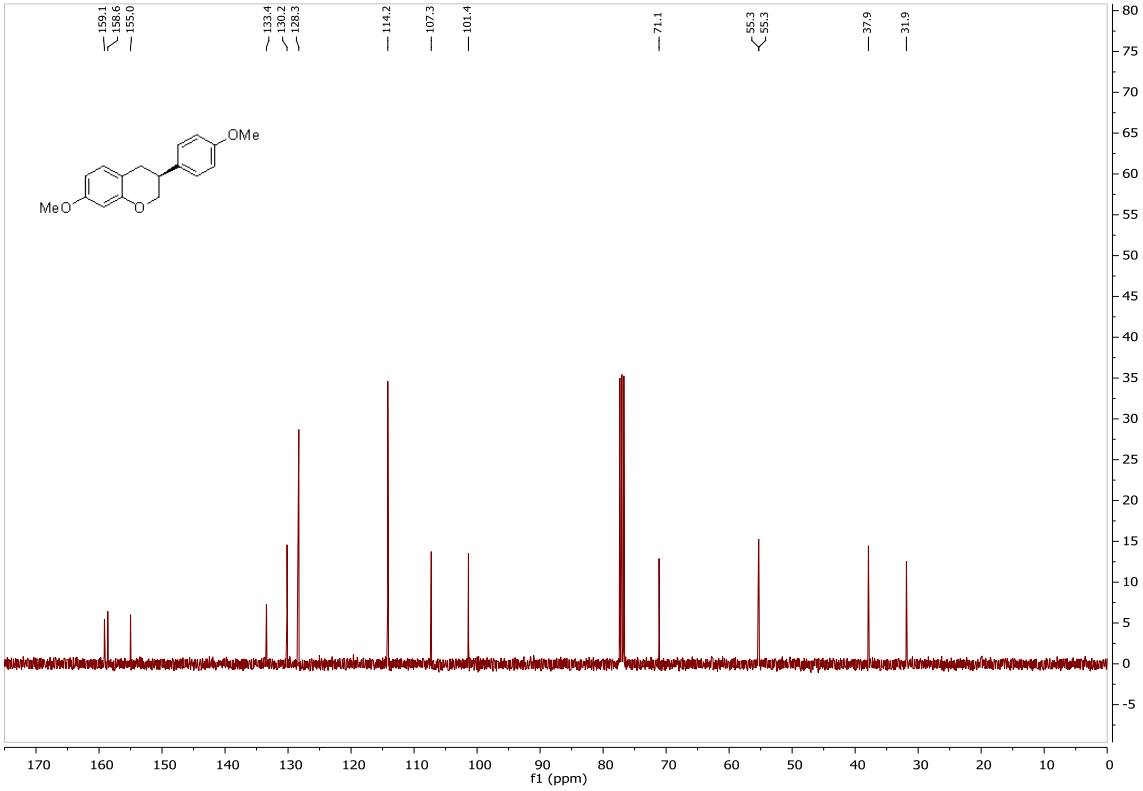

^{13}C NMR spectrum of compound (-) 30

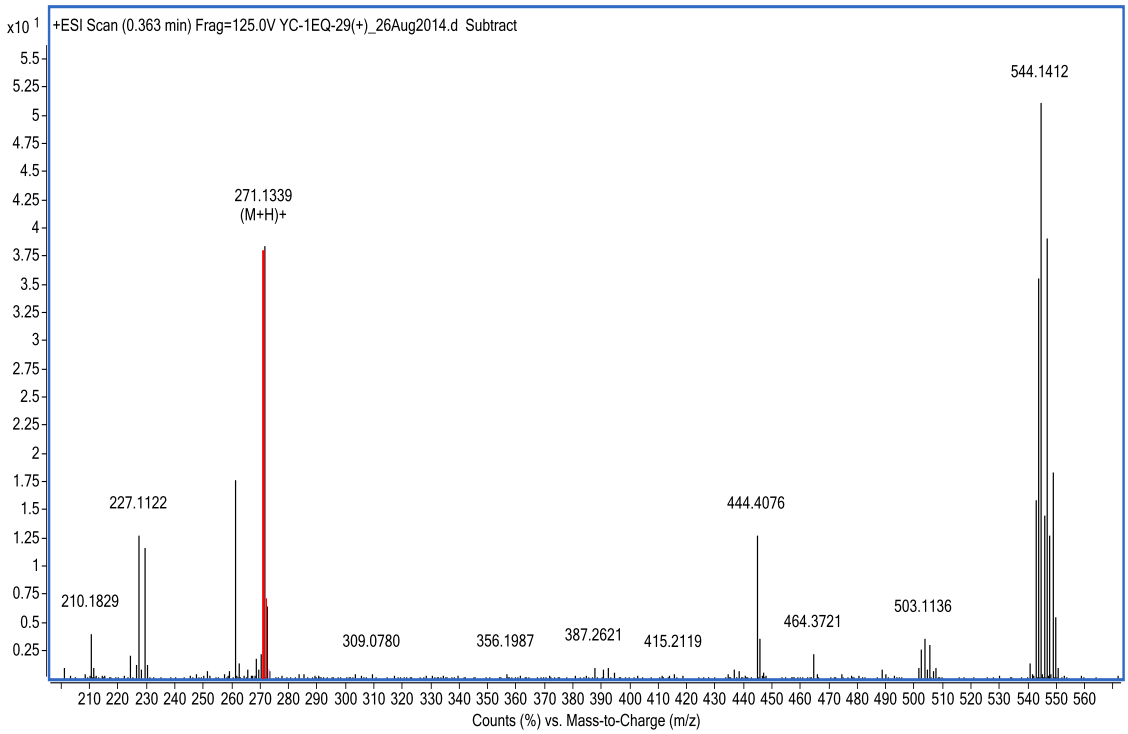

ESI-HRMS of compound (-)-30

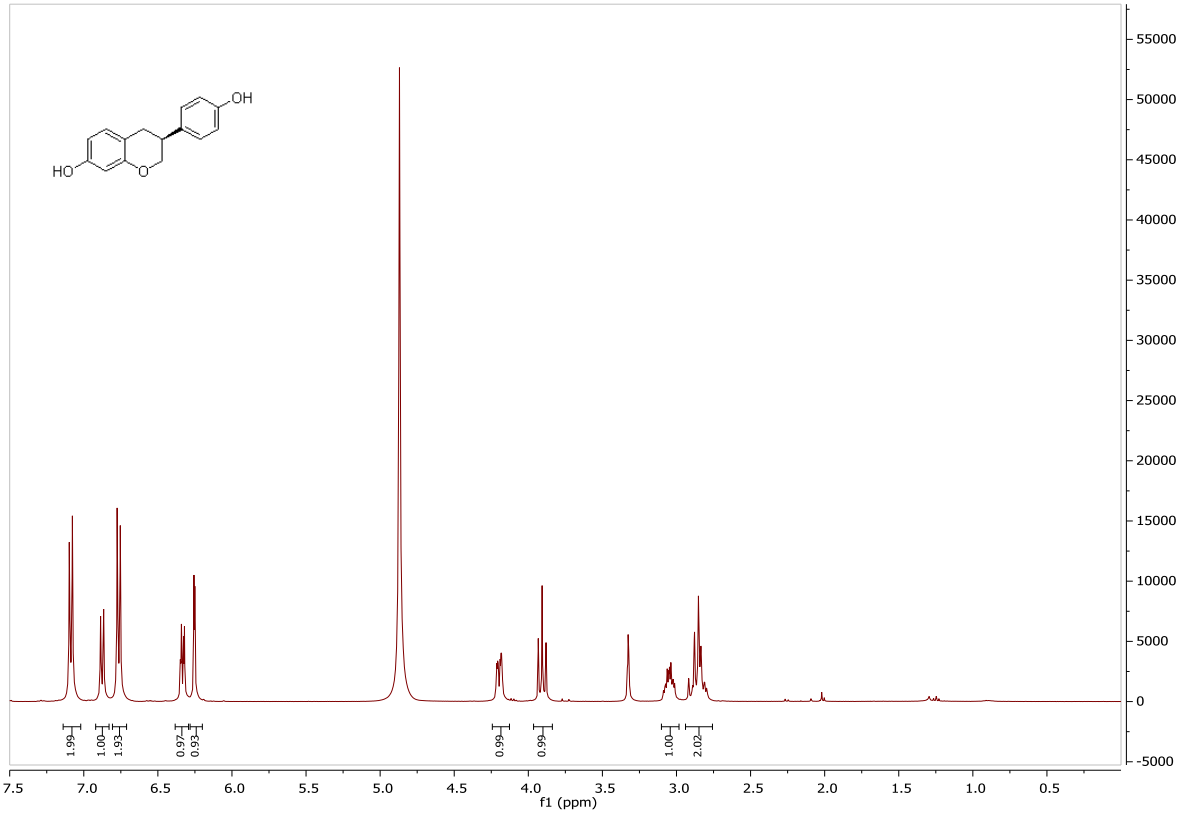

^{1}H NMR spectrum of compound S-Equol (-)-7

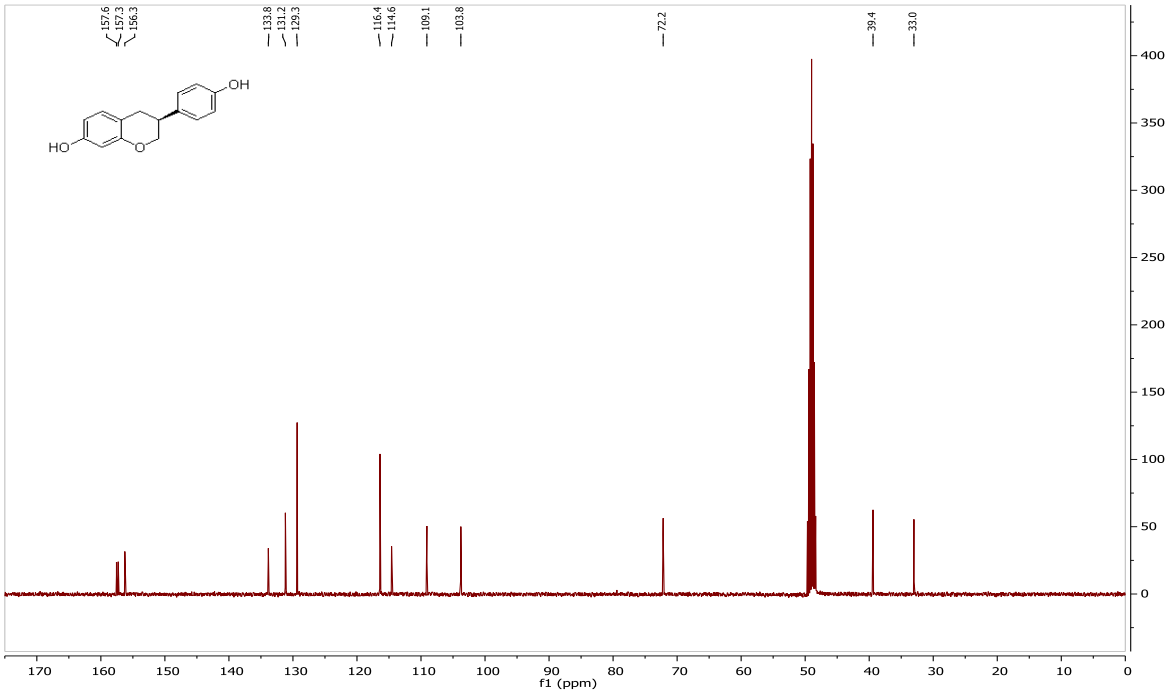

^{13}C NMR spectrum of compound S-Equol **(-) 7**

SI Spectral Data 4. Spectral date of the compounds for Synthesis of *R*-Equol.

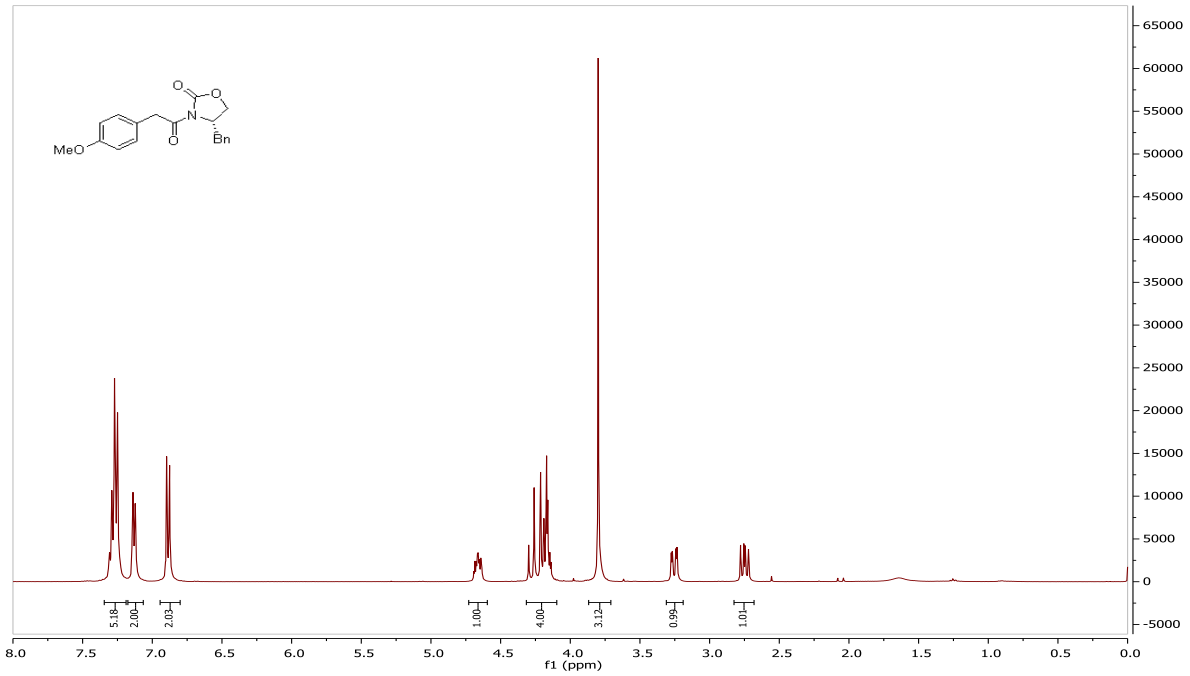

^{1}H NMR spectrum of compound (+) 26

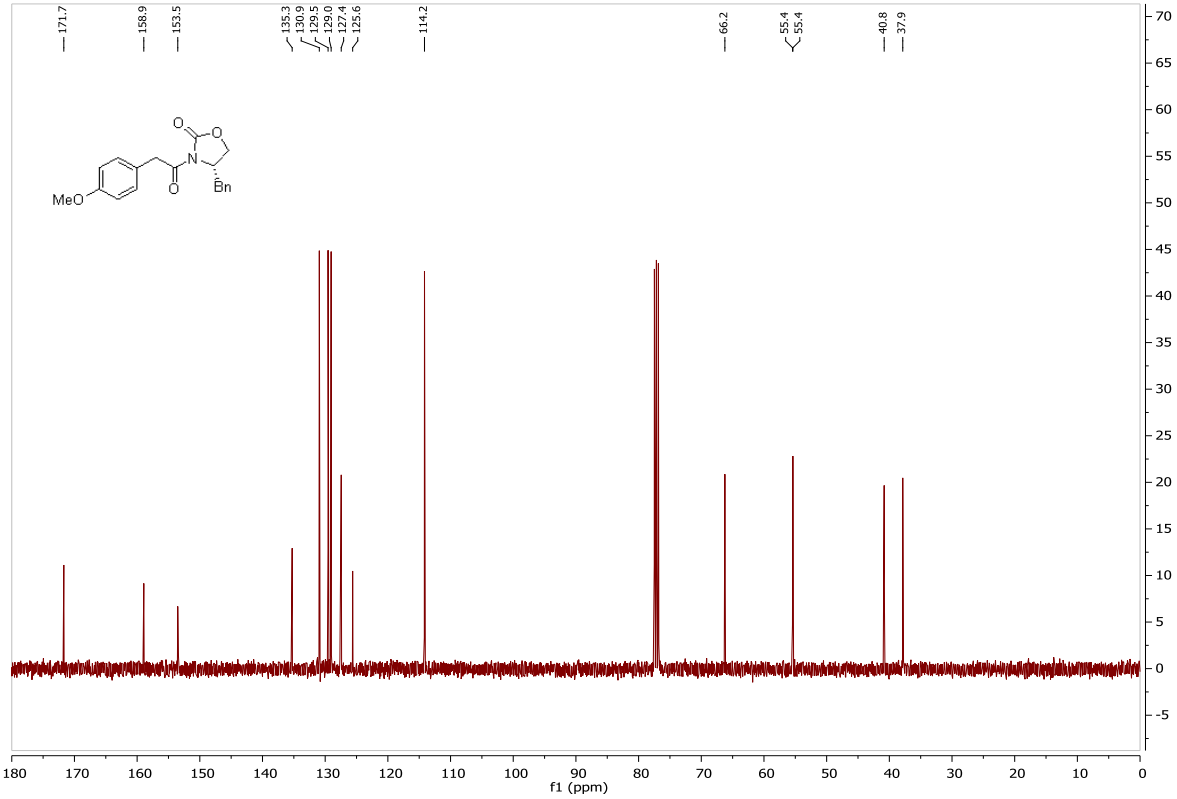

^{13}C NMR spectrum of compound (+) 26

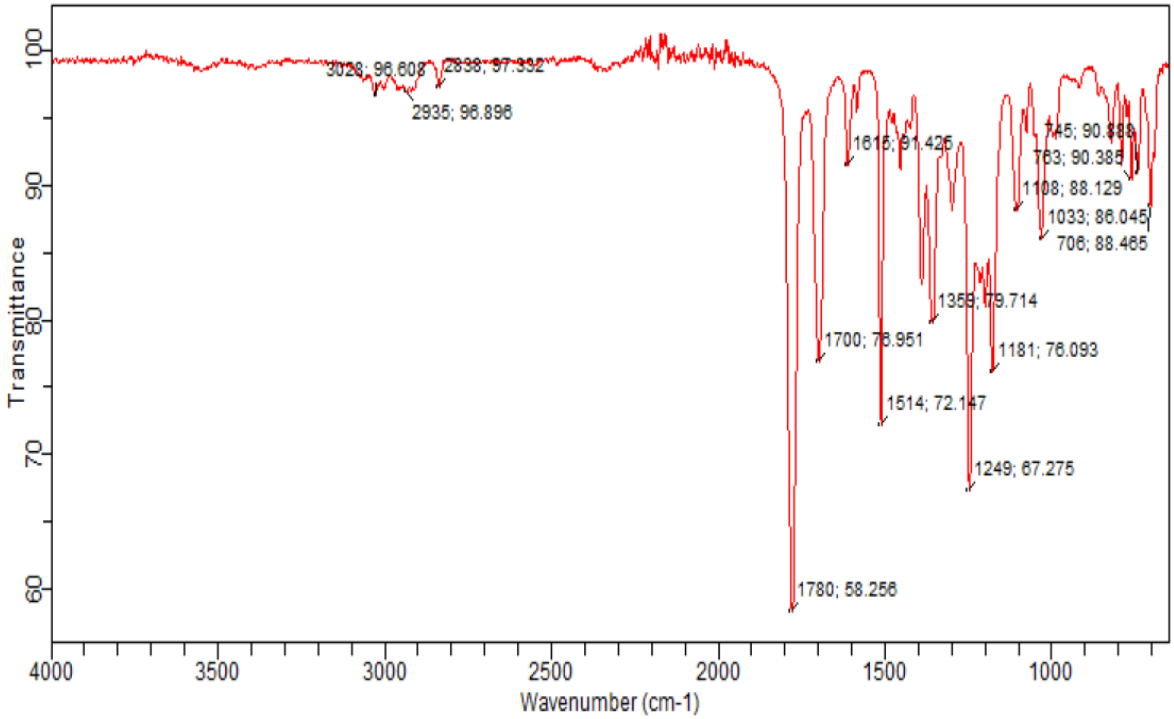

IR spectrum of compound (+) 26

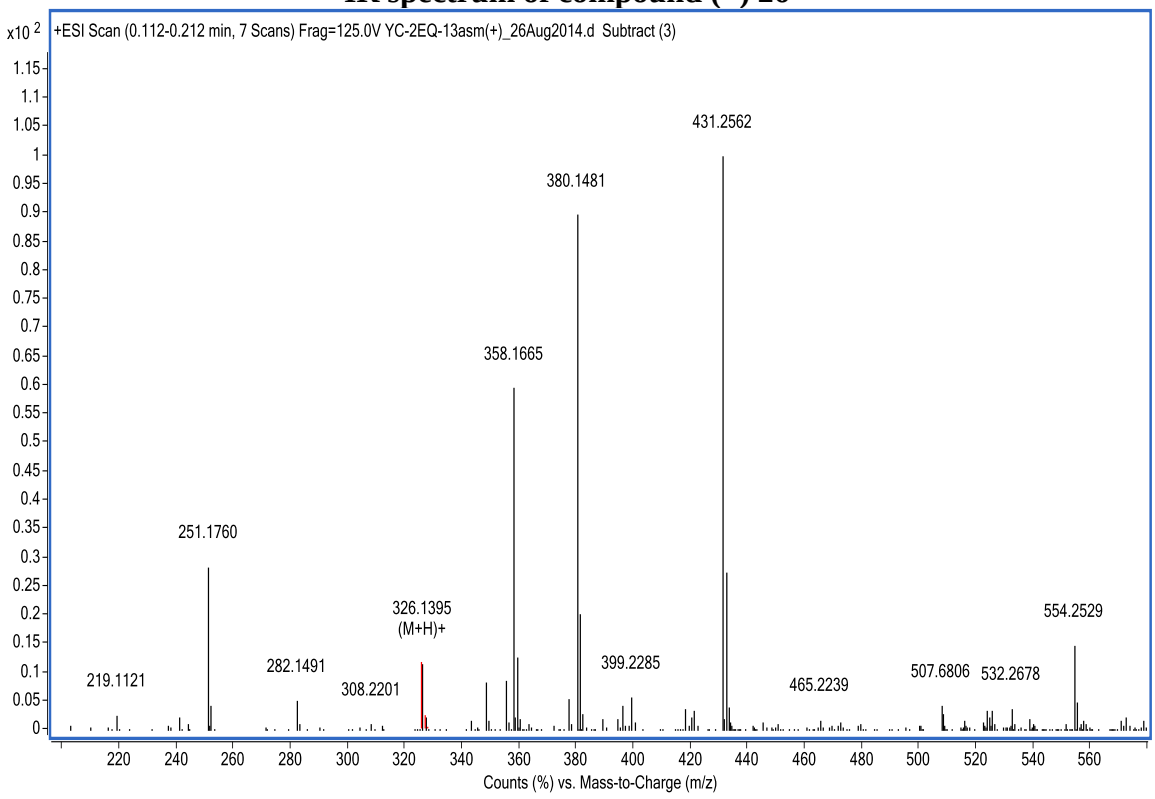

ESI-HRMS of compound (+) 26

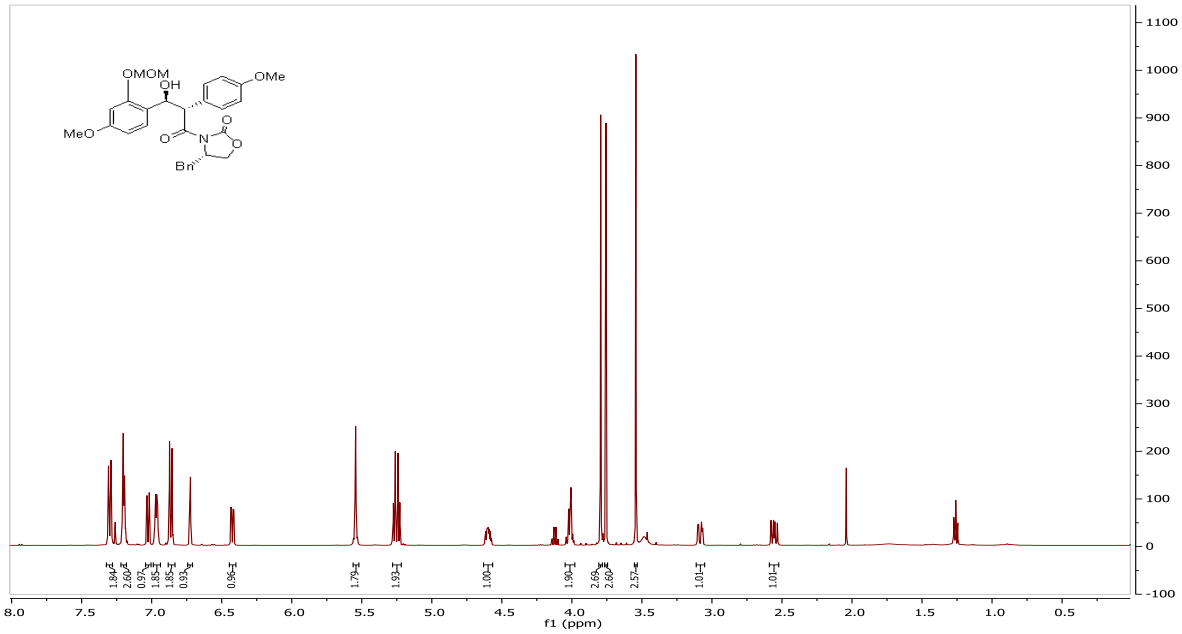

^{1}H NMR spectrum of compound (-) 44

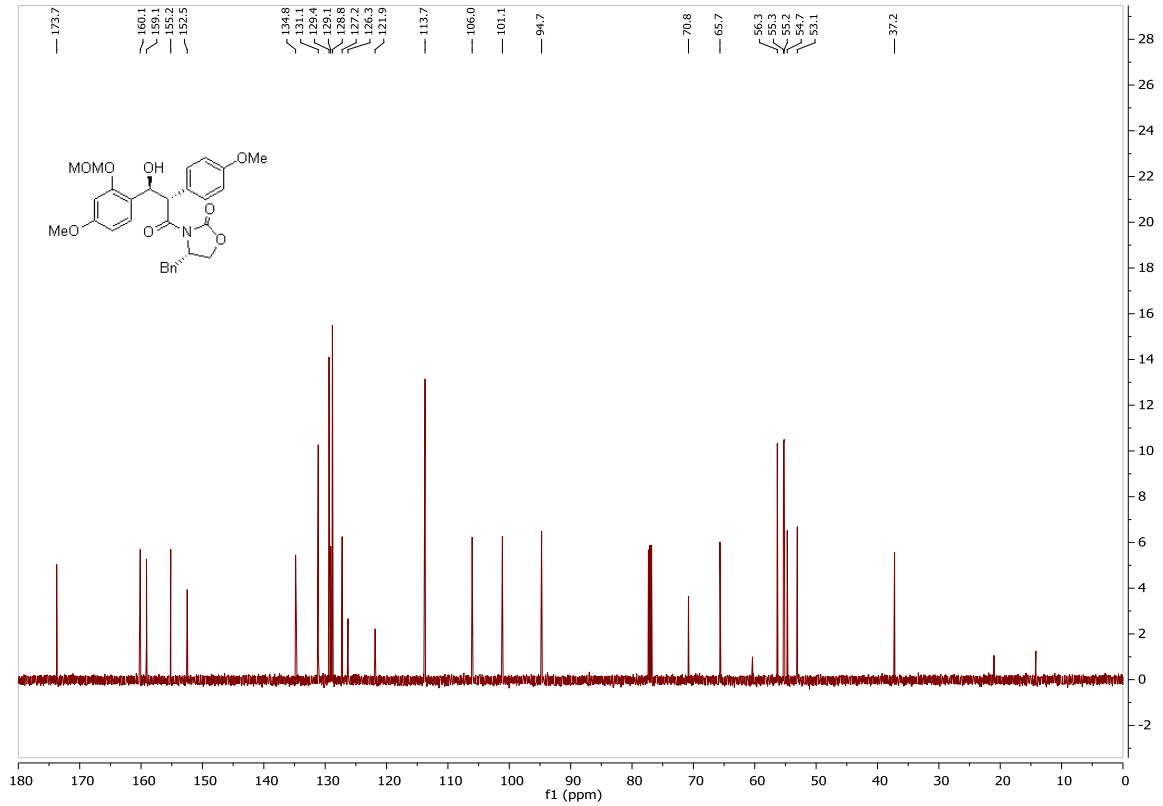

^{13}C NMR spectrum of compound (-) 44

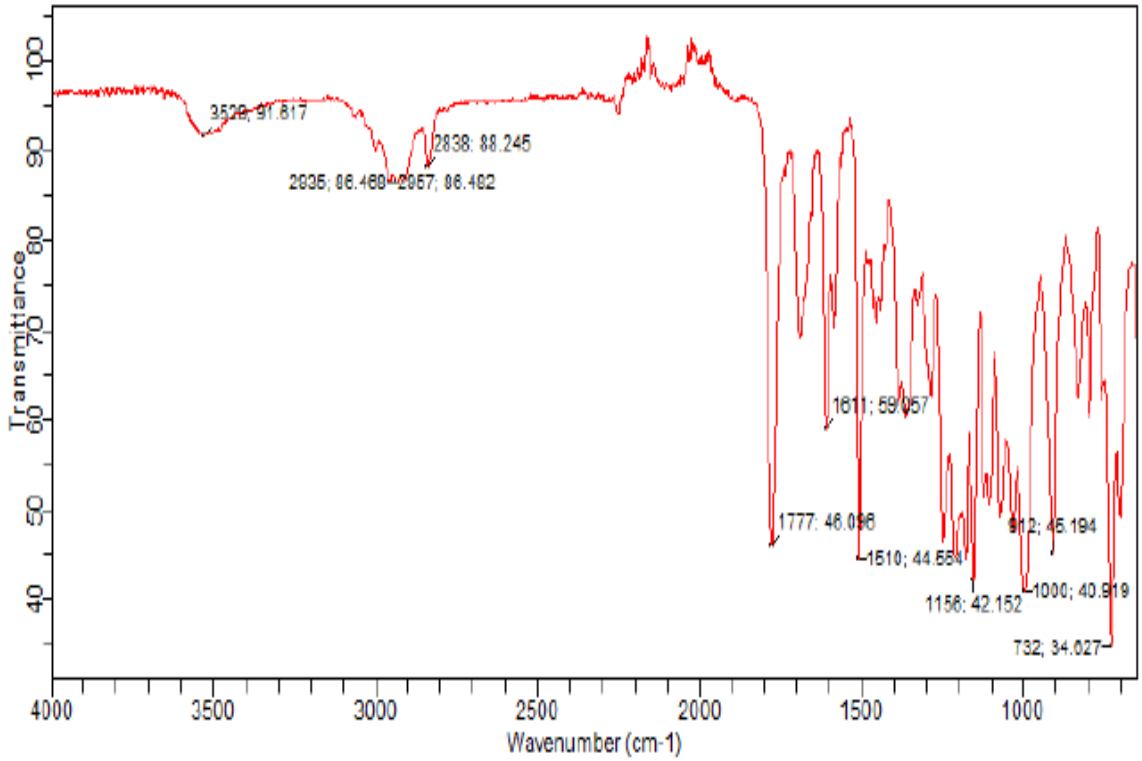

IR spectrum of compound (-) 44

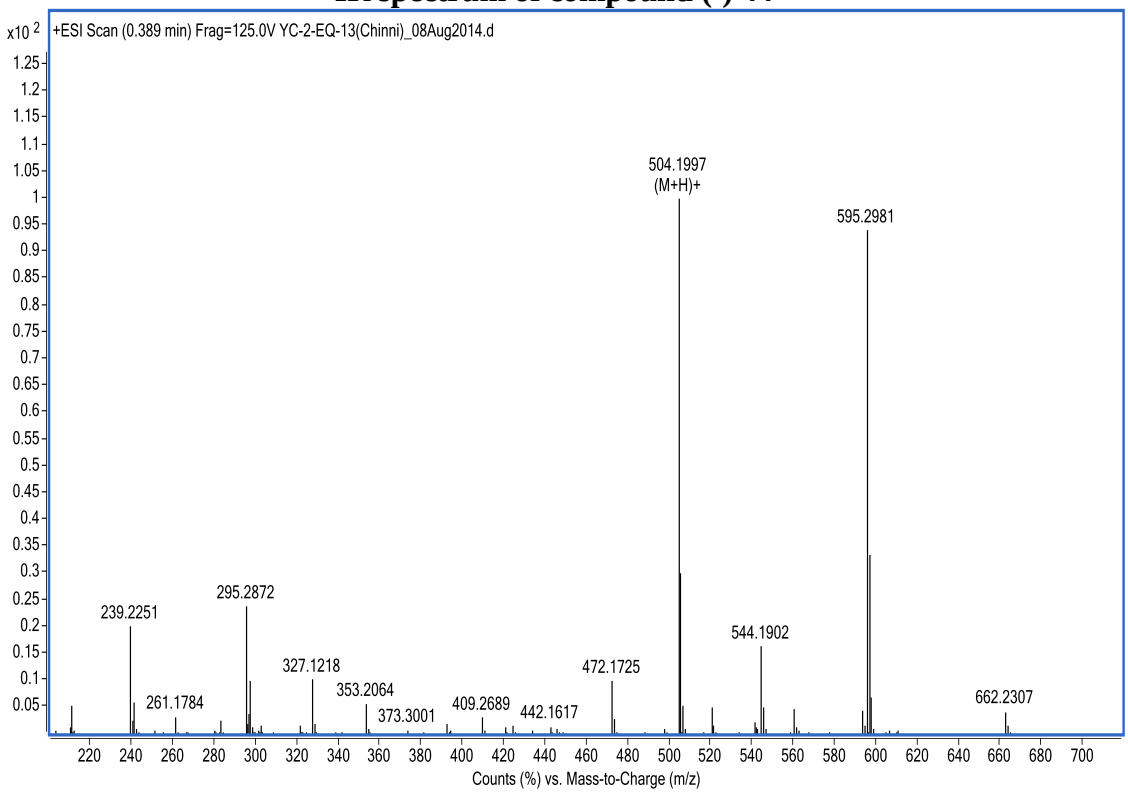

ESI-HRMS of compound (-) 44

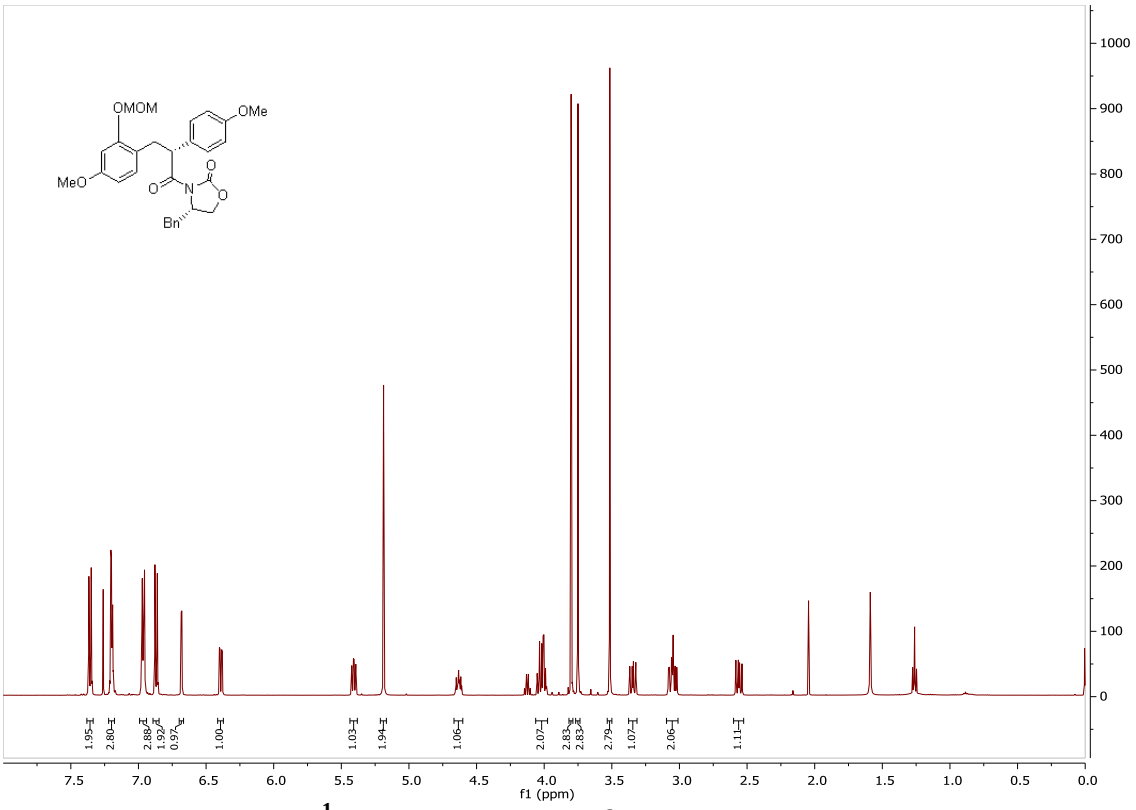

^{1}H NMR spectrum of compound (-) 54

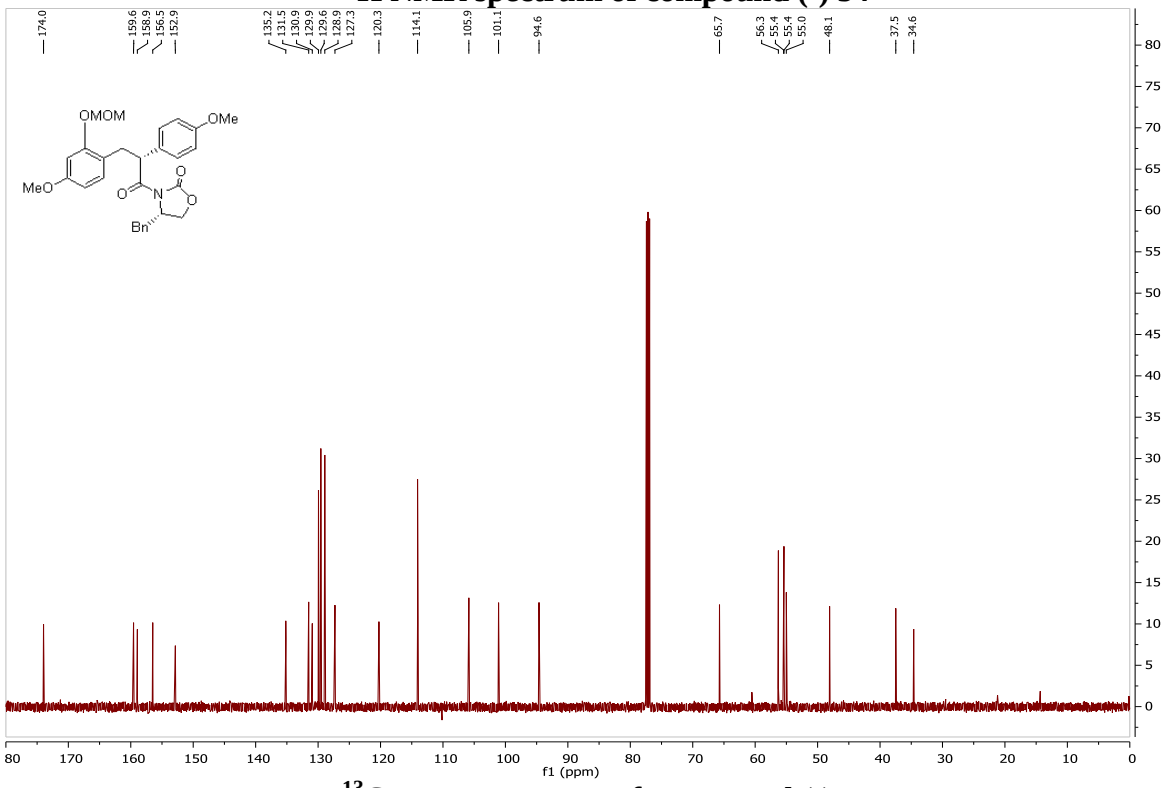

^{13}C NMR spectrum of compound (-) 54

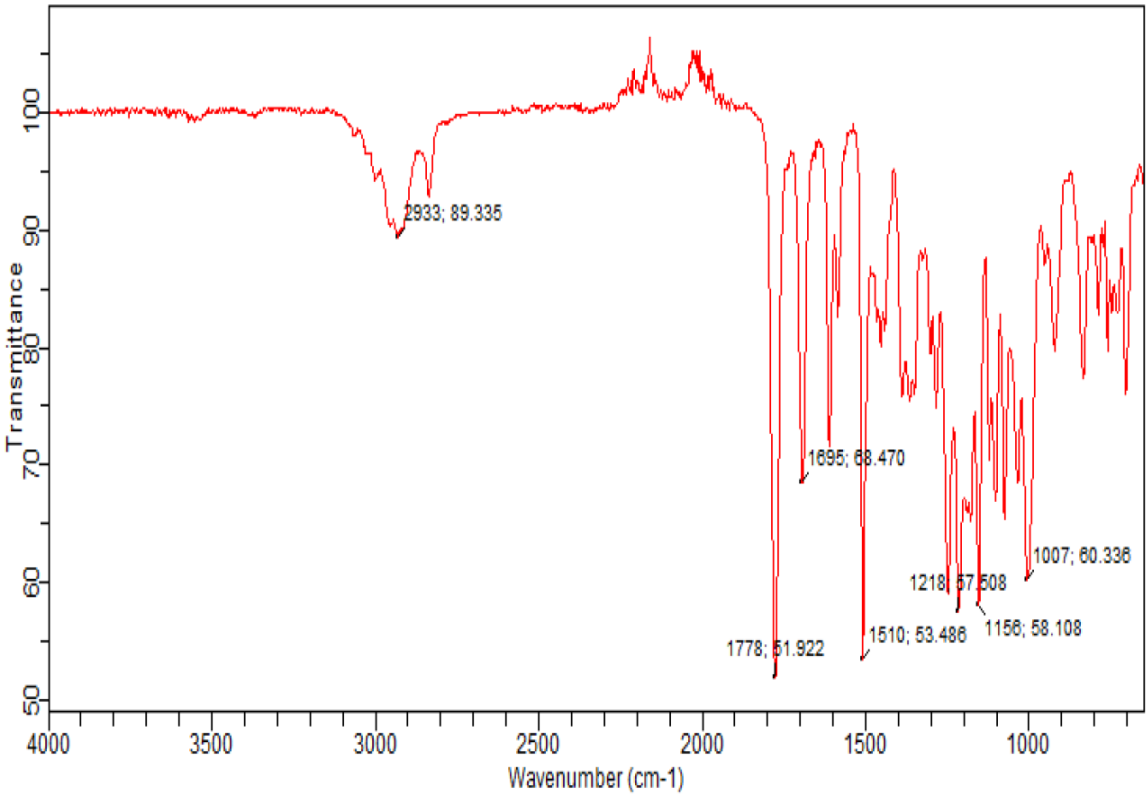

IR spectrum of compound (-) 54

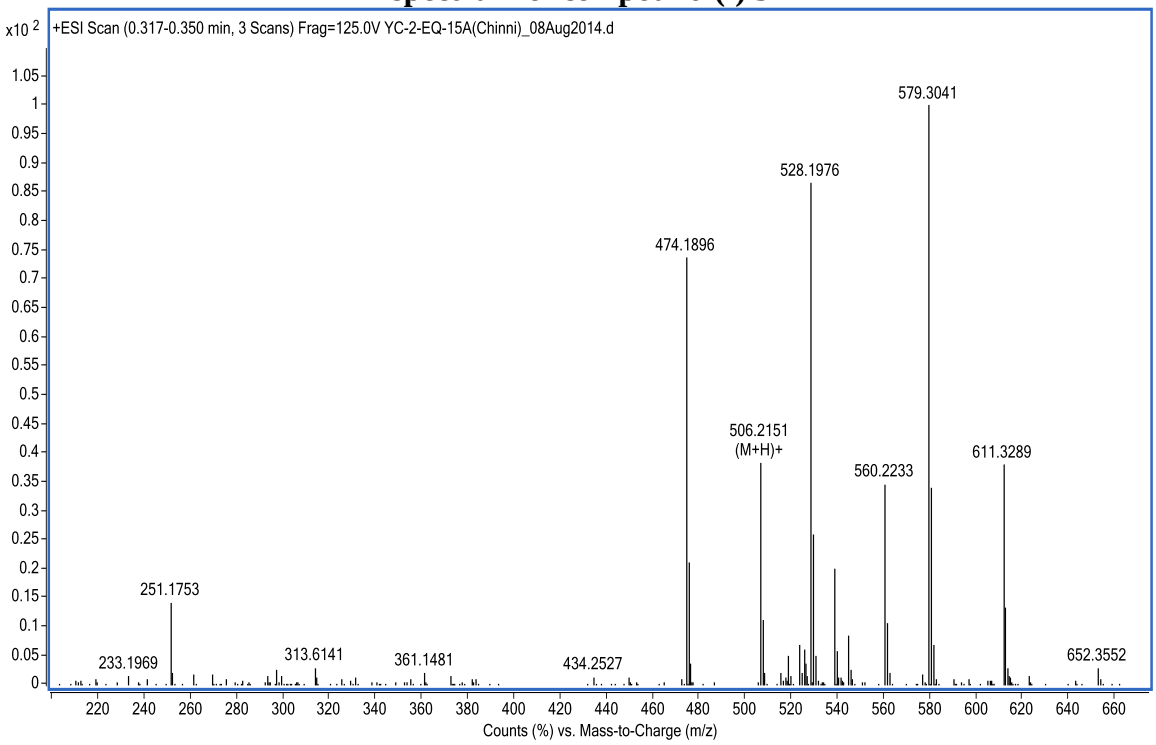

ESI-HRMS of compound (-) 54

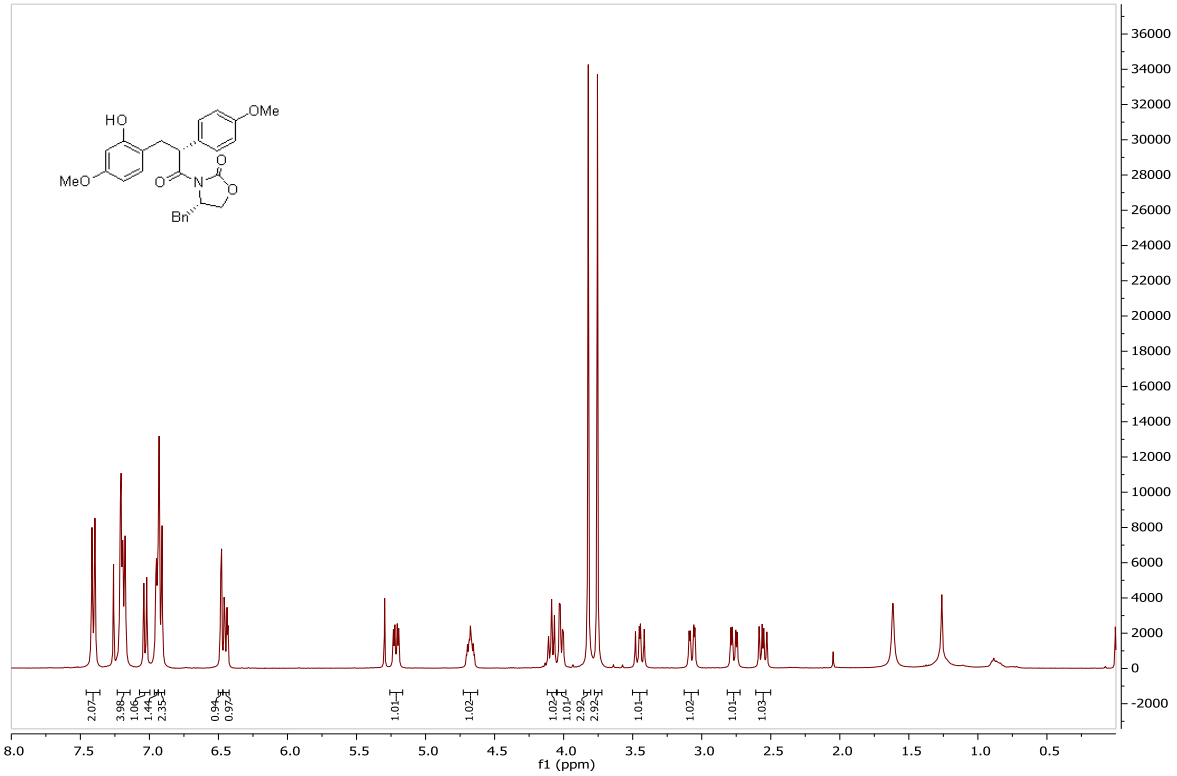

^{1}H NMR spectrum of compound (-) 55

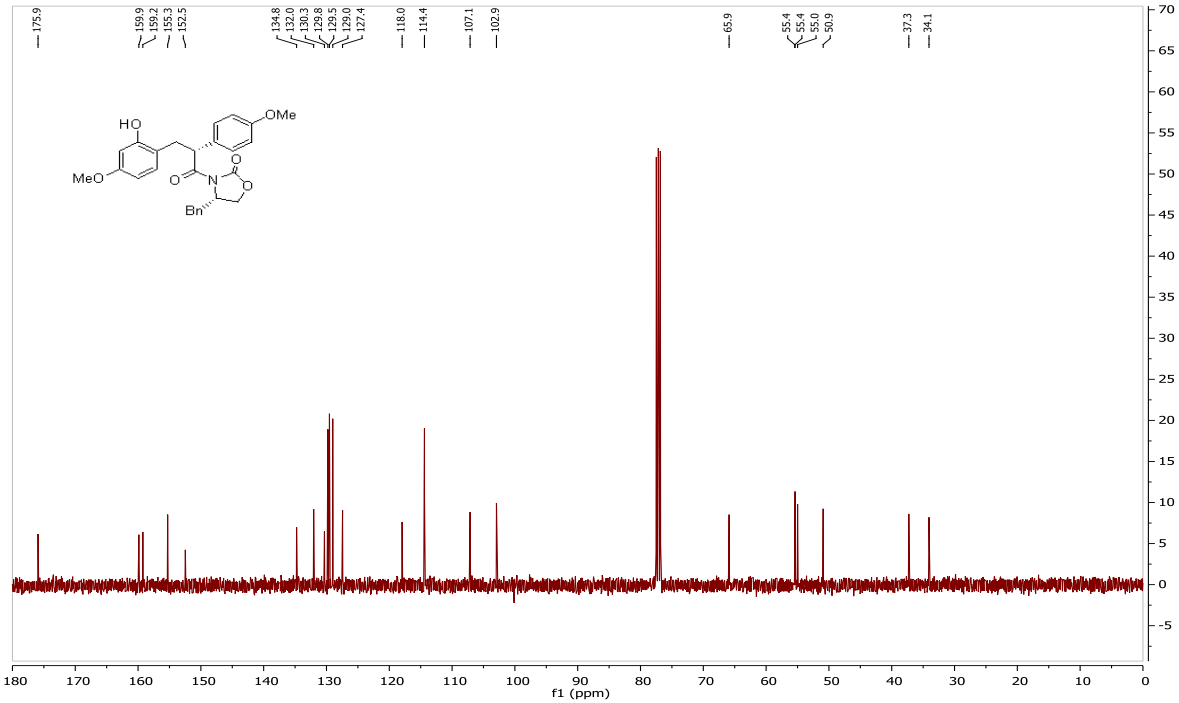

^{13}C NMR spectrum of compound (-) 55

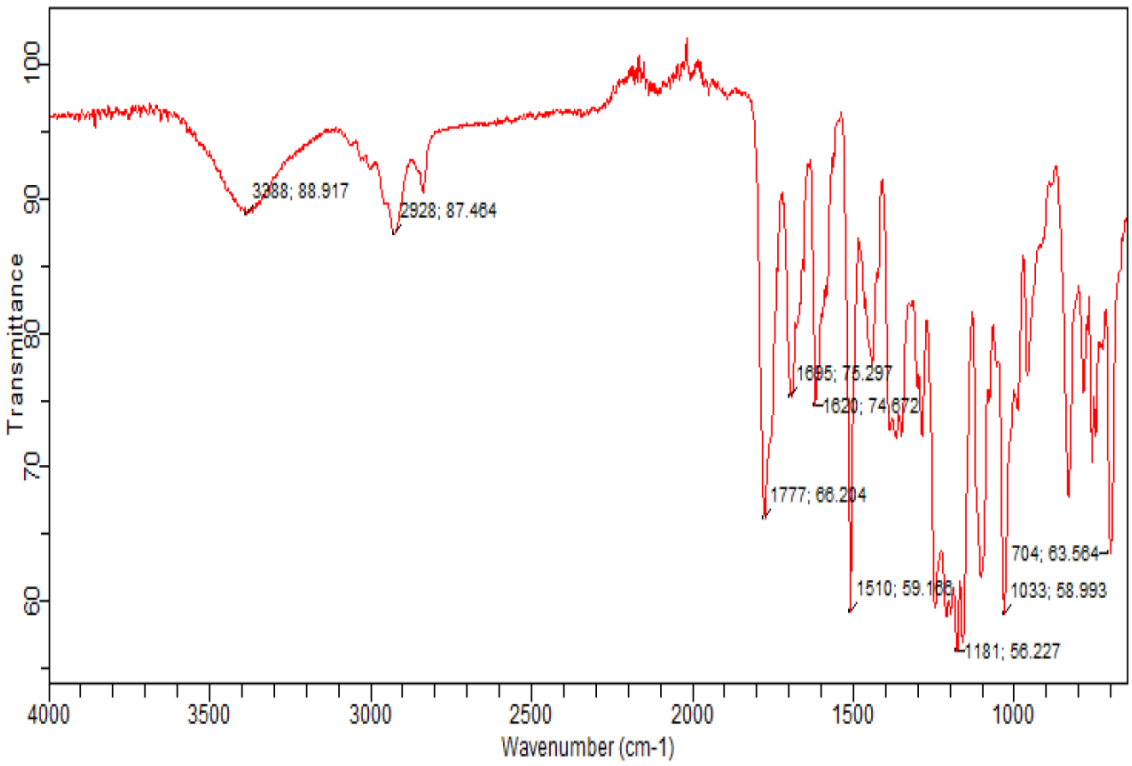

IR spectrum of compound (-) 55

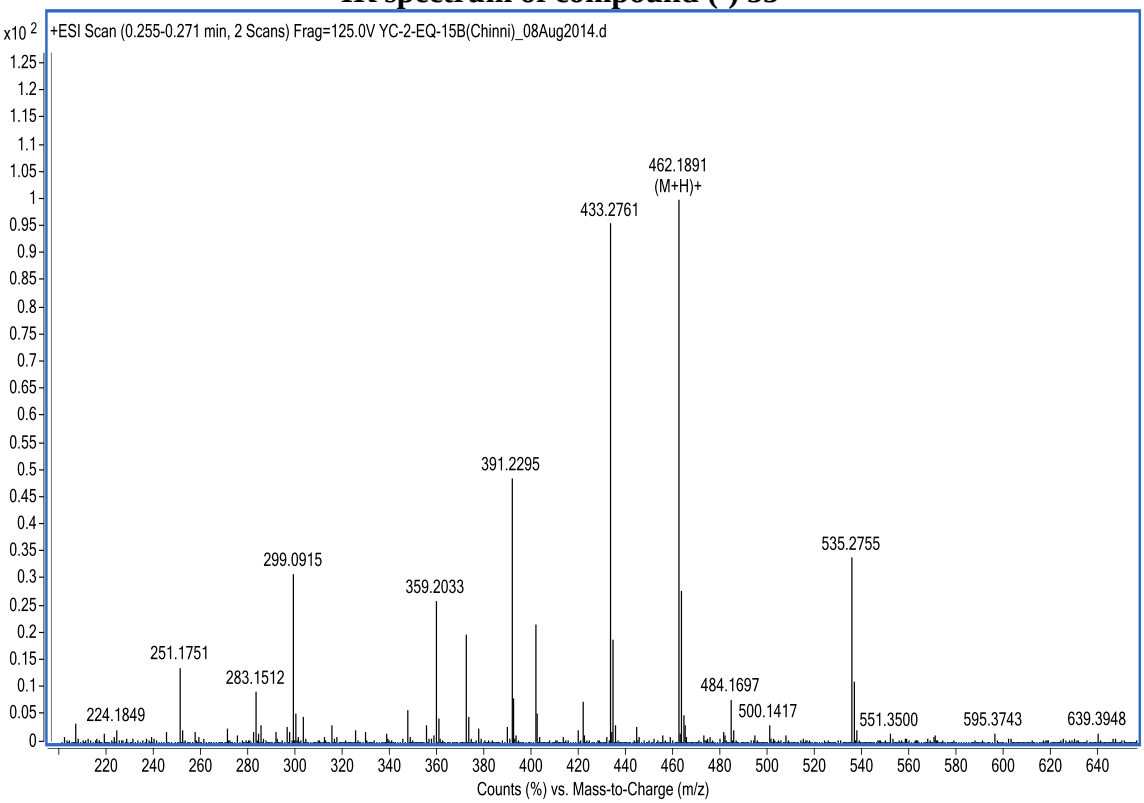

ESI-HRMS of compound (-) 55

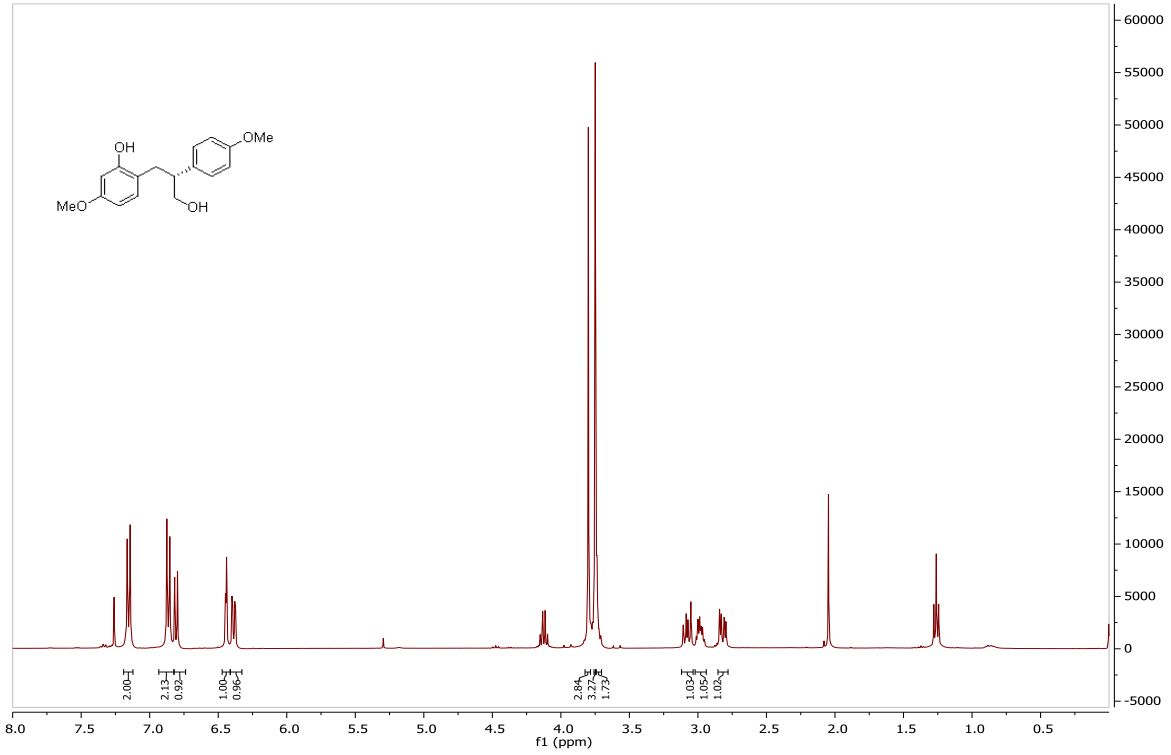

^{1}H NMR spectrum of compound (-) 42

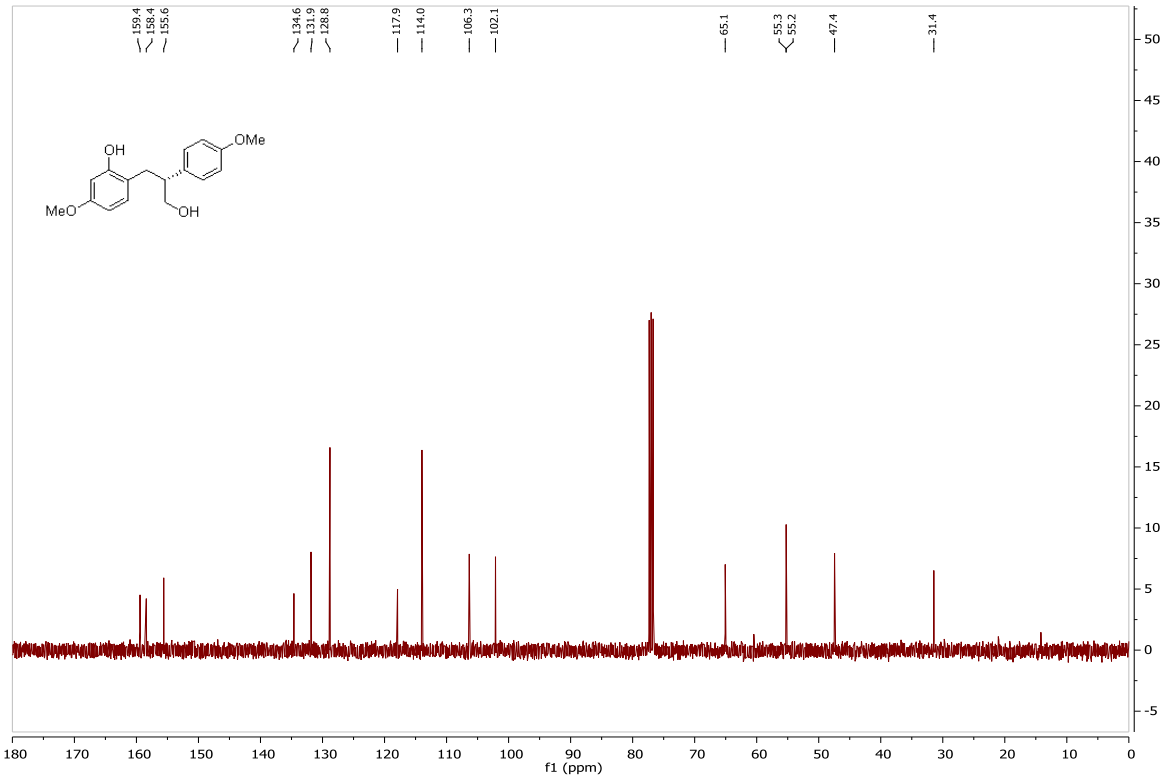

13 C NMR spectrum of compound (-) 42

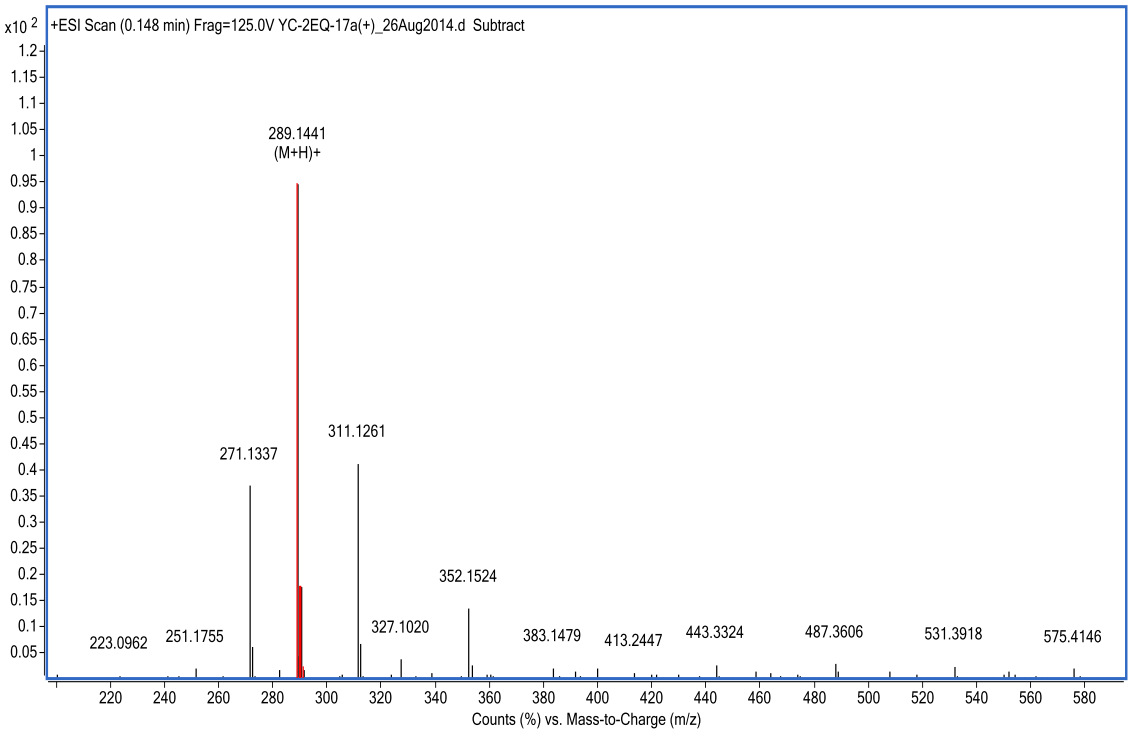

ESI-HRMS of compound (-) 42

SI Spectral Data 5. Spectral data of the compounds for synthesis of *S*-Sativan

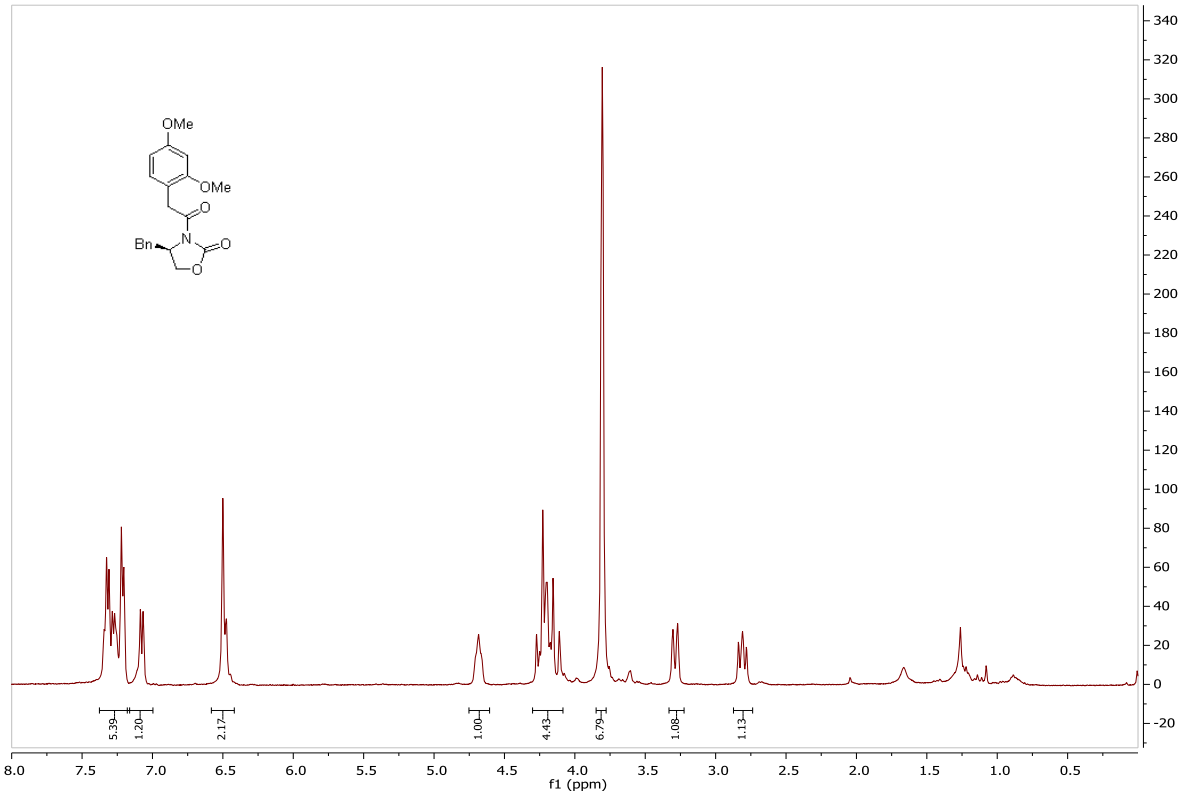

^{1}H NMR spectrum of compound (-) 48

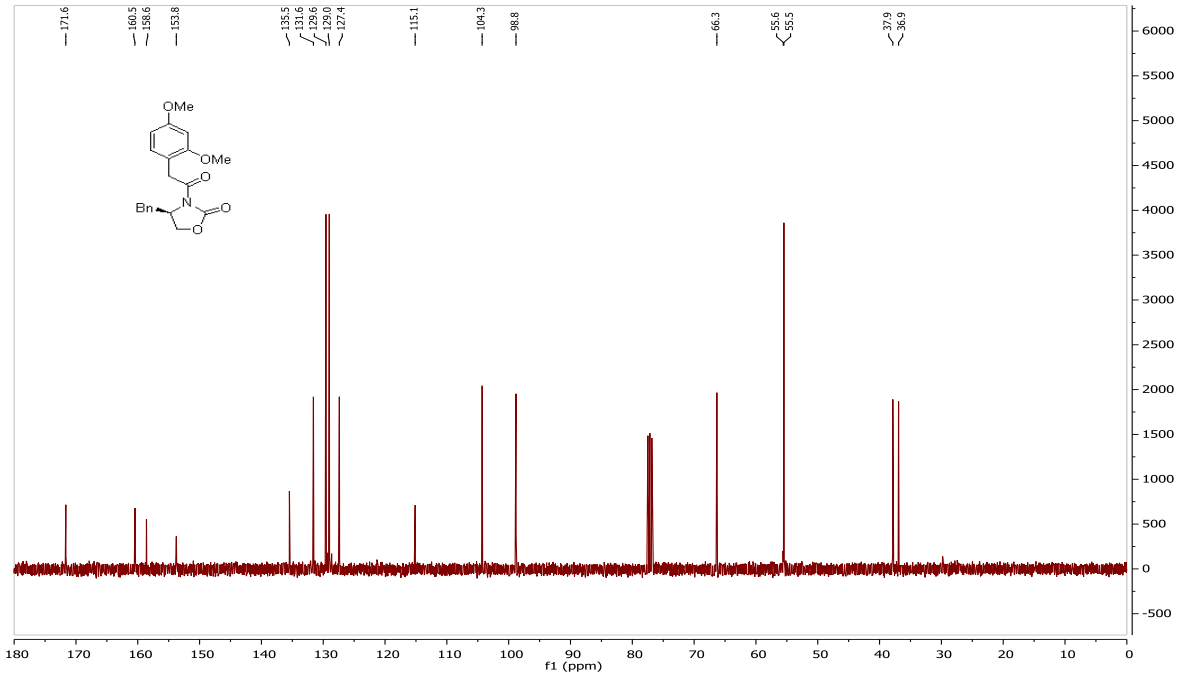

^{13}C NMR spectrum of compound (-) 48

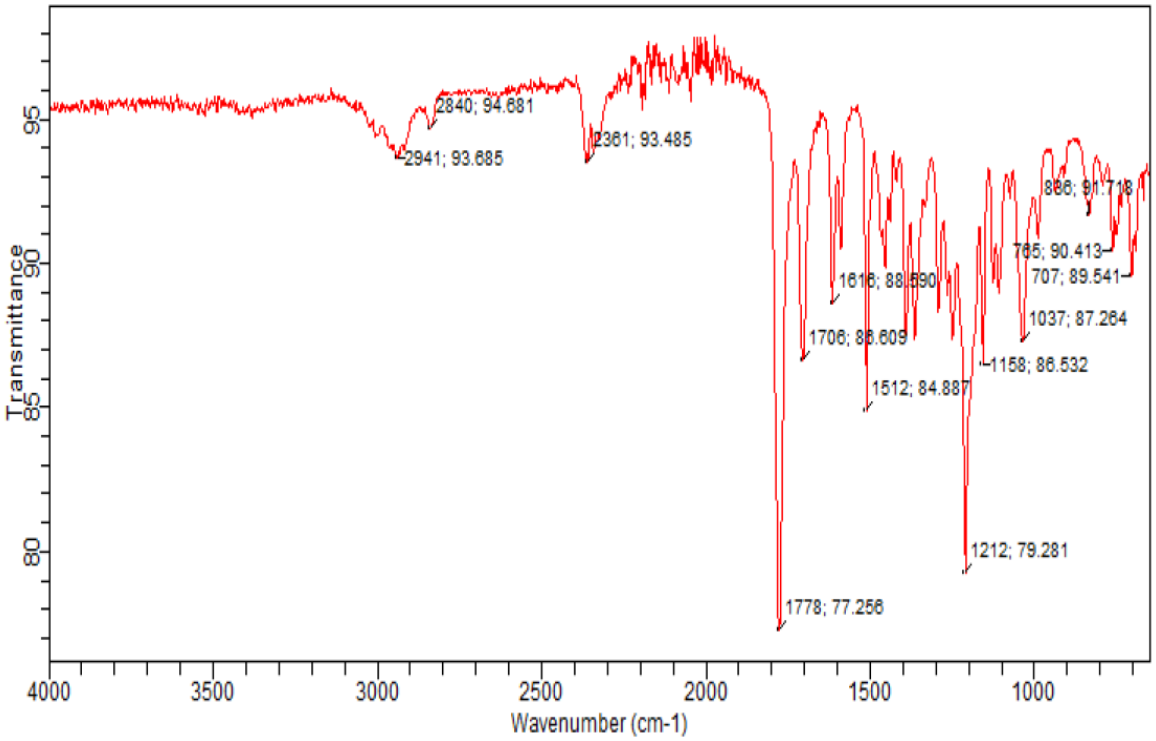

IR spectrum of compound (-) 48

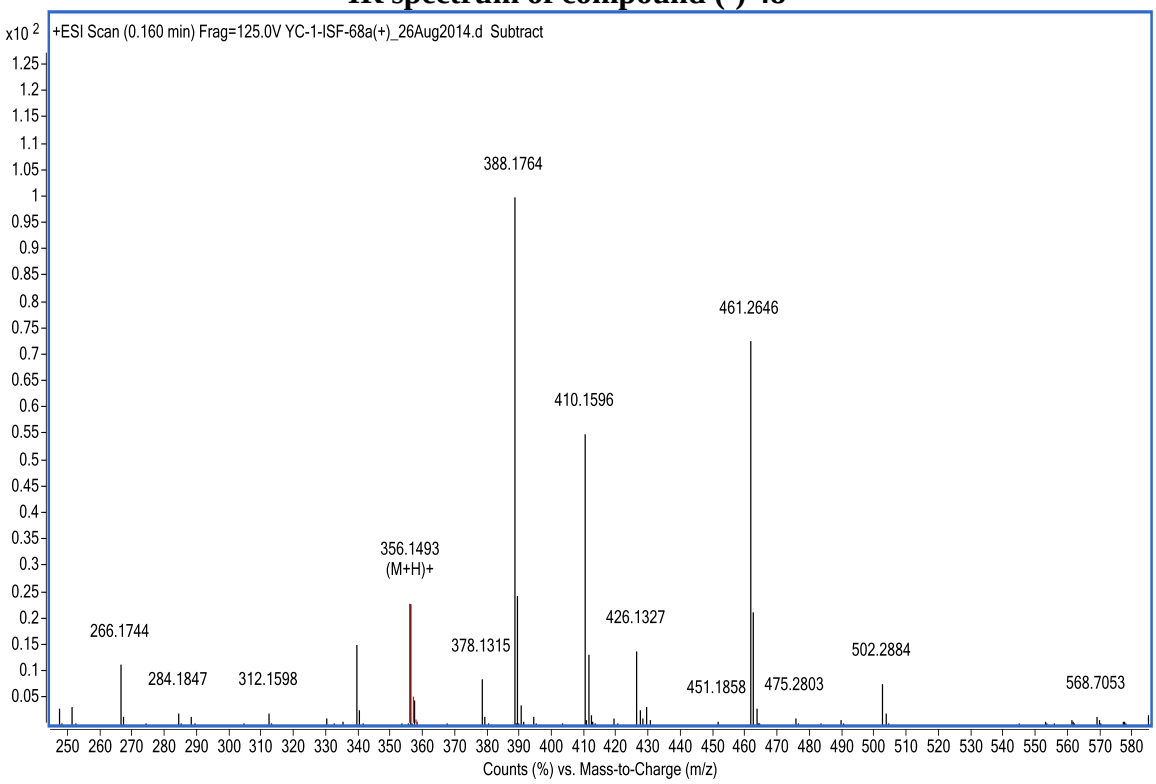

ESI-HRMS of compound (-) 48

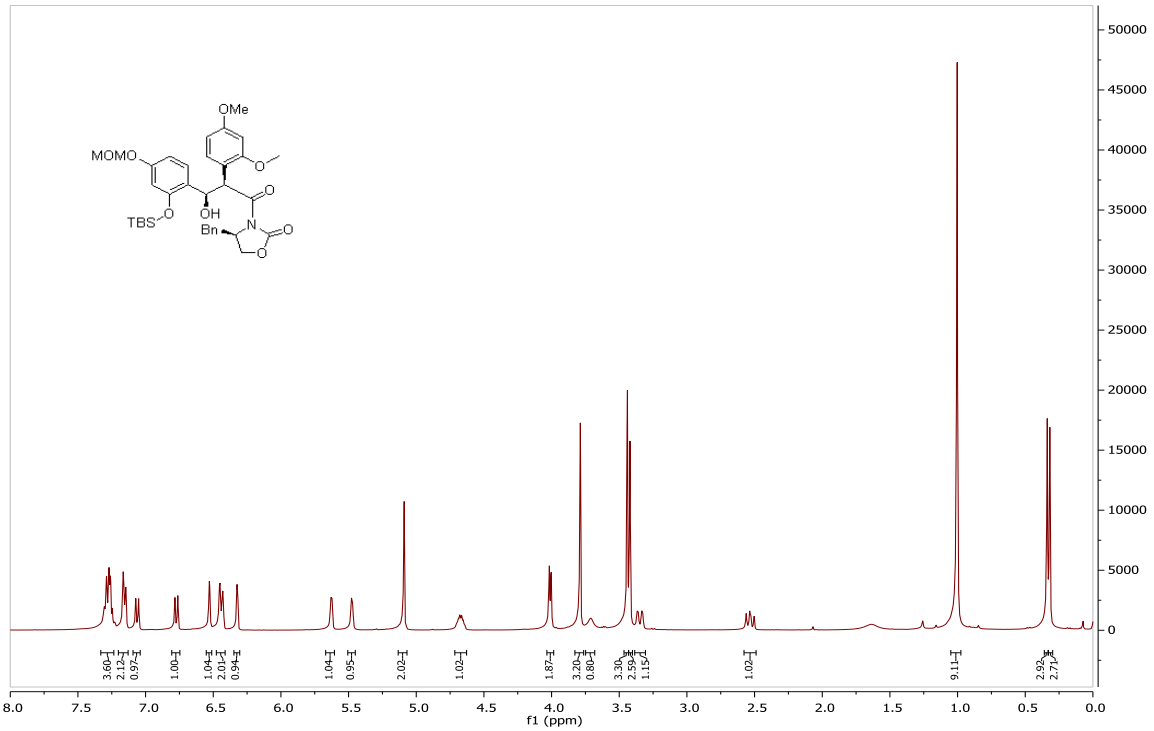

^{1}H NMR spectrum of compound (+) 45

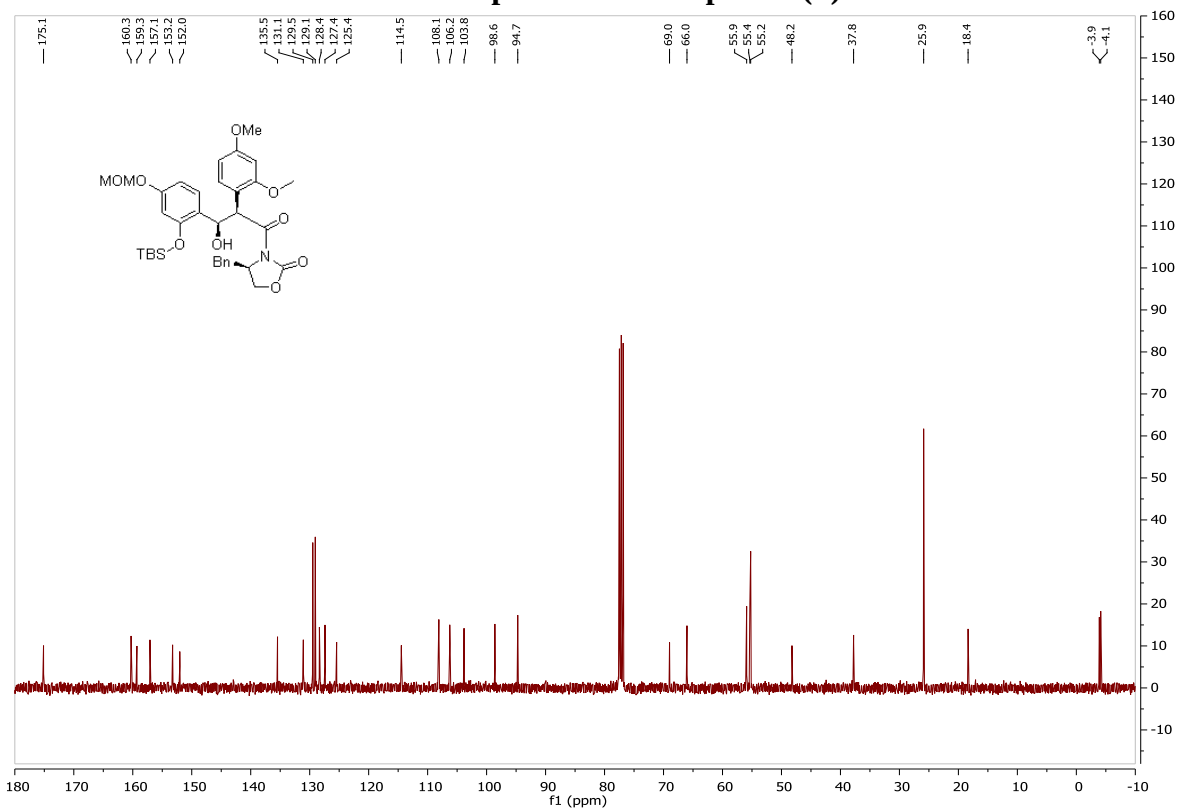

^{13}C NMR spectrum of compound (+) 45

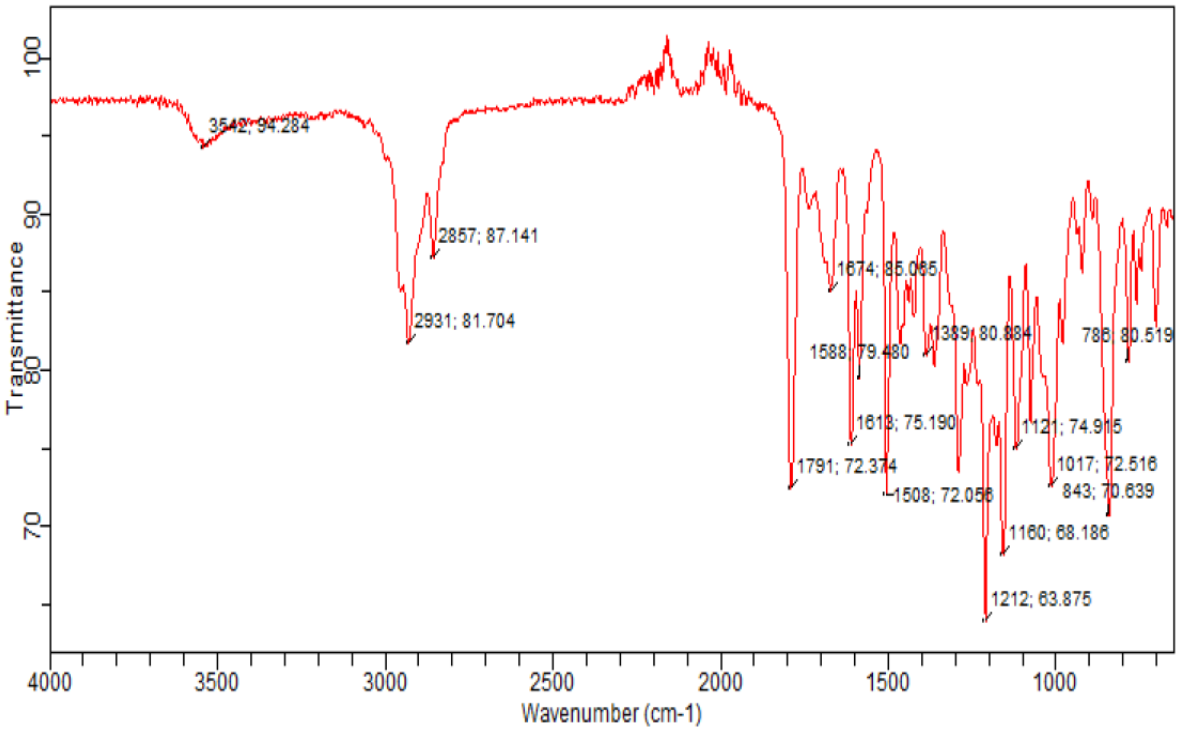

IR spectrum of compound (+) 45

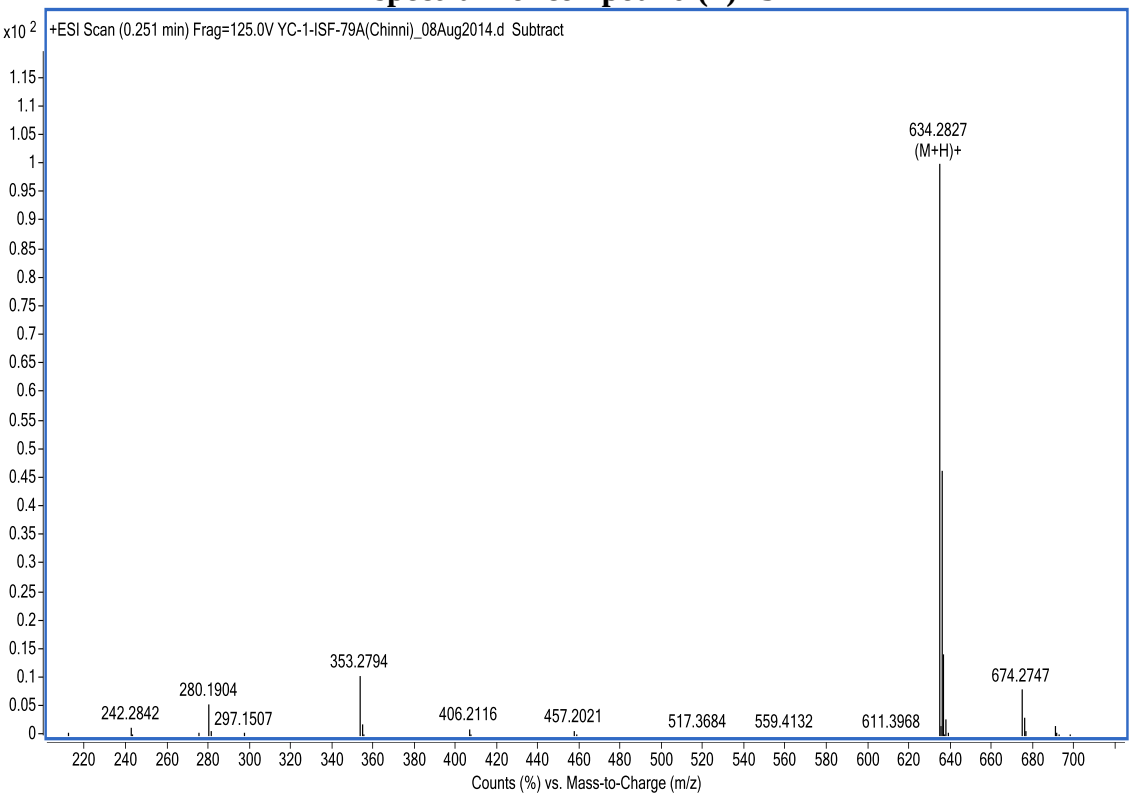

ESI-HRMS of compound (+) 45

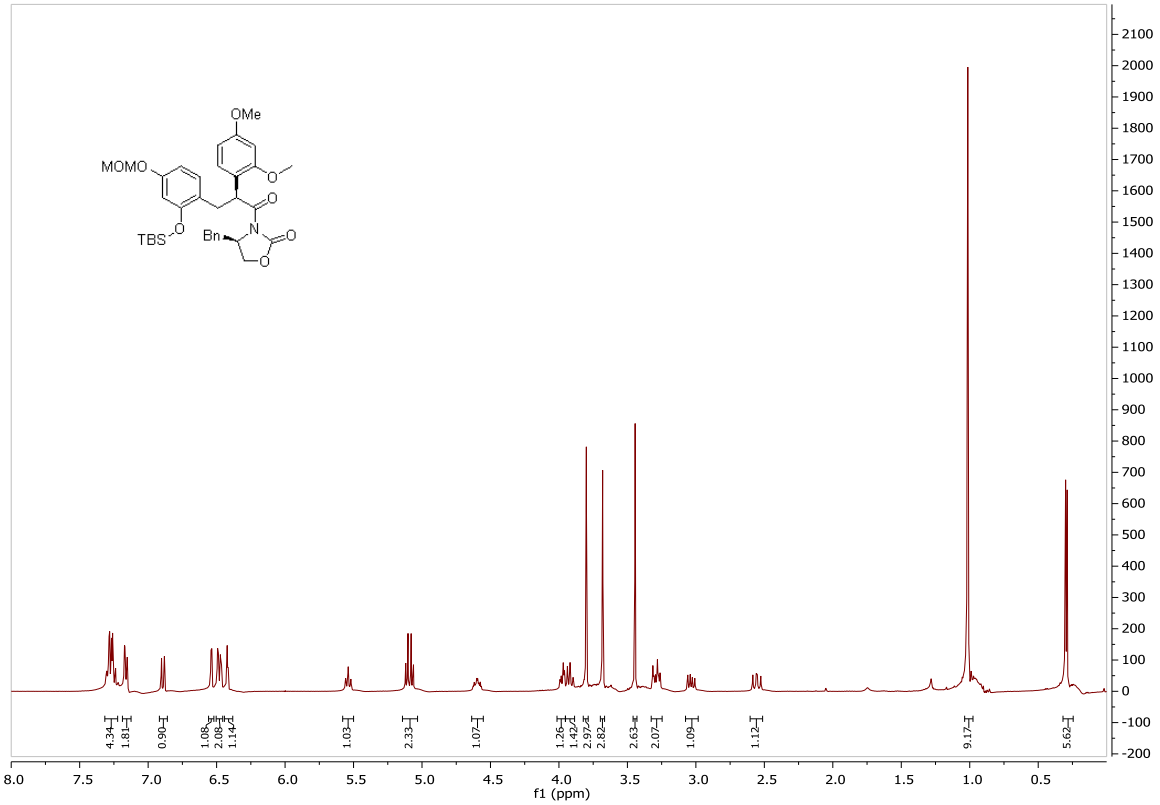

^{1}H NMR spectrum of compound (+) 56

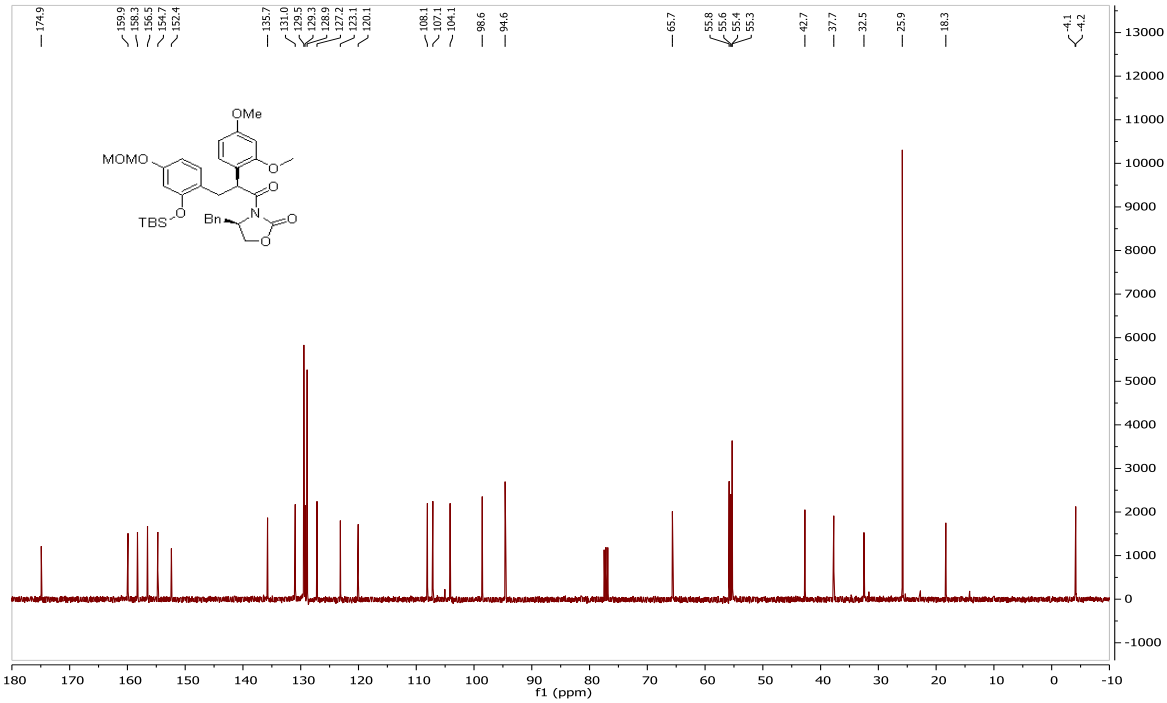

^{13}C NMR spectrum of compound (+) 56

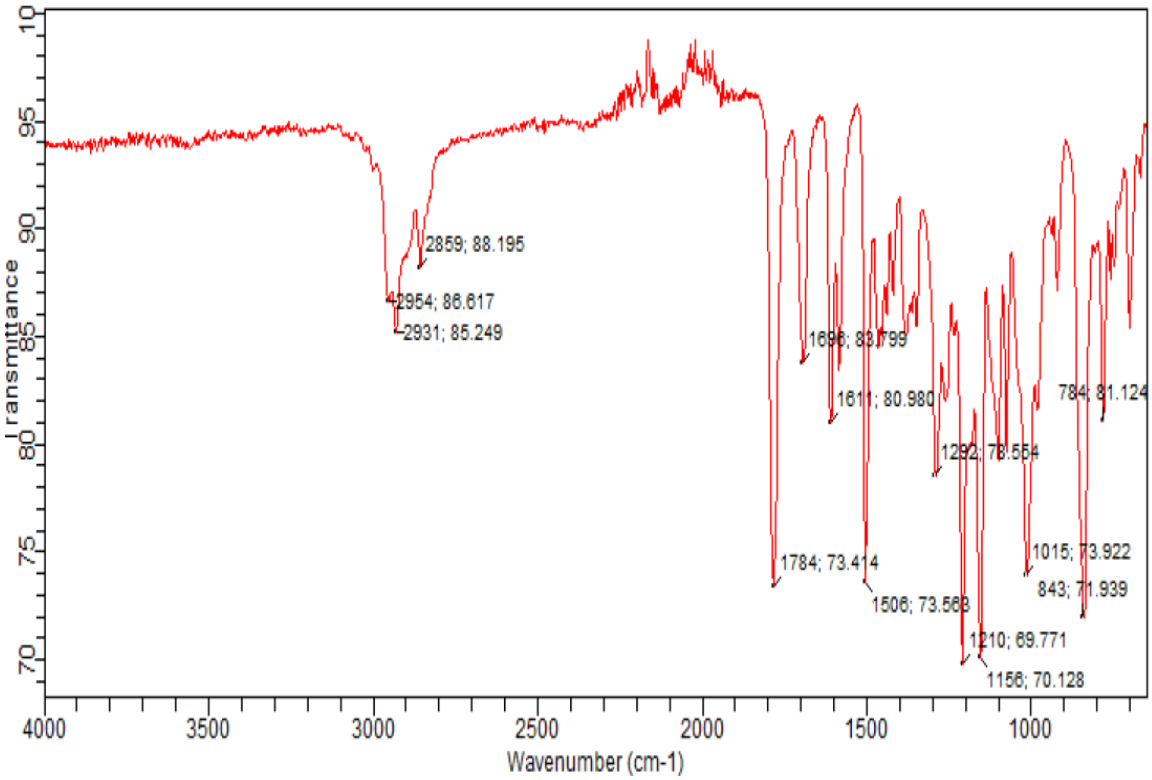

IR spectrum of compound (+) 56

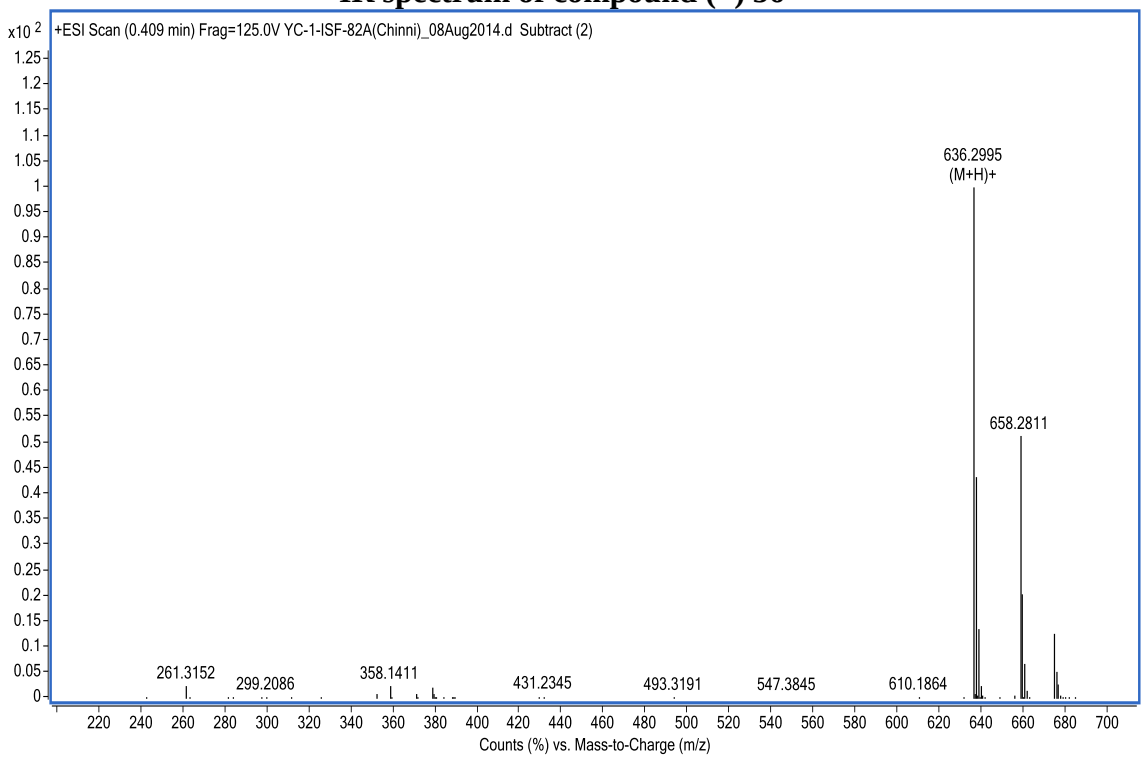

ESI-HRMS of compound (+) 56

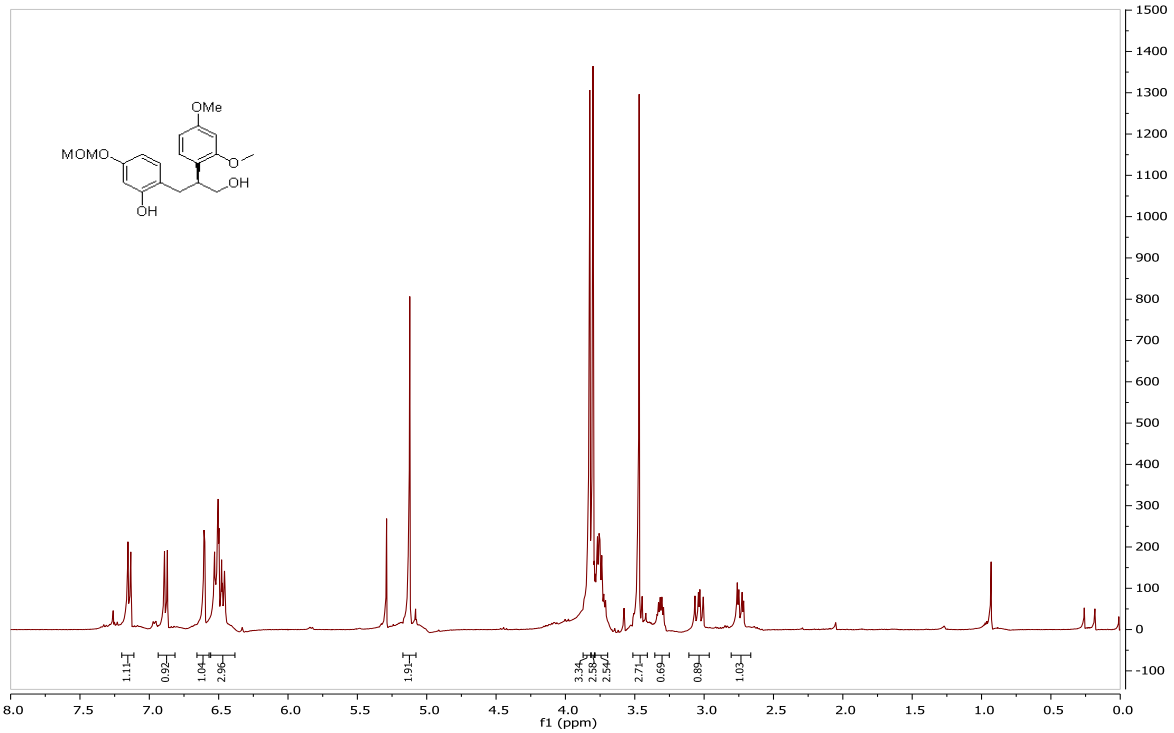

^{1}H NMR spectrum of compound (+) 43

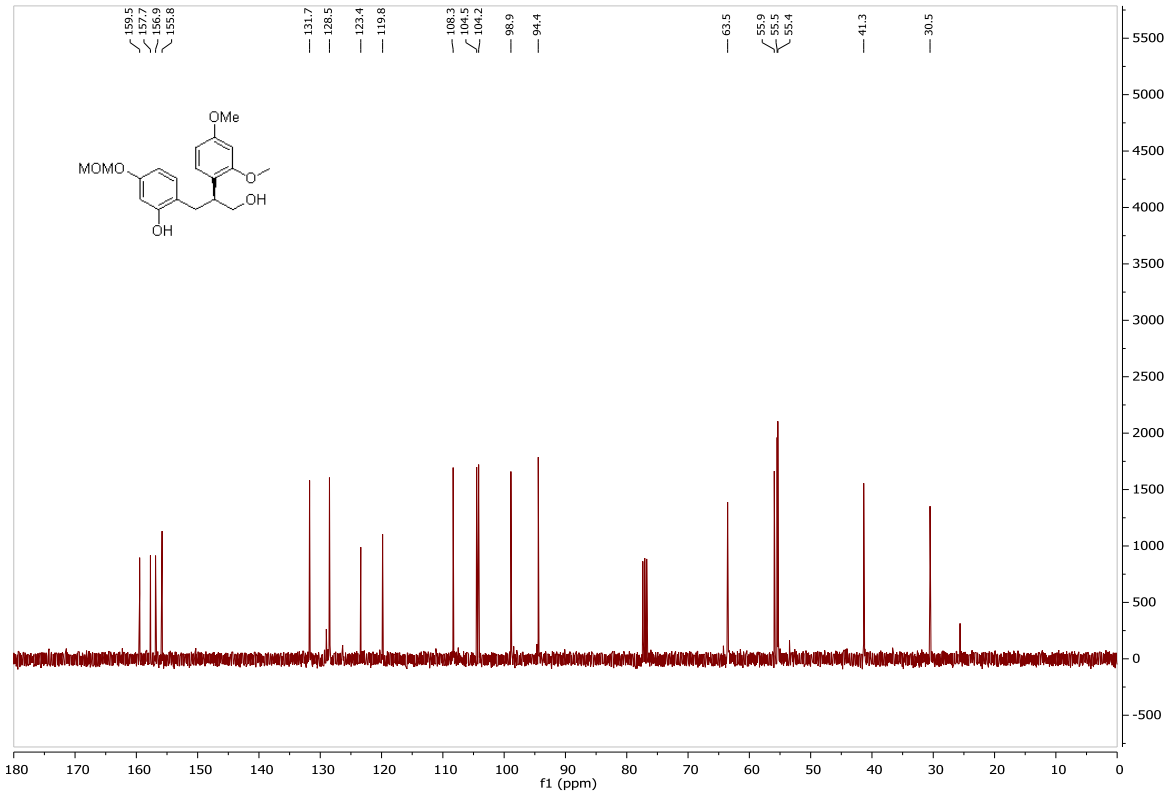

^{13}C NMR spectrum of compound (+) 43

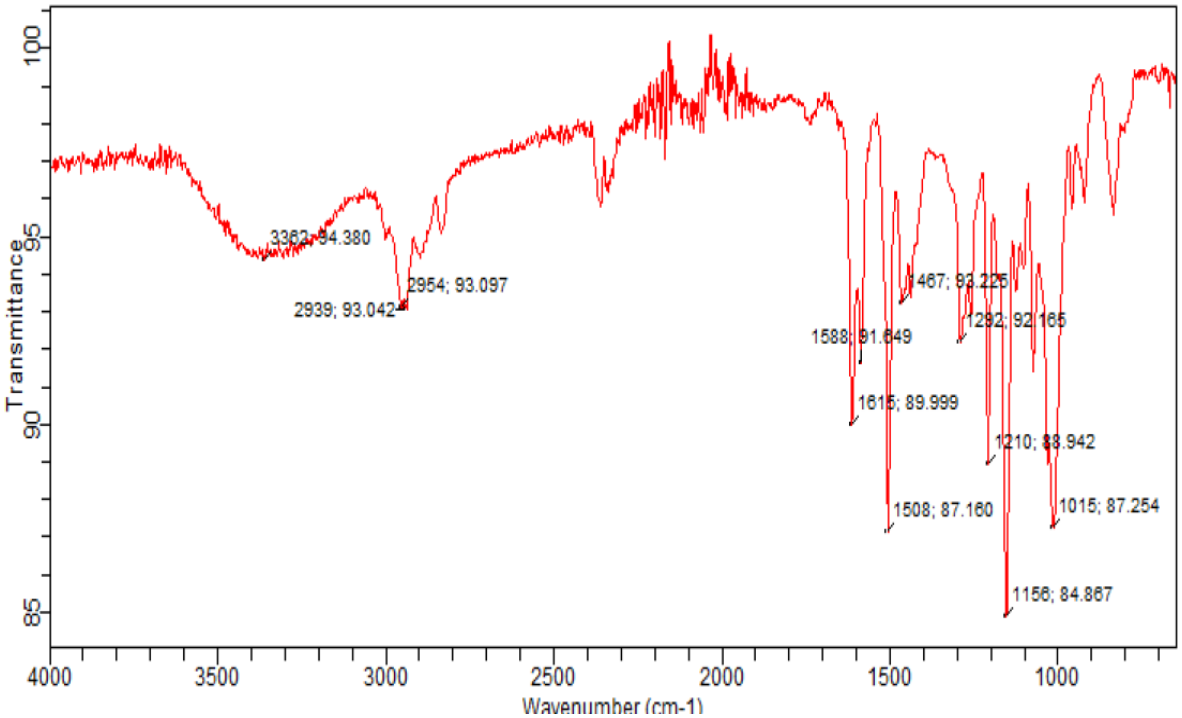

IR spectrum of compound (+) 43

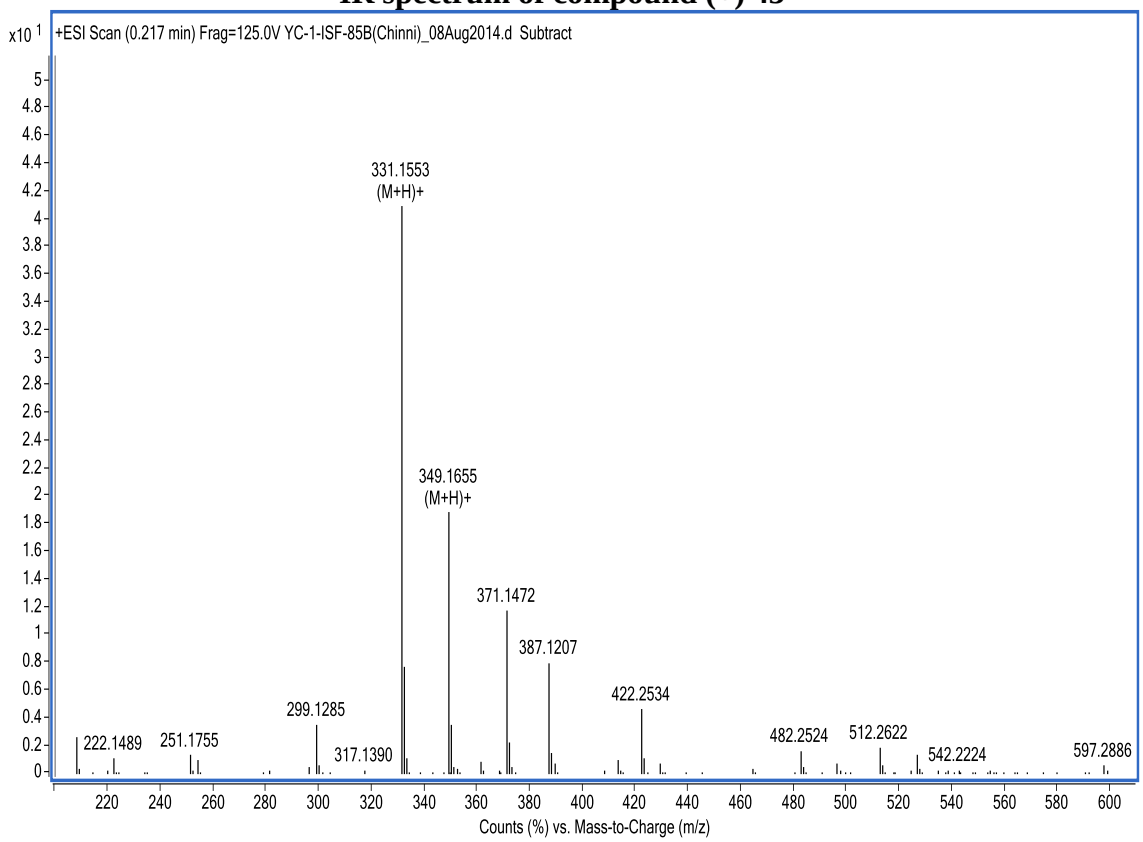

ESI-HRMS of compound (+) 43

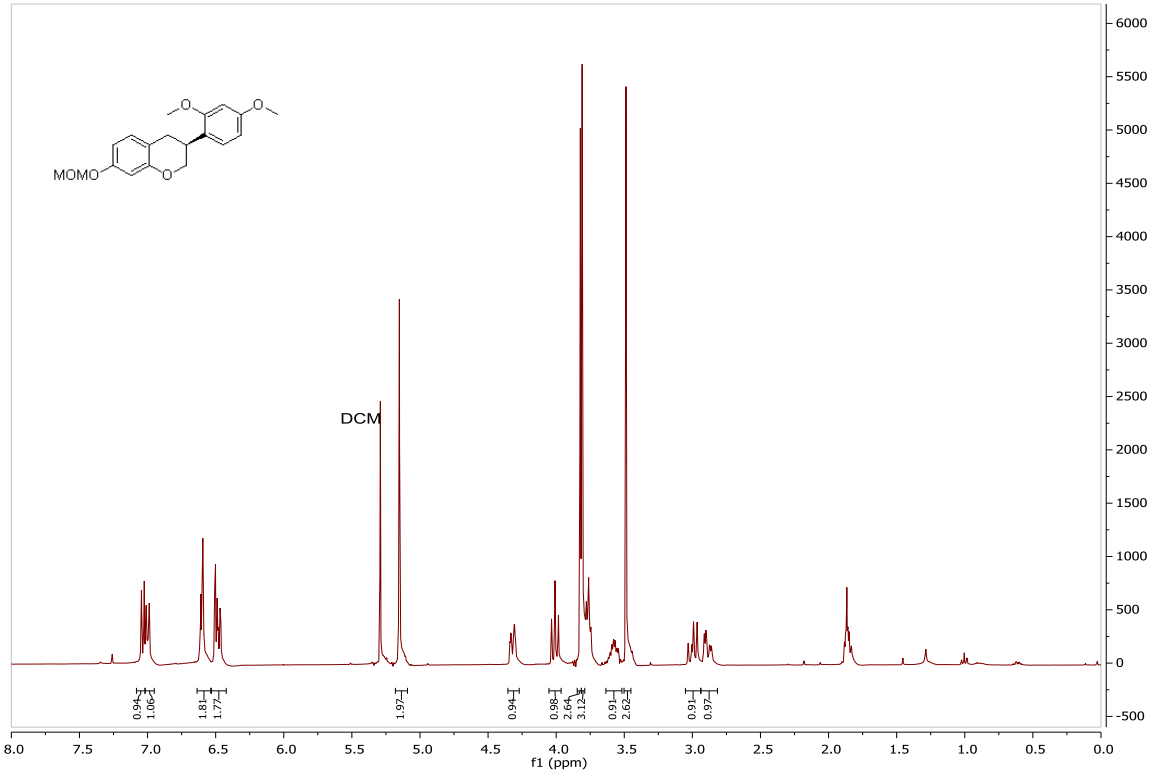

^{1}H NMR spectrum of compound (+) 57

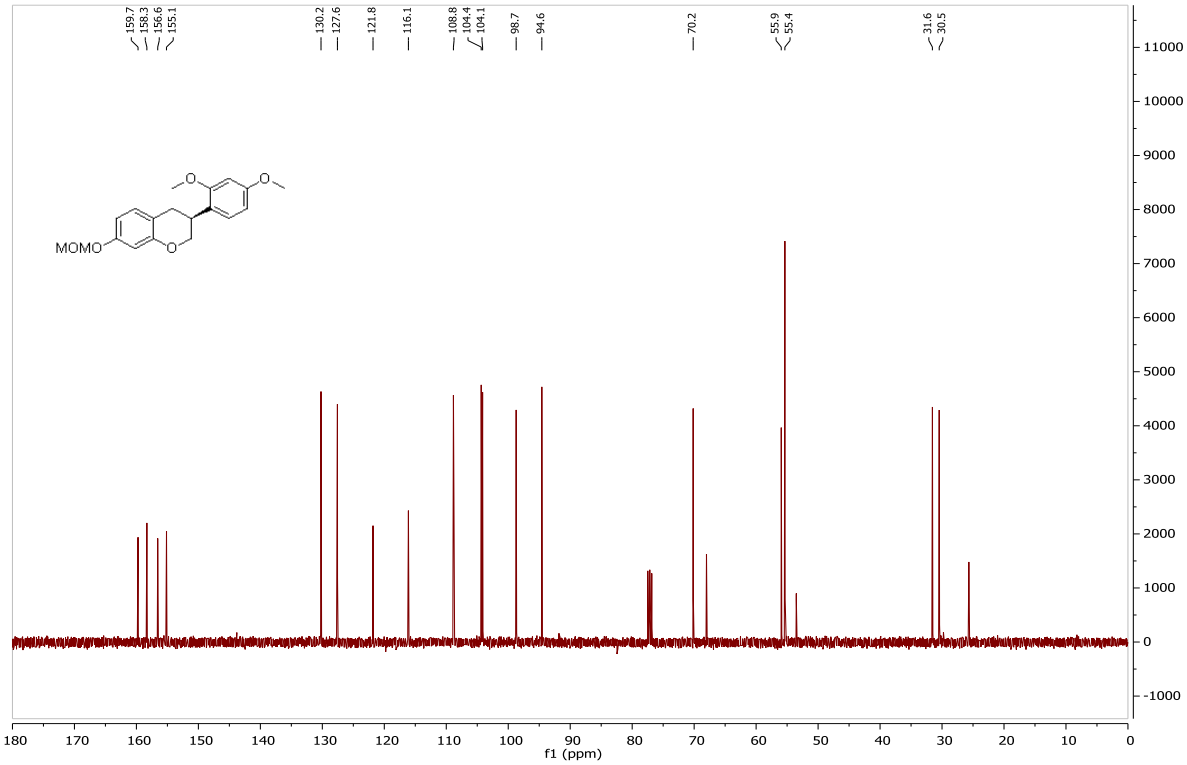

13C NMR spectrum of compound (+) 57

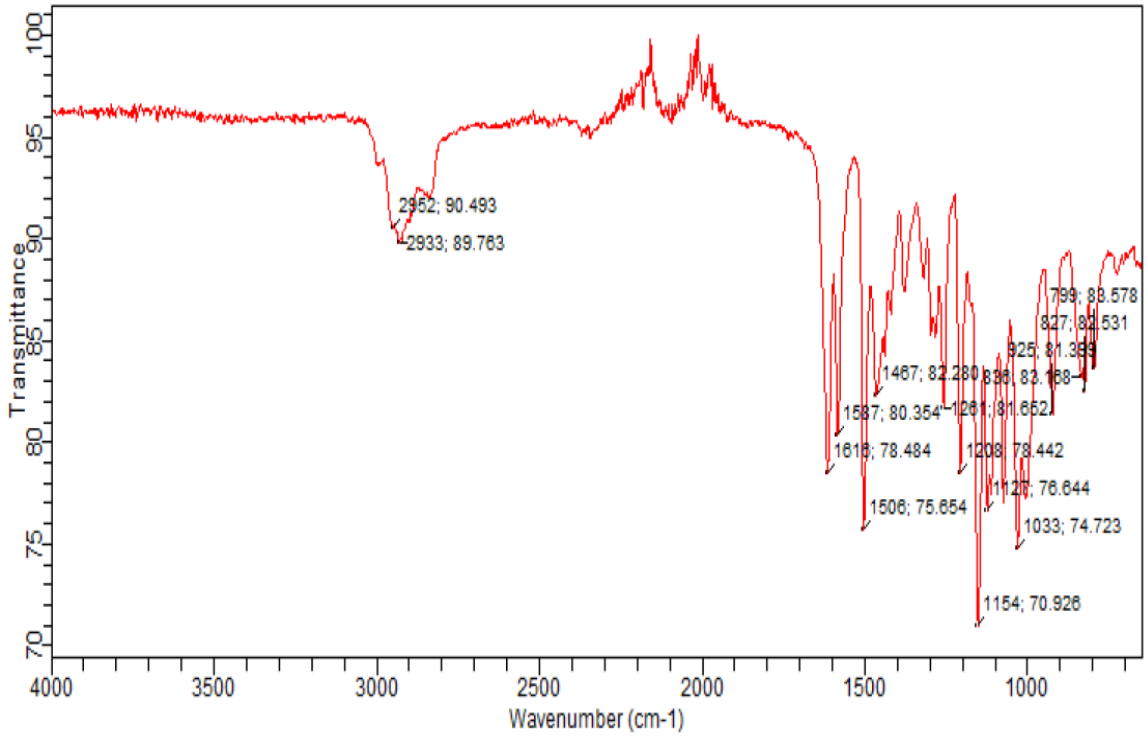

IR spectrum of compound (+) 57

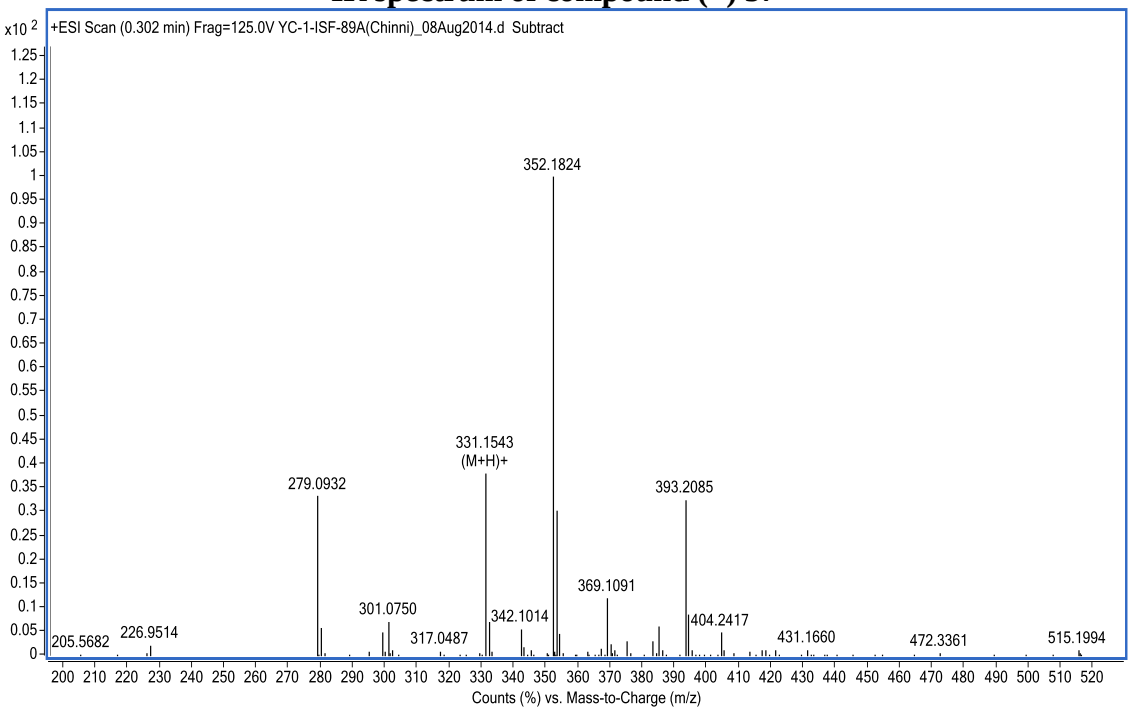

ESI-HRMS of compound (+) 57

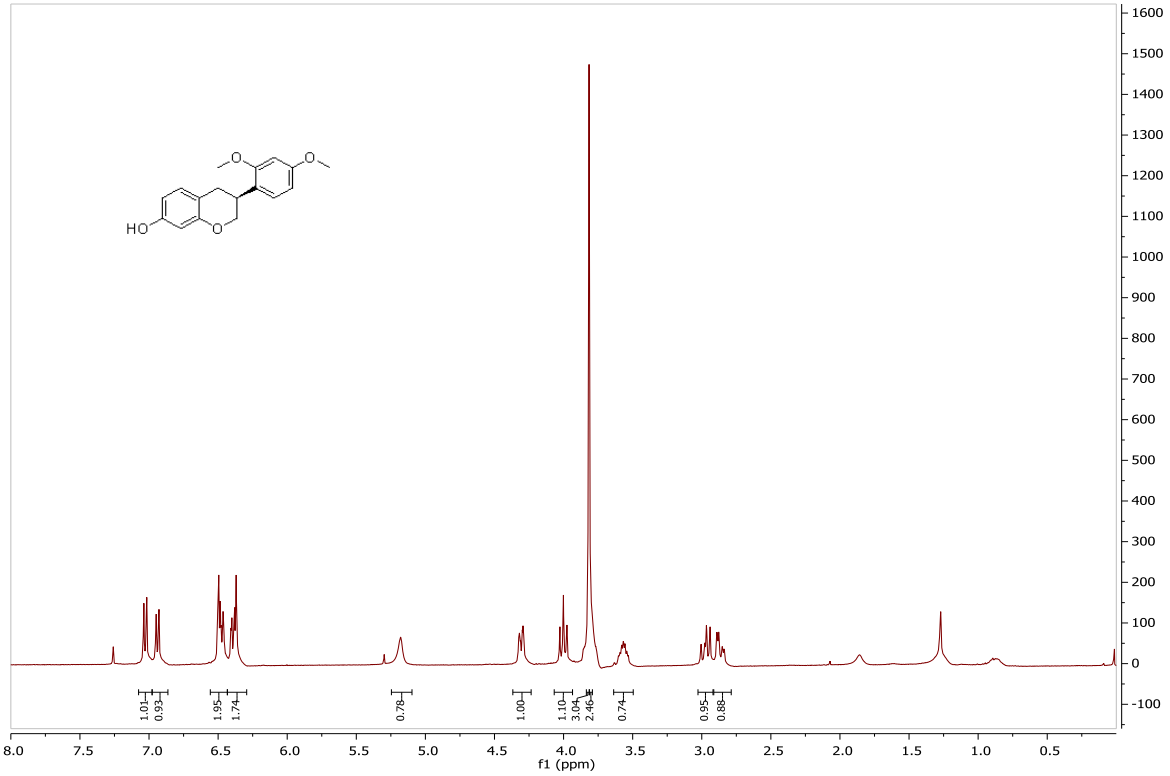

^{1}H NMR spectrum of compound (+) 8

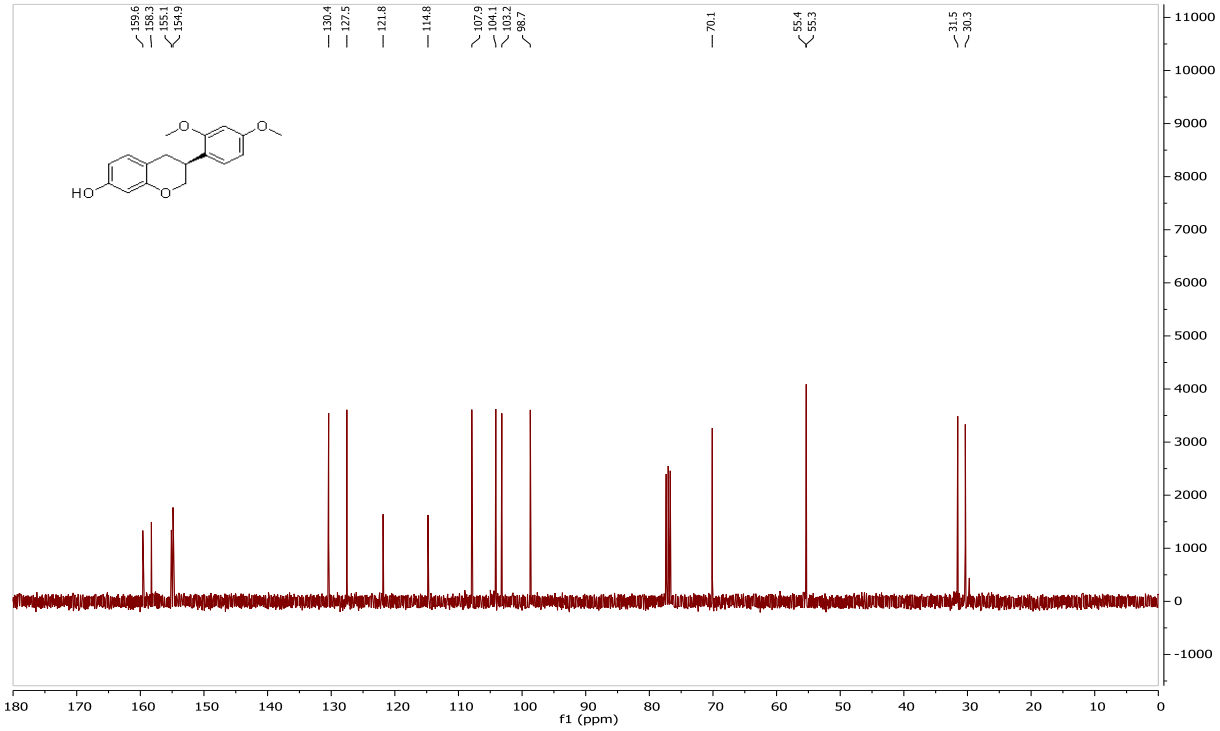

^{13}C NMR spectrum of compound (+) 8

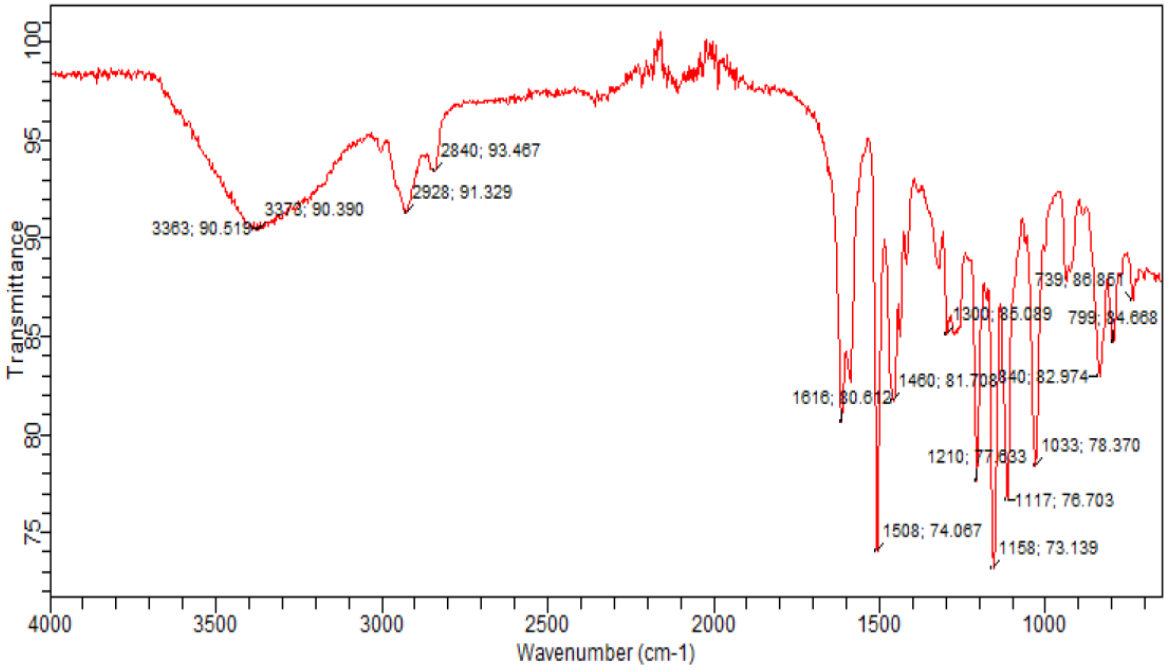

IR spectrum of compound (+) 8

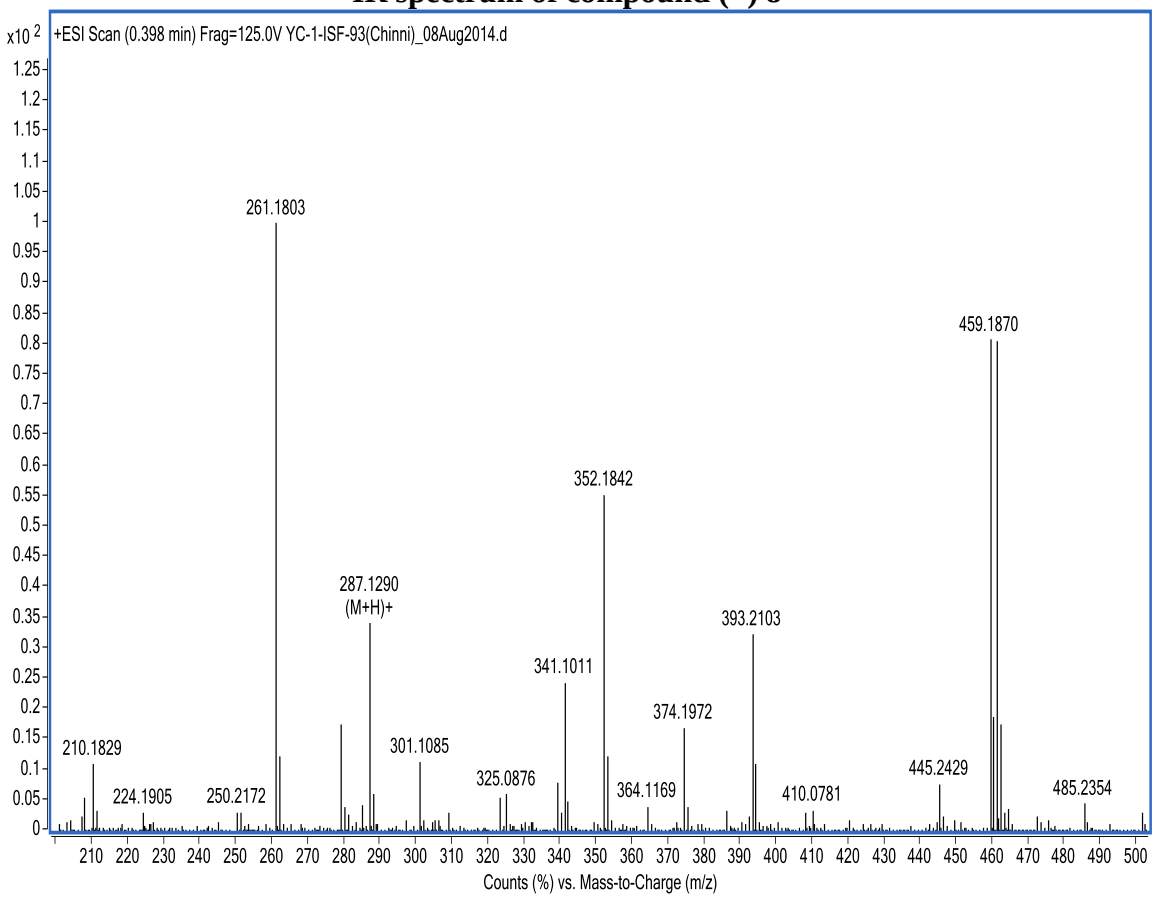

ESI-HRMS of compound (+) 8

SI Spectral Data 6. Spectral data of the compounds for synthesis of *R*-Sativan **8**.

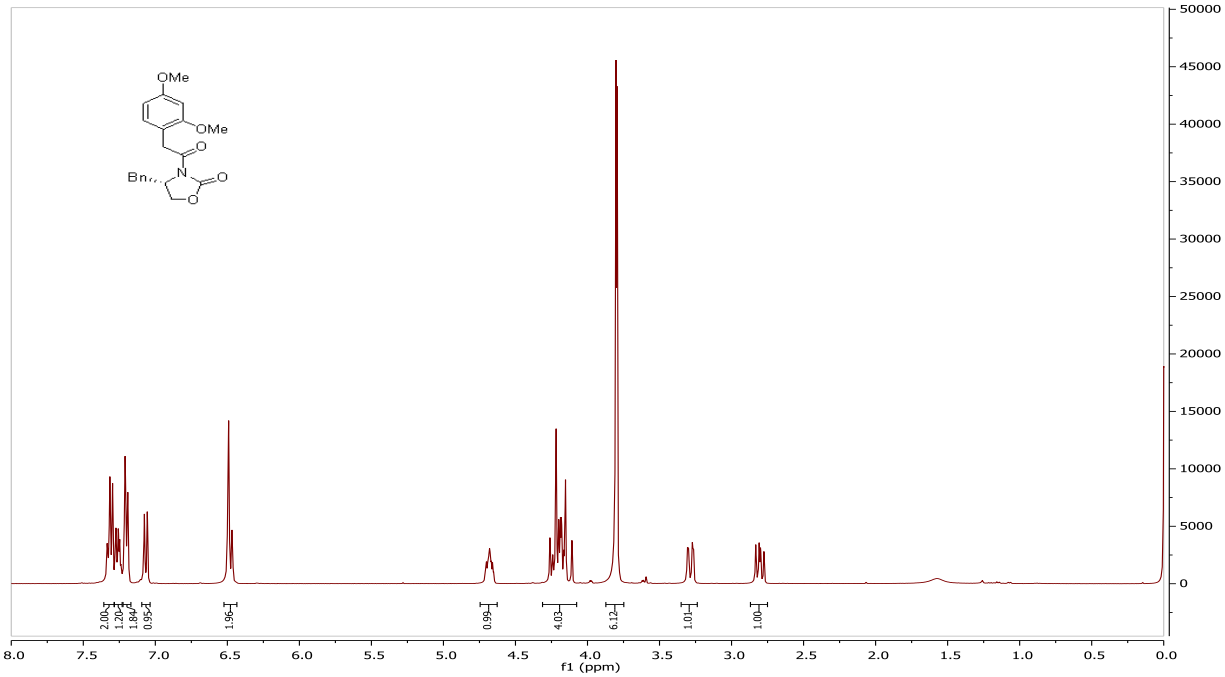

^{1}H NMR spectrum of compound (+) 48

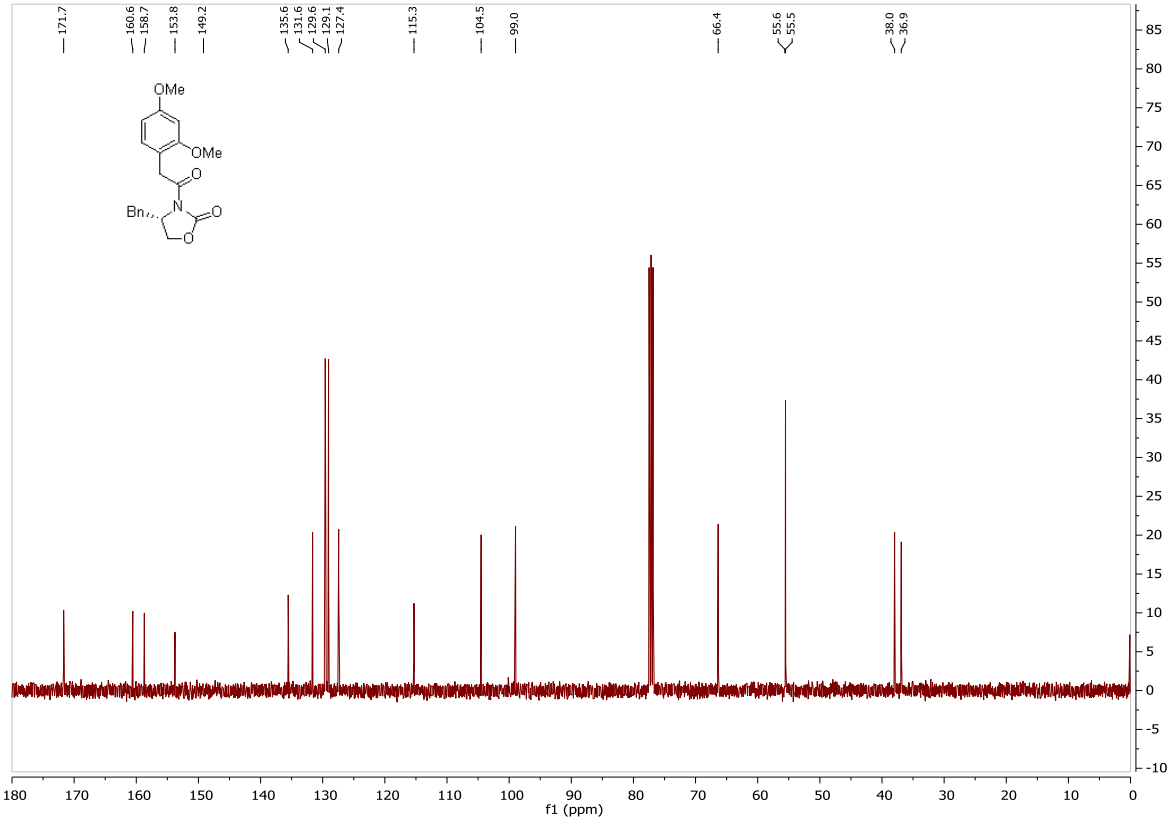

^{13}C NMR spectrum of compound (+) 48

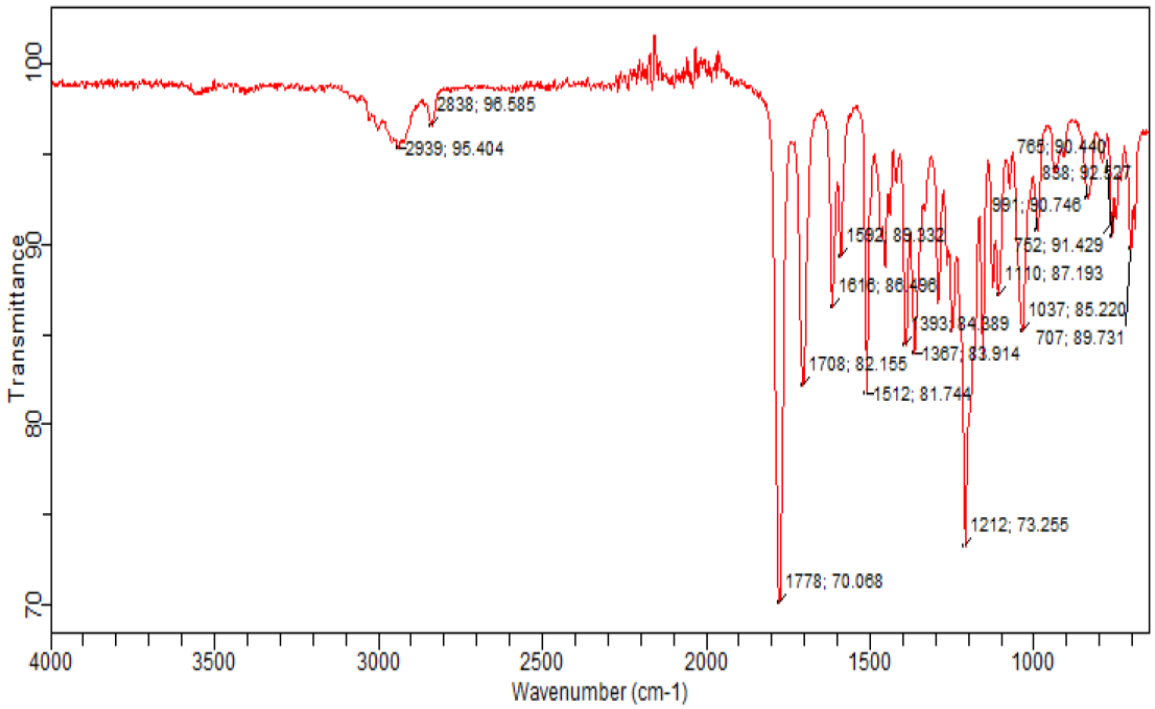

IR spectrum of compound (+) 48

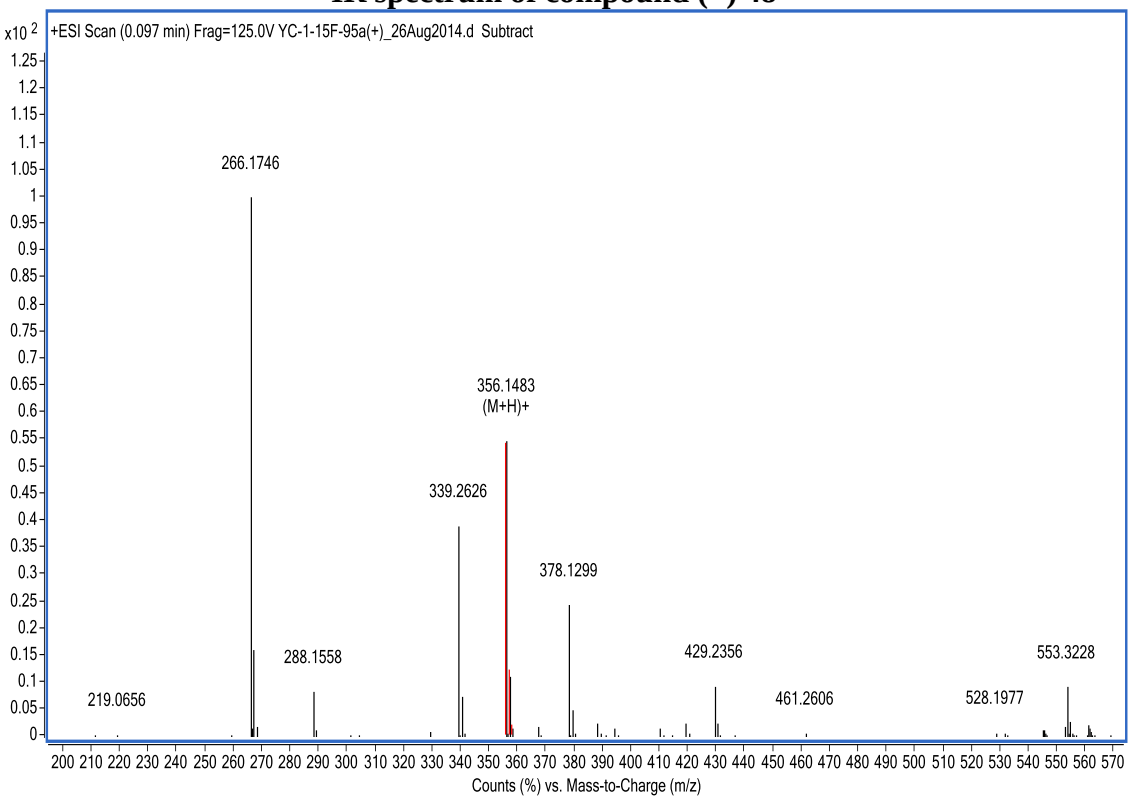

ESI-HRMS of compound (+) 48

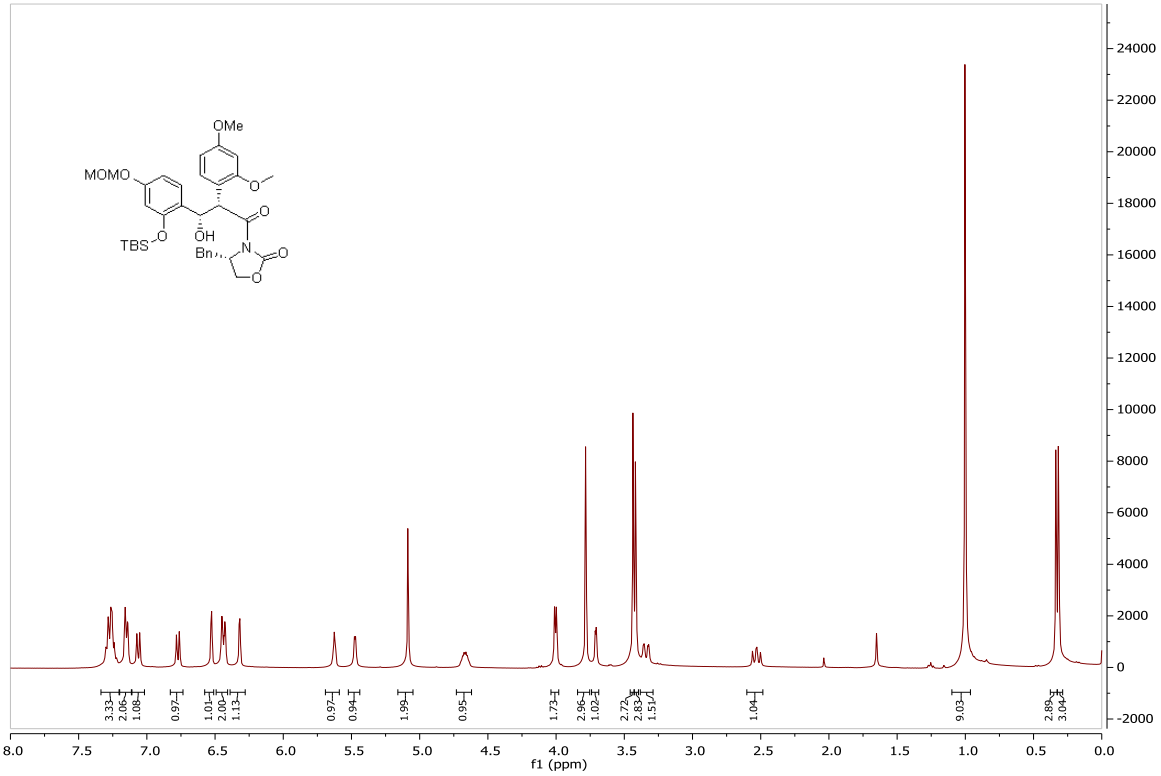

^{1}H NMR spectrum of compound (-) 45

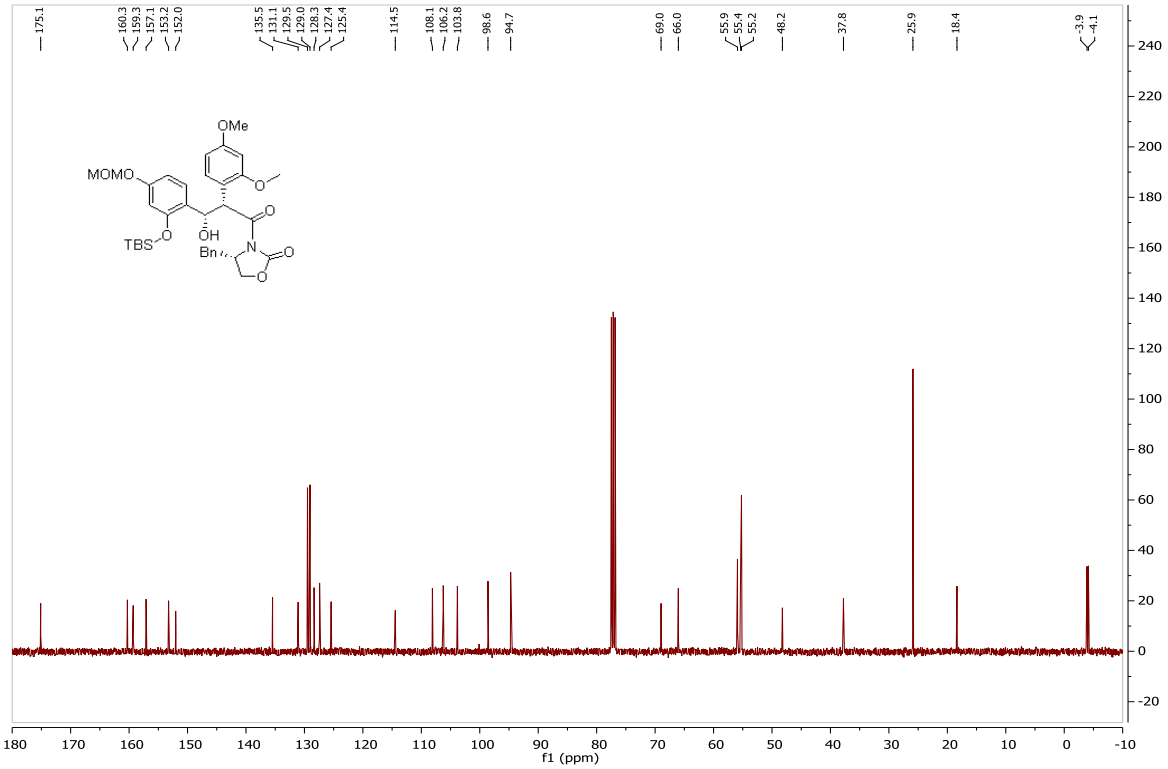

^{13}C NMR spectrum of compound (-) 45

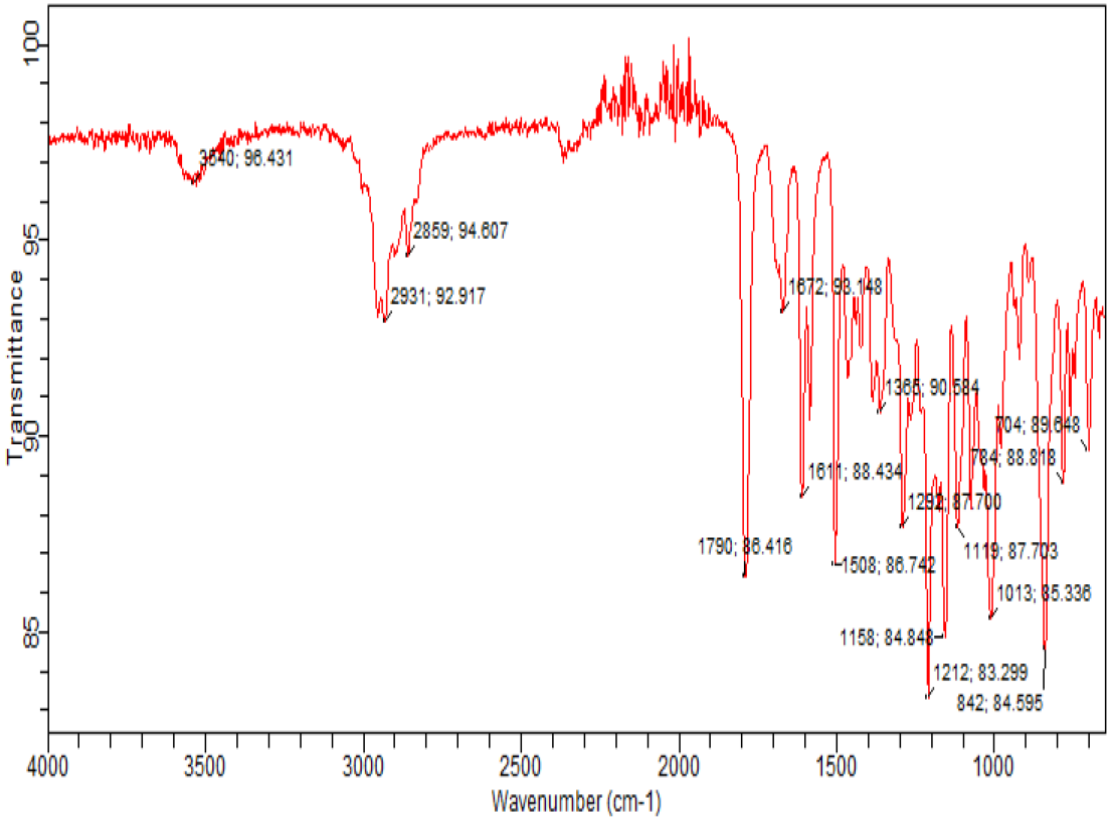

IR spectrum of compound (-) 45

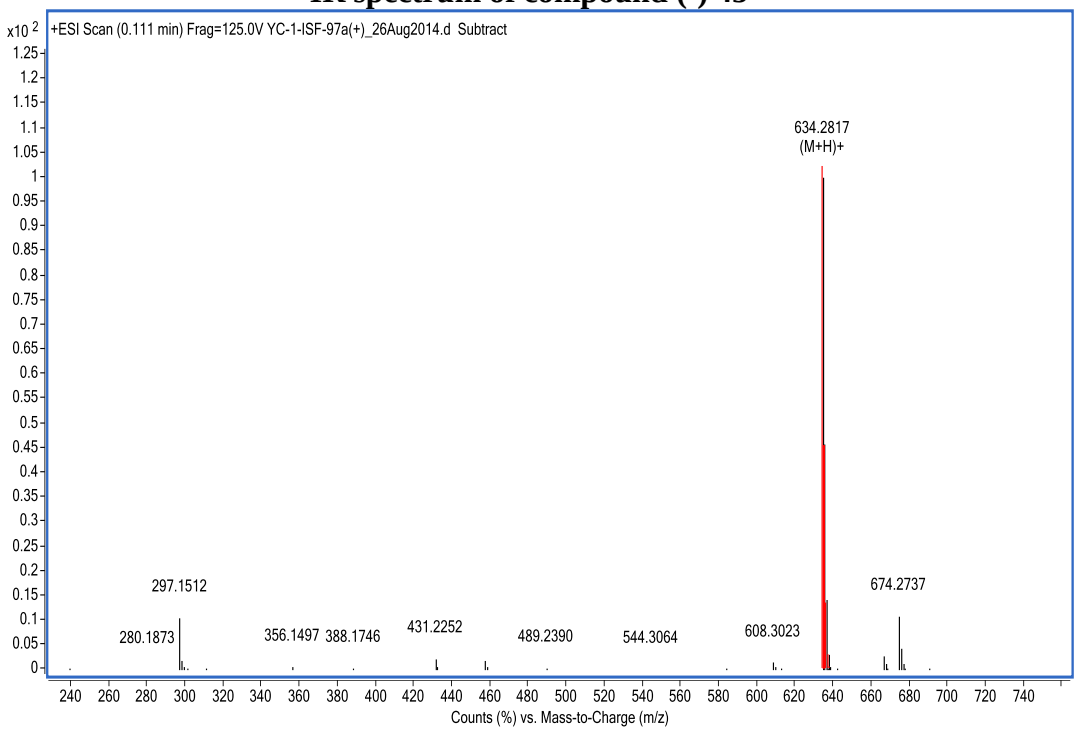

ESI-HRMS of compound (-) 45

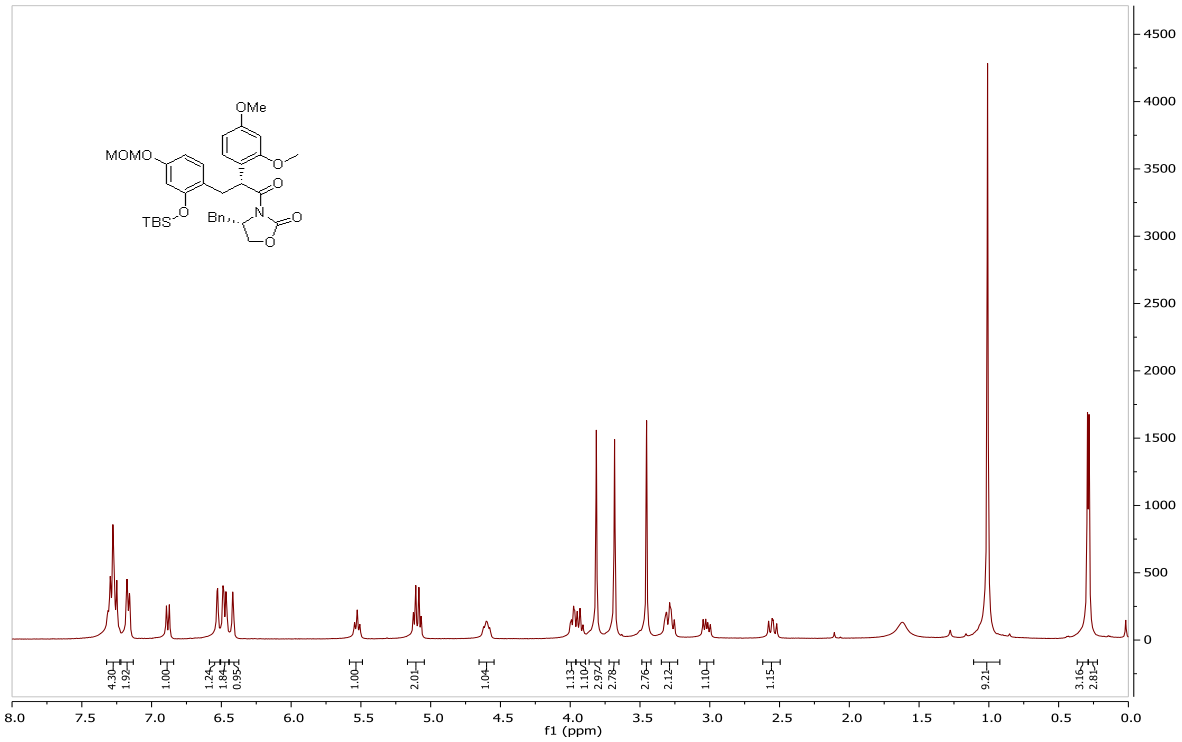

^{1}H NMR spectrum of compound (-) 56

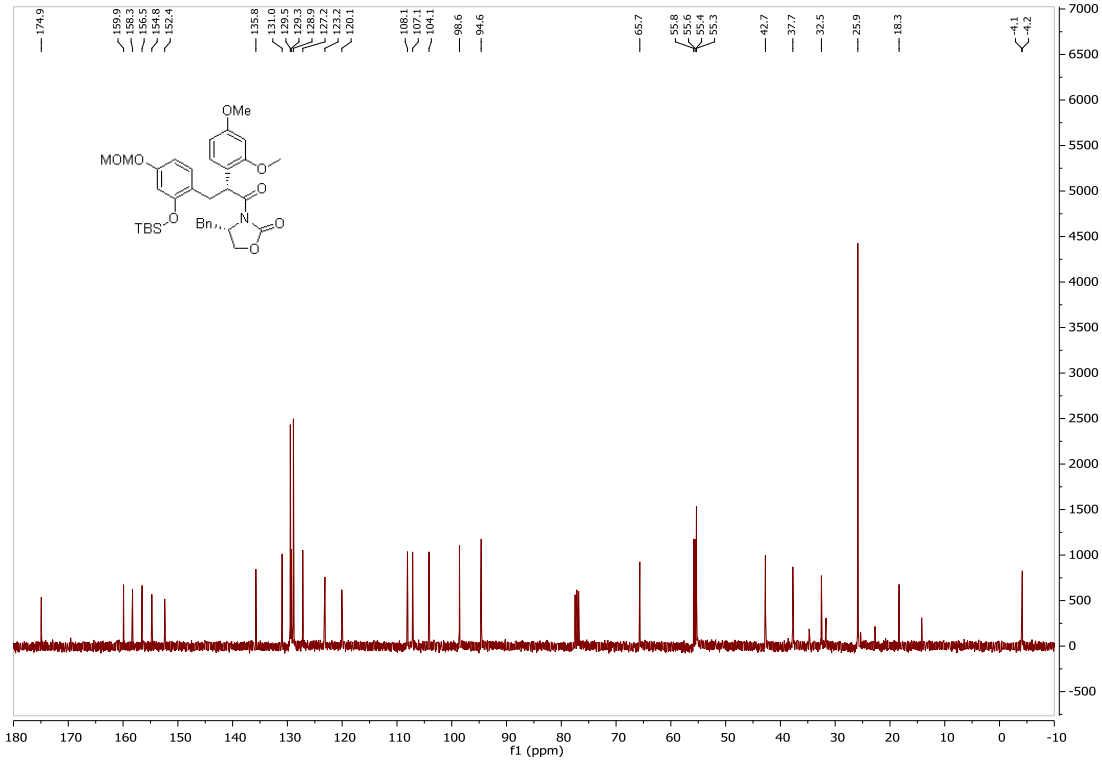

^{13}C NMR spectrum of compound (-) 56

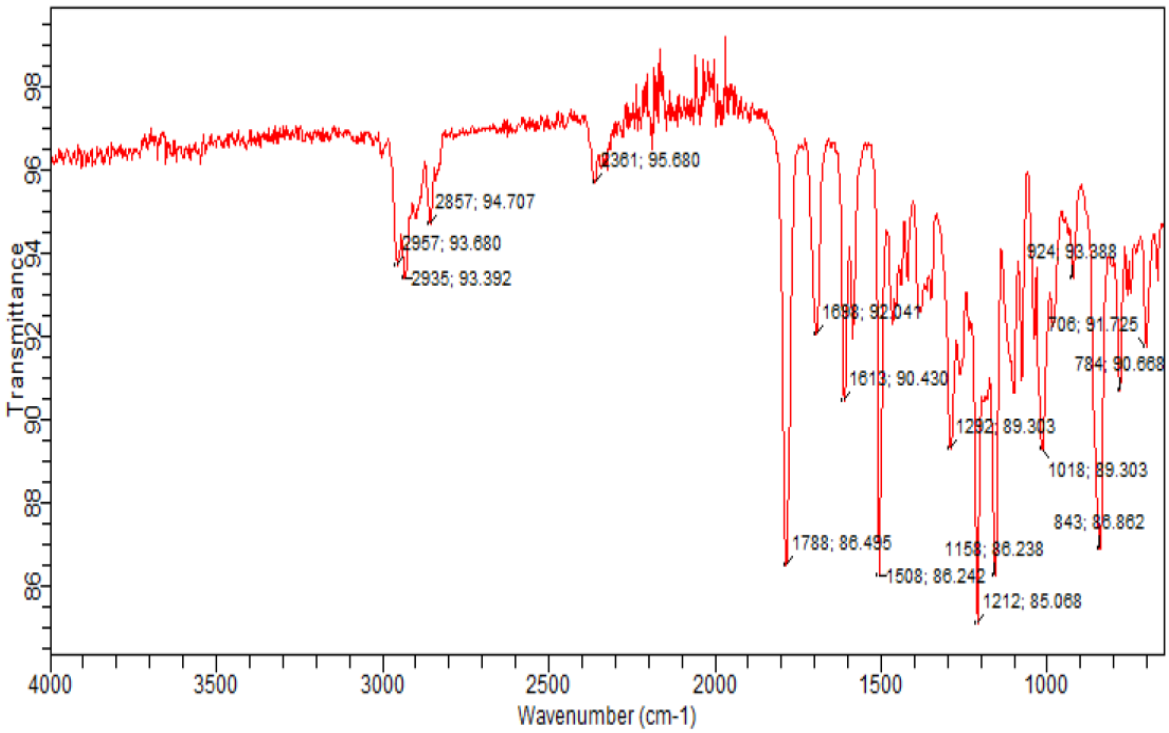

IR spectrum of compound (-) 56

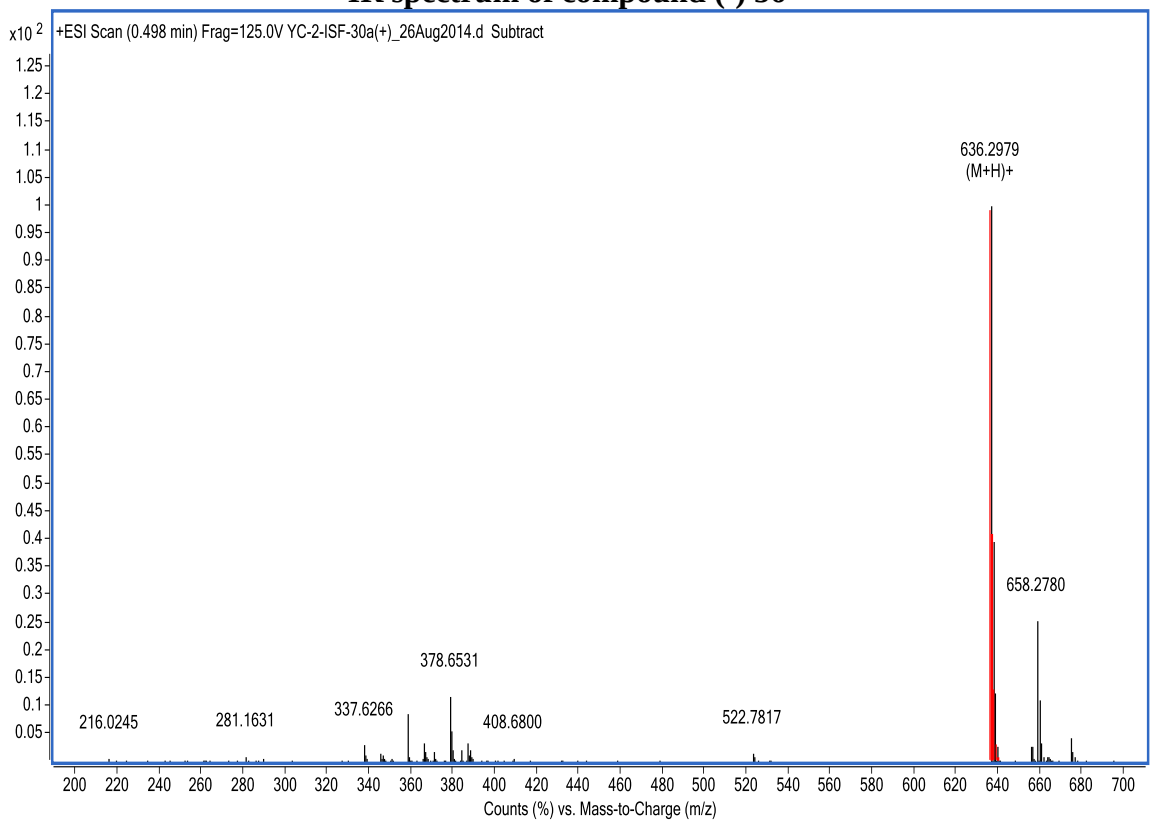

ESI-HRMS of compound (-) 56

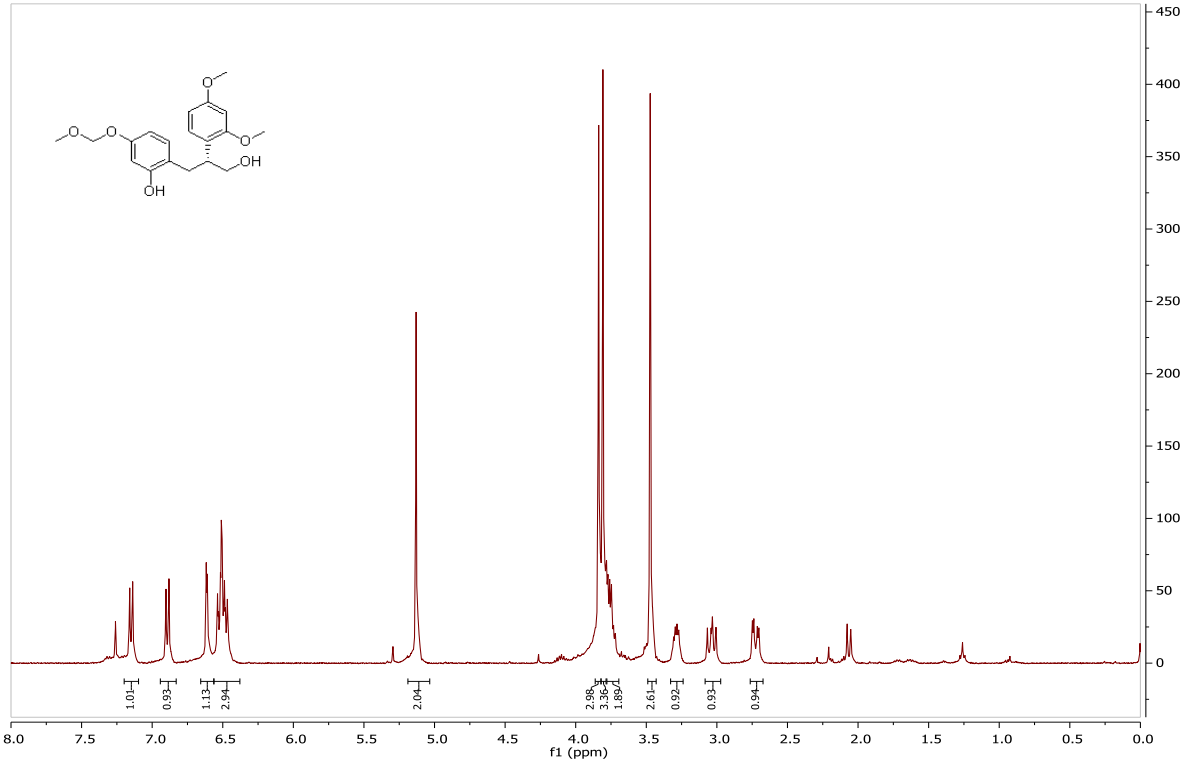

^{1}H NMR spectrum of compound (-) 43

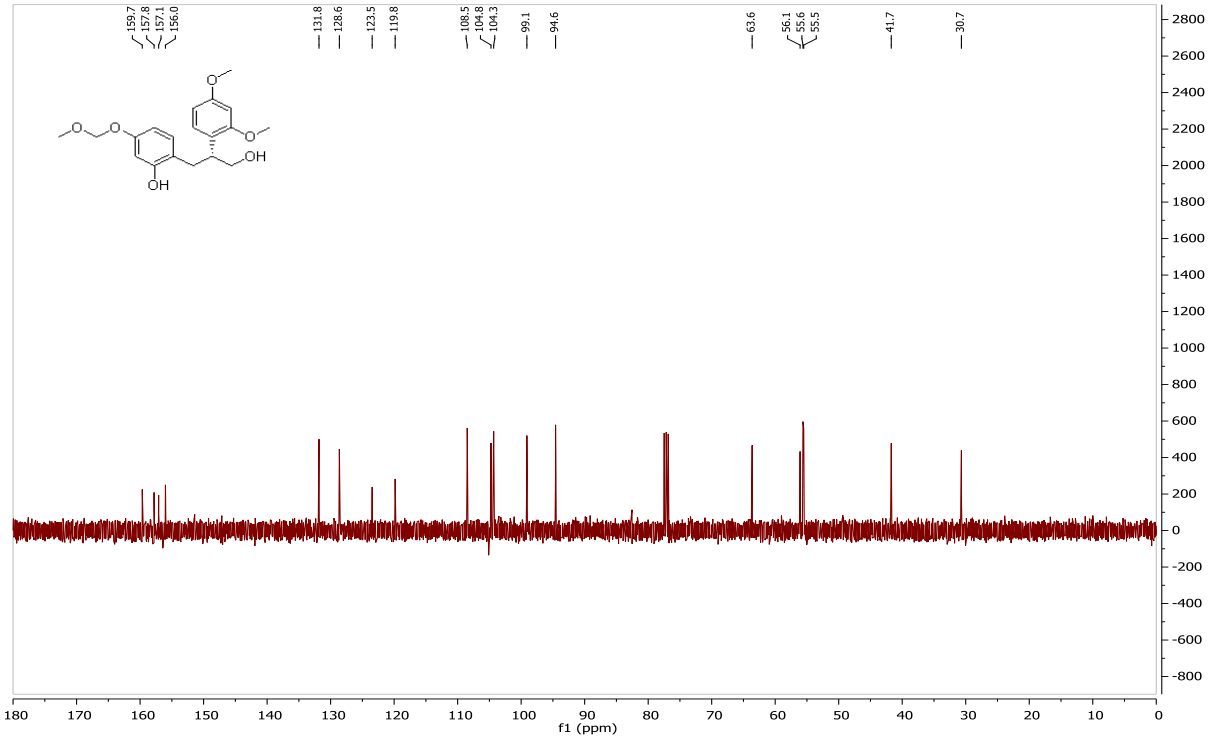

^{13}C NMR spectrum of compound (-) 43

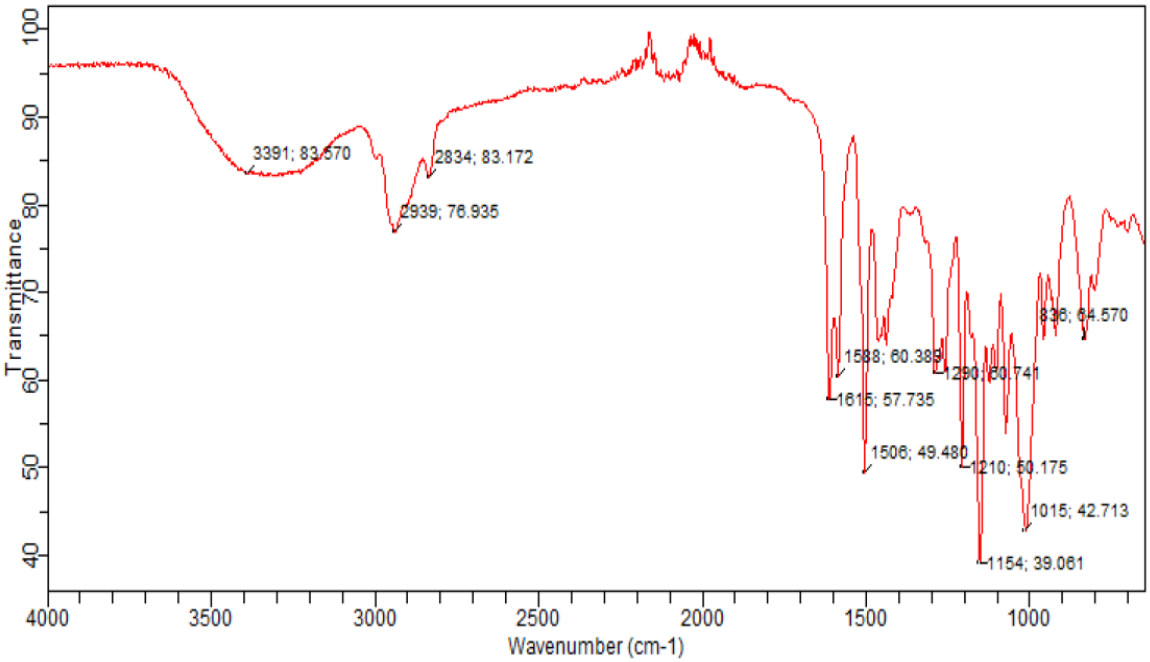

IR spectrum of compound (-) 43

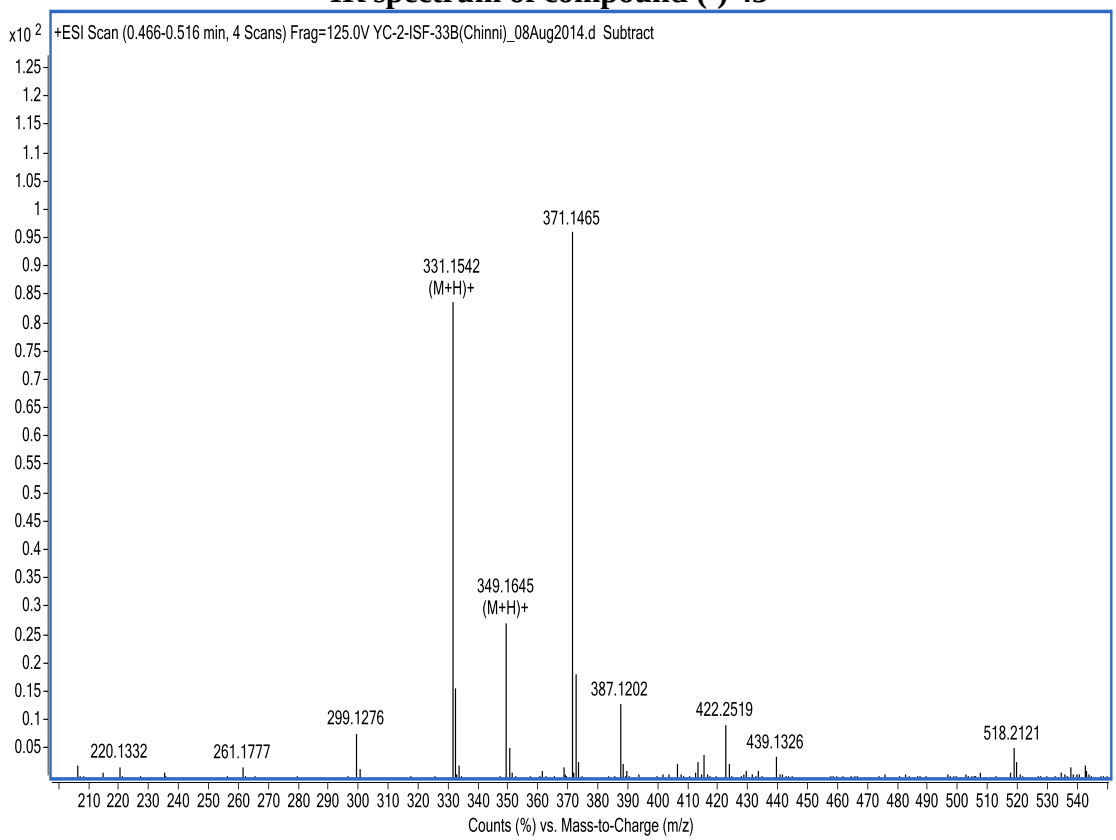

ESI-HRMS of compound (-) 43

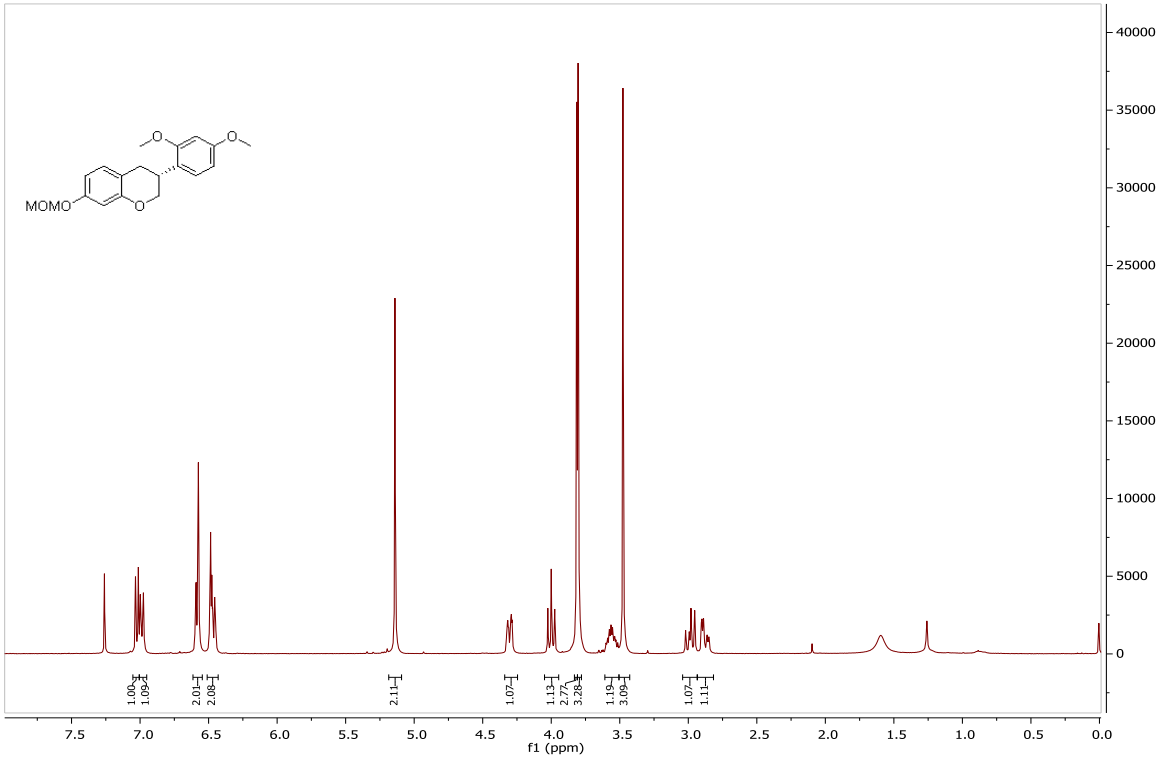

^{1}H NMR spectrum of compound (-) 57

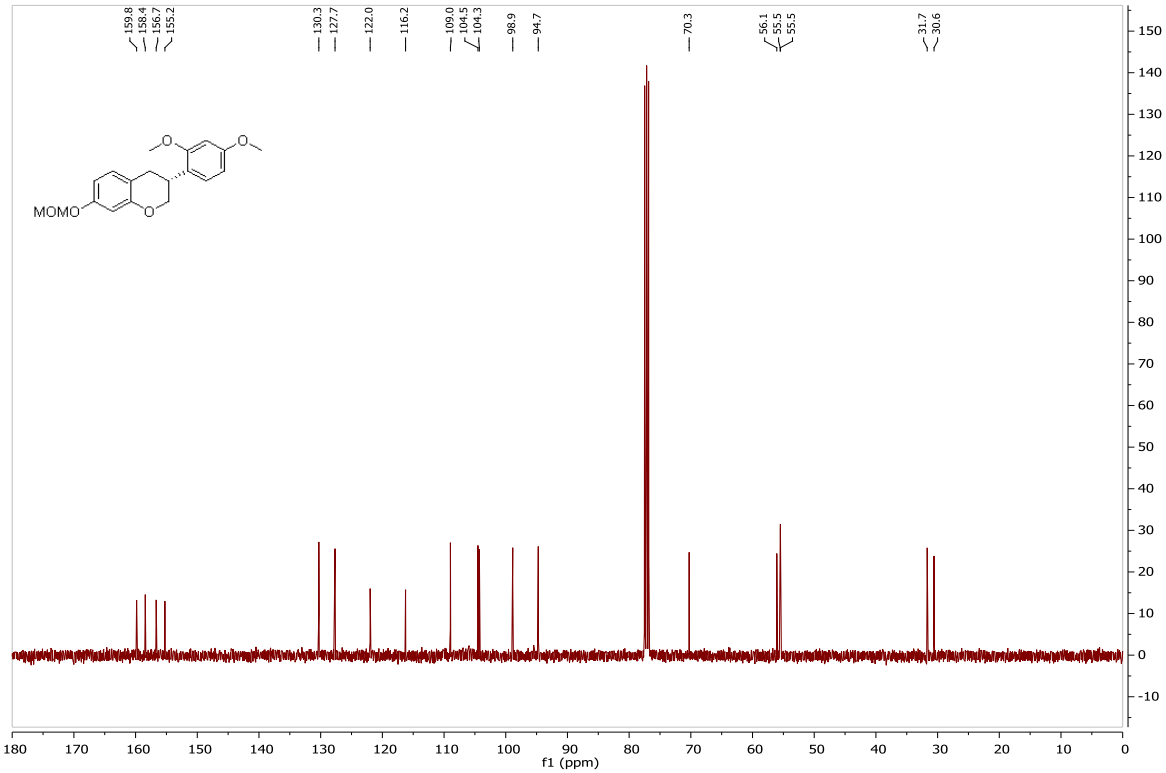

^{13}C NMR spectrum of compound (-) 57

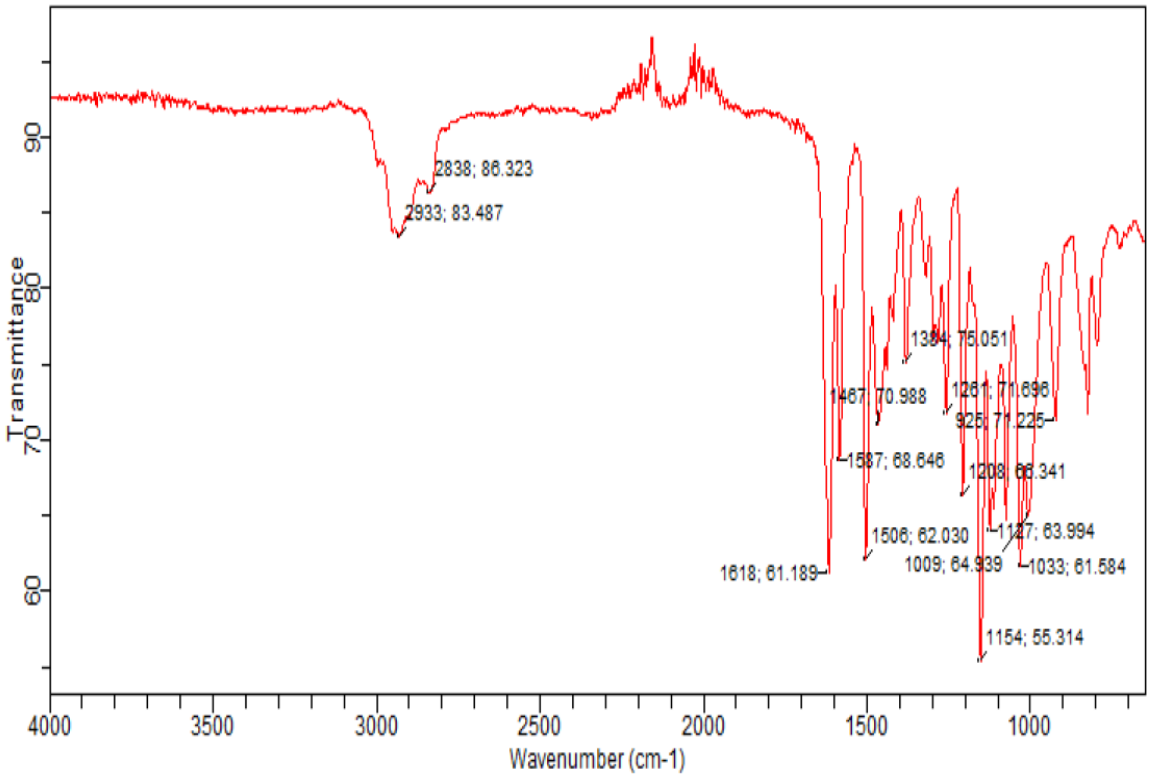

IR spectrum of compound (-) 57

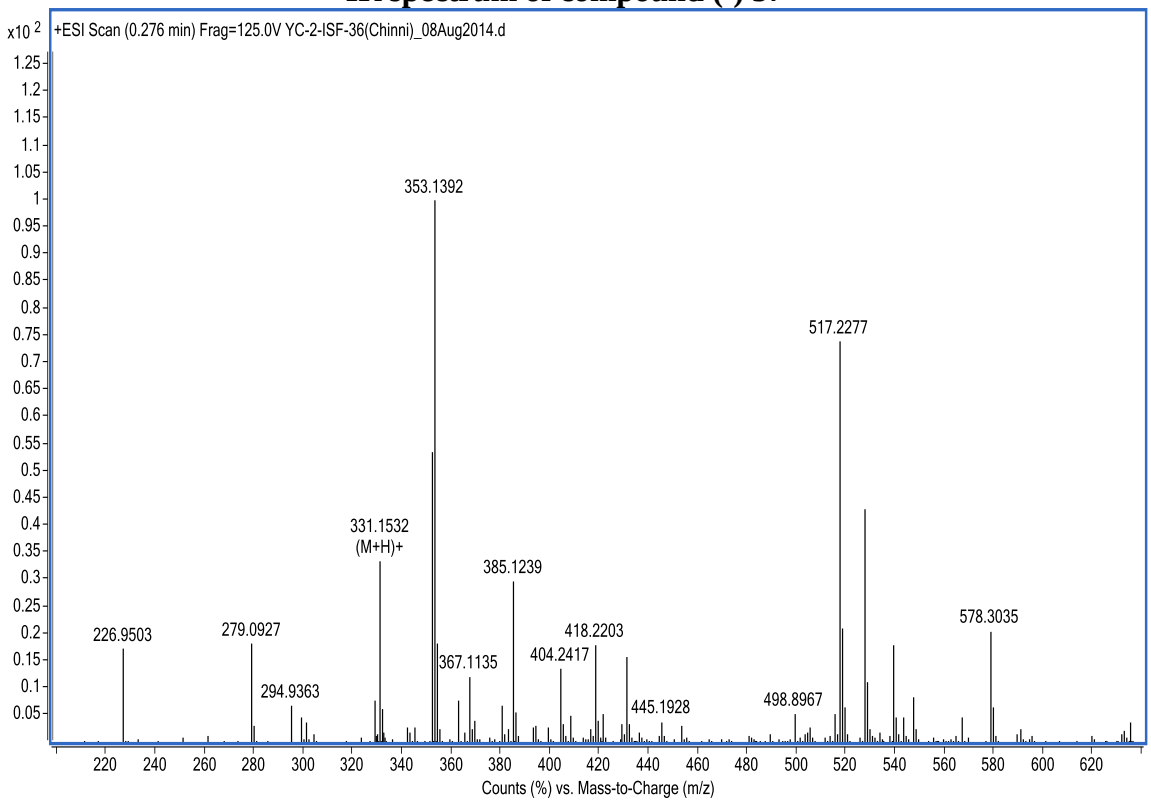

ESI-HRMS of compound (-) 57

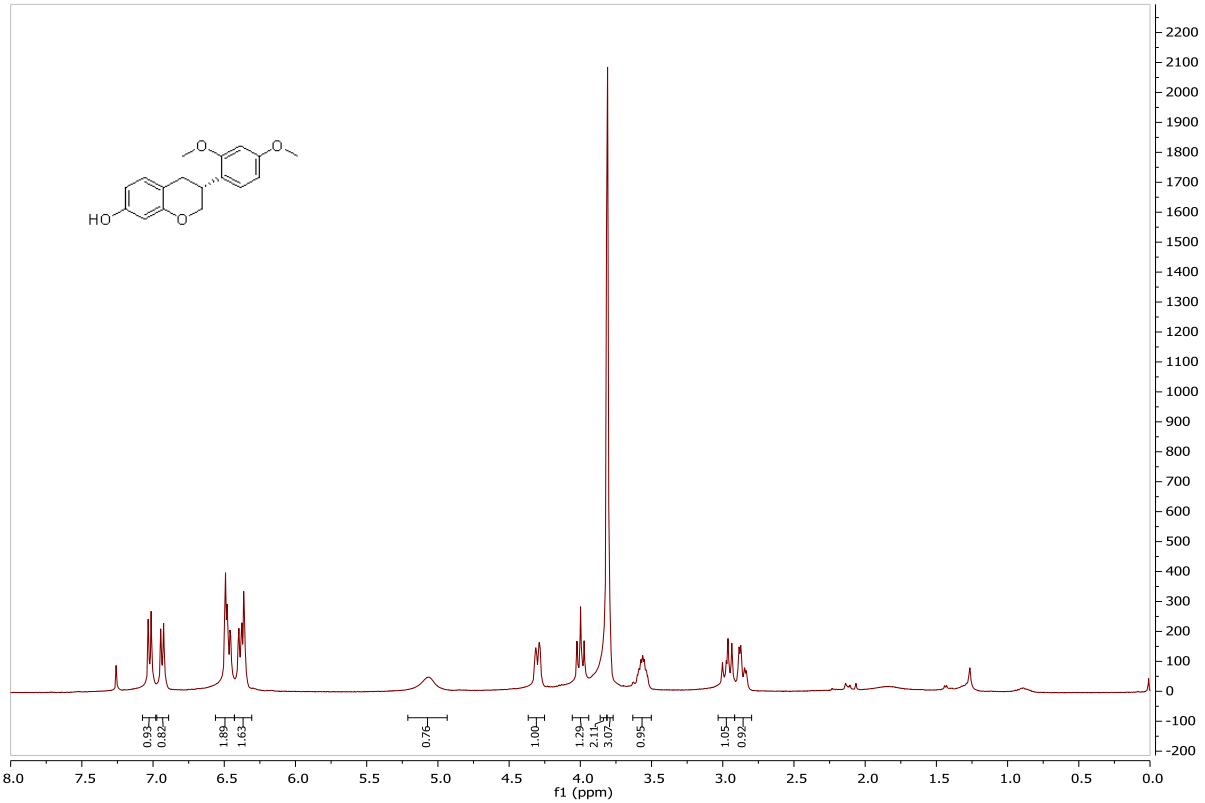

^{1}H NMR spectrum of compound (-) 8

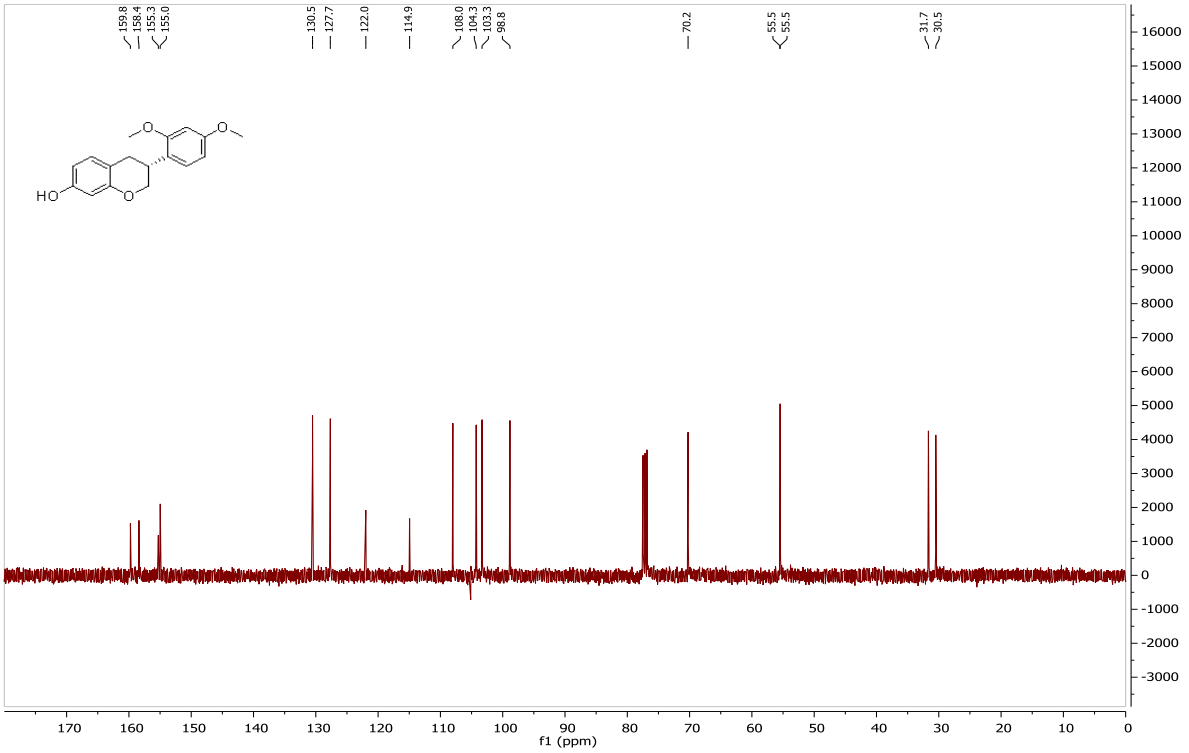

^{13}C NMR spectrum of compound (-) 8

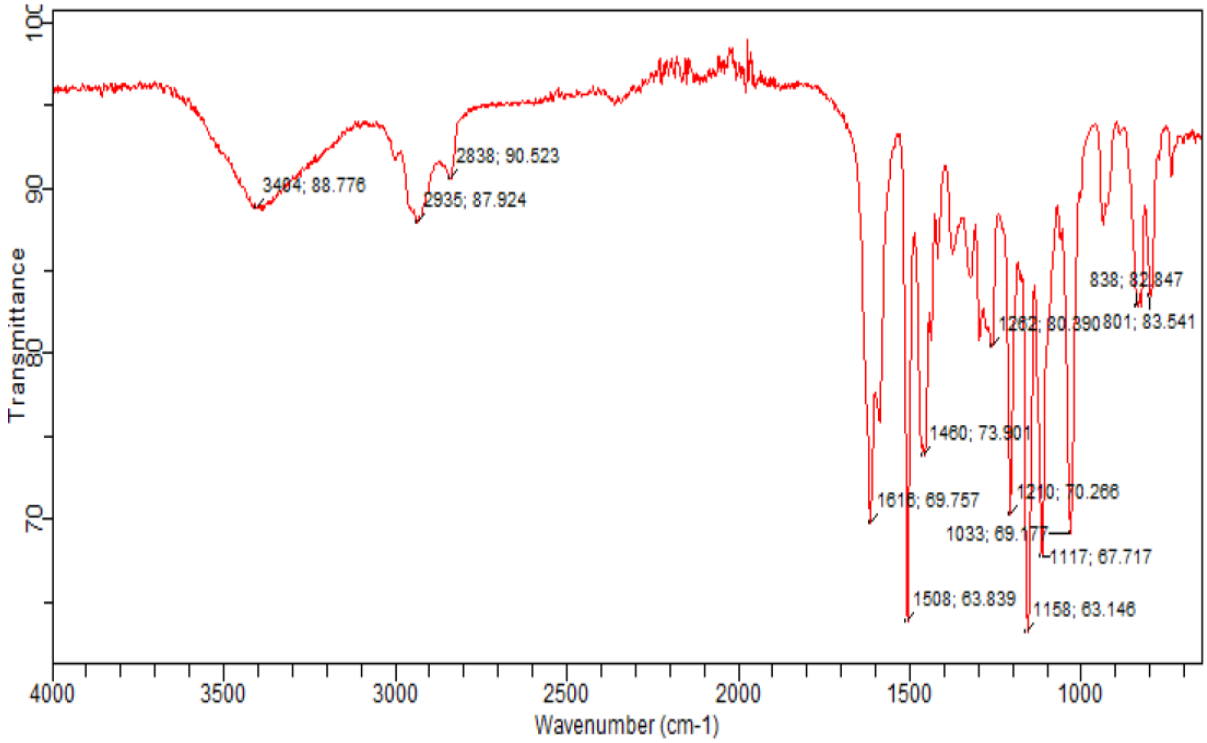

IR spectrum of compound (-) 8

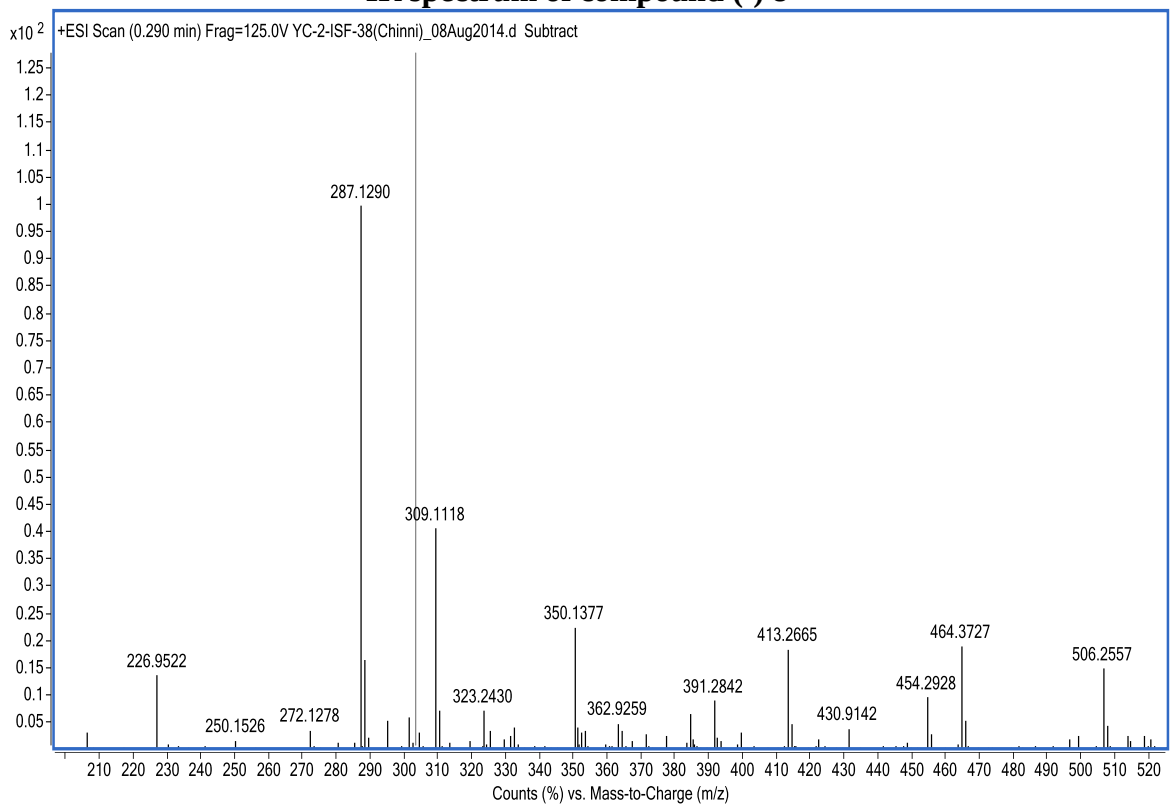

ESI-HRMS of compound (-) 8

VITA

CHINNI YALAMANCHILI

SUMMARY

Extensive experience in drug discovery, synthesis and biology, utilizing computer-aided drug discovery and HPLC-based bioassays, synthesis of polymers.
Hands on NMR, chromatography, characterization, and analysis of natural products and polymer
Research experience on bio-based carbohydrate polymers.
Experience in analysis of formulations.

EDUCATION

2010-present	Doctor of Philosophy Pharmaceutical Sciences (Pharmacognosy).
2006-2009	Master of Science (Chemistry), Mississippi State University. Teaching Assistant.
2002–2006	Bachelors of Pharmacy, Acharya Nagarjuna University.

SKILLS

- Skilled/experienced in analytical techniques: NMR, HRMS, HPLC, Chromatography, Size exclusion chromatography (SEC), Spectroscopic techniques (FTIR), zetasizer, TGA, polarimeter, column chromatography.
- Modelling and analysis software: PyMOL, Schrodinger software, Python, SAS, Matlab.

AWARDS

- 2015-2016, Dr. Charles D. Hufford Graduate Student Award.
- Best Poster, 3rd place in 16th annual Oxford ICSB/5th Interim ASP meeting in Oxford, MS (April 2016).
- 2015 AAPS Travelship Award (Drug Discovery and Development Interface-AAPS)
- Special mention award: "*Stereoselective Synthesis of S-(-)-Equol*" at International Conference on Science of Botanicals (ICSB), 2012.
- First prize, Presentation "*Alzheimer's disease–its science*" National pharmacy week celebrations, 2005, KVSR Siddhartha College of Pharmacy, India.

AFFLIATIONS

- American Association of Pharmaceutical Scientists (2014-current)
- American Society of Pharmacognosy (2013-current)
- Registered Pharmacist, TN, India (2014-2019)

PUBLICATIONS

Communications/abstracts

1. **Yalamanchili, C.;** Chittiboyina, A. G.; Vasquez, Y.; Khan, S.; Khan, I. A., Screening for antidiabetic compounds from Goji berries: Identification of novel small molecule PPARγ activators. *Planta Med* **2015,** 81, (11), PK26.
2. **Yalamanchili, C**.; Manda, V. K.; Chittiboyina, A. G.; Harrell Jr, W. A.; Webb, R. P.; Khan, I. A., Identification of novel inhibitors of botulinum neurotoxin A. *Planta Med* **2015,** 81, (11), PK12.
3. **Yalamanchili, C**.; Manda, V. K.; Chittiboyina, A. G.; HarrellJr, W. A.; Webb, R. P.; Khan, I. A., Identification of novel phytochemical inhibitors of botulinum neurotoxin A, *Planta Med* 2014, *80*, PH13.
4. Chittiboyina, A.; Rotte, S.; **Yalamanchili, C.**; Smillie, T. J.; Khan, I. A., Stereoselective Synthesis of S(-) Equol. *Planta Med* 78, (05), P41, **2012**.
5. Chittiboyina, A. G.; **Yalamanchali, C**.; Vasquez, Y.; Khan, S. I.; Khan, I. A., In Silico Screening for Antidiabetic Compounds from Goji Berries: Identification and Lead Optimization of Novel PPARγ Activators. *Planta Med* 77, (05), P16, **2011**.
6. **Yalamanchili, C.**; Rotte, S.; Smillie, T. J.; Khan, I. A., Aldol condensation of Evans Chiral enolates with benzaldehydes: Application to the stereoselective synthesis of phytoestrogens (submitted**).**
7. **Yalamanchili, C**; Chittiboyina, A. G.; Vasquez, Y.; Khan, S. I.; Khan, I. A.; Identification and lead optimization of novel PPARγ activators from Goji berries. (under preparation)
8. Chinni Yalamanchili, Vamshi K. Manda, Amar G. Chittiboyina, Rebecca L. Guernieri, William A. Harrell Jr, Robert P. Webb, Leonard A. Smith and Ikhlas A. Khan "Utilizing Ayurvedic Literature for the Identification of Novel Phytochemical Inhibitors of Botulinum Neurotoxin A" Journal of Ethnopharmacology , **2016** (In press).

PRESENTATIONS

1. "Identification of novel inhibitors of botulinum neurotoxin A"(Podium) MALTO meeting, University, MS (May **2015**).
2. Yalamanchili, C.; Manda, V. K.; Chittiboyina, A. G.; Harrell Jr, W. A.; Webb, R. P.; Khan, I. A., "Identification of novel phytochemical inhibitors of botulinum neurotoxin A" at American society of Pharmacognosy Conference (ASP, August, **2014**).
3. Chittiboyina, A.; Rotte, S.; Yalamanchili, C**.**; Smillie, T. J.; Khan, I. A., "Stereoselective Synthesis of S(-) Equol" at International Conference on Science of Botanicals (ICSB), **2012**.
4. Chittiboyina, A. G.; Yalamanchali, C.; Vasquez, Y.; Khan, S. I.; Khan, I. A., "*In Silico* Screening for Antidiabetic Compounds from Goji Berries: Identification and lead optimization of Novel PPARγ Activators." International Conference on Science of Botanicals (ICSB), **2011**.
5. Chinni, Y., "Drug interactions with natural products", National seminar on recent advances in pharmacy, **2006**, Bapatla, India.
6. Chinni, Y., "Alzheimer's disease–its science" national pharmacy week celebrations, **2005**, KVSR Siddhartha College of Pharmacy, Vijayawada, India.